

## INFORMATION TO USERS

This manuscript has been reproduced from the microfilm master. UMI films the text directly from the original or copy submitted. Thus, some thesis and dissertation copies are in typewriter face, while others may be from any type of computer printer.

**The quality of this reproduction is dependent upon the quality of the copy submitted.** Broken or indistinct print, colored or poor quality illustrations and photographs, print bleedthrough, substandard margins, and improper alignment can adversely affect reproduction.

In the unlikely event that the author did not send UMI a complete manuscript and there are missing pages, these will be noted. Also, if unauthorized copyright material had to be removed, a note will indicate the deletion.

Oversize materials (e.g., maps, drawings, charts) are reproduced by sectioning the original, beginning at the upper left-hand corner and continuing from left to right in equal sections with small overlaps. Each original is also photographed in one exposure and is included in reduced form at the back of the book.

Photographs included in the original manuscript have been reproduced xerographically in this copy. Higher quality 6" x 9" black and white photographic prints are available for any photographs or illustrations appearing in this copy for an additional charge. Contact UMI directly to order.

# UMI

A Bell & Howell Information Company  
300 North Zeeb Road, Ann Arbor MI 48106-1346 USA  
313/761-4700 800/521-0600



**University of Alberta**

**Site Characterization and Foundation Design in Sands**

**by**

**Soheil Eslaamizaad** ©

**A thesis submitted to the Faculty of Graduate Studies and Research  
in partial fulfillment of the requirements for the degree of  
Doctor of Philosophy**

**in**

**Geotechnical Engineering**

**Department of Civil and Environmental Engineering**

**Edmonton, Alberta**

**Fall 1997**



National Library  
of Canada

Acquisitions and  
Bibliographic Services

395 Wellington Street  
Ottawa ON K1A 0N4  
Canada

Bibliothèque nationale  
du Canada

Acquisitions et  
services bibliographiques

395, rue Wellington  
Ottawa ON K1A 0N4  
Canada

*Your file* *Votre référence*

*Our file* *Notre référence*

The author has granted a non-exclusive licence allowing the National Library of Canada to reproduce, loan, distribute or sell copies of this thesis in microform, paper or electronic formats.

The author retains ownership of the copyright in this thesis. Neither the thesis nor substantial extracts from it may be printed or otherwise reproduced without the author's permission.

L'auteur a accordé une licence non exclusive permettant à la Bibliothèque nationale du Canada de reproduire, prêter, distribuer ou vendre des copies de cette thèse sous la forme de microfiche/film, de reproduction sur papier ou sur format électronique.

L'auteur conserve la propriété du droit d'auteur qui protège cette thèse. Ni la thèse ni des extraits substantiels de celle-ci ne doivent être imprimés ou autrement reproduits sans son autorisation.

0-612-22980-7

University of Alberta

Library Release Form

**Name of Author:** Soheil Eslaamizaad

**Title of Thesis:** Site Characterization and Foundation Design in Sands

**Degree:** Doctor of Philosophy

**Year this Degree Granted:** 1997

Permission is hereby granted to the University of Alberta Library to reproduce single copies of this thesis and to lend or sell such copies for private, scholarly, or scientific research purposes only.

The author reserves all other publication and other rights in association with the copyright in the thesis, and except as hereinbefore provided, neither the thesis nor any substantial portion thereof may be printed or otherwise reproduced in any material form whatever without the author's prior written permission.

Soheil Eslaamizaad

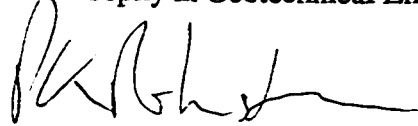
169 Mehr Street, Narmak, Tehran  
Iran, 16498

Oct. 2, 97  
Date submitted to the Faculty of  
Graduate Studies and Research

University of Alberta

Faculty of Graduate Studies and Research

The undersigned certify that they have read, and recommend to the Faculty of Graduate Studies and Research for acceptance, a thesis entitled **Site Characterization and Foundation Design in Sands** submitted by **Soheil Eslaamizaad** in partial fulfillment of the requirements for the degree of Doctor of Philosophy in Geotechnical Engineering.



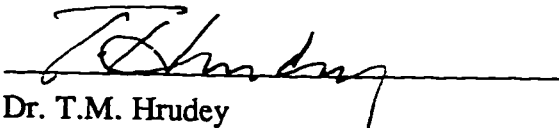
Dr. P.K. Robertson (Supervisor)



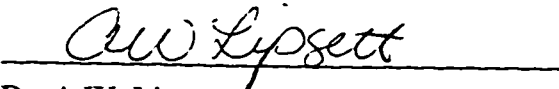
Dr. D. Chan



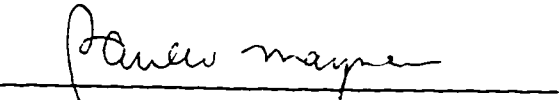
Dr. D.C. Sego



Dr. T.M. Hruday



Dr. A.W. Lipsett



Dr. P.W. Mayne (External Examiner)

Sept. 29, 97  
Date of Approval by Committee

*Dedicated to my family*

*and*

*in ever-loving memory of my father*

## ABSTRACT

A major concern in soil characterization is whether the soil is tested in its natural physical and chemical environment. In particular, where cohesionless soils are encountered, reliable soil characterization is difficult using conventional sampling and laboratory testing, due to unavoidable disturbance and difficulties associated with sampling. Consideration is therefore directed to alternative methods of in situ testing.

Much of the existing research work on sand is based on ideal uncemented low to medium compressible sand. Hence, engineering design based on these studies may not always be valid for all sands. A comprehensive procedure to identify and to evaluate 'unusual' sands has not yet been established. The effect of cementation on the strength-deformation behavior of sands is often ignored since cementation usually improves the shear strength. However, neglecting cementation can result in an overly conservative design of shallow and deep foundations as well as slopes and retaining walls. The stress history and age of the deposit are among the important factors which control the deformation characteristics of the soil. A reliable procedure for determining horizontal in situ stress has also not yet been established for cohesionless soils.

Few attempts have been made to estimate the ultimate bearing capacity of shallow footings directly from CPT data. The ultimate bearing capacity of shallow footings on sand is often overpredicted using correlations based on test results from calibration chamber tests performed on uncemented unaged sands while some natural sands are lightly cemented. Most of the methods for the prediction of settlement of footings on sand have been based on the conventional elastic formula. An equivalent soil modulus is frequently estimated based on in-situ testing measurements using empirical correlations.



The objective of this research has been to identify new ways to evaluate cohesionless soils, based on seismic techniques, such as the Seismic CPT. The research has focused on the identification of unusual sands, such as, highly compressible and/or cemented sands, and the quantification of their compressibility, stiffness, level of cementation, and in-situ stress and stress history. Relationships and methods have also been developed to evaluate the bearing capacity, and settlement of shallow footings on sand.

## ACKNOWLEDGMENTS

I would like to express my appreciation to my supervisor, Dr. Peter K. Robertson for the great interest he took in my research, and his generous support and continuous encouragement throughout the development of this thesis. The direction offered by Dr. Robertson, and his most valuable suggestions and comments during various stages of research are gratefully acknowledged.

I would like to thank Dr. Dave Chan for his advice and guidance during the early stage of research. My gratitude also goes to Dr. M. Jamiolkowski for his encouragement and valuable comments on my papers, to Dr. P.W. Mayne for his assistance in providing field data, and to Dr. T. Lunne for his contribution in evaluation the findings of this research.

I wish to express my gratitude to my wife, Atekeh, my daughter, Yasaman, and my son, Sahand, for their invaluable support and understanding throughout the course of this study. I also recognize and appreciate the lifelong influence of my parents, especially my late father for his love and encouragement in my higher education.

The seismic CPT results were provided by CANLEX office of Edmonton and ConeTec Investigation Ltd. of Vancouver. Their assistance are appreciated. The help of Dr. C. Wride of CANLEX office is gratefully acknowledged.

I would like to acknowledge the financial support of the Ministry of Science and Higher Education of Islamic Republic of Iran (9/92-8/96), and the partial financial support of the Natural Sciences and Engineering Research Council of Canada (NSERC) (6/93-12/96).

## TABLE OF CONTENTS

Page

### LIST OF TABLES

### LIST OF FIGURES

### LIST OF SYMBOLS

### CHAPTER 1: INTRODUCTION

1.1	Overview.....	1
1.2	Thesis Objectives .....	3
1.3	Methodology .....	4
	References .....	7

### CHAPTER 2: A FRAMEWORK FOR IDENTIFICATION OF UNUSUAL SANDS USING SEISMIC CPT

2.1	Introduction.....	8
2.2	The correlation between shear modulus and cone resistance .....	11
2.3	Proposed framework for identification of unusual sands .....	14
2.4	Summary and conclusions.....	18
	References .....	29

### CHAPTER 3: ESTIMATION OF LEVEL OF CEMENTATION IN CEMENTED SANDS BASED ON SEISMIC CPT RESULTS

3.1	Introduction.....	32
3.2	Influence of cementation on cone penetration resistance in sands.....	35
3.3	Influence of cementation on small strain shear modulus in sands.....	36
3.4	Proposed method for estimation of degree of cementation.....	39
3.5	Estimation of relative density in cemented sands.....	43

3.6	Summary and conclusions .....	43
	References .....	55

#### **CHAPTER 4: EVALUATION OF COMPRESSIBILITY OF UNCEMENTED SANDS**

4.1	Introduction.....	58
4.2	Evaluation of sand compressibility from Seismic CPT.....	62
	4.2.1 Constrained modulus.....	62
	4.2.2 Bulk modulus .....	66
	4.2.3 Example application .....	67
4.3	A procedure to evaluate sand compressibility from CPT results .....	68
	4.3.1 Constrained modulus.....	68
	4.3.2 Bulk modulus .....	70
	4.3.3 Example application .....	70
4.4	Summary and conclusions .....	72
	References .....	94

#### **CHAPTER 5: EVALUATION OF IN SITU LATERAL STRESS AND OCR IN UNCEMENTED SANDS**

5.1	Introduction.....	97
5.2	Evaluation of in situ lateral stress in sands.....	101
5.3	Estimation of stress history in sands .....	105
5.4	Applications .....	106
5.5	Discussion .....	107
5.6	A modified method for a direct estimation of $K_0$ .....	108
5.7	Summary and conclusions.....	111
	References .....	124

## **CHAPTER 6: A METHOD FOR EVALUATING BEARING CAPACITY OF FOUNDATIONS IN SANDS FROM CONE PENETRATION TEST (CPT)**

6.1	Introduction.....	126
6.2	Proposed method for evaluation of bearing capacity of footing in sands .....	130
6.3	Estimation of ultimate end bearing capacity of deep foundations .....	135
6.4	Summary and conclusions.....	136
References	.....	146

## **CHAPTER 7: EVALUATION OF SETTLEMENT OF FOOTINGS ON SAND FROM SEISMIC IN SITU TESTS**

7.1	Introduction.....	149
7.2	Depth of influence and evaluation of equivalent modulus.....	152
	7.2.1 Background .....	152
	7.2.2 Proposed method for evaluation of equivalent modulus .....	156
7.3	Operational stiffness of ground .....	158
	7.3.1 Modulus degradation relationships .....	159
	7.3.2 Increase in soil stiffness due to loading of footing .....	162
7.4	First proposed method to estimate settlement based on an equivalent homogeneous medium beneath the footing .....	165
	7.4.1 A summary of the first method.....	165
	7.4.2 Worked example .....	166
7.5	Second proposed method to estimate settlement for a non-homogeneous medium beneath the footing.....	167
	7.5.1 Computation of settlement.....	168
	7.5.2 Evaluation of increase in modulus with depth, $\alpha(z)$ due to increase in confinement stress.....	169
	7.5.3 Evaluation of reduction of modulus with depth, $\beta(z)$ due to increase in shear stress .....	170
	7.5.4 Strain influence factor $I_L$ .....	171
	7.5.5 A summary of the second method .....	171
	7.5.6 Worked example .....	173

7.6	Summary and conclusions.....	173
	References .....	199

## **CHAPTER 8: CONCLUSIONS AND RECOMMENDATIONS**

8.1	Conclusions .....	202
	8.1.1 Identification of unusual sands.....	203
	8.1.2 Evaluation of level of cementation.....	203
	8.1.3 Evaluation of compressibility.....	204
	8.1.4 Evaluation of in situ lateral stress and stress history.....	204
	8.1.5 Evaluation of bearing capacity.....	205
	8.1.6 Evaluation of settlement.....	206
8.2	Recommendations .....	207
	References .....	209

## **APPENDIX A**

.....	210
-------	-----

## LIST OF TABLES

	Page
<b>CHAPTER 2</b>	
2.1	Index properties of sands tested at calibration chamber ..... 20
2.2	Index properties of sands tested at field..... 21
<b>CHAPTER 3</b>	
3.1	Penetration test results of artificially cemented Monterey sand (after Puppala et al., 1995) ..... 46
<b>CHAPTER 4</b>	
4.1	Summary of calibration chamber test results for constrained modulus factor $\alpha_k$ (after Lunne and Kleven, 1981) ..... 75
4.2	Average sand compressibility parameters from laboratory tests (after Byrne et al., 1987) ..... 76
4.3	Evaluation of the proposed method of estimation of sand compressibility using SCPT ..... 77
4.4	Evaluation of the proposed method of estimation of sand compressibility using CPT..... 78
4.5	Validation of the proposed method of estimation of constrained modulus in sands (after Lunne, 1996) ..... 79
<b>CHAPTER 7</b>	
7.1	Detailed data for tested low compressible Toyoura sand (after Teachavorasinskun et al., 1990) ..... 176
7.2	$q_{ult}$ and $\lambda$ values for typical low compressible sands with different density and stress history ..... 177

7.3	Summary of subsoil condition at the Texas Experimentation site (after Tand et al., 1995) .....	178
7.4	Cross-hole test results (after Briaud and Gibbens, 1994) .....	179
7.5	Evaluation of settlement for a 3.0 m square footing on sand based on the first proposed method.....	180
7.6	Distribution of factor $I'_z$ in depth for NC and OC sands .....	181
7.7	Evaluation of settlement for a 3.0 m square footing on sand based on the second proposed method.....	182

## APPENDIX A

A.1	Index parameters for Phase II CANLEX sites (after Wride and Robertson, 1997) .....	211
-----	--	-----



## LIST OF FIGURES

Page

### CHAPTER 2

- 2.1 Chart that estimates cohesion intercept ( $c$ ) and relative density ( $D_r$ ) from cone penetration resistance ( $q_c$ ) and sleeve friction in Cone Penetration Testing (after Puppala et al., 1993) ..... 22
- 2.2 Correlation for estimating slope of the steady state line ( $\lambda$ ) for uncemented sand from seismic CPT results (after Robertson et al., 1995) ..... 23
- 2.3 Relationship between cone bearing and dynamic shear modulus for normally consolidated, uncemented, quartz sands (after Robertson and Campanella, 1983) ..... 24
- 2.4  $q_{cs}$  versus  $G_o$  correlation for uncemented, predominantly quartz sands (after Jamiolkowski and Robertson, 1988) ..... 25
- 2.5 Correlation between  $q_c$  and  $G_o$  (after Baldi et al., 1989) ..... 26
- 2.6 Soil behavior type chart based on normalized CPT penetration resistance and the ratio of small strain shear modulus with penetration resistance (after Robertson et al., 1995) ..... 27
- 2.7 Proposed chart for identification of unusual sands ..... 28

### CHAPTER 3

- 3.1 Effect of cementation on the cone penetration resistance and the sleeve friction (after Rad and Tumay, 1986) ..... 47
- 3.2 Effect of cohesion intercept of cemented sands on the cone penetration resistance and the sleeve friction (after Rad and Tumay, 1986) ..... 48
- 3.3 Relative effect of very weak cementation on the cone penetration in Monterey sand (after Puppala et al., 1995) ..... 49
- 3.4 Correlation between normalized cone resistance, attraction parameter, and relative density ..... 50
- 3.5 Correlation between normalized small strain shear modulus, attraction parameter, and relative density ..... 51

3.6	Estimation of attraction parameter from SCPT for cemented sands.....	52
3.7	Estimation of relative density for cemented Utah tailings sands.....	53
3.8	Comparison of conventional method and proposed method for estimation of relative density for cemented Utah tailings sands.....	54

## CHAPTER 4

4.1	Relationship between cone penetration resistance and constrained modulus for normally consolidated, uncemented quartz sands (after Robertson and Campanella, 1983) .....	80
4.2	Relationship between cone penetration resistance and constrained modulus for NC and OC, uncemented unaged quartz sands (after Baldi et al., 1986) .....	81
4.3	Constrained modulus vs. cone resistance based on calibration chamber test in Toyoura sand (after Fioravante et al., 1991) .....	82
4.4	Correlation between $M_t$ , $q_c$ and $V_v$ for normally consolidated uncemented sands.....	83
4.5	Correlation between $M_t$ , $q_c$ , $V_v$ , and OCR for overconsolidated uncemented sand.....	84
4.6	Relationship between $k_M$ , $q_c$ and $V_v$ for uncemented sands .....	85
4.7	Predicted versus measured normalized constrained modulus (using Eq. 4.9 and 4.12).....	86
4.8	Relationship between $k_B$ , $q_c$ and $V_v$ for uncemented sands .....	87
4.9	Correlation between $M_t$ and $q_c$ for normally consolidated uncemented sands.....	88
4.10	Correlation between $M_t$ , $q_c$ and OCR for overconsolidated uncemented sand.....	89
4.11	Relationship between $k_M$ and $V_v$ for uncemented sands .....	90
4.12	Predicted versus measured normalized constrained modulus (using Eq. 4.18 and 4.20) .....	91
4.13	Relationship between $k_B$ and $q_c$ for uncemented sands .....	92
4.14	$k_B$ values from laboratory and field tests (after Byrne et al., 1987).....	93

## CHAPTER 5

5.1	Estimation of $K_o$ from Durgunoglu and Mitchell (after Kulhawy et al., 1989) .....	113
5.2	$K_o$ as a function of sleeve friction and overconsolidation ratio (after Masood and Mitchell, 1993).....	114
5.3	Correlation between $\sigma'_{ho}$ , $q_c$ , $G_o$ and $\sigma'_{vo}$ .....	115
5.4	Measured versus predicted normalized horizontal effective stress for calibration chamber tests.....	116
5.5	Correlation between OCR and $K_o$ .....	117
5.6	Evaluation of $K_o$ from SCPT for unaged, uncemented sands .....	118
5.7	Predicted $K_o$ , based on Eq. 5.12 versus measured $K_o$ for calibration chamber tests .....	119
5.8	Correlation between $q_c$ , $V_v$ and $\sigma'_{vo}$ for uncemented quartz sands .....	120
5.9	Predicted $K_o$ , based on Eq. 5.17 versus measured $K_o$ for calibration chamber tests .....	121
5.10	Evaluation of $K_o$ from SCPT for unaged, uncemented sands .....	122
5.11	Correlation between $q_c$ , $V_v$ and $\sigma'_{vo}$ for carbonate Quiou sands .....	123

## CHAPTER 6

6.1	Allowable bearing pressure estimated from Cone Penetrometer (after Meyerhof, 1956) .....	138
6.2	Correlation between $q_c$ and allowable bearing pressure $q_a$ , for various sizes of footings (after Goel, 1982) .....	139
6.3	Bearing ratio versus width of footing (after Tand et al., 1995) .....	140
6.4	Application of CPT to pile design (after Schmertmann, 1978) .....	141
6.5	Modes of foundation failure in sand (after Vesic, 1973) .....	142
6.6	Regression analysis to evaluate the empirical correlation factor, $\alpha$ .....	143
6.7	Correlation between bearing capacity of footings on cohesionless soils and average cone resistance, $\bar{q}_c$ .....	144

6.8	Correlation between bearing capacity of deep footings in cohesionless soils and average cone resistance, $\bar{q}_c$ .....	145
-----	--	-----

## CHAPTER 7

7.1	Relationship between B and depth of influence $Z_f$ (after Burland and Burbidge, 1985).....	183
7.2	Distribution of settlement with depth for a circular rough rigid foundation on isotropic non-homogeneous elastic soil (after Burland and Burbidge, 1985) .....	184
7.3	Distribution of the strain influence factors in depth for various Poisson's ratios .....	185
7.4	Recommended distribution of strain influence factors in depth .....	186
7.5	Secant shear moduli for NC sand specimens and OC sand specimens (after Teachavorasinskun et al., 1991) .....	187
7.6	Curve fitting for NC sands .....	188
7.7	Curve fitting for OC sands.....	189
7.8	Average increasing factor, $\alpha$ , of sand moduli due to increase in confinement.....	190
7.9	Average decreasing factor, $\beta$ , of sand moduli due to increase in shear strain.....	191
7.10	Factor, $\psi$ , versus $q/q_{ult}$ , for sands with various density and stress history .....	192
7.11	Comparison of the first method of prediction of settlement with load settlement curve of 3m square footings at Texas Experimentation Site.....	193
7.12	Distribution of shear stress with depth for Poisson's ratio of 0.30 (after Poulos and Davis, 1974).....	194
7.13	variation of $\mu(z)$ with depth.....	195
7.14	Distribution of factor $I'_z$ in depth for NC sands.....	196
7.15	Distribution of factor $I'_z$ in depth for OC sands .....	197
7.16	Comparison of the first method of prediction of settlement with load settlement curve of 3m square footings at Texas Experimentation Site.....	198

## APPENDIX A

A.1	Kidd Site in the Fraser River Delta (after Lawrence, 1995) .....	212
A.2	Corrected (a) SPT, (b) CPT and $V_s$ profiles at the Kidd Site.....	213
A.3	Massey Site in the Fraser River Delta (after Lawrence, 1995) .....	214
A.4	Corrected (a) SPT, (b) CPT and $V_s$ profiles at the Massey Site.....	215
A.5	CPT profile at the Alaska Site .....	216
A.6	$V_s$ profile at the Alaska Site.....	217
A.7	CPT profile of Utah tailings sand.....	218
A.8	$V_s$ profile of Utah tailings sand.....	219
A.9	CPT profile of Alabama residual soil at Auburn Test Site, Test C41.....	220
A.10	CPT profile of Alabama residual soil at Auburn Test Site, Test C42.....	221
A.11	$V_s$ profile of Alabama residual soil at Auburn Test Site, Test C41 and Test C42 .....	222
A.12	CPT profile at Holmen .....	223
A.13	CPT profile at Sleipner.....	224

## LIST OF SYMBOLS, NOMENCLATURE AND ABBREVIATIONS

$A, A_0, A_1, A_2$	= constant parameter
$A_x$	= factor which is computed for estimation of $K_0$
$a$	= radius of circular footing
$a'_p$	= attraction intercept = $c'_p / \tan \phi'_p$
$B$	= width of the footing
$B_t$	= tangent bulk modulus
$B_0, B_1, B_2$	= constant parameter
B.C.	= British Columbia in Canada
CC	= degree of cementation
$C$	= constant parameter, empirical parameter
$C_0, C_1, C_2, C_3$	= constant parameter
CANLEX	= Canadian Liquefaction Experiment
CPT	= cone penetration test
CPTU	= cone penetration test with pore pressure measurement
$c$	= cohesion intercept
$c'$	= drained cohesion intercept
$c'_p$	= peak drained cohesion intercept
$D$	= depth of footing
$D_1$	= constant parameter
$D_r$	= relative density
$D_{50}$	= grain size of the soil particle which 50% of grains are smaller than that
$d_c$	= cone diameter
$E'_0$	= Young's modulus at surface
$E_{eq}$	= equivalent Young's modulus
$E_i$	= Young's modulus for layer I
$E_s$	= equivalent stress-strain Young's modulus
$E_{si}$	= stress-strain Young's modulus estimated from CPT for layer i
$E_z$	= operational Young's modulus at depth z
$e$	= void ratio
$e_{max}$	= maximum void ratio
$e_{min}$	= minimum void ratio
$F$	= shape factor
$f$	= constant parameter

$f_n, f_{n-1}$	= influence factor for settlement as defined by Schultz and Sherif (1973)
$f_s$	= CPT sleeve friction
$G_o$	= small strain shear modulus
$G_i$	= small strain shear modulus for layer i
$G_{ou}$	= small strain shear modulus of corresponding uncemented sand
$G_{eq}$	= equivalent small strain shear modulus
$G_{oeq}$	= equivalent small strain shear modulus
$G_{o1}$ to $G_{o4}$	= small strain shear modulus for layer 1 to 4, respectively
$G_s$	= soil specific gravity
$G_z$	= operational shear modulus at depth z
$G_{oz}$	= small strain shear modulus at depth z
$g$	= constant parameter
$H$	= depth of influence
$I_z$	= strain influence factor
$I'_z$	= influence factor for estimation of settlement based on small strain shear modulus
$K_o$	= coefficient of earth pressure at rest
$K_{oNC}$	= coefficient of earth pressure at rest for normally consolidated sands
$K_1$	= a correction factor for depth of foundation
$K_2$	= a correction factor for creep
$k$	= constant parameter
$k$	= rate of increase of Young's modulus with depth
$k_B$	= bulk modulus number
$k_M$	= constrained modulus number
$L$	= length of footing
$M$	= constrained modulus
$M_t$	= tangent constrained modulus
$m_v$	= volumetric change per unit of pressure increase
$N$	= SPT blow number
$N_m$	= mean value of SPT blows
$N_\gamma, N_q$	= bearing capacity factor
NC	= normally consolidated
$n$	= power term of confining pressure in relationship of small strain shear modulus of sands
OC	= overconsolidated

OCR	= overconsolidation ratio
$p'$	= mean effective stress
$p'_o$	= initial mean effective stress
$P_a$	= atmospheric pressure
$q$	= pressure of footing
$q_a$	= allowable bearing pressure
$q_c$	= cone penetration resistance
$q_n$	= net cone penetration resistance = $q_c - \sigma'_{vo}$
$q_{c1}$	= normalized cone penetration resistance
$\bar{q}_c$	= average cone resistance within the zone of influence
$q_{ct}$	= total cone penetration resistance
$q_{ult}$	= ultimate bearing capacity
$R_c$	= ratio between small strain shear modulus of cemented sand to that of similar uncemented sand
$R$	= correlation factor in regression analysis
$R_k$	= ratio between ultimate bearing capacity and cone penetration resistance as defined by Tand et al. (1995)
$S$	= stiffness coefficient for uncemented sand
SPT	= standard penetration test
SCPT	= seismic cone penetration test
SCPT-DH	= down hole seismic cone penetration test
SCPT-XH	= cross hole seismic cone penetration test
$s$	= settlement
$s_o$	= settlement at surface
$V_a$	= velocity of sound in air
$V_s$	= shear wave velocity
$V_o$	= initial volume
$V_{s1}$	= normalized shear wave velocity
$Y$	= a conversion factor between $V_s$ , $q_c$ and $\sigma'_{vo}$ (after Robertson et al., 1995)
$Z_1$	= depth of influence
$z$	= variable depth beneath the footing
$\alpha_u$	= empirical correlation factor to correlate cone penetration resistance and ultimate bearing capacity
$\alpha_b$	= installation coefficient of pile



$\alpha_E$	= coefficient between Young's modulus and cone penetration resistance
$\alpha_f$	= empirical correlation factor of bearing capacity
$\alpha_m$	= constrained modulus factor
$\alpha_M$	= coefficient between constrained modulus and cone penetration resistance
$\alpha(z)$	= a factor to measure increase in modulus with depth due to increase in confinement stress
$\bar{\alpha}$	= average factor for the increase in modulus within depth of influence due to increase in confinement stress
$\beta$	= average factor for the reduction of modulus with depth due to increase in shear stress
$\beta(z)$	= a factor to measure reduction of modulus with depth due to increase in shear stress
$\chi$	= factor between volumetric strain and vertical effective strain
$\Delta G_o$	= increase in modulus due to cementation
$\Delta\sigma_x$	= increase in stress in direction x due to loading
$\Delta\sigma_y$	= increase in stress in direction y due to loading
$\Delta\sigma_z$	= increase in stress in direction z due to loading
$\Delta V$	= volume change
$\Delta z_i$	= thickness of layer i
$\epsilon_i$	= vertical strain for layer i
$\epsilon_z$	= vertical strain at depth of z
$\phi_{cv}$	= constant volume friction angle
$\phi'$	= drained friction angle
$\phi'_p$	= peak drained friction angle
$\gamma$	= soil weight density
$\eta$	= distribution factor of changes of stress with depth

$\varphi$	= constant exponent
$\kappa$	= $N_\gamma / N_q$
$\lambda$	= parameter equal to $0.4 N_\gamma$
$\lambda_{st}$	= slope of the steady state line
$\mu(z)$	= variable factor with depth between $\tau/\tau_{max}$ and $q/q_{ult}$
$\theta$	= constant exponent
$\rho$	= soil mass density
$\sigma'_a$	= effective stress in the direction of seismic wave propagation
$\sigma'_b$	= effective stress in the direction of soil particle motion
$\sigma'_{ho}$	= horizontal effective stress
$\sigma'_m$	= mean effective stress
$\sigma_v$	= vertical total stress
$\sigma'_v$	= vertical effective stress
$\sigma_{vo}$	= initial vertical total stress
$\sigma'_{vo}$	= initial vertical effective stress
$\tau$	= shear stress
$\tau_{max}$	= maximum shear stress
$\nu$	= Poisson's ratio

## CHAPTER 1

### INTRODUCTION

#### 1.1 Overview

A major concern in soil characterization is whether the soil is tested in its natural physical and chemical environment. Common causes of disturbances to the sample are mechanical disturbance of the soil structure during drilling, sampling, transportation, storage and handling in the lab as well as changes in water content and stress conditions and possible chemical changes and mixing and segregation of the soil constituents. In particular, where cohesionless soils are encountered, reliable soil characterization is difficult using conventional sampling and laboratory testing, due to unavoidable disturbance and difficulties associated with sampling. Drilling techniques generally produce considerable disturbance to the materials surrounding the drill hole, which can have a significant effect on subsequent sample quality. Undisturbed sampling in soils with little or no cohesion can be difficult and expensive. In addition, some natural cohesionless soils may be lightly cemented and standard sampling techniques often break the bonds, resulting in disturbance. Consideration is therefore directed to alternative methods of in situ testing to characterize sands, and to determine bearing capacity and settlement of footings on sand.

Much of the existing research work on sand is based on ideal uncemented low to medium compressible sand. Therefore, engineering design based on these studies may not always be valid for all sands. Evaluation of compressibility and level of cementation in cohesionless soils based on laboratory tests can be difficult and sometimes unreliable due to the often unavoidable sample disturbance. In such circumstances in situ tests are generally preferred. However, a comprehensive procedure to identify 'unusual' sands has not yet been established.

Most natural soils have components of stiffness and strength which are difficult to account for by classical soil mechanics and are generally due to the presence of structure in soils (inter-particle bonding and fabric). Cementation is a process which frequently exists in many natural deposits of granular soils. Recent data and evidence suggest that even the cleanest natural sand deposits may be very weakly cemented (Puppala et al. 1995). Hence,

engineering judgment made based on test results from uncemented specimens reconstituted in the laboratory may not be valid (Mitchell and Solymar, 1984). The effect of cementation on the strength-deformation behavior of sands is often ignored since cementation often improves the strength. However, neglecting cementation can result in an overly conservative design of shallow and deep foundations, as well as slopes and retaining walls.

Compression in granular soils involves both rearrangement and crushing of particles. The significant effect of sand mineralogy and confining pressures on compression behavior of sands has been broadly recognized. Other influencing factors include initial relative density, stress history, cementation, particles size and distribution, angularity and gradation. Evaluation of compressibility in cohesionless soils based on laboratory tests can be difficult and unreliable due to the often unavoidable sample disturbance. In such circumstances in situ tests are generally preferred. However, a comprehensive procedure for determining compressibility from in situ tests, applicable to sands with different mineralogy ranging from clean silica sand to calcareous carbonate sand, has not yet been established.

The stress history and age of the deposit are among the important factors which control the soil modulus and, hence, the deformation characteristics of the soil. Extensive studies of penetration testing mostly in calibration chamber have shown that the stiffness of sands is very sensitive to stress history. A reliable procedure for determining horizontal in situ stress has also not yet been established for cohesionless soils .

Extensive research has been performed to correlate cone resistance to the bearing capacity of deep footings. However, few attempts have been made to estimate the ultimate bearing capacity ( $q_{ult}$ ) of shallow footings directly from CPT data. The most widely used procedure for computing  $q_{ult}$  using CPT data is indirect and is based on the general bearing capacity theory in which either internal friction angle or bearing capacity factors are estimated from empirical correlations or published charts. However, the ultimate bearing capacity of shallow footings on sand is often overpredicted using correlations that relate cone resistance to friction angle because such relationships are most frequently based on test results from calibration chamber tests performed on uncemented unaged sands while some natural sands are lightly cemented.

Numerous articles have appeared in the literature related to the prediction of settlement of footings on sand by means of in-situ tests. Most of these methods have been based on the

conventional elastic formula, where the ground is assumed to be an elastic homogeneous halfspace. Sand deposits are often non-homogeneous in nature in which the stiffness varies with depth. Hence, an equivalent soil modulus is frequently estimated based on in-situ testing measurements. Empirical correlations exist relating in-situ test results to the ground stiffness from which the equivalent ground modulus can be obtained. In general, a depth of influence is defined within which an average value of soil modulus, is computed. Seismic tests are among the few in-situ tests that produce little or no soil disturbance. Such techniques induce very small strain in the ground that preserve its natural features. Swiger (1974) applied in-situ seismic techniques in the evaluation of ground settlement using conventional linear elastic theory. In his approach, the measured small strain moduli are softened using reduction curves developed by Seed (1969) based on the strain level in the ground. However, the curves given by Seed do not distinguish between sand stress history and sand grain mineralogy. More realistic computation of settlement of footings on sands can be obtained when appropriate modulus degradation curves are utilized in determining operational modulus of the ground from the measured small strain modulus. Hence, prior knowledge of stress history and compressibility of sand are required to select an appropriate modulus degradation curve.

## 1.2 Thesis Objectives

The objective of this research has been to identify new ways to evaluate cohesionless soils, based on seismic techniques, such as the Seismic CPT. The research has focused on the identification of unusual sands, such as, highly compressible and/or cemented sands, and the quantification of their compressibility, stiffness, level of cementation, and in-situ stress and stress history. Based on this information the second objective has been to develop techniques to estimate the bearing capacity, and settlement of shallow footings on sand.

Settlement in sands is a function of sand mineralogy, level of cementation, stress history and degree of loading. A major component of the settlement of footings on compressible sands with high mica or carbonate contents can be volumetric deformation due to crushing of particles which is not incorporated in shear deformation based conventional elastic formula for settlement calculation. Also cemented sands generally have smaller deformation compared with uncemented sands. Hence, a prior knowledge of sand compressibility and cementation both qualitatively and quantitatively is of great importance. The objectives of Chapter 2, 3 and 4 will be to develop procedures to identify compressible

sands and cemented sands and to evaluate the level of cementation and modulus of volumetric deformation from in situ testing.

The stress history of the sand deposit is an important factor which controls the soil modulus, and hence, the deformation characteristics of the sand. Chapter 5 presents a method to evaluate in situ lateral stress and overconsolidation ratio from a combined measurement of cone penetration resistance and shear wave velocity in sands using the results from the seismic CPT.

In the design process of a footing, loading should be compared with the bearing capacity to evaluate the safety factor against failure. In addition, the soil modulus is a function of degree of loading, that is load to bearing capacity ratio. A larger ratio of degree of loading associates with a smaller soil modulus due to inherent nonlinearity of the stress strain relationship which results in larger settlement. In Chapter 6 a direct method is developed for predicting ultimate bearing capacity of footings in cohesionless soils using cone penetration resistance.

The objective of Chapter 7 will be to develop a method to evaluate settlement of footings on sand from a direct measurement of soil modulus using seismic methods.

### **1.3 Methodology**

The most rapidly developing site characterization techniques for geotechnical purposes involve direct push technology, i.e. penetration tests. The electric cone penetration test (CPT) has become increasingly more popular due to the continuous nature of the data, reliable and repeatable results and cost effectiveness. The cone has an apex angle of 60 degree and the base area is  $10 \text{ cm}^2$ . The friction sleeve is located immediately behind the cone and has an area of  $150 \text{ cm}^2$ . The penetration rate is  $2 \text{ cm/s}$ . Seismic tests are among the few in situ tests that produce little or no disturbance. Such techniques induce very small strain in the ground that preserve its natural feature. Seismic methods measure small strain response of a large volume of the ground, whereas the penetration of the cone measures large strain response of the ground since average stress levels around the cone approximately equals failure in the soil. The addition of a small velocity seismometer to the cone penetrometer provided additional measurement of shear wave velocity during cone penetration testing (Robertson et al., 1986). This test is called the seismic cone penetration

test (SCPT). During the SCPT, both cone penetration resistance and shear wave velocity are measured from the same sounding in the same soil. The small strain shear modulus can be determined from shear wave velocity based on elastic theory. Cone penetration resistance depends on the relative density, vertical and horizontal effective stress, compressibility, and structure of sand. On the other hand, small strain shear modulus is a function of relative density, vertical and horizontal effective stress, and structure of the soil. This suggests that various geotechnical properties can be determined by means of a proper correlation between cone penetration resistance and small strain shear modulus. In addition, the seismic CPT measures both small strain and large strain response of the ground. Therefore, the seismic CPT has the potential to provide a wide range of in situ geotechnical properties from a single sounding.

Many researchers have expressed sand compressibility in terms of confining pressure, relative density and stress history (e.g. Baldi et al., 1986). Cone penetration resistance and small strain shear modulus of sands are functions of the same variables. Therefore, a combined measurement of cone penetration resistance ( $q_c$ ) and small strain shear modulus ( $G_s$ ) can be used to identify compressible sands and to compare sands of various compressibility.

Preliminary studies on the possible effects of very weak cementation on cone penetration test (CPT) results indicate that low levels of cementation can have a substantial effect on penetration resistance at shallow depth. In addition, small strain stiffness of sand is also highly influenced by low levels of cementation. Hence, the potential exists to identify cemented sands and to quantify the level of cementation in cemented sands with a combined measurement of cone penetration resistance ( $q_c$ ) and small strain shear modulus ( $G_s$ ).

Many empirical correlations have been developed between cone penetration resistance and modulus in sands. Application of the available methods is limited to low to moderately compressible silica sands. Moreover, they often require a prior knowledge of relative density and stress history. In general, the cone penetration test can not be used to determine the preconsolidation pressure in prestressed sands. Since the estimated compressibility of sand is highly influenced by whether it is normally consolidated or overconsolidated, this can be a serious limitation if the stress history of the deposit is unknown. An assessment of calibration chamber test results can provide an empirical basis to relate tangent constrained modulus with cone penetration resistance and shear wave velocity in sands.

Experimental evidence indicates that the penetration of the cone destroys the effect of the previous stress and strain history of the sand (Baldi et al. 1986). Nevertheless, cone penetration resistance ( $q_c$ ) is strongly influenced by the current level of horizontal effective stress ( $\sigma'_{ho}$ ) (e.g. Baldi et al. 1986). Cone penetration resistance and small strain shear modulus in uncemented sands depend significantly on the in situ effective stress state. Hence, the potential exists to relate horizontal stress with cone resistance and small strain shear modulus.

For shallow foundations, the method by Meyerhof (1956) and recently the method by Tand and Funegard (1995) are distinguished since they predict the ultimate bearing capacity of footings directly from the CPT data and include the effect of embedment and footing size. As mentioned earlier, the penetration of the cone measures large strain response of the ground since average stress levels around the cone approximately equals failure in the soil. Hence, a correlation should exist between cone penetration resistance and ultimate bearing capacity of footing. However, the influence of size and shape of the footing in the relationship should be incorporated. Recently, the results of 9 load tests of full size shallow footings on sand have been reported in the literature. The footings were loaded to failure to measure bearing capacity and displacements (Briaud and Gibbens 1994, Tand et al. 1994). Based on these test results, the impact of shape, size and depth of the footing as well as sand density on the ultimate bearing can be evaluated.

Conventional elastic formula can be used for the evaluation of settlement of footings on sand. Modulus of sand can be determined directly from the measurement of shear wave velocity. However, sand modulus should be softened based on degree of loading, stress history and sand compressibility. Teachavorasinskun et al. (1991) reported the results of drained simple shear testing to evaluate the stiffness of low compressible Toyoura sand for strains from  $10^{-6}$  to those at peak strength. They obtained the relationship between the secant shear modulus and the corresponding shear stress for Toyoura sand with various relative density and stress history. These test results can be used to soften measured sand modulus.



## References

- Baldi G., Bellotti R., Ghionna N., Jamiolkowski M. and Pasqualini E. 1986. Interpretation of CPT's and CPTU's 2nd Part: Drained Penetration of Sands. Proceedings of Fourth International Geotechnical Seminar on Field Instrumentation and In situ Measurements, Singapore.
- Briaud, J. L., and Gibbens, R. M. 1994. Predicted and measured behavior of five spread footings on sand. ASCE geotechnical special publication No. 41.
- Meyerhof, G. G. 1956. Penetration tests and bearing capacity of cohesionless soils. Journal of Soil Mechanics and Foundations Division, ASCE, Vol. 82 No. SM 1, pp. 1-19.
- Mitchell, J. K., and Solymar, Z. V. 1984. Time dependent strength gain in freshly deposited or densified sands, Journal of Geotechnical Engineering, ASCE, Vol. 110, No. 11, pp. 1559-1576.
- Puppala, A. J., Acar, Y. B. and Tumay, M. T. 1995. Cone penetration in very weakly cemented sand, Journal of Geotechnical Engineering, Vol. 121, ASCE, pp. 589-601.
- Robertson P. K., Campanella R. G., Gillespie D., and Rice A. 1986. Seismic CPT to measure in situ shear wave velocity. Journal of Geotechnical Engineering Vol. 122, No. 8, ASCE, pp. 791-803.
- Seed H. B. 1969. Influence of local soil conditions on earthquake damage. Proc., 7th International Conference on Soil Mech. and Found. Eng., Mexico city .
- Swiger W. F. 1974. Evaluation of soil moduli. Proc., Conference on Analysis and Design in Geotech. Engrg., ASCE, Austin, Texas, Vol. 2.
- Tand K. E., Funegard E.G. and Warden P. E. 1994. Footing Load Test on Sand. Vertical and Horizontal Deformations of Foundations and Embankments, ASCE Geotechnical Special Publication No. 40, Vol. 1, pp. 164-178.
- Tand K. E., Funegard E.G. and Warden P. E. 1995. Predicted/ Measured Bearing Capacity of Shallow Footings on Sand. Proceeding of CPT'95, Volume 2, Sec. 3.33, pp. 589-594.
- Teachavorasinskun S., Shibuya S. and Tatsuoka F. 1991. Stiffness of sands in monotonic and cyclic simple shear. Proceeding of Geotechnical Engineering Congress, Boulder, Clorado, ASCE, pp. 863-878.

## CHAPTER 2

### A FRAMEWORK FOR IDENTIFICATION OF UNUSUAL SANDS USING SEISMIC CPT <sup>1</sup>

#### 2.1 Introduction

Most of the available research work on sand has been carried out largely on ideal uncemented, unaged, predominantly quartz sand. However, most natural sands rarely meet all these qualifiers. Hence, engineering design based on results from those studies may not always be valid for all sands.

Unusual sands can be defined as: a) sands in which the primary constituents are not quartz particles or b) sands which are cemented and/or aged.

Sands with a high mica content or carbonate and calcareous sands with a high carbonate content made up of shell fragments with low resistance to fracturing can be termed as unusual sands. The significant effect of grain mineralogy on compression behavior of sands has been broadly recognized. Compression in granular soils involves both rearrangement and crushing of particles. Mineralogy and confining pressure play a major role on the compression behavior of sands. Other influencing factors include initial relative density, stress history, cementation, particles size, angularity and gradation. At low confining pressures, the volume changes in sands occur primarily due to elastic compression of the soil skeleton and particle movements by sliding and rolling whereas, at high pressures there can be considerable volume change due to crushing of grains. Initial relative density, stress history and level of cementation of sands can affect the compression behavior of sands in the low stress regime. The threshold stress of particle crushing is basically a function of sand mineralogy. Nevertheless, the physical properties such as particle size, angularity and gradation can influence both the onset and development of particle crushing. In clean silica sands, in which the primary constituent is quartz with high

---

<sup>1</sup> A version of part of this chapter has been published. *Eslaamizaad, S. and Robertson P.K. 1996. A Framework for In-Situ Determination of Sand Compressibility, Proc. of the 49th Canadian Geotechnical Conference, St. John's, Newfoundland, 419-428.*

resistance to fracturing, the threshold stress of particle crushing can be as high as 1 MPa whereas, in sands with a high mica or carbonate content, the threshold stress can be lower than 100 kPa.

A significant variation in both stiffness and strength in natural sands can be caused by changes in soil structure by either cementation or aging, or a combined effect.

Cemented sands are found in many areas of the world and one of their distinguishing characteristics is their ability to stand in steep natural slopes. Slope failures in these areas are not uncommon. They occur rapidly under gravity and/or earthquake loading which can easily lead to loss of life and property. Cementation is a process which frequently exists in many natural deposits of granular soils. Recent data and evidence suggest that even the cleanest natural sand deposits may be very weakly cemented (Puppala et al. 1995). Even a small degree of cementation can have an important influence on soil stiffness, especially at small and intermediate strain levels. However, in general, inter-particle bonding is destroyed at large strains.

Aging influences the mechanical properties of granular soils. Recent Holocene deposits with ages ranging from 3000 to 15000 years are generally considered as unaged deposits. Many researchers have suggested that the small strain shear modulus increases with time due to secondary compression or aging effects (e.g. Mesri et al., 1990). However, the influence of aging on the penetration resistance is not well understood. Nevertheless, Mesri et al. (1990) concluded that aging influences to a similar extent the increase of cone penetration resistance  $q_c$ , and small strain shear modulus  $G_o$ .

Evaluation of compressibility and level of cementation in cohesionless soils based on laboratory tests can be difficult and unreliable due to the often unavoidable sample disturbance. In such circumstances in-situ tests are generally preferred. However, a comprehensive procedure to identify 'unusual' sands has not yet been established.

Based on the bearing capacity theory by Janbu and Senneset (1974), Puppala et al. (1993) proposed a chart, from which the cohesion intercept and relative density of cemented sands at shallow depths can be estimated from both cone resistance and sleeve friction in penetration testing. They assumed a linear variation of cone resistance with vertical effective stress. Puppala et al. mentioned that in granular soils, for all practical purposes, at shallow depths (vertical stress less than 200 kPa) and for relative densities less than

90%, normalizing  $q_c$  with  $\sigma'_v$  is appropriate and can eliminate the influence of vertical stress. However, it is widely known that cone resistance in granular soils increase approximately in proportion to the square root of the vertical effective stress. In addition, the sleeve friction is the least reliable and repeatable measured parameter in cone penetration testing. Figure 2.1 illustrates their proposed chart.

Robertson et al. (1995) proposed to estimate sand compressibility using a ratio of

$$[2.1] \quad Y = \frac{V_s}{\left[ q_c^{0.25} \left( \frac{\sigma'_{vo}}{P_a} \right)^{0.125} \right]}$$

in which,  $V_s$  is shear velocity in m/s,  $\sigma'_{vo}$  is vertical effective stress,  $P_a$  is atmospheric pressure (in same units as  $\sigma'_{vo}$ ) and  $q_c$  is cone penetration resistance in MPa. For more compressible sands the parameter  $Y$  seems to be higher than that of low compressible sands. According to Robertson and his coworkers, the parameter  $Y$  is controlled by grain characteristics, sand compressibility, age and level of cementation. Based on the seismic test results and laboratory testing from a number of sites Robertson et al. developed a preliminary correlation between the slope of the steady state line  $\lambda_{ss}$ , and the parameter  $Y$ , as shown in Fig. 2.2.

Many researchers have expressed sand compressibility in terms of confining pressure, relative density and stress history (e.g. Baldi et al., 1986). Cone penetration resistance and small strain shear modulus of sands are functions of the same variables. Therefore, a combined measurement of cone penetration resistance ( $q_c$ ) and small strain shear modulus ( $G_p$ ) can be used to identify compressible sands and to compare sands of various compressibility.

Preliminary studies on the possible effects of very weak cementation on cone penetration test (CPT) results indicate that low levels of cementation can have a substantial effect on penetration resistance at shallow depth. In addition, small strain stiffness of sand is also highly influenced by low levels of cementation. Hence, the potential exists to identify cemented sands with a combined measurement of cone penetration resistance ( $q_c$ ) and small strain shear modulus ( $G_p$ ).

The seismic CPT (SCPT) in which both cone resistance and small strain shear modulus are measured from a single sounding, can be used to identify 'unusual' sands. During the SCPT, the shear wave velocity ( $V_s$ ) can be measured. Based on elastic theory, the small strain shear modulus ( $G_o$ ) can be determined from the seismic shear wave velocity ( $V_s$ ) using:

$$[2.2] \quad G_o = \rho(V_s)^2$$

where,  $\rho$  is soil mass density.

The objective of this chapter is to present a method for the identification of unusual sands using the combined measurement of cone penetration resistance and small strain shear modulus. The method is based on published data from three different large CPT calibration chamber test programs and resonant column tests performed on sands with various history and compressibility. The proposed method can be used to compare qualitatively sands with different levels of compressibility and cementation.

## **2.2 The correlation between shear modulus and cone resistance.**

The penetration of the cone causes large strains to the surrounding sand in vicinity of cone and deletes to a large extent the effects of aging, and stress history of the deposit. A large number of available experimental data, including laboratory and calibration chamber studies, have shown that small strain shear modulus is mostly a function of density and stress level in much the same manner as penetration resistance, and it is influenced very little by the stress and strain history of the sand. Therefore, it appears that penetration resistance  $q_c$ , and stiffness  $G_o$ , are two different functions of the same variables and despite their incompatible strain levels a moderate association between  $G_o$  and  $q_c$  is possible (Baldi et al., 1986). However, it should be recognized that the compressibility of the sands can be expected to significantly affect any correlation between cone bearing and modulus. The correlation indicates a clear trend of decreasing  $G_o$  to  $q_c$  ratio with increasing normalized cone tip resistance (or relative density). This reflects the very different influence that changes in relative density ( $D_r$ ) have on  $G_o$  and  $q_c$ . These correlations have been established for recent Holocene deposits with ages ranging from 3000 to 15000 years.

Jamiolkowski et al. (1989) stated that their use in uncemented Pleistocene deposits having similar characteristics might lead to a tolerable underestimate of  $V_t$ . Rix and Stokoe (1991) noted that for an individual sand, the ratio of  $G_o$  to  $q_c$  as a function of the normalized cone tip resistance can be well defined, but the values of this ratio differ from sand to sand. They added that there may be factors such as fines content, particle angularity, and particle mineralogy that influence  $G_o$  and/or  $q_c$  that are not included in these correlations between  $G_o/q_c$  and normalized tip resistance. This speculation has not been supported by other researchers. Baldi et al. (1986) noted the relatively poor agreement between measured and predicted  $G_o/q_c$  ratios at shallow depths. They explained that this might be due to a limited number of calibration chamber and resonant column tests run at low initial mean effective stress (less than 100 kPa) and/or lack of reliability of the  $V_t$  measured at shallow depth.

Robertson and Campanella (1983) combined the relative density-cone resistance relationship developed by Baldi et al. (1981) with the relative density-small strain shear modulus relationship proposed by Seeds and Idriss (1970) and Hardin and Drnevich (1972) and developed a series of curves relating  $G_o$  to  $q_c$  for normally consolidated, uncemented quartz sands where  $G_o$  is a function of  $q_c$  and  $\sigma'_{vo}$ , as shown in Fig. 2.3.

Baldi et al. (1986) developed a correlation between  $G_o$  and  $q_c$  for NC and OC Ticino sand based on regression analyses of the results of calibration chamber tests and resonant column tests performed on both NC and OC specimens of Ticino sand, in the form of:

$$[2.3] \quad \frac{G_o}{q_c} = 44.4(\sigma'_m)^{-0.12} \exp(-1.92Dr)$$

in which  $\sigma'_m$  is initial mean effective stress.

Among the attempts to correlate  $q_c$  and  $G_o$  for uncemented, predominately silica sands, the correlation proposed by Jamiolkowski and Robertson (1988), as shown in Fig. 2.4, has been of practical interest. They plotted the correlation in a diagram of  $G_o/q_c$  versus  $q_c/\sqrt{\sigma'_{vo}}$  indicating a zone for unaged uncemented low compressible sands. It summarizes the results of laboratory tests performed on pluvially deposited Ticino sand with  $G_o$  determined from resonant column tests and  $q_c$  from CPT performed in a large calibration chamber. Also shown are the individual points corresponding to field data from

three different Holocene deposits in which  $q_c$  has been assessed from CPT and  $G_o$  has been calculated from  $V_s$  measured using seismic cone and/or crosshole tests. The difference between the continuous (OCR = 1) and dotted (OCR = 10) lines for laboratory tests is due to the variation of in-situ stress ( $K_o$ ) and, hence, the mean effective stress  $p'$ , caused by mechanical overconsolidation. This correlation provides an estimate of  $G_o$  from CPT but is limited to cohesionless Holocene deposits. Jamiolkowski and Robertson stated that with increasing age, fines content and gravel content the correlation underestimates the shear wave velocity. Baldi et al. (1989) noted that although the data were obtained on recently deposited unaged sand, the results in Fig. 2.4 displays good agreement with the data of natural cohesionless deposits having an age of 3000 to 20000 years at the maximum depth of 30 m. Jamiolkowski and Robertson (1988) mentioned that traditionally many natural sands are considered to be normally consolidated. However, considerable evidence exists to suggest that most natural sands with an age greater than about 3000 years behave as overconsolidated sands for most loading conditions. This is probably due to factors such as aging, cementation or stress or strain history. The same factors have been recognized for some time to produce similar apparent preconsolidation in clay soils.

For two natural sands in Italy, Lo Presti and Lai (1989) have performed a regression analysis using  $q_c$  and  $\sigma'_{vo}$  as independent variables and derived a relationship for Italian sands in the form of

$$[2.4] \quad V_s = 277(q_c)^{0.13}(\sigma'_{vo})^{0.27}$$

where  $V_s$  is in m/s, and  $q_c$  and  $\sigma'_{vo}$  are in MPa.

Based on the work by Jamiolkowski and Robertson (1988), Baldi et al. (1989) proposed a correlation between  $G_o$  and  $q_c$  for uncemented predominantly silica sands, as illustrated in Fig. 2.5. They noted that such a correlation is not influenced heavily by aging.

Rix and Stokoe (1991) examined the correlation suggested by Baldi et al. (1989) with additional data from a series of calibration chamber tests performed with washed mortar sand and in-situ seismic measurements and CPT in sands at the Heber Road site in the Imperial Valley of California. They suggested the following relationship for quartz sands:

$$[2.5] \quad G_o = 1634(q_c)^{0.25}(\sigma'_{vo})^{0.375}$$

where  $G_o$ ,  $q_c$ , and  $\sigma'_{vo}$  are in kPa.

Based on calibration chamber tests in Toyoura quartz sand, Fioravante et al. (1991) proposed the following correlations between  $q_c$  and  $G_o$  for different cone diameters:

$$[2.6] \quad G_o = 1.76q_c + 57.25 \quad \text{for } d_c = 20.0 \text{ mm}$$

$$[2.7] \quad G_o = 2.26q_c + 59.2 \quad \text{for } d_c = 35.7 \text{ mm}$$

where,  $d_c$  is the cone diameter,  $G_o$  and  $q_c$  are in MPa.

Hegazy and Mayne (1995) collected data from 24 sites worldwide and proposed a new correlation for  $V_s$ - $q_c$  based on regression analyses as:

$$[2.8] \quad V_s = 13.18(q_c)^{0.192}(\sigma'_{vo})^{0.179}$$

where  $V_s$  is in m/s, and  $q_c$  and  $\sigma'_{vo}$  are in kPa. They indicated that the predicted values of  $V_s$  compare well with the measured values except at shallow depths.

### 2.3 Proposed framework for identification of unusual sands

To develop a method for identification of unusual sands from a combined measurement of small strain shear modulus and cone penetration resistance, the existing correlations between  $G_o$  and  $q_c$  are examined with the results of calibration chamber tests and field experiments.

Gillespie (1988) suggested a chart to estimate soil behavior type based on CPT penetration resistance and the ratio of small strain shear modulus to cone penetration resistance,  $G_o/q_c$ . Gillespie (1988) found that the ratio  $G_o/q_c$  varies from about 4 to 20 in sands. Robertson et al. (1995) modified and updated the soil classification chart by Gillespie, as illustrated in Fig. 2.6, where cone penetration resistance is normalized in the form of  $(q_t - \sigma_v)/\sigma'_v$ . They



noted that since increasing sand compressibility will decrease the cone penetration resistance and increasing age and cementation will tend to increase the penetration resistance, the regions where aged, cemented and compressible sands should fall, can be distinguished. On this basis, they recommended to use the chart for identification of 'unusual' soils such as cemented or aged soils that fall outside the central region of the chart.

Schmertmann (1976) and Harman (1976) noted that relative density  $D_r$ , and effective stress  $\sigma'_v$ , are the most important variables affecting the cone penetration resistance and suggested the following empirical relationship for sands:

$$[2.9] \quad q_c = C_o \sigma'^{C_1} \text{Exp}(C_2 D_r)$$

in which,  $C_o$ ,  $C_1$  and  $C_2$  are experimental coefficients, and in the case of normally consolidated sands  $\sigma' = \sigma'_v$  and for overconsolidated sands  $\sigma' = \sigma'_m$  where  $\sigma'_m$  is mean effective stress. Baldi et al. (1986) back-calculated  $C_1$  for low compressible Ticino and Hokksund sands as 0.55. This indicates that a linear normalization of cone penetration resistance with vertical stress is not entirely correct for sands of constant  $D_r$ . It should be noted that  $\sigma'_m$  can be substituted with  $\sigma'_v$  and overconsolidation ratio OCR to include the influence of stress history or coefficient of earth pressure at rest  $K_o$ .

Olson and Malone (1988) discussed that cone penetration resistance should be normalized with vertical effective stress in a form of power function rather than a linear form and proposed following relationship:

$$[2.10] \quad q'_{c1} = \frac{q_c}{(\sigma'_v)^n}$$

in which  $n$  is the appropriate exponent from approximately 0.60 for coarse sands to slightly under unity for clays,  $\sigma'_v$  is vertical effective stress and  $q'_{c1}$  is the normalized cone resistance.

As mentioned earlier, in an attempt to estimate small strain shear modulus from cone resistance in sands, Jamiolkowski and Robertson (1988) plotted the correlation between  $G_o$

and  $q_c$  in a diagram of  $G_s/q_c$  versus  $q_c/\sqrt{\sigma'_{vo}}$  indicating that the cone penetration resistance in sands should be normalized with square root of effective stress. This is in good agreement with the findings of Baldi et al. and Olson and Malone where they suggested an exponent of 0.55 and 0.60 respectively.

As a result of the above discussion, an exponent of 0.5 is taken for normalization of penetration resistance with vertical effective stress in sands for this study.

To investigate the influence of cementation and soil compressibility in its broadest sense, including grain crushability, on the correlation between  $G_s$  and  $q_c$ , different sets of data with various degrees of compressibility and cementation, as illustrated in Fig. 2.7, are plotted in a diagram of  $G_s/q_c$  versus normalized cone penetration  $q_{c1}$  in log-log scale where normalized cone penetration resistance is defined as:

$$[2.11] \quad q_{c1} = \left( \frac{q_c}{p_a} \right) \left( \frac{p_a}{\sigma'_{vo}} \right)^{0.5}$$

in which  $p_a$  is atmospheric pressure in the same units as  $q_c$  and  $\sigma'_{vo}$ .

The relationship by Baldi et al. (1989), agrees very well with the bounded zone in Fig. 2.7.

A total of 8 soils have been evaluated using available SCPT data. Three (3) of the soils (Ticino, Toyoura, Quiou) have data available from calibration chamber studies (Baldi et al. 1986, Fioravante et al. 1991 and Almeida et al. 1991). The data have been corrected for calibration chamber size and boundary effects. A summary of their index properties are given in Table 2.1. Extensive calibration studies have been carried out on Ticino sand, which is a clean, uniform quartz sand of moderate compressibility. Limited calibration chamber results are available on Quiou sand, which is a highly compressible carbonate sand (Almeida et al. 1991). The remaining five (5) soils (Kidd, Massey, Alaska, Alabama residual soil, Utah tailing) have data available from SCPT profiles carried out in-situ. Typical SCPT profiles for these sites are given in Appendix A.

The Kidd and Massey sites are located near Vancouver, B.C. Both sites contain natural alluvial sediments as part of the Fraser River delta. At both sites, SCPT data are within a 20 to 30 m thick complex of distributary channel sands that underlies most of the delta plain (Monahan et al., 1995). Fraser River sand is a young, uncemented predominantly quartz

sand with some mica and feldspar, has a  $D_{50} = 0.30$  mm and contains on average about 5% fines. Measured in-situ void ratio has been reported as 0.85 to 0.95 at Kidd site, and 0.9 to 1.0 at Massey site. Seismic CPT's have been performed at various depths and locations at these sites. Both sites have been identified as normally consolidated sands having a coefficient of earth pressure of about  $K_o = 0.4$  based on self boring pressuremeter test results. Both sites were part of the CANLEX project (Robertson et al., 1995).

Alaska sand is a tailings deposit which has been deposited into the sea and has a 30% fines content. The fines have a high crushed shell content and, hence, Alaska sand has high compressibility.

Table 2.1 summarizes the index properties of sands (Ticino, Toyoura, Quiou) tested in calibration chamber. Similarly, Table 2.2 presents the index properties of the sands (Massey, Kidd, Alaska) tested in-situ.

Utah tailings sand is a tailings from a mine in Utah and recognized to be a lightly cemented sand while Kidd, Massey and Alaska sands are uncemented sands.

The residual soil from Alabama has variable cementation due to the variation in weathering profile (Mayne, 1996). This soil belongs to a group of residual silty and sandy soils known as the Piedmont (means foot-of-the mountains) Formation. The Piedmont have been eroded away since Paleozoic times. The remaining overburden consists of residual soil that was derived from the in-place decomposition of the underlying metamorphic and igneous rocks. These primarily include schist, gneiss, and granite. The SCPT was performed at Auburn University Test Site in Opelika. The Opelika site is located near the southern tip of the Piedmont Province in Alabama. Weathering has resulted in residuum composed of approximately 50 percent silt and 50 percent fine sand. Figure A.9, Fig. A.10, and Fig. A.11 in Appendix A, illustrate results of the seismic piezocone penetration tests in Alabama residual soil (Mayne, 1997).

Figure 2.7 shows that sands with different compressibility plot essentially within the same band. This indicates that the correlation between  $G_o$  and  $q_c$  is not highly influenced by soil compressibility. However, more compressible sands have low values of normalized cone resistance  $q_{c1}$  and high ratios of  $G_o/q_c$ . Compressible sands with high  $G_o/q_c$  (often greater than 10) and low  $q_{c1}$  (less than 50) can be distinguished as they plot in the lower half of the bounded zone. Also shown in Fig. 2.7 are data from artificially cemented Monterey sand

with 0%, 1% and 2% cement content (Puppala et al., 1995). Cemented sands, however, fall outside the bounded zone. Hence, the chart shown in Fig. 2.7 can be used to identify potentially cemented sands and to compare sands of different compressibility. Seismic CPT testing can be performed to obtain both the cone resistance and small strain shear modulus during the same sounding in the same soil. These data should then be plotted in the proposed chart to identify compressible and/or cemented sands.

## 2.4 Summary and conclusions

Much of the existing research work on sand is based on ideal uncemented low to medium compressible sand. Therefore, engineering design based on results from these studies may not always be valid for all sands.

Evaluation of compressibility and level of cementation in cohesionless soils based on laboratory tests can be difficult and sometimes unreliable due to the often unavoidable sample disturbance. In such circumstances in-situ tests are generally preferred. However, a comprehensive procedure to identify 'unusual' sands has not yet been established.

Puppala et al. (1993) proposed a chart, from which the cohesion intercept and relative density of cemented sands at shallow depths can be estimated from both cone resistance and sleeve friction in penetration testing. However, the application of this chart for natural cemented and uncemented soils has been poor.

Robertson et al. (1995) modified and updated the soil classification chart by Gillespie (1988). They noted that since increasing sand compressibility will decrease the cone penetration resistance and increasing age and cementation will tend to increase the penetration resistance, the regions where aged, cemented and compressible sands should fall can be distinguished. On this basis, they recommended to use the chart for identification of 'unusual' soils such as cemented or aged soils that fall outside the central region of the chart. In the same work, Robertson et al. (1995) proposed to compare sand compressibility using a parameter,  $Y$ , based on a combined measurement of shear wave velocity and cone penetration resistance. Robertson and his co-workers developed a preliminary correlation between the slope of steady state line  $\lambda_{ss}$ , and the parameter  $Y$ .

In this chapter, a procedure has been presented to identify 'unusual' sands using in-situ seismic CPT results. The method is based on the correlation between small strain shear

modulus and cone penetration resistance. Based on a review of the work by Baldi et al. (1986), Olson and Malone (1988), Jamiolkowski and Robertson (1988), it has been suggested to normalize cone penetration resistance with square root of effective stress. Figure 2.7 shows that uncemented and unaged sands with different compressibility plot within same band. This indicates that the correlation between  $G_s$  and  $q_c$  is not highly influenced by sand mineralogy. However, more compressible sands have low values of normalized cone resistance  $q_{c1}$  and high ratios of  $G_s/q_c$ . Compressible sands with high  $G_s/q_c$  (often greater than 10) and low  $q_{c1}$  (less than 50) can be distinguished as they plot in the lower half of the bounded zone. Cemented and aged sands, however, appear to fall outside the bounded zone. Hence, the chart shown in Fig. 2.7 can be used to identify potentially cemented sands and to compare sands of different compressibility. For a given sand, the compressibility varies with density (this is expressed by the variation of  $q_{c1}$ ). Hence, loose sand appears to be more compressible than dense sand of the same mineralogy. Seismic CPT testing can be performed to obtain both the cone resistance and small strain shear modulus during the same sounding in the same soil. These data should then be plotted in the proposed chart to identify compressible and/or cemented sands.

Reliable field data for cemented and/or aged sands is rare. Hence, there is limited data to evaluate the proposed chart in Fig. 2.7. Published results from a cemented sand will be presented in Chapter 3.

	<i>Toyoura</i>	<i>Ticino</i>	<i>Quiou</i>
<b>Mineralogy</b>	90% Quartz 3% Chert	95% Quartz 5% Feldspar	12% Quartz 74% Shell fragments 14% Cal. carbonate aggregates
<b><math>D_{50}</math> (mm)</b>	0.16	0.54	1.04
<b>Coefficient of uniformity <math>U=D_{60}/D_{10}</math></b>	1.50	1.13	2.9
<b><math>G_s</math></b>	2.65	2.67	2.66
<b><math>e_{min}</math></b>	0.605	0.52	0.831
<b><math>e_{max}</math></b>	0.977	0.89	1.281
<b>Grain shape</b>	subangular	subrounded	subangular to subrounded
<b>Fine content %</b>	< 5	< 5	3 - 4

Table 2.1 Index properties of sands tested at calibration chamber

	<i>Kidd</i>	<i>Massey</i>	<i>Alaska</i>
<b>Mineralogy</b>	70% quartz 15% feldspar 5% mica 5% Kaolinite 5% chlorite & smectie	70% quartz 15% feldspar 5% mica 5% Kaolinite 5% chlorite & smectie	70% quartz 30% calcium carbonate aggregate
<b><math>D_{50}</math> (mm)</b>	0.30	0.30	0.12
<b>Coefficient of uniformity <math>U=D_{60}/D_{10}</math></b>	2.50	2.14	
<b><math>G_s</math></b>	2.72	2.68	2.90
<b><math>e_{min}</math></b>	0.703	0.677	0.70
<b><math>e_{max}</math></b>	1.061	1.056	1.78
<b>Grain shape</b>	subrounded	subrounded	Angular
<b>Fine content %</b>	5	5	30

Table 2.2 Index properties of sands tested at field

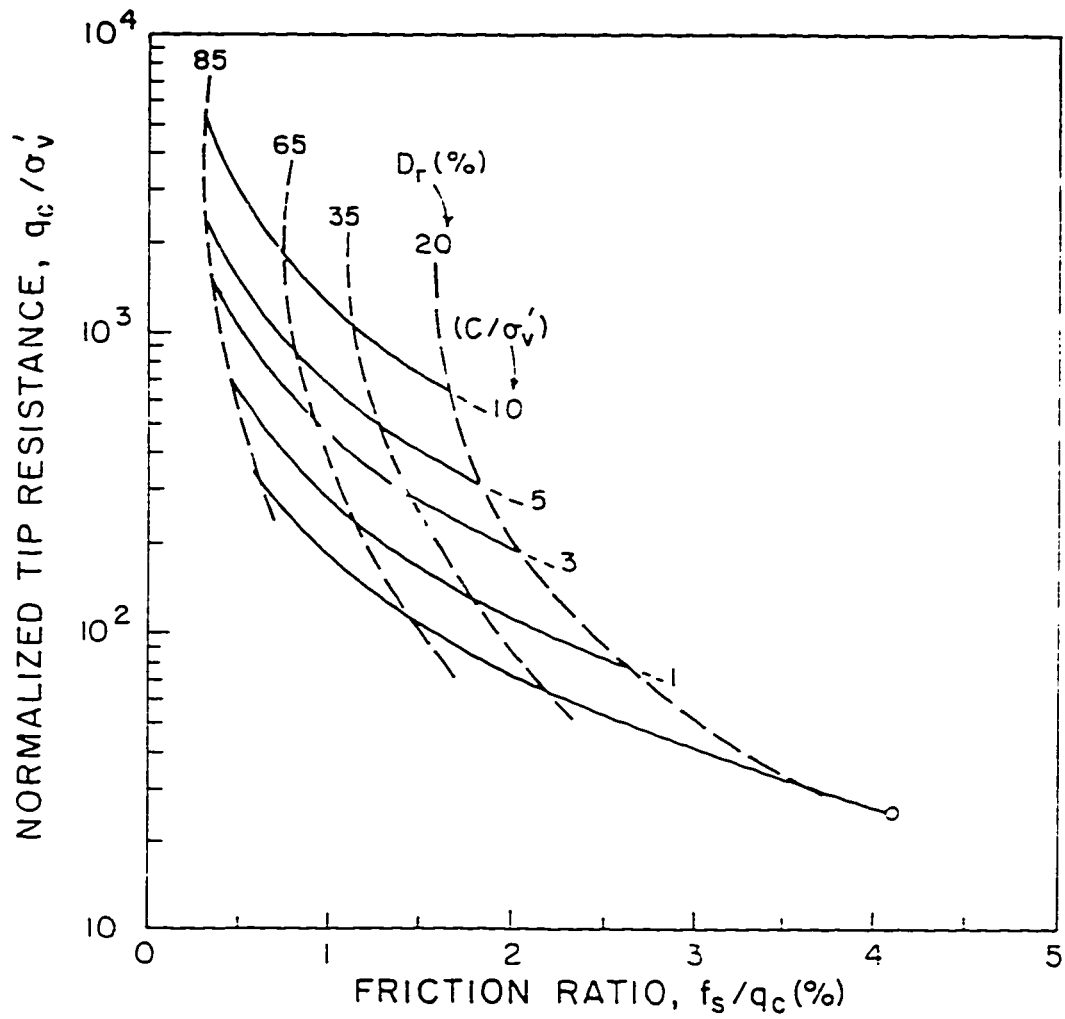


Fig. 2.1 Chart that estimates cohesion intercept ( $c$ ) and relative density ( $D_r$ ) from cone penetration resistance ( $q_c$ ) and sleeve friction in Cone Penetration Testing of cemented sands (after Puppala et al., 1993)



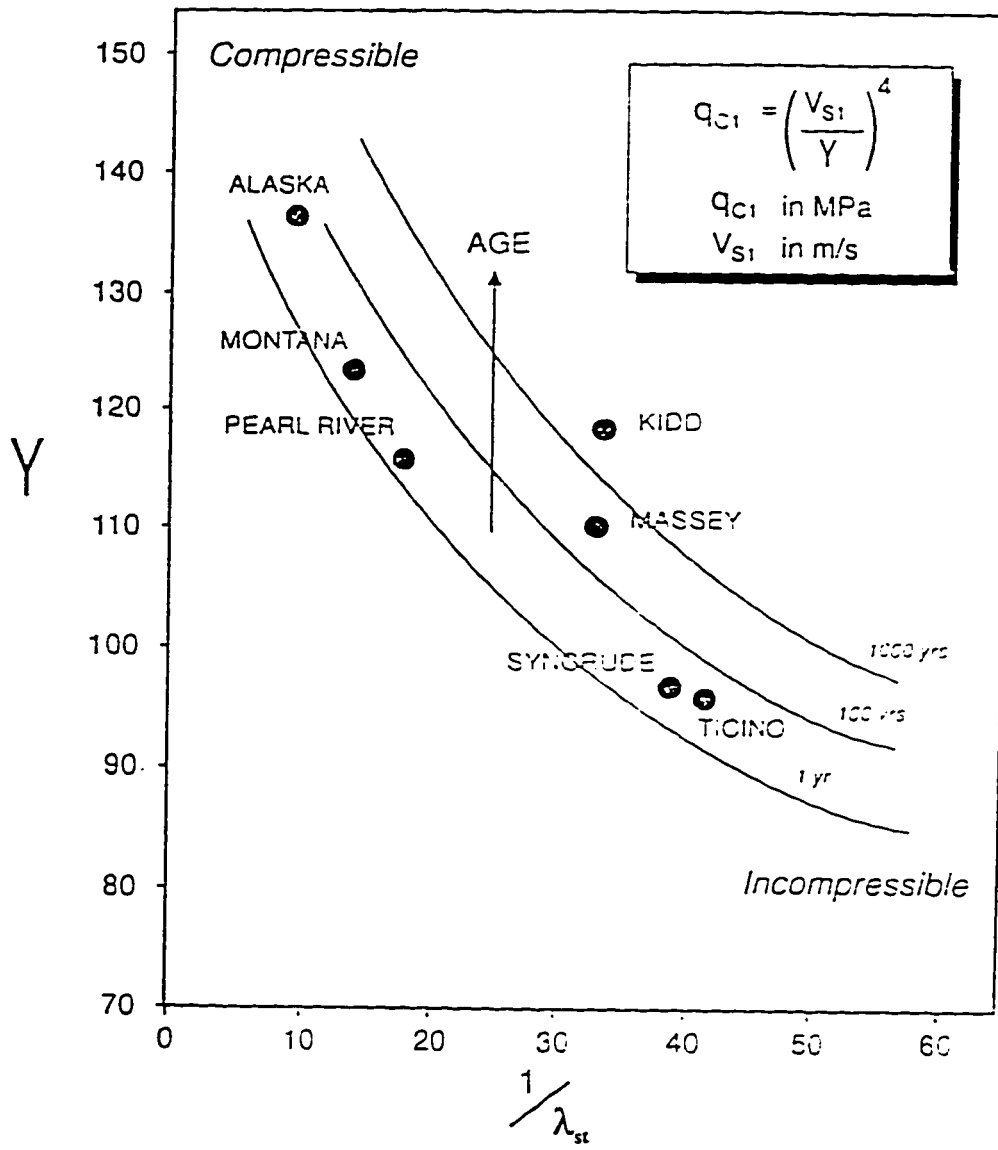


Fig. 2.2 Correlation for estimating slope of the steady state line ( $\lambda$ ) for uncemented sand from seismic CPT results (after Robertson et al., 1995)

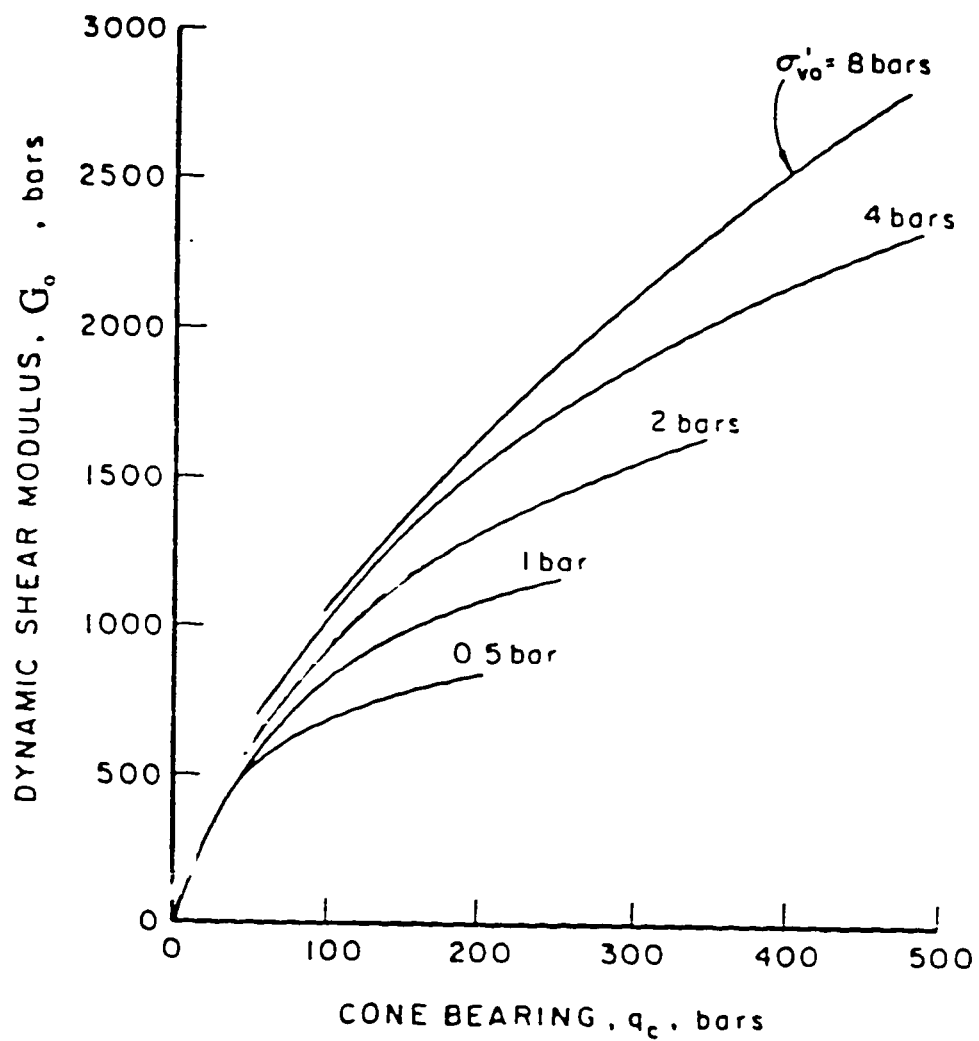


Fig. 2.3 Relationship between cone bearing and dynamic shear modulus for normally consolidated, uncemented, quartz sands (after Robertson and Campanella, 1983)

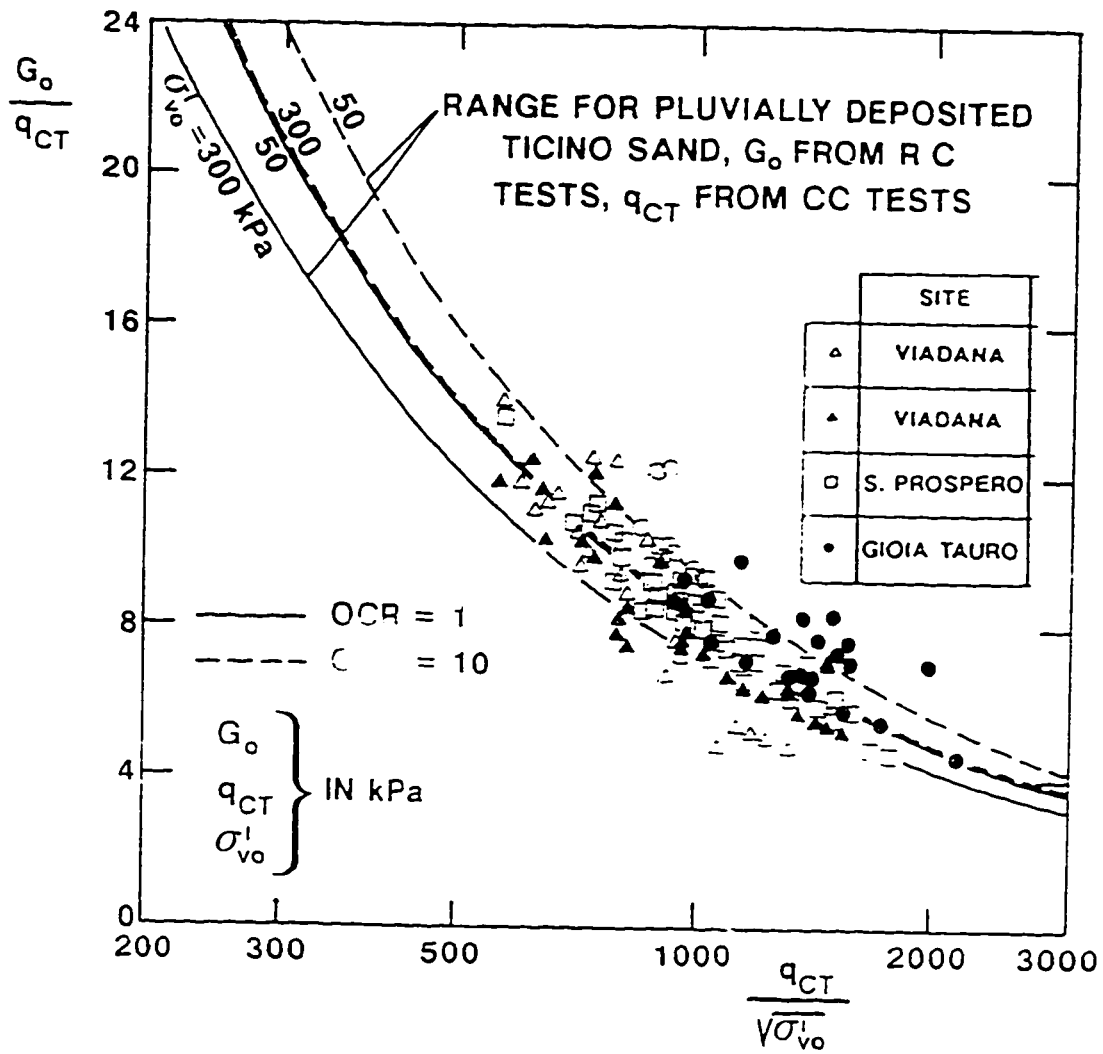


Fig. 2.4  $q_{ct}$  versus  $G_o$  correlation for uncemented, predominantly quartz sands (after Jamiolkowski and Robertson, 1988)

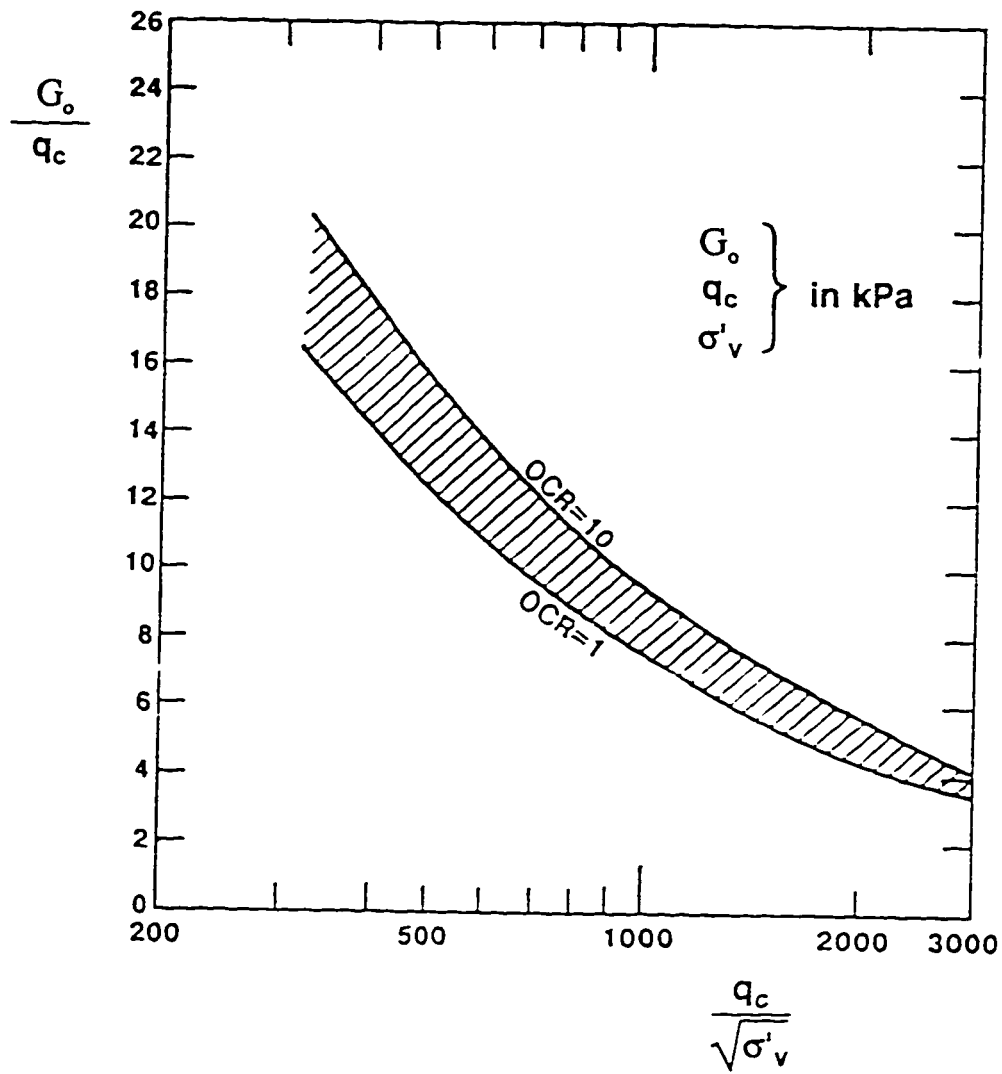


Fig. 2.5 Correlation between  $q_c$  and  $G_0$  (after Baldi et al., 1989)

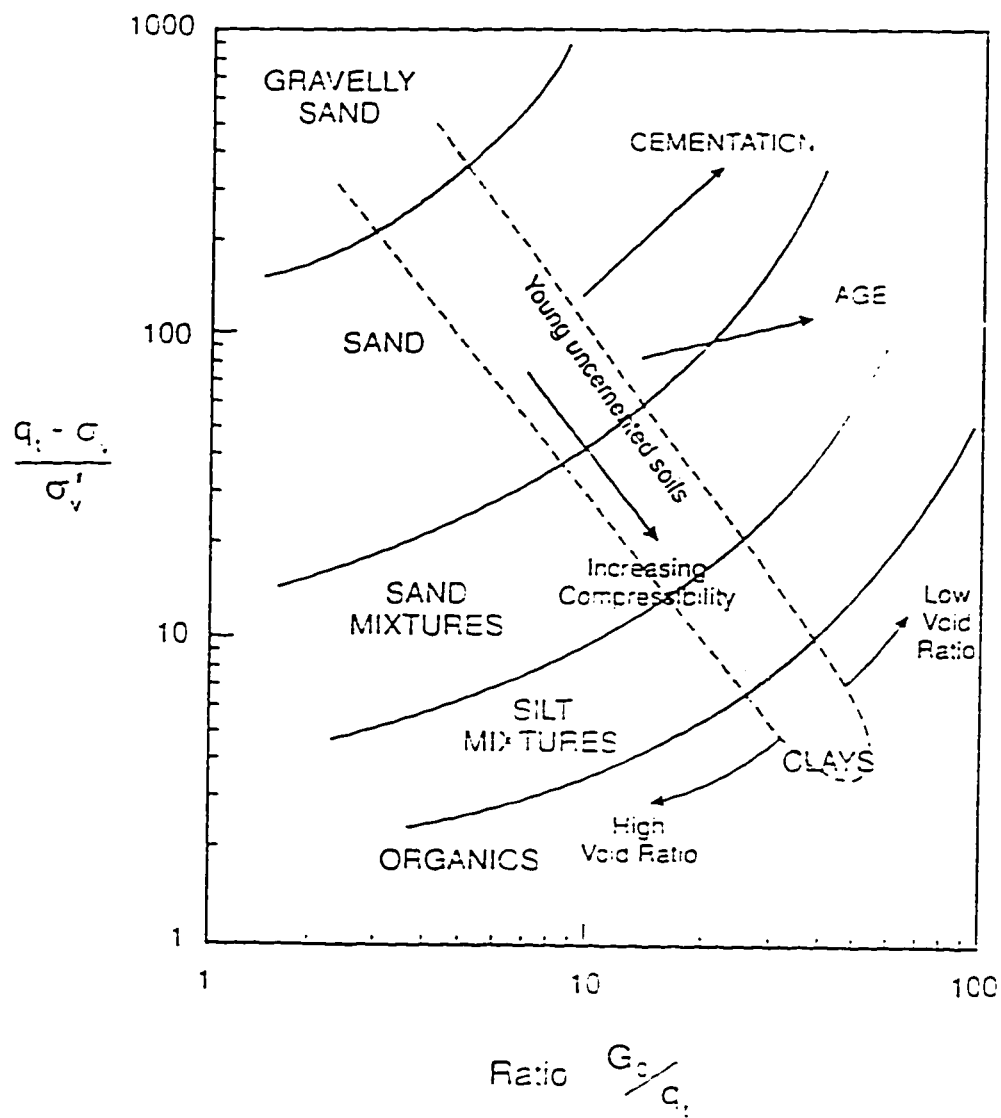


Fig. 2.6 Soil behavior type chart based on normalized CPT penetration resistance and the ratio of small strain shear modulus with penetration resistance (after Robertson et al., 1995)

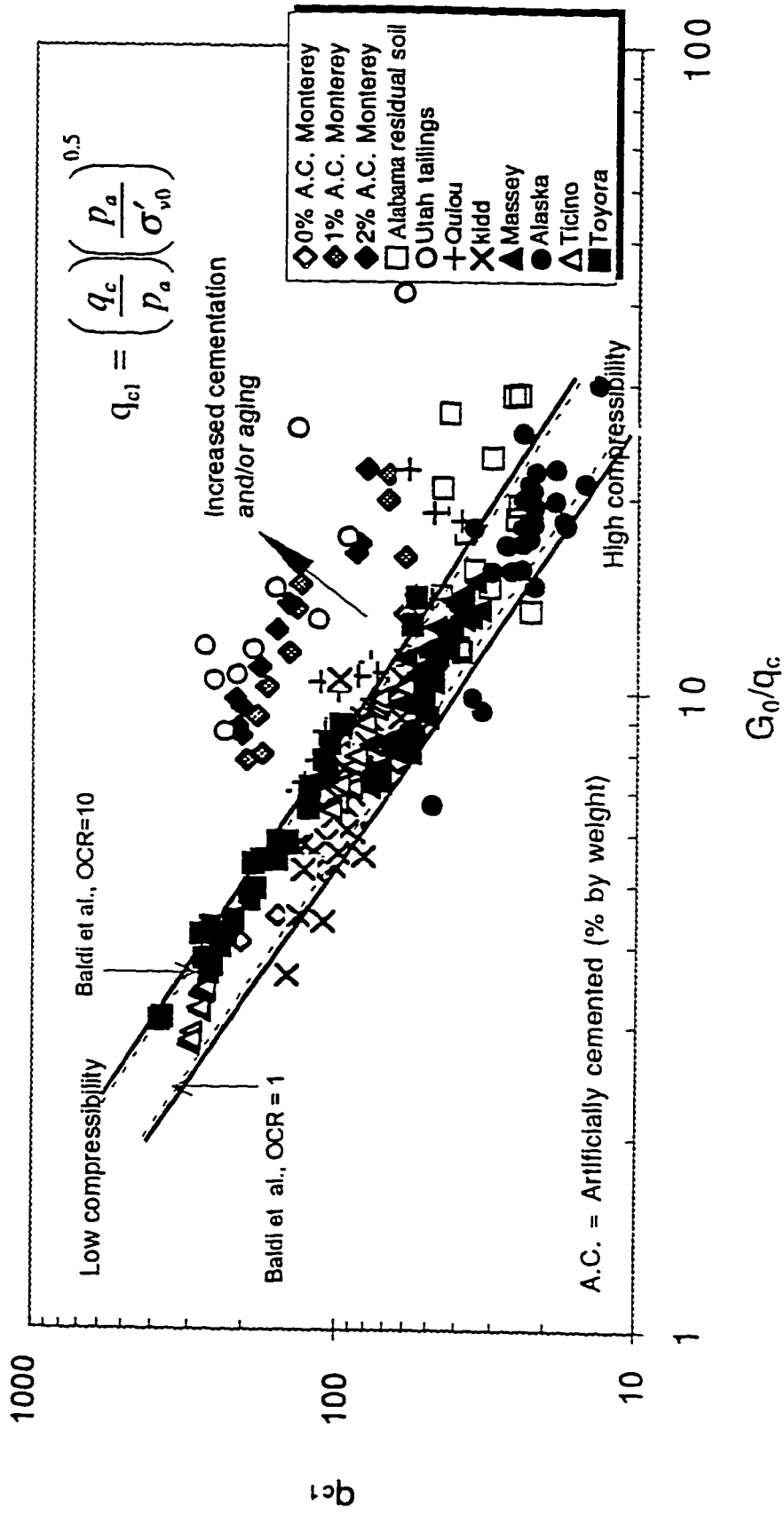


Fig. 2.7 Proposed chart for identification of unusual sands

## References

- Almeida M.S., Jamiolkowski M., and Peterson R.W. 1991. Preliminary results of CPT in tests in calcareous Quiou sand, Proceedings of the First International Symposium on Calibration Chamber Testing ISOCCT1, Potsdam, New York, Edited by An-Bin Huang, pp. 41-53.
- Baldi, G., Bellotti, R., Ghionna, V., Jamiolkowski, M. and Pasqualini, E. 1981. Cone resistance of a dry medium sand, Proceedings of 10th International Conference on Soil Mechanics and Foundation Engineering, Stockholm, Vol. 2, pp. 425-438.
- Baldi, G., Bellotti, R., Ghionna, V., Jamiolkowski, M. and Pasqualini, E. 1986. Interpretation of CPT's and CPTU's, 2nd part: Drained penetration of sands, 4th Int. Geotechnical Seminar, Nanyang Technological Institute, Singapore, Field Inst. & In-situ measurements, pp. 143-162.
- Baldi, G., Bellotti, R., Ghionna, V., Jamiolkowski M. and Lo Presti D.C.F. 1989. Modulus of sands from CPT's and DMT's. Proceedings, XII International Conference of Soil Mechanics and Foundation Engineering, Vol. 1, pp. 165-170., Rio De Janeiro.
- Gillespie 1988 Ph.D. Thesis, University of British Columbia, Vancouver, British Columbia.
- Harman, D. E. 1976. A statistical study of static cone bearing capacity, vertical effective stress, and relative density of dry and saturated fine sands in a large triaxial test chamber. Master's Thesis. University of Florida.
- Hardin, B.O., and Drnevich, V.P. 1972. Shear modulus and damping in soils: design equations and curves, ASCE Journal of the Soil Mechanics and Foundation Division, 98(SM7), pp. 667-692.
- Hegazy, Y.A., and Mayne P.W. 1995. Statistical correlations between Vs and cone penetration data for different soil types, Proceedings of CPT'95, pp. 173-178.
- Fioravante V., Jamiolkowski M., Tanizawa F., and Tatsuoka F. 1991. Results of CPT's in Toyoura quartz sand., Proceedings of the First International Symposium on Calibration Chamber Testing ISOCCT1, Potsdam, New York, Edited by An-Bin Haung, pp. 135-146.
- Jamiolkowski, M., and Robertson, P.K. 1988. Future trends for penetration testing., Proceedings of conference, Penetration testing in the U.K., Birmingham, pp. 21-42.

- Jamiolkowski, M., Lo Presti, D., Manfredini, C. and Rix C.J. 1989. Italian experience in assessing shear wave velocity from CPT and SPT. Proceedings of XII ICSMFE, Rio.
- Janbu, N., and Senneset, K. 1974. Effective stress interpretation of in-situ static penetration tests. Proc. European Symp. on Penetration Testing, ESOPT I, A.A. Balkema, Rotterdam, The Netherlands, Vol. 1.2., pp. 479-488.
- Lo Presti, D. 1987. Behavior of Ticino sand during resonant column test, Ph.D. Thesis, Technological University of Turin.
- Lo Presti, D., and Lai C. 1989. Shear wave velocity from penetration tests. *Arti del Dipartimento di Ingegneria Strutturale, Politecnico di Torino, Torino.*
- Mayne, P.W. 1996. Personal communications with P.K. Robertson.
- Mayne, P.W. 1997. Characterization of Piedmont residual Silts, Proceedings of 14th ICSMFE, Hamburg.
- Mesri, G. Feng, T.W., and Benak J.M. 1990. Postdensification resistance of clean sands. *Journal of Geotechnical Engineering, Vol. 116, No. 7, ASCE, pp. 1095-1115.*
- Monahan, P. A., Luternauer, J. L., and Barrie, J. V. 1995. The geology of the CANLEX Phase II sites in Delta and Richmond, British Columbia. Proceedings of the 48th Canadian Geotechnical Conference, Vancouver, B.C., pp. 59-68.
- Olson, R. S., and Malone P. G. 1988. Soil classification and site characterization using the cone penetrometer test. Proceedings of the first international symposium on penetration testing/ISOPT-1, Orlando, pp. 887-893.
- Puppala, A. J., Acar, Y. B. and Senneset K. 1993. Cone penetration in cemented sand: Bearing capacity interpretation. *Journal of Geotechnical Engineering, Vol. 119, ASCE, pp. 1990-2001.*
- Puppala, A. J., Acar, Y. B. and Tummy, M. T. 1995. Cone penetration in very weakly cemented sand, *Journal of Geotechnical Engineering, Vol. 121, ASCE, pp. 589-601.*
- Rix G.J. and Stokoe K.H. II. 1991, Correlation of Initial tangent Modulus and Cone Penetration Resistance. Proceedings of the First International Symposium on Calibration Chamber Testing/ISOCCT1, Potsdam, New York, Edited by An-Bin Huang, pp. 351-362.
- Robertson, P. K. and Campanella, R. G. 1983, Interpretation of cone penetration tests. Part I: sand., *Canadian Geotechnical Journal* 20, pp. 718-733.
- Robertson, P.K., Fear C.E., Woeller D.J. and Weemee I. 1995. Estimation of sand compressibility from Seismic CPT, Proceeding of 48th Canadian Geotechnical Conference, Vancouver.



- Robertson, P.K., List B.R. and Hofmann B.A. 1995. CANLEX (Canadian Liquefaction Experiment): A One Year Update, Proceeding of Third International Conference on Recent Advances in Geotechnical Earthquake Engineering and Soil Dynamics.
- Schmertmann, J.H. 1976. An updated correlation between relative density,  $D_r$ , and Fugro-Type electric cone bearing,  $q_c$ . Unpublished report to WES, Vicksburg, Miss.
- Seed, H. B., and Idriss, I. B. 1970. Soil moduli and damping factors for dynamics response analysis, Report No. EERC 70-10, University of California, Berkeley.

## CHAPTER 3

### ESTIMATION OF LEVEL OF CEMENTATION IN CEMENTED SANDS BASED ON SEISMIC CPT RESULTS<sup>1</sup>

#### 3.1 Introduction

Most natural soils have components of stiffness and strength which can not easily be accounted for by classical soil mechanics. These components are generally due to the presence of structure in soils (inter-particle bonding and fabric). Soil structure can be considered to be all the physical features which are present in intact samples but can be difficult to duplicate in reconstituted samples. The principal components of soil structure are fabric and bonding or cementing. Fabric includes inhomogenities, layering, particle orientation and fissuring. In general, the term structure can be used to account for differences between the properties of a soil in its natural state and of the same soil at the same void ratio but thoroughly remolded, or between the soil in its natural state and after remolding and the re-application of the original stress state. Usually, structured soils are destructured by straining. Hence, the thoroughly remolded and reworked soil is said to be destructured (Mitchell, 1993).

It is noted that a significant variation in both stiffness and strength in natural sands can be caused by changes in soil structure (fabric and bonding). Natural sands often exhibit an enhanced structure which can distinctly yield at a pressure greater than the past maximum vertical pressure. Hence, the effect of soil structure on the mechanical behavior of soils can be qualitatively similar to stress history; both can increase soil stiffness, strength and brittleness, and can enlarge the stress domain in which soil exhibits a stiff (elastic) behavior. Some differences between structural and stress history effects are worth noting. Yielding in structured natural soils can be rather distinct and abrupt. This behavior, which is typical for highly consolidated soils, occurs at relatively low values of OCR for structured soils. Hence, it appears that structure-induced overconsolidation has a much

---

<sup>1</sup> A version of part of this chapter has been published. *Eslaamizaad, S. and Robertson P.K. 1996. Seismic Cone Penetration Test To Identify Cemented Sands, Proc. of the 49th Canadian Geotechnical Conference, St. John's, Newfoundland, 849-858.*

stronger influence on deformability characteristics than mechanical stress-induced overconsolidation (Burghignoli et al., 1991).

Cemented sands are found in many areas of the world and one of their distinguishing characteristics is their ability to stand in steep natural slopes. However, slope failures in these areas are not uncommon. They can occur rapidly under gravity and/or earthquake loading which can easily lead to loss of life and property.

Cementation is a process which frequently exists in many natural deposits of granular soils. The cementation agents are often carbonates, silica, hydrous silicates, and hydrous iron oxides deposited at the point of contact between sand particles (Clough et al., 1981). In some cases, the cementation is due to welding at the contact points (Lee, 1975). This type of cementation generally results in low to moderate degrees of cementation.

Recent data and evidence suggest that even the cleanest natural sand deposits may be very weakly cemented (Puppala et al. 1995). Hence, engineering judgment made based on test results from uncemented specimens reconstituted in the laboratory may not be valid (Mitchell and Solymar, 1984). Light cementation can seldom be detected by conventional site investigation techniques. The influence of light cementation on the stress-strain and strength behavior of granular soils has been extensively investigated through testing reconstituted artificially cemented sands in the laboratory (e.g. Dupas and Pecker 1979, Clough et al. 1981, Acar and El-Tahir 1986, Saxena et al. 1987 and Puppala et al. 1995). Based on these studies cementation can be considered to provide some value of cohesion intercept  $c'$  for sand, with an almost negligible influence on the peak angle of shearing resistance  $\phi'_p$ . For lightly cemented sands the magnitude of  $c'$  does not exceed 20 to 40 kPa. In general, large strain characteristics of cemented sands are similar to those of uncemented sands. In contrast, even a small degree of cementation can have an important influence on soil stiffness, especially at small and intermediate strain levels. Hence, adding a cohesion intercept and a tensile strength to the sand increases its stiffness but does not change its friction angle significantly. However, inter-particle bonding is often destroyed at large strains.

The effect of cementation on the strength-deformation behavior of sands is often ignored since cementation often improves the strength. However, neglecting cementation can result

in an overly conservative design of shallow and deep foundations as well as slopes and retaining walls.

Most of the available research work on sand has been largely on ideal uncemented, unaged, predominantly quartz sand. However, natural sand deposits hardly ever meet all these qualifiers and in many areas of the world natural sands are found to be cemented. Application of the results from ideal sands to cemented sands can be misleading and sometimes unsafe. Undisturbed sampling in cemented sands can be difficult, time consuming and costly. Hence, there is a need to have the ability to identify cemented sands and to quantify the level of cementation through simple in-situ testings.

A comprehensive procedure to identify cemented sands in-situ has not yet been established. Based on the bearing capacity theory by Janbu and Senneset (1974), Puppala et al. (1993) proposed a chart, from which the cohesion intercept and relative density of cemented sands at shallow depths can be estimated from both cone resistance and sleeve friction in penetration testing. This chart has been previously illustrated in Fig. 2.1. Limitations to the method has been discussed in Chapter 2, Section 2.1.

Preliminary studies on the possible effects of very weak cementation on cone penetration test (CPT) results indicate that low levels of cementation can have a substantial effect on penetration resistance at shallow depth. In addition, as described earlier, small strain stiffness of sand is also highly influenced by low levels of cementation. Hence, the potential exists to identify cemented sands with a combined measurement of cone penetration resistance ( $q_c$ ) and small strain shear modulus ( $G_o$ ). This can be accomplished by using the seismic CPT (SCPT) in which both cone resistance and small strain shear modulus are measured from a single sounding. During the SCPT, the shear wave velocity ( $V_s$ ) can be measured. Based on elastic theory, the small strain shear modulus ( $G_o$ ) can be determined from the seismic shear wave velocity ( $V_s$ ) using:

$$[3.1] \quad G_o = \rho(V_s)^2$$

where,  $\rho$  is soil mass density.

In this chapter, the available literature on the influence of cementation on both cone penetration resistance and small strain shear modulus is reviewed, then the potential of

using SCPT to quantify level of cementation in sands is studied in which new methods are developed to quantify level of cementation and to estimate relative density in cemented sands.

### **3.2 Influence of cementation on cone penetration resistance in sands**

The cone penetrometer is one of the most widely used in-situ testing equipments. The ease of testing, reliability, and repeatability of the results, as well as its cost effectiveness have resulted in ever increasing use of the cone penetrometer in geotechnical investigation of different subsurface soil conditions. As mentioned earlier, the effect of cementation on the strength and deformation characteristics of soils has also gained increasing attention during last two decades. However, little information is currently available on the effect of cementation on the penetration resistance of soils. Limited studies, mainly on artificially cemented sands, have been conducted by Rad and Tumay (1986), Akili and Al-Joulani (1988), Puppala et al. (1993), and Puppala et al. (1995).

Rad and Tumay (1986) conducted a laboratory study to investigate the effect of cementation on the cone penetration resistance of sand. Artificially cemented specimens of Monterey sand No. 0, with 1 to 2% cement content and relative densities ranging from 18 to 80% were tested. Portland cement was used as cementing agent. Rad and Tumay noted that the effect of cementation on the cone penetration resistance is similar to that of relative density. Hence, using available correlations for uncemented sands to estimate the relative density or internal friction angle of naturally deposited, and possible cemented sands, can be misleading. Generally, existing correlations may predict values of relative density and internal friction angle higher than those actually available for the cemented sands. Rad and Tumay concluded that cementation has a pronounced effect on the cone penetration resistance of sand. Increasing the cement content increases the cone penetration resistance and the sleeve friction, as illustrated in Fig. 3.1. Similarly, they noted that an increase in the cohesion intercept of cemented sands enhances the cone penetration resistance and sleeve friction, while reducing friction ratio  $f_s/q_c$ . Rad and Tumay mentioned that there seems to be a unique correlation between the cohesion intercept and the cone penetration resistance, sleeve friction, or the friction ratio of cemented sands independent of their cement content or relative density. Figure 3.2 shows the effect of cohesion intercept of cemented sands on the cone penetration resistance and the sleeve friction of the cone penetrometer.

Puppala et al. (1995) conducted a series of tests on artificially weakly cemented Monterey 0/30 sand in a calibration chamber to investigate effects of cementation on cone penetration resistance. Monterey 0/30 is a clean sand with subangular to subrounded particles which is considered to be of medium to low compressibility. The maximum and minimum void ratios of this sand are 0.85 and 0.56, respectively. The specific gravity is 2.65 and the grain size distribution has a uniformity coefficient of 1.50. A total of 37 tests were carried out on uncemented, 1% and 2% cemented specimens. Cementation levels are expressed by dry weight of sand. Calibration cone penetration tests were performed on specimens with relative density of between 47 to 90 per cent. The initial vertical effective stress was in the range of 0.5 to 3.0 atmospheric pressure (i.e. 50 kPa and 300 kPa). They concluded that very weak cementation at these levels may increase significantly cone penetration resistance at a shallower depth, where  $(\sigma'_v/P_a) < 1.0$ . Figure 3.3 illustrates the relative influence of very weak cementation on cone penetration resistance. It indicates that the increase in confinement with depth gradually dominates the effect of very weak cementation. Nevertheless, Puppala and his co-workers reported that even at vertical effective stresses of 300 kPa, cone penetration resistance is about 40-45% higher than uncemented values when the cohesion intercept is only 32 kPa.

### 3.3 Influence of cementation on small strain shear modulus in sands

Information on the influence of low to moderate degrees of cementation on deformation behavior of sands, especially at small strains is limited. It is widely recognized that adding a cohesion intercept and a tensile strength to the sand increases its stiffness at low to moderate strain levels. However, large strain characteristics of cemented sands are considered to be similar to uncemented sands.

Chiang and Chae (1972) conducted resonant column tests with cement-treated sand and proposed the following equation:

$$[3.2] \quad G_o = [G_{ou} - 0.343CC(\sigma'_v)^{0.5}] (\sigma'_v)^{0.06CC}$$

in which, CC is cement content in percentage, expressed by dry weight of sand,  $\sigma'_o$  is effective confining pressure,  $G_o$  and  $G_{ou}$  are small strain shear modulus, in psi (1 psi = 6.89 kPa), of cemented and uncemented sands, respectively. They recommended to compute small strain shear modulus of corresponding uncemented sand ( $G_{ou}$ ) based on the relationships by Hardin and Drenvich (1972a, b).

Acar et al. (1986) performed a series of resonant column tests on both uncemented and artificially cemented specimens of Monterey 0/30 sand to study the effect of cementation on small strain shear modulus. Specimens were prepared using 0, 1, 2 and 4% cement by weight and cured for 14 days before testing. Relative density of specimens were 25, 35, 50 and 75 percent. They proposed a relationship to estimate small strain shear modulus of cemented sands as:

$$[3.3] \quad G_o = R_c \left( \frac{S}{0.3 + 0.7e^2} \right) (p_a)^{0.57} (\sigma'_m)^{0.43}$$

in which

$$[3.4] \quad R_c = (1 + CC^{0.49} - 2.0CC^{0.1} e^{4.6})$$

where CC is the cement content,  $e$  is void ratio,  $S$  is the stiffness coefficient for uncemented sand (a mean value of 631 was found for Monterey sands),  $R_c$  is the ratio between small strain shear modulus of cemented sand to that of similar uncemented sand, and  $\sigma'_m$  is mean effective stress.

Acar et al. discussed that an increase in the confining pressure leads to an increase in the number of particle bonds contributing to the resistance of the specimen to deformation. Hence, the cementation-induced increase in the stiffness, implies that cement particles provide a confinement effect at sand to sand interfaces. Nevertheless, Saxena et al. (1987) argued that the value of  $R_c$  as given by Eq. 3.4 depends only on the cement content and void ratio, and the contribution of confining pressure comes only through the relationship which provides the contribution of sand from its uncemented form. Hence, the increase in modulus due to the contribution of confining pressure for the cemented condition or the

process of cementation is not included in the relationship proposed by Acar and his co-workers.

Based on resonant column tests on artificially cemented Monterey No. 0 sand specimens, Saxena et al. (1987) proposed empirical relationships to estimate small strain shear modulus of cemented sands. Using regression analysis on the test results, they obtained the following correlations to compute the increase in modulus due to cementation,  $\Delta G_o$ :

- for cement content (CC) less than 2%:

$$[3.5] \quad \frac{\Delta G_o}{P_a} = \frac{172}{(e - 0.5168)} (CC)^{0.88} \left( \frac{\sigma'_o}{P_a} \right)^{(0.515e - 0.13CC + 0.285)}$$

- for cement content (CC) greater than 2% up to 8%:

$$[3.6] \quad \frac{\Delta G_o}{P_a} = \frac{773}{e} (CC)^{1.2} \left( \frac{\sigma'_o}{P_a} \right)^{(0.698e - 0.04CC - 0.2)}$$

where,  $e$  is void ratio, and  $\Delta G_o$  is in the same unit as  $\sigma'_o$  and  $P_a$ .

According to Saxena et al. (1987) small strain shear modulus of cemented sand should be computed as:

$$[3.7] \quad G_o = G_{ou} + \Delta G_o$$

where,  $G_{ou}$  is small strain shear modulus for the corresponding uncemented sand which should be computed from the following relationship:

$$[3.8] \quad \frac{G_{ou}}{P_a} = \frac{428.2}{(0.3 + 0.7e^2)} \left( \frac{\sigma'_o}{P_a} \right)^{0.574}$$



### 3.4 Proposed method for estimation of degree of cementation

Bearing capacity theories are often used as an analytical model for cone penetration (Durgunoglu and Mitchell 1973; Janbu and Senneset 1974). In these theories, experimentally-determined failure mechanisms are used to calculate ultimate bearing capacities with the limit equilibrium approach. The theory by Janbu and Senneset (1974) is a variation of the Prandtl model, recognizing that the failure zone does not close onto the penetrometer. According to this theory, when drained conditions govern around a penetrating cone, the bearing capacity can be expressed as:

$$[3.9] \quad q_c + a'_p = N_q (\sigma'_{vo} + a'_p)$$

where  $q_c$  is cone resistance,  $\sigma'_{vo}$  is effective overburden pressure,  $N_q$  is bearing capacity factor, and  $a'_p$  is an attraction intercept which is defined as:

$$[3.10] \quad a'_p = \frac{c'_p}{\tan \phi'_p}$$

where  $c'_p$  is the peak cohesion intercept and  $\phi'_p$  is the peak drained friction angle.

This theory suggests that for cemented sands a surcharge can be assumed to replicate the effect of the cohesion due to cementation. The equivalent surcharge is referred to as the attraction parameter  $a'_p$  as defined above. As a result, in cemented sands vertical stress  $\sigma'_v$  can be replaced with  $(\sigma'_v + a'_p)$  to account for cementation. This concept will be used to obtain a correlation between cone resistance  $q_c$  and relative density  $Dr$  in the form of:

$$[3.11] \quad \frac{q_c}{p_a} = A_o \left( \frac{\sigma'_v + a'_p}{p_a} \right)^{A_1} \text{Exp}(A_2 Dr)$$

where,  $p_a$  is atmospheric pressure.

As mentioned earlier, Acar et al. (1986) also noted that cement particles provide an apparent confinement effect at sand to sand interfaces. This implies that the effect of cementation

can be replaced with a larger equivalent confining pressure. This concept which has been supported by Saxena et al. (1987) is in good agreement with the proposed procedure based on the bearing capacity theory, i.e. to replace  $\sigma'_v$  with  $(\sigma'_v + a'_p)$  to account for the effect of cementation.

For uncemented sands in which  $a'_p = 0$ , Schmertmann (1976) and Harman (1976) suggested an empirical relationship of similar form. However, mean effective stress is here replaced with vertical effective stress to reduce the number of unknowns.

This study is based mainly on the published data by Puppala et al. (1995), as summarized in Table 3.1, from the calibration chamber tests on artificially cemented Monterey sand. When cone penetration resistance, relative density, vertical effective stress and attraction are related in the form given in Eq. 3.11, it is found that the factor  $A_0$  is highly influenced by variation in the attraction parameter. In addition, cone penetration resistance in uncemented sands increases nonlinearly with vertical effective stress. The variation of  $q_c$  with depth is often a function of  $(\sigma'_v)^{0.5}$  for uncemented sands. This suggests that exponent  $A_1$  in Eq. 3.11 can be fixed as 0.5 in the regression analysis. Hence, Eq. 3.11 is modified to the following form:

$$[3.12] \quad \frac{q_c}{p_a} = C_0 \left( 1 + \frac{a'_p}{p_a} \right)^\phi \left( \frac{\sigma'_v + a'_p}{p_a} \right)^{0.5} \text{Exp}(C_1 Dr)$$

where  $\phi$  is varied to obtain the best fit correlation.

Based on the data base by Puppala et al. (1995), a new correlation is developed for cemented sands between cone penetration resistance  $q_c$ , vertical effective stress  $\sigma'_v$ , attraction parameter  $a'_p$ , and relative density  $Dr$  as:

$$[3.13] \quad \frac{q_c}{p_a} = 17.635 \left( 1 + \frac{a'_p}{p_a} \right)^{1.19} \left( \frac{\sigma'_v + a'_p}{p_a} \right)^{0.5} \text{Exp}(2.40 Dr)$$

The correlation factor for the regression analysis is  $R = 0.9145$ . Figure 3.4 illustrates this relationship based on the data published by Puppala et al. (1995). When uncemented sand

is encountered, i.e.  $a'_p = 0$ , Eq. 3.13 is in reasonable agreement with the correlations given by Baldi et al. (1986) for uncemented medium compressible Ticino sand.

Using a similar concept, i.e. to replace vertical stress  $\sigma'_v$  with  $(\sigma'_v + a'_p)$  to account for cementation, it is possible to generate a relationship between small strain shear modulus  $G_o$  and relative density as:

$$[3.14] \quad \frac{G_o}{p_a} = B_o \left( \frac{\sigma'_v + a'_p}{p_a} \right)^{B_1} \text{Exp}(B_2 Dr)$$

This relationship is similar to the correlation developed by Lo Presti (1987) for uncemented Ticino sand. However, mean effective stress is again replaced with vertical stress for the sake of simplicity.

In this study, Eq. 3.3, proposed by Acar et al. (1986) is used to evaluate the small strain shear moduli for the calibration chamber tests performed by Puppala et al. (1995). Then attempts were made to relate small strain shear modulus, relative density, vertical effective stress and attraction in the form given in Eq. 3.14. However, it was found that the factor  $B_o$  is also affected by the variation of attraction parameter. As a result, the relationship is modified to the following form and  $\theta$  is varied to obtain the best fit for the correlation.

$$[3.15] \quad \frac{G_o}{p_a} = D_o \left( 1.0 + \frac{a'_p}{p_a} \right)^\theta \left( \frac{\sigma'_v + a'_p}{p_a} \right)^{D_1} \text{Exp}(0.60 Dr)$$

The regression analysis of the data from the calibration chamber specimens yields the following relationship:

$$[3.16] \quad \frac{G_o}{p_a} = 596.01 \left( 1.0 + \frac{a'_p}{p_a} \right)^{2.467} \left( \frac{\sigma'_v + a'_p}{p_a} \right)^{0.48} \text{Exp}(0.60 Dr)$$

The correlation factor for the regression analysis is  $R = 0.9203$ . Figure 3.5 displays this relationship. It should be noted that the factor 0.60 for  $Dr$  has been fixed in the regression analysis to obtain an ultimate correlation of  $G_o$  versus  $q_c^{0.25}$  when  $Dr$  is eliminated between Eq. 3.13 and Eq. 3.16. A similar form of relationship between  $G_o$  and  $q_c$  for uncemented

sands has been reported by several researchers (Jamiolkowski and Robertson 1988, Baldi et al. 1989, Rix and Stokoe 1991). When uncemented sand is encountered, i.e.  $a'_p = 0$ , Eq. 3.16 is in good agreement with the correlations given by Lo Presti (1987) for uncemented medium compressible Ticino sand.

After manipulation between Eq. 3.13 and Eq. 3.16 relative density  $D_r$  can be eliminated and the following correlation between  $G_o$  and  $q_c$  is obtained for cemented sands:

$$[3.17] \quad \frac{G_o}{p_a} = 290.84 \left( \frac{q_c}{p_a} \right)^{0.25} \left( \frac{\sigma'_{v'} + a'_p}{p_a} \right)^{0.355} \left( 1.0 + \frac{a'_p}{p_a} \right)^{2.1695}$$

The exponents in Eq. 3.17 (0.25 and 0.355) are in good agreement with those (on average, 0.25 and 0.375) given in the correlation of  $G_o$  versus  $q_c$  by other researchers for uncemented sands (e.g. Rix and Stokoe, 1991). Equation 3.17 can be applied to seismic CPT test results, to investigate whether a sand is cemented and to quantify the amount of cementation in a given sand. Figure 3.6 illustrates a set of contours developed based on Eq. 3.17. Figure 3.6 can be used to identify cemented sands and/or to evaluate the attraction parameter.

Figure 3.6 illustrates the application of the proposed correlation to identify cemented sands and to evaluate cementation level. As seen in Fig. 3.6, a set of contours has been developed by which the attraction parameter  $a'_p$  can be estimated, based on a set of  $G_o$ ,  $q_c$  and  $\sigma'_{v'}$  values from the results of seismic CPT in a sand. Also shown on Fig. 3.6 is the application of these contours to estimate  $a'_p$  for Kidd, Massey, Alaska, Utah tailings sands and a residual soil from a site in Alabama. More details about the above soils, have been given in Chapter 2, Section 2.3.

Based on additional field data and the method proposed by Eslaamizaad and Robertson (1996), the residual soil from Alabama is identified as a compressible, very lightly cemented soil. In addition, the Utah tailings sand is of moderate compressibility and more cemented than the Alabama residual soil. These are confirmed in Fig. 3.6. On average, for lightly cemented Utah tailings sand the attraction is estimated to be  $0.25p_a$  (i.e. 25 kPa) in Fig. 3.6. Generally, for lightly cemented sands in which the level of cementation is around 1% and 2% by weight, the magnitude of  $a'_p$  does not exceed 40 kPa (Puppala et al., 1995).

### 3.5 Estimation of relative density in cemented sands

The available reference charts (Baldi et al., 1986) developed for clean uncemented sands overestimate relative density for cemented sands. The methodology developed in this paper can provide a means to evaluate relative density of cemented sands. Once a sand is identified as cemented and the attraction parameter  $a'_p$  is determined, it is then possible to estimate relative density of cemented sand using Eq. 3.13. Figure 3.7 shows a set of contours based on Eq. 3.13, from which the relative density of cemented sands can be evaluated.

Figure 3.7 also shows the application of the proposed approach to estimate the relative density of Utah tailings sands. Knowing  $a'_p = 0.25$ , the Seismic CPT data of Utah tailings sands are plotted in the proposed chart. For Utah tailings sand at the given site, a relative density of 50% is estimated at shallow depths increasing to about 90% with depth. Using the conventional  $D_r$  charts for  $a'_p = 0$  (Baldi et al., 1986), the relative density would be estimated to be from 90% to 120% over the same depth, which is not possible. Figure 3.8 compares relative density at various depths corrected for cementation based on Eq. 3.13 with corresponding relative density based on the method by Baldi et al. (1986), which has not been corrected for cementation.

### 3.6 Summary and conclusions

Most natural soils have components of stiffness and strength which can not be accounted for by classical soil mechanics which are generally due to the presence of structure in the soils (inter-particle bonding and fabric).

Cementation is a process which frequently exists in many natural deposits of granular soils. Recent data and evidence suggest that even the cleanest natural sand deposits may be very weakly cemented (Puppala et al. 1995). Hence, engineering judgment made based on test results from uncemented specimens reconstituted in the laboratory may not be valid (Mitchell and Solymar, 1984).

The effect of cementation on the strength-deformation behavior of sands is often ignored since cementation often improves the strength. However, neglecting cementation can result

in an overly conservative design of shallow and deep foundations as well as slopes and retaining walls.

The influence of light cementation on the stress-strain and strength behavior of granular soils has been extensively investigated through testing reconstituted artificially cemented sands in the laboratory (e.g. Dupas and Pecker 1979, Clough et al. 1981, Acar and El-Tahir 1986, Saxena et al. 1987 and Puppala et al. 1995). Based on these studies cementation can be considered to provide some value of cohesion intercept  $c'$  for sand, with an almost negligible influence on the peak angle of shearing resistance  $\phi'_p$ . In general, large strain characteristics of cemented sands are similar to that of uncemented sands. In contrast, even a small degree of cementation can have an important influence on soil stiffness, especially at small and intermediate strain levels. However, in general, inter-particle bonding is destroyed at large strains.

A comprehensive procedure to identify cemented sands in-situ has not yet been established. Puppala et al. (1993) proposed a chart, from which the cohesion intercept and relative density of cemented sands at shallow depths can be estimated from both cone resistance and sleeve friction in penetration testing.

Preliminary studies on the possible effects of very weak cementation on cone penetration test (CPT) results indicate that low levels of cementation can have a substantial effect on penetration resistance at shallow depth (Rad and Tumay 1986, Akili and Al-Joulani 1988, Puppala et al. 1993, and Puppala et al. 1995). Small strain stiffness of sand is also highly influenced by low levels of cementation (Chiang and Chae 1972, Acar et al. 1986, Saxena et al. 1987). Hence, the potential exists to quantify level of cementation in cemented sands with a combined measurement of cone penetration resistance ( $q_c$ ) and small strain shear modulus ( $G_o$ ). On this basis, and using calibration chamber test results on artificially cemented sands, relationships have been developed from which the level of cementation in terms of the attraction parameter can be obtained and hence, the relative density of cemented sands estimated. These correlations are in good agreement with similar relationships developed for uncemented sands by other researchers. Application of the proposed procedure to natural sand deposits has been illustrated. Further field data from SCPT in cemented sands is required to evaluate the proposed relationships.

It should be noted that, the available data base is limited since only one type of sand, a medium compressible Monterey No, 0/30 sand, has been used in the present study. Therefore, the developed interpretation correlation and method are considered valid only for cemented, medium compressible sands. It is necessary to enlarge the database and complement them with field studies before precise predictions could be made.

$C_r$ (%) (1)	$D_r$ (%) (2)	$(\sigma'_t/\sigma_a)$ (3)	$(q/\sigma_a)$ (4)	$(f/\sigma_a)$ (5)	$\sigma'_t/\sigma_a$ (6)
0	55	0.50	45	0.20	0.41
0	49	1.00 (0.96)	60	0.20	0.44
0	72	1.00	84	0.20*	0.42
0	86	1.00	103	0.30*	0.37
0	89	1.00	125	0.80	0.35
0	90	1.00	122	0.34*	0.34
0	56	2.00	75	0.45	0.35
0	69	2.00	176	0.79	0.48
0	90	2.00	218	0.60*	0.44
0	55	3.00	115	0.73	0.62
0	57	3.00	110	0.80	0.46
0	71	3.00	203	1.31	0.40
0	74	3.00	205	1.30	0.38
0	88	3.00	350	1.73	0.40
1	50	0.50	57	0.22	0.39
1	49	1.00	68	0.20	0.36
1	68	1.00	131	0.74	0.37
1	86	1.00	168	0.95	0.54
1	47	2.00	97	0.72	0.41
1	66	2.00	191	0.86	0.63
1	85	2.00	254	1.55	1.00**
1	45	3.00	80	0.70	0.43
1	53	3.00	104	1.00	0.57
1	70	3.00	246	1.21	0.49
1	88	3.00	300	1.40	0.35*
1	89	3.00	338	1.98	0.49
2	52	0.50	70	0.28	0.41
2	47	1.00	80	0.40	0.44
2	70	1.00	143	0.80	0.42
2	85	1.00	202	1.10	0.54
2	54	2.00	120	0.75	0.35
2	69	2.00	220	1.20	0.48
2	81	2.00	300	2.00*	0.43
2	86	2.00	295	1.75	0.59
2	52	3.00	150	1.01	0.62
2	72	3.00	307	1.31	0.40
2	84	3.00	350	2.11	0.40

Note:  $q_t$  = tip resistance,  $f_s$  = sleeve friction,  $\sigma_a$  = atmospheric pressure (approximated to be 100 kPa.)

\*Problems in sleeve friction measurements. Excluded from analysis

\*\*Leak between piston and inner cell

\*Test stopped due to buckling of the cone. Actual tip resistance value may be higher.

Table 3.1 Penetration test results of artificially cemented Monterey sand. (after Puppala et al., 1995)



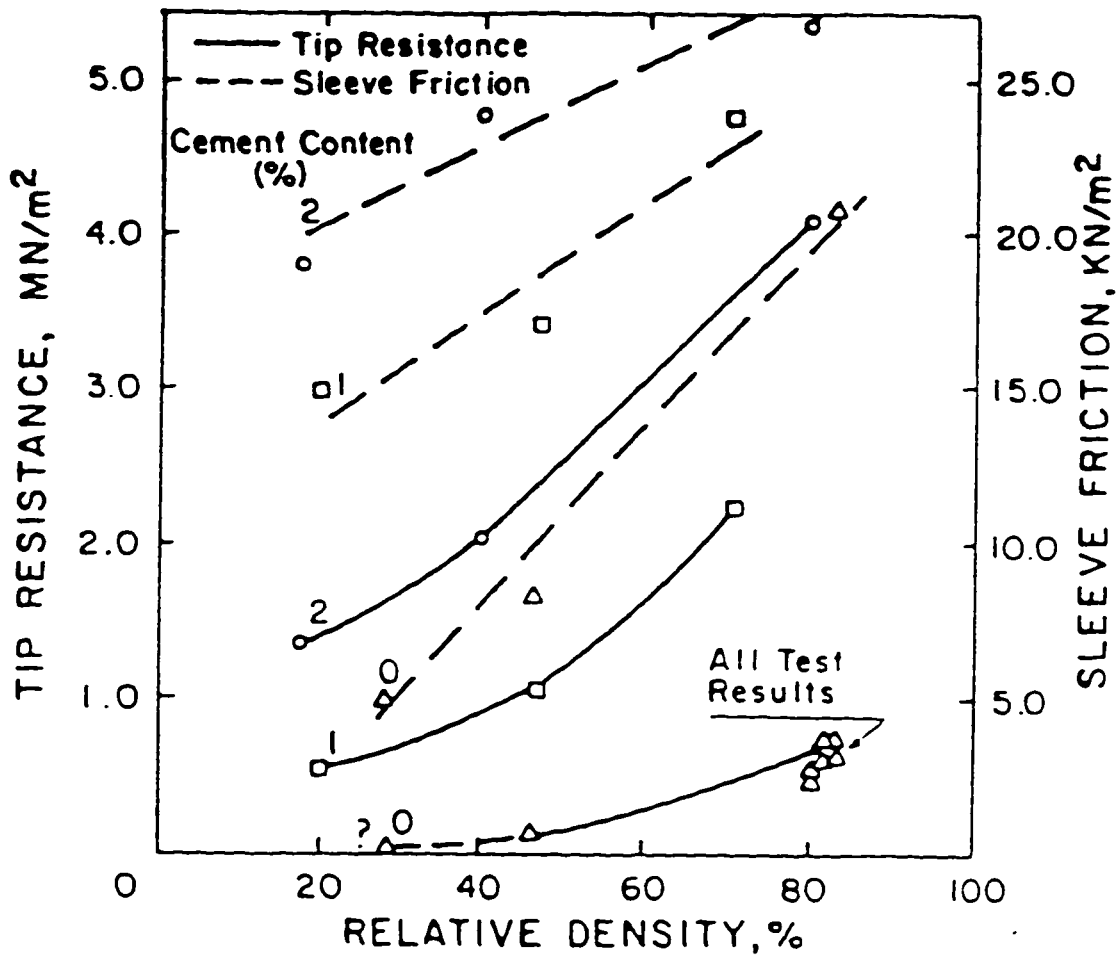


Fig. 3.1 Effect of cementation on the cone penetration resistance and the sleeve friction. (after Rad and Tumay, 1986)

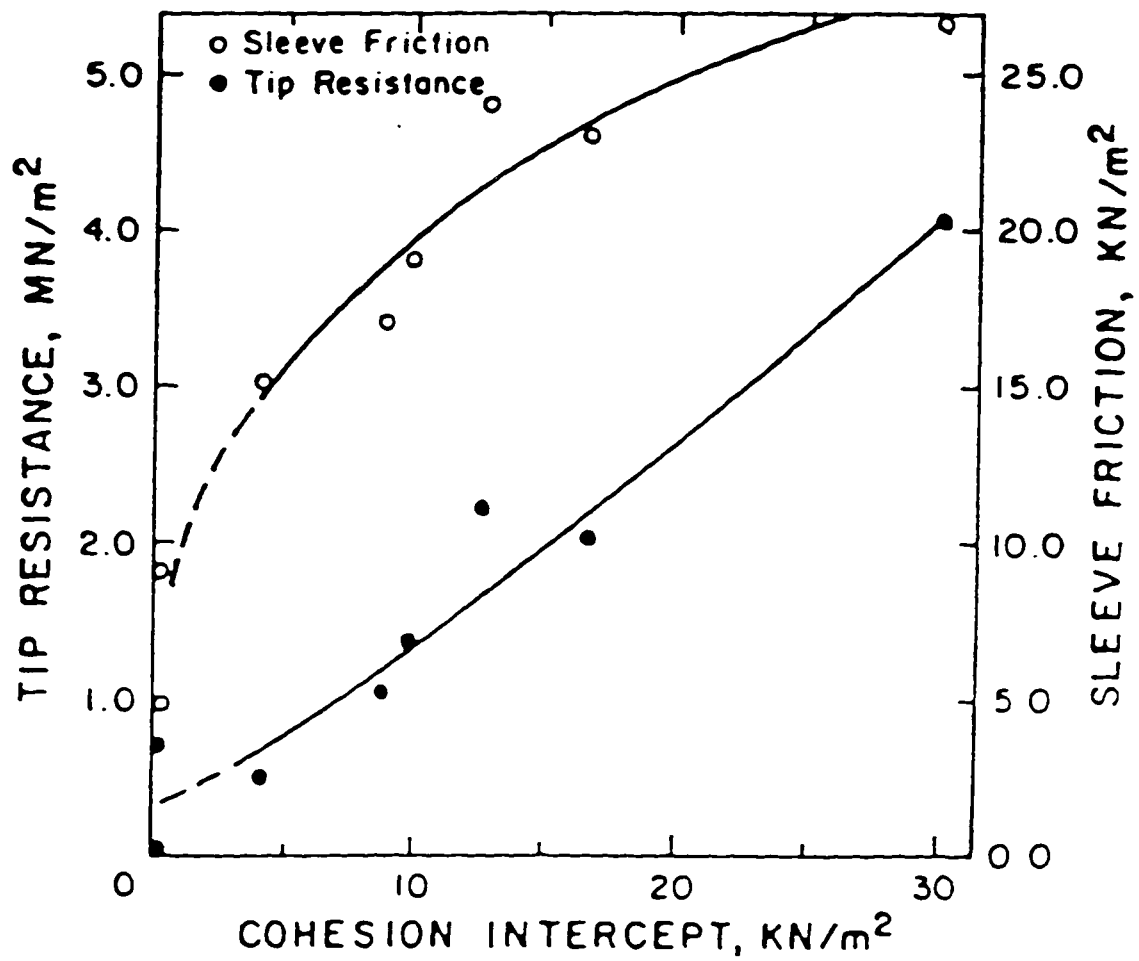


Fig. 3.2 Effect of cohesion intercept of cemented sands on the cone penetration resistance and the sleeve friction. (after Rad and Tumay, 1986)

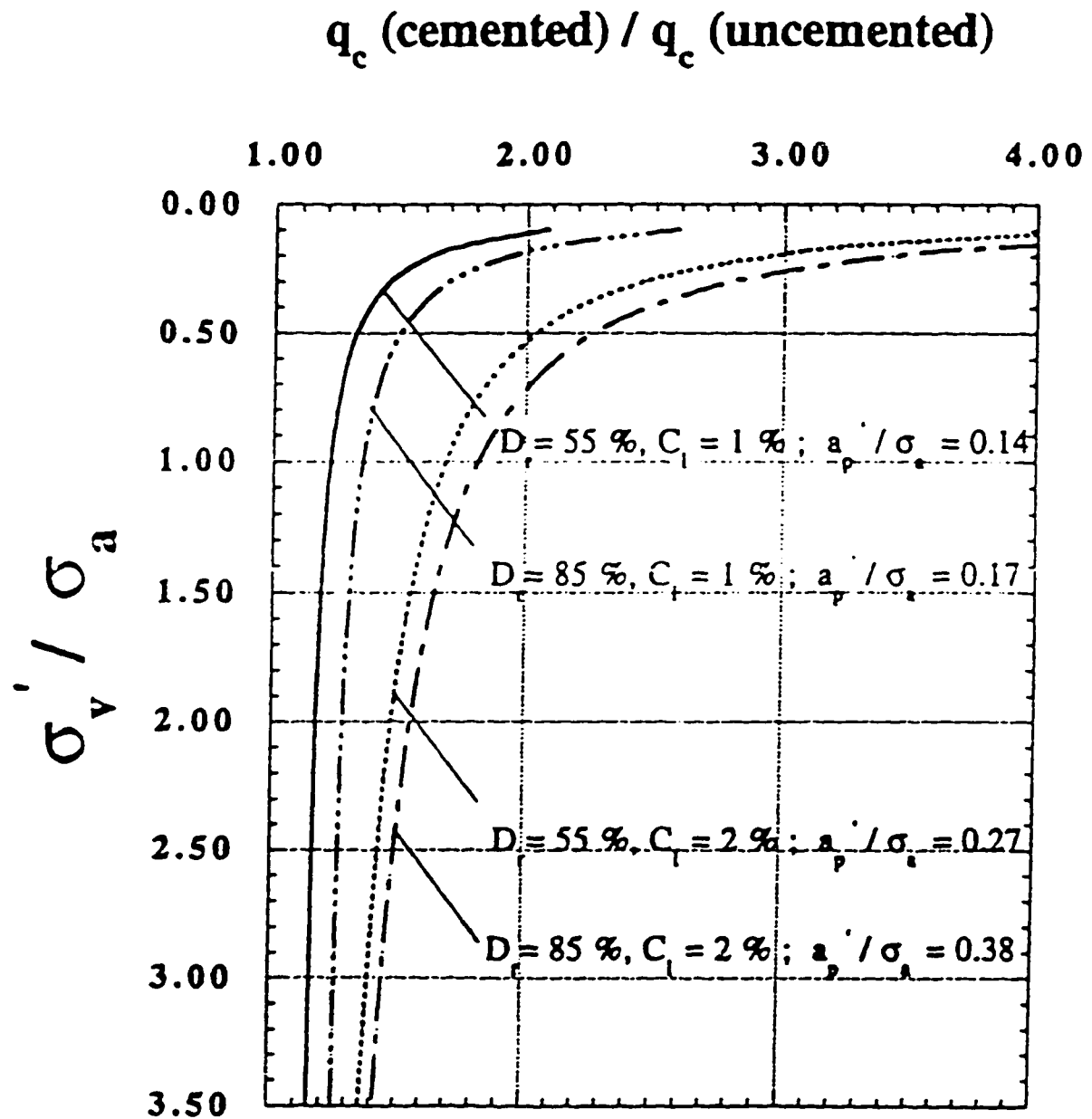


Fig. 3.3 Relative effect of very weak cementation on the cone penetration resistance in Monterey sand. (after Puppala et al., 1995)

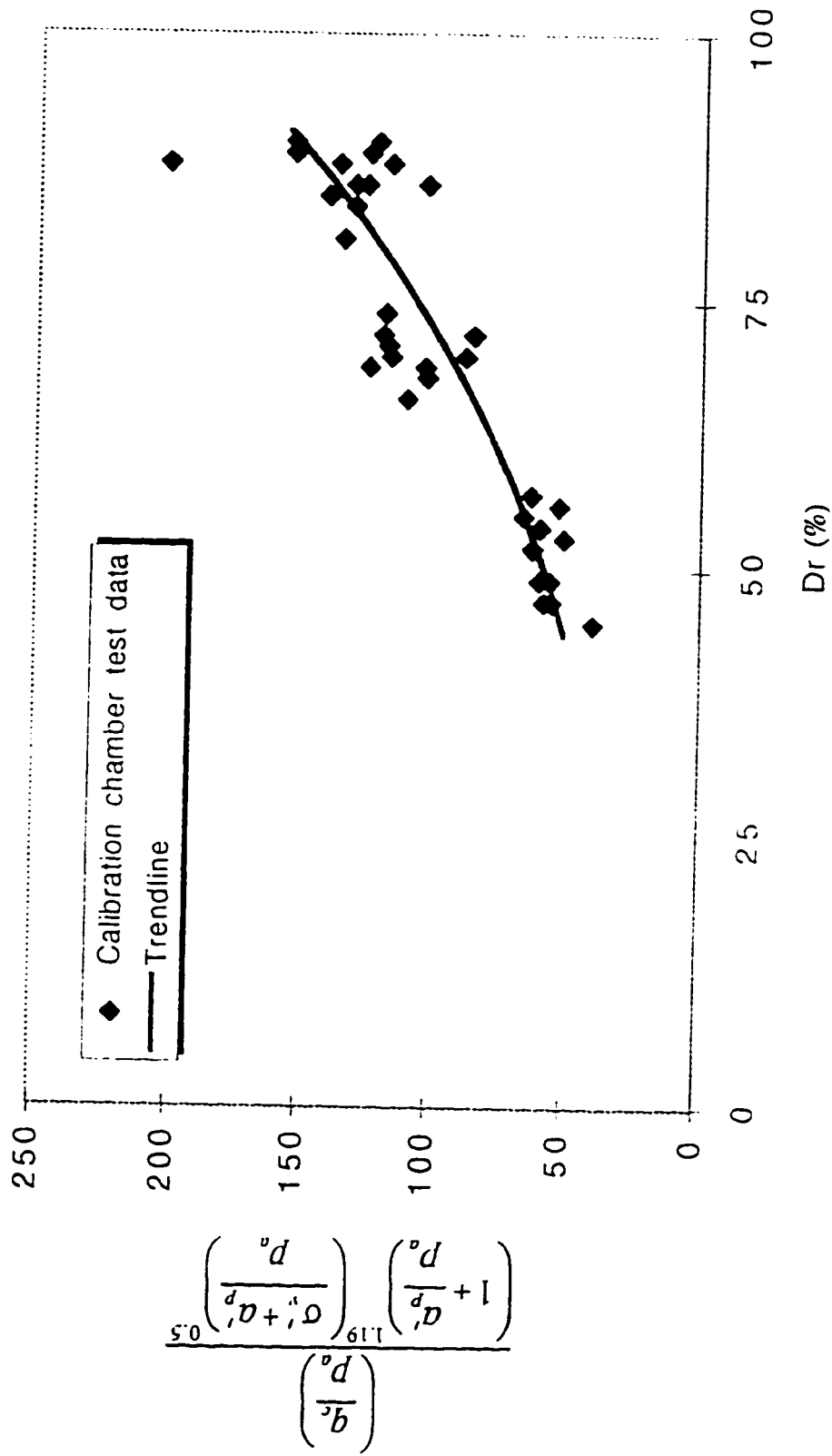


Fig. 3.4 Correlation between normalized cone resistance, attraction parameter, and relative density.

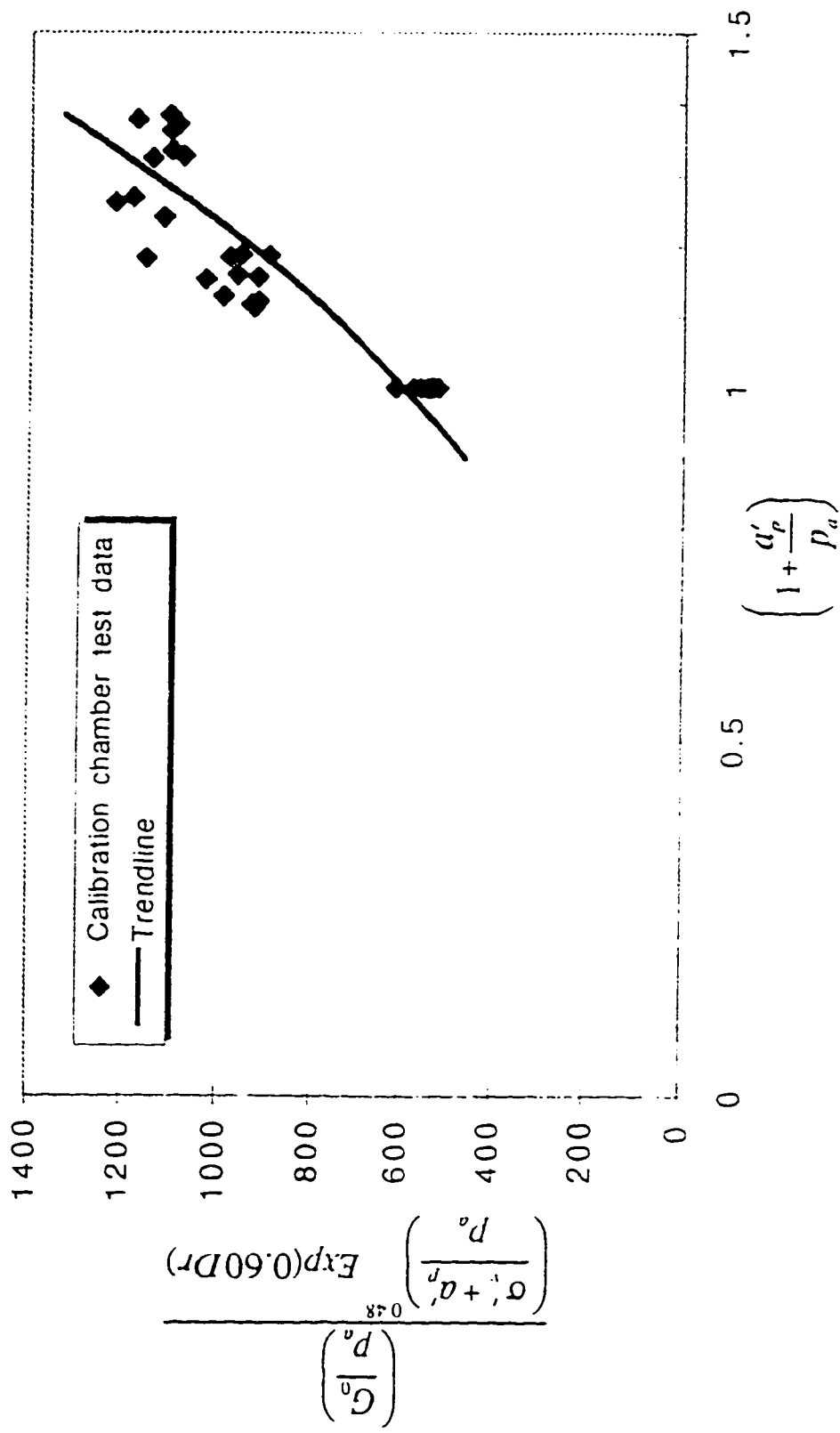


Fig. 3.5 Correlation between normalized small strain shear modulus, attraction parameter, and relative density.

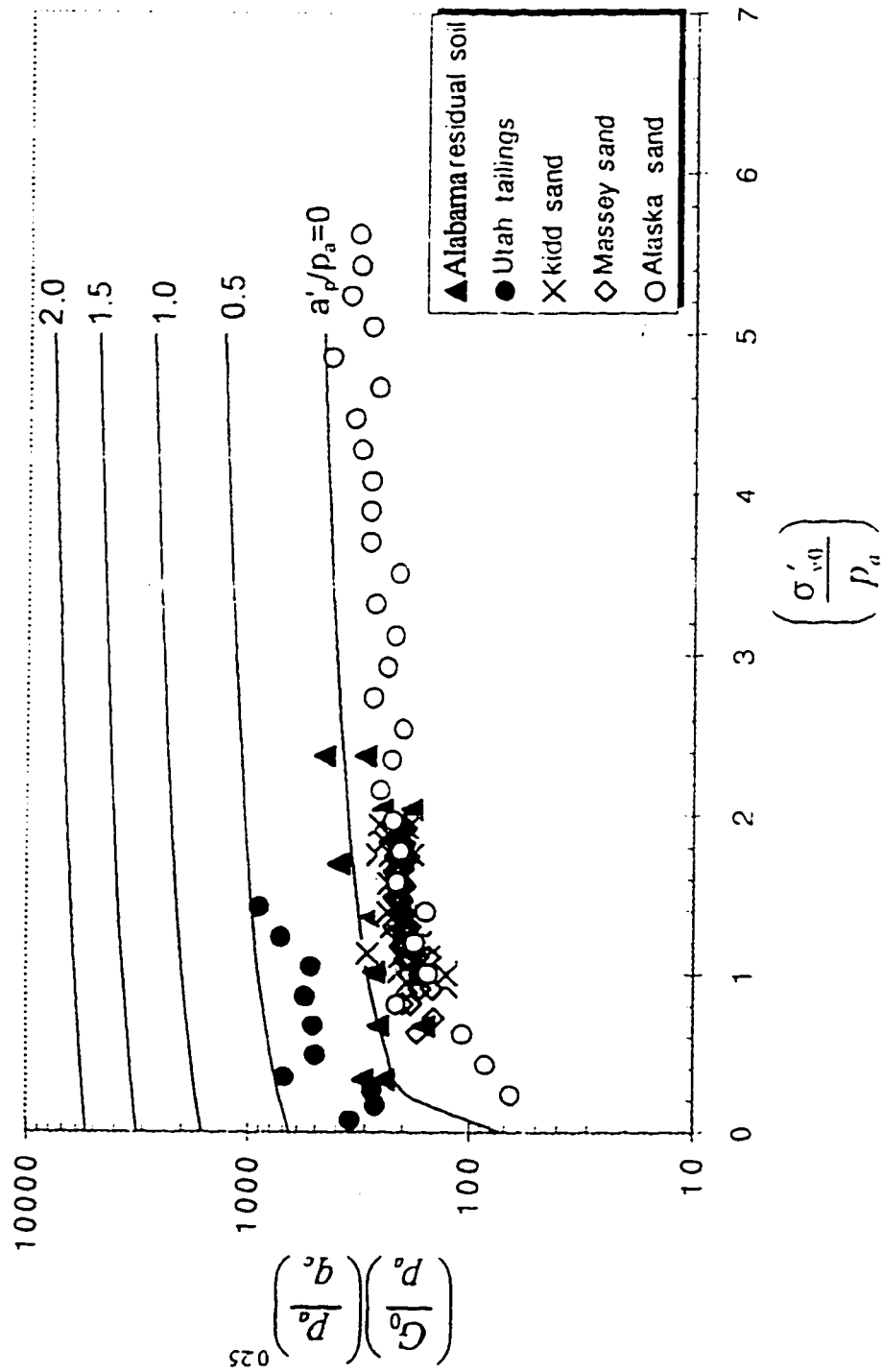


Fig. 3.6 Estimation of attraction parameter from SCPT for cemented sands.

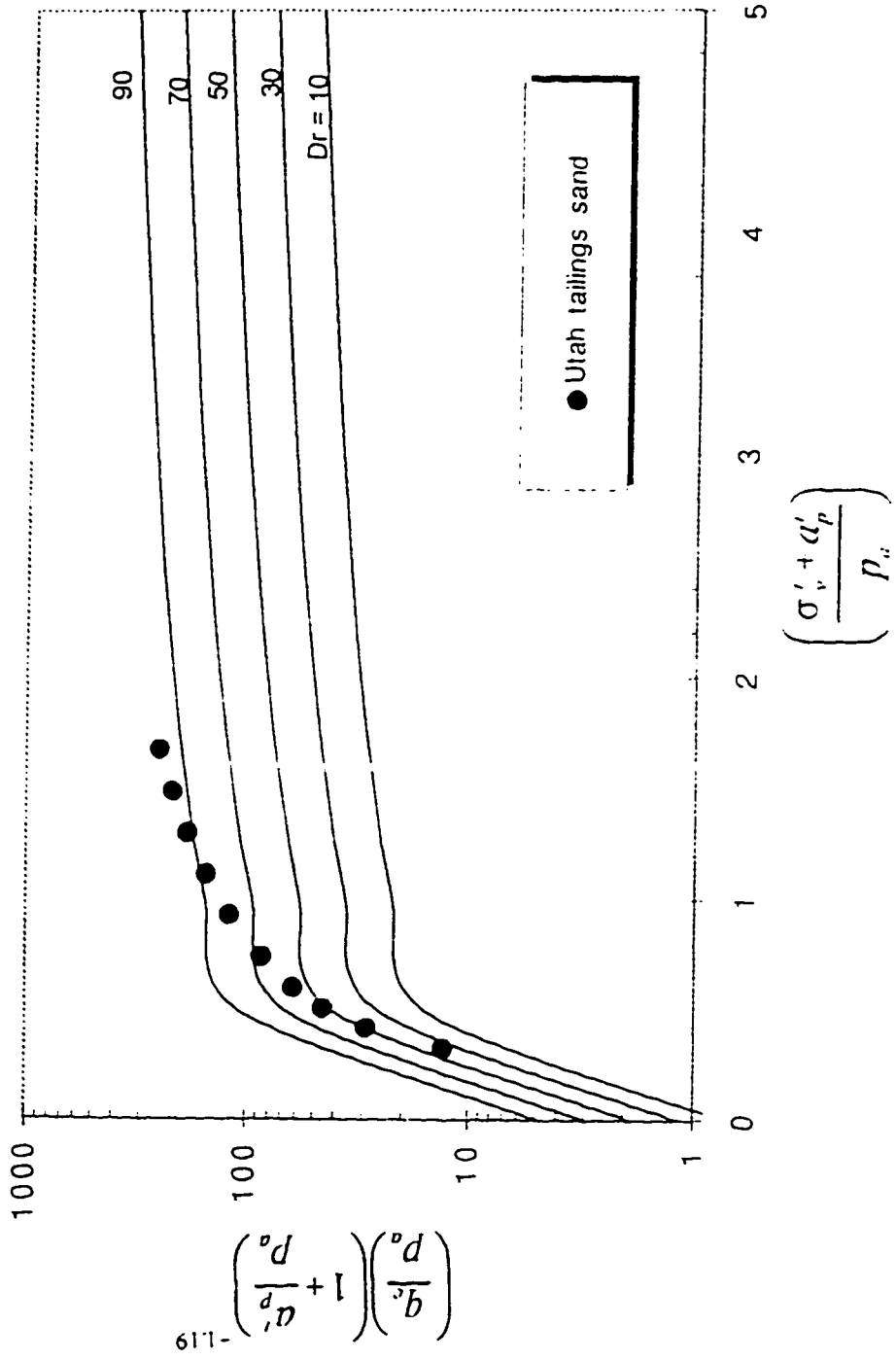


Fig. 3.7 Estimation of relative density for cemented Utah tailings sands.

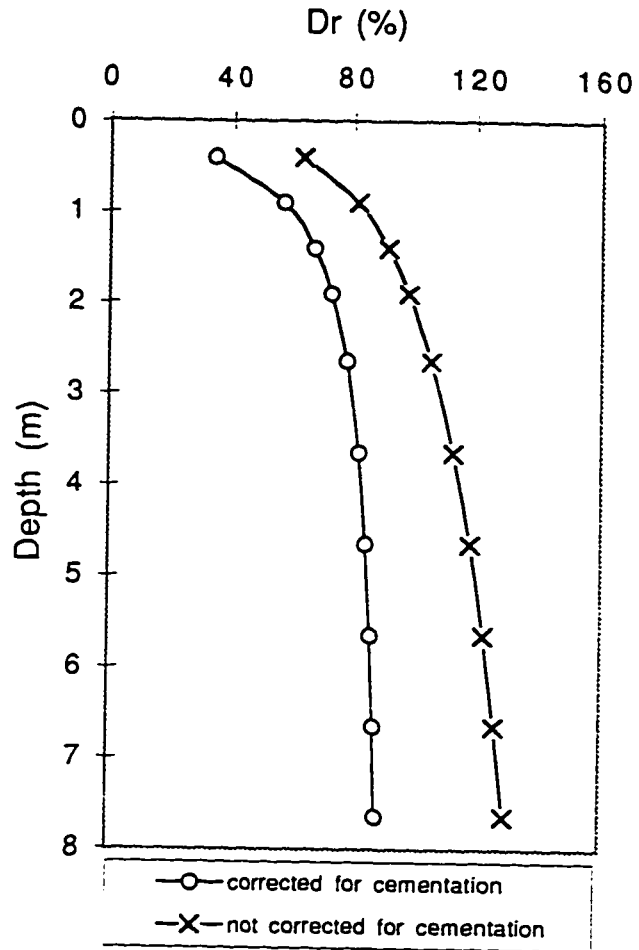


Fig. 3.8 Comparison of conventional method and proposed method for evaluation of relative density for cemented Utah tailings sand



## References

- Acar, Y. B. and El-Tahir, E. A. 1986. Low strain dynamic properties of artificially cemented sand. *Journal of Geotechnical Engineering*, Vol. 112, No. 11, ASCE, pp. 1001-1015.
- Akili, W. and Al-Joulani, N. M. 1988. Cone penetration tests on artificially cemented sands, *Proceedings of the First Int. Symp. on Penetration Testing, ISOPT-I, the Orlando*, pp. 607-614.
- Baldi, G., Bellotti, R., Ghionna, V., Jamiolkowski, M. and Pasqualini, E. 1986. Interpretation of CPT's and CPTU's, 2nd part: Drained penetration of sands, 4th Int. Geotechnical Seminar, Nanyang Technological Institute, Singapore, Field Inst. & In-situ measurements, pp. 143-162.
- Baldi, G., Bellotti, R., Ghionna, V., Jamiolkowski M. and Lo Presti D.C.F. 1989. Modulus of sands from CPT's and DMT's. *Proceedings, XII International Conference of Soil Mechanics and Foundation Engineering, Vol. 1*, pp. 165-170., Rio De Janeiro.
- Burghignoli, A., Pane, V., and Cavalera, L. 1991. Monotonic Loading, *Proceedings, 10th European Conference of Soil Mechanics and Foundation Engineering, Deformation of soils and displacement of structures*, pp. 961-979.
- Chiang, Y. C., and Chae, Y. S. 1972. Dynamic properties of cement treated soils, *Highway Research Record, No. 379*, pp. 39-51.
- Clough, G. W., Sitar, N., Bachus, R. C., and Rad, N. S. 1981. Cemented sands under static loading, *Journal of Geotechnical Engineering*, Vol. 107, No. GT6, ASCE, pp. 799-816.
- Dupas, J. M. and Pecker, A., 1979. Static and dynamic properties of sand-cement, *Journal of Geotechnical Engineering*, Vol. 105, No. GT3, ASCE, pp. 419-436.
- Durgunoglu, H. T., and Mitchell, J. K. 1973. Static penetration resistance of soils, Rep., Space Sciences Laboratory, University of California, Berkeley, Calif.
- Eslaamizaad, S. and Robertson, P.K. 1996. A framework for in-situ determination of sand compressibility. *Proceedings of 49th Canadian Geotechnical Conference, St. John's, NF, Canada*.
- Hardin, B. O., and Drenvich, V. P. 1972a. Shear modulus and damping in soils; measurement and parameter effect. *ASCE Journal of Soil Mechanics and Foundation Division, Vol. 98, SM6*, pp. 603-624.

- Hardin, B. O., and Drenvich, V. P. 1972b. Shear modulus and damping in soils; design equations and curves. *ASCE Journal of Soil Mechanics and Foundation Division*, Vol. 98, SM7, pp. 667-692.
- Harman, D. E. 1976. A statistical study of static cone bearing capacity, vertical effective stress, and relative density of dry and saturated fine sands in a large triaxial test chamber. Master's Thesis. University of Florida.
- Jamiolkowski, M., and Robertson, P.K. 1988. Future trends for penetration testing., *Proceedings of conference, Penetration testing in the U.K.*, Birmingham, pp. 21-42.
- Janbu, N., and Senneset, K. 1974. Effective stress interpretation of in-situ static penetration tests. *Proc. European Symp. on Penetration Testing, ESOPT I*, A.A. Balkema, Rotterdam, The Netherlands, Vol. 1.2., pp. 479-488.
- Lee, K.L. 1975. Formation of adhesion bonds in sands at high pressure. Rep. No. UCLA. Eng. 7586. UCLA School of Engrg. and Appl. Sci., Los Angeles, Calif.
- Lo Presti, D. 1987. Behavior of Ticino sand during resonant column test, Ph.D. Thesis, Technological University of Turin.
- Mitchell, J. K., and Solymar, Z. V. 1984. Time dependent strength gain in freshly deposited or densified sands, *Journal of Geotechnical Engineering, ASCE*, Vol. 110, No. 11, pp. 1559-1576.
- Mitchell, K. J. 1993. *Fundamentals of soil behavior*, Second edition, John Wiley & Sons, Inc.
- Puppala, A. J., Acar, Y. B. and Senneset K. 1993. Cone penetration in cemented sand: Bearing capacity interpretation. *Journal of Geotechnical Engineering*, Vol. 119, ASCE, pp. 1990-2001.
- Puppala, A. J., Acar, Y. B. and Tumay, M. T. 1995. Cone penetration in very weakly cemented sand, *Journal of Geotechnical Engineering*, Vol. 121, ASCE, pp. 589-601.
- Rad, N. S., and Tumay, M. 1986. Effect of cementation on the cone penetration resistance of sand: A model study, *American Society for Testing and Materials, Geotechnical Testing Journal*, pp. 117-125
- Rix G.J. and Stokoe K.H. II. 1991, Correlation of Initial tangent Modulus and Cone Penetration Resistance. *Proceedings of the First International Symposium on Calibration Chamber Testing/ISOCCT1*, Potsdam, New York, Edited by An-Bin Huang, pp. 351-362.

- Saxena, S. K., Avramidis, A. S. and Reddy, K. R. 1987. Dynamic moduli and damping ratios for cemented sands at low strains, Canadian Geotechnical Journal, Vol. 25, pp. 353-368.
- Schmertmann, J.H. 1976. An updated correlation between relative density,  $D_r$ , and Fugro-Type electric cone bearing,  $q_c$ . Unpublished report to WES, Vicksburg, Miss.

## CHAPTER 4

### EVALUATION OF COMPRESSIBILITY OF UNCEMENTED SANDS<sup>1</sup>

#### 4.1 Introduction

Compression in granular soils involves both rearrangement and crushing of particles. The significant effect of sand mineralogy and confining pressures on compression behavior of sands has been broadly recognized. Other influencing factors include initial relative density, stress history, cementation, particles size, angularity and gradation. At low pressures, the volume changes in sands occur due to elastic compression of the soil skeleton and particle movements by sliding and rolling whereas, at high pressures there can be considerable volume change due to crushing of grains. Initial relative density, stress history and level of cementation of sands can affect the compression behavior of sands in the low stress regime. The threshold stress of particle crushing is basically a function of sand mineralogy. Nevertheless, the physical properties such as particle size, angularity and gradation can influence both the onset and development of particle crushing. In clean silica sands, in which the primary constituent is quartz particles with high resistance to fracturing, the threshold stress of particle crushing can be as high as 1 MPa whereas, in sands with a high mica or carbonate content made up of shell fragments, the threshold stress can be lower than 100 kPa. The amount of crushing increases with increasing level of anisotropic stress state (i.e. shear stress) in the soil.

A number of investigators have studied the compressibility of sand in one-dimensional compression in the laboratory and in the field. The results of these studies indicate that sand is relatively incompressible at low pressure, but at high pressures there can be considerable volume change due to crushing of the grains, and that compression can continue for a considerable period of time. The consolidation curves are parabolic over the major part of the stress range and the relationship can be represented by the equation:

---

<sup>1</sup> A version of part of this chapter has been published. Eslaamizaad, S. and Robertson P.K. 1996. A Framework for In-Situ Determination of Sand Compressibility, Proc. of the 49th Canadian Geotechnical Conference, St. John's, Newfoundland, 419-428.

$$[4.1] \quad \frac{\Delta V}{V_0} = \chi \sqrt{\sigma'_v}$$

where,  $\chi$  is a function of the relative density of the sand, and  $\sigma'_v$  is effective vertical stress in kPa.

Evaluation of compressibility in cohesionless soils based on laboratory tests can be difficult and unreliable due to the often unavoidable sample disturbance. In such circumstances in-situ tests are generally preferred. However, a comprehensive procedure for determining compressibility from in-situ tests, applicable to sands with different mineralogy ranging from clean silica sand to calcareous carbonate sand, has not yet been established.

The cone penetration test (CPT) has become increasingly more popular due to the continuous nature of the data, reliable and repeatable results and cost effectiveness. The penetration resistance of a soil is a complex function of its strength and compressibility characteristics. Hence, comprehensive analytical solutions for penetration resistance as a function of compressibility are not yet available. Grain crushing in sands is likely during cone penetration for cone resistance  $q_c$ , greater than 10 MPa (Thomas, 1968), whereas, it would be unlikely under typical working load conditions for most well designed foundations. Nonetheless, many empirical correlations have been developed between cone penetration resistance and compressibility in sands. In general, the cone penetration test can not be used to determine the preconsolidation pressure in prestressed sands. Since the compressibility of sand is highly influenced by whether it is normally consolidated or overconsolidated, this can be a serious limitation if the stress history of the deposit is unknown (Mitchell and Gardner, 1975).

Based on a review of such correlations for sands, Mitchell and Gardner (1975) concluded that the correlations generally are in the form of:

$$[4.2] \quad M = \alpha_M q_c$$

where  $M$  is the drained constrained modulus (equal to  $1/m_v$  from oedometer test,  $m_v$  is volumetric change per unit of pressure increase) and the factor  $\alpha_M$  is a function of relative

density and stress history, and is generally in the range of 1.5 to 4.0. For a given sand  $\alpha_M$  is not constant and varies with at least variations in relative density and confining pressure, Vesic (1970) found the following relationship for Ogeechee River sand

$$[4.3] \quad \alpha_M = 2(1 + Dr^2)$$

This indicates that  $\alpha_M$  should vary from 2 for very loose sands to 4 for very dense sands.

Lunne and Kleven (1981) reviewed calibration chamber test results, as summarized in Table 4.1. They concluded that  $\alpha_M = 3.0$  provide the most conservative estimate of constrained modulus and the choice of  $\alpha_M$  depends on judgment and experience.

Senneset et al. (1982) suggested a parabolic form of

$$[4.4] \quad M_t = A\sqrt{q_n p_a}$$

in which  $M_t$  is the tangent constrained modulus,  $p_a$  is atmospheric pressure,  $q_n$  is the net cone resistance equal to  $(q_c - \sigma'_{vo})$ , and the coefficient  $A$  varies between 30 and 50 depending on sand relative density. This equation would appear to apply for all stress levels and OCR.

Lunne and Christoffersen (1983), reviewed data from various field and laboratory sources and recommended the following relationships for normally consolidated sands:

$$[4.5] \quad \begin{array}{lll} M_t = 4q_c & \text{for} & q_c < 10 \text{ MPa} \\ M_t = 2q_c + 20 & \text{for} & 10 \text{ MPa} < q_c < 50 \text{ MPa} \\ M_t = 120 \text{ MPa} & \text{for} & q_c > 50 \text{ MPa} \end{array}$$

They also proposed the following relationships for overconsolidated sands:

$$[4.6] \quad \begin{array}{lll} M_t = 5 q_c & \text{for} & q_c < 50 \text{ MPa} \\ M_t = 250 \text{ MPa} & \text{for} & q_c > 50 \text{ MPa} \end{array}$$

When these relations are superimposed graphically, they plot as an approximate parabolic relationship which supports the work by Senneset et. al (1982). The proposed relationships suggest a constant constrained modulus beyond a certain value of cone penetration resistance of 50 MPa. In addition, in overconsolidated sands, the predicted constrained modulus is independent of degree of overconsolidation.

Based on calibration chamber test results on Ticino sands, Baldi et al. (1981) and Baldi et al. (1982) developed correlations between relative density and constrained modulus number, as well as relative density and cone resistance  $q_c$ , respectively. Robertson and Campanella (1983) combined the above correlations and developed a series of curves for normally consolidated, uncemented quartz sands, relating tangent constrained modulus  $M_t$ , to cone resistance  $q_c$ , for different levels of vertical effective stress  $\sigma'_{vo}$ , as shown in Fig. 4.1.

Based on the tangent moduli corresponding to the last load increment for samples of Ticino sand tested in large calibration chamber, Baldi et al. (1986) developed a correlation between  $M_t$  and  $q_c$  in the form of :

$$[4.7] \quad \frac{M_t}{q_c} = C_0 p_a \left( \frac{\sigma'_o}{p_a} \right)^{C_1} OCR^{C_2} \text{Exp}(C_3 Dr)$$

in which  $\sigma'_o$  is mean effective stress and for Ticino sand  $C_0 = 14.48$ ;  $C_1 = -0.116$ ;  $C_2 = 0.313$  and  $C_3 = -1.123$ . Equation 4.7 is illustrated in Fig. 4.2. The proposed equation includes the influence of stress history, relative density and confining stress. A comparison between typical relationship as given by Eq. 4.7 and Eq. 4.2, suggests that the influence of relative density as well as stress history are included quantitatively, and an additional term is introduced in Eq. 4.7 for the effect of confining pressure. However, since there is a small exponent of -0.116, the effect of confining pressure can be neglected for practical purposes.

Fioravante et al. (1991) proposed an empirical correlation for normally consolidated Toyoura sands based on the tangent modulus measured at the last increment of consolidation in calibration chamber as

$$[4.8] \quad M_t = (13 \text{ to } 15)q_c^{0.5}$$

in which  $M_t$  and  $q_c$  are in MPa. The above relationship is illustrated in Fig. 4.3.

Application of the available methods is limited to low to moderately compressible silica sands. Moreover, they often require a prior knowledge of relative density and stress history. In addition, experimental evidence indicates that the penetration of the cone alters almost completely the previous stress and strain history of sand (Baldi et al. 1986) since average stress level around the cone approximately equals failure in the soil, whereas, the compressibility of sands is significantly influenced by whether it is normally consolidated or overconsolidated. Seismic tests are among the few in-situ tests that produce little or no soil disturbance. Such techniques induce very small strains in the ground that preserve its natural feature. Seismic methods measure the small strain response of a large volume of the ground. Hence, the potential exists to evaluate directly the sand compressibility with a combined measurement of cone penetration resistance ( $q_c$ ) and shear wave velocity ( $V_s$ ).

In this chapter the potential of using SCPT to quantify sand compressibility is studied. Correlations are developed to evaluate initial tangent constrained modulus and bulk modulus in sands with different stress history.

## 4.2 Evaluation of sand compressibility from Seismic CPT

### 4.2.1 Constrained modulus

Extensive studies have been conducted by several researchers (e.g. Robertson and Campanella 1983, Baldi et al. 1986, Jamiolkowski and Robertson 1988, Baldi et al. 1989, Fioravante et al. 1991, Rix and Stokoe 1991) to relate small strain shear modulus  $G_o$ , with cone penetration resistance  $q_c$ , performed in unaged, uncemented predominantly quartz sands. Based on a comprehensive review of calibration chamber test results, Eslaamizaad and Robertson (1996a) (Chapter 2) investigated the influence of sand compressibility on the correlation between  $G_o$  and  $q_c$  and concluded that compressible sands have a high ratio of  $G_o/q_c$  (often greater than 10), hence, sand compressibility can be evaluated from a combined measurement of  $G_o$  and  $q_c$ . This implies that a potential exists to correlate  $G_o/q_c$  (or  $V_s^2/q_c$ ) with sand compressibility.



The tangent constrained modulus is frequently measured during the last step of one-dimensional compression stage of a sand specimen in a large calibration chamber prior to penetration testing. A large published database derived from 2 different series of CPT calibration chamber (Baldi et al. 1986, Fioravante et al. 1991) and resonant column tests on silica sands with different stress history was reviewed to investigate a relationship between  $M_t$ ,  $q_c$  and  $G_o$  or  $V_s$ .

A unique correlation between penetration resistance and deformation modulus can not exist due to the importance of stress history. Hence, all the relationships between cone penetration resistance and deformation modulus should make a clear distinction between normally consolidated (NC) and overconsolidated (OC) sands (Jamiolkowski et al. 1988).

Based on calibration chamber test results on uncemented normally consolidated Ticino sand and Toyoura sand (134 tests), a relationship was developed as part of this study for the evaluation of the tangent constrained modulus from SCPT data in the form of:

$$[4.9] \quad \frac{M_t}{p_a} = 35.475 \frac{\left(\frac{q_c}{p_a}\right)^{0.5034} \left(\frac{\sigma'_{vo}}{p_a}\right)^{0.3675}}{\left(\frac{V_s}{V_a}\right)^{1.0068}}$$

in which  $V_a$  is the velocity of sound in air assumed to be 340 m/s (1110 ft/s). In the above correlation, shear wave velocity has been back-calculated from the small strain shear modulus. For Toyoura sand the relationship developed by Iwasaki and Tatsuoka (1977) using resonant column test results, has been applied. For Ticino sand the relationship proposed by Lo Presti (1987) based on resonant column test results, has been applied. Figure 4.4 presents a summary of the calibration test results in the form of Eq. 4.9. The correlation factor for the above regression analysis is  $R = 0.9066$ . To correlate initial tangent constrained modulus with  $V_s^2/q_c$ , the exponent of normalized shear wave velocity and normalized cone resistance have been fixed in the regression analysis as 2.0 and 1.0 respectively whereas, the exponent of normalized vertical stress is varied to obtain the best fit correlation. In Eq. 4.9, the exponent of cone resistance equals to 0.5034. This supports the approximate parabolic form of the correlation between tangent constrained modulus and

cone penetration resistance assumed by other researchers (Senneset et al. 1982, Lunne and Christoffersen 1983).

Equation 4.9 can be compared with the empirical formula proposed by Janbu (1963) in the form of:

$$[4.10] \quad M_t = k_M p_a \left( \frac{\sigma'_{vo}}{p_a} \right)^n$$

where  $k_M$  is modulus number and  $n$  is the modulus exponent. This implies that the stress exponent  $n = 0.37$  which is in good agreement with the findings of other researchers of about 0.40 (e.g. Robertson and Campanella, 1983). Hence, for normally consolidated sands, the modulus number can be obtained from the following relationship:

$$[4.11] \quad k_M = 35.475 \frac{\left( \frac{q_c}{p_a} \right)^{0.5034}}{\left( \frac{V_s}{V_a} \right)^{1.0068}}$$

Similarly using published calibration chamber test results (71 tests) on uncemented overconsolidated Ticino sand and Toyoura sand (Baldi et al. 1986, Fioravante et al. 1991), a relationship is developed for the evaluation of the tangent constrained modulus from SCPT data in the form of:

$$[4.12] \quad \frac{M_t}{p_a} = 932.95 \frac{\left( \frac{q_c}{p_a} \right)^{0.1466} \left( \frac{\sigma'_{vo}}{p_a} \right)^{0.1847}}{\left( \frac{V_s}{V_a} \right)^{0.2932} (OCR)^{0.3225}}$$

Figure 4.5 presents a summary of the calibration chamber test results in the form of Eq. 4.12. The correlation factor for the above regression analysis is  $R = 0.8960$ . Similarly, to correlate initial tangent constrained modulus with  $V_s^2/q_c$ , the exponent of normalized shear wave velocity and normalized cone resistance have been fixed in the regression analysis as 2.0 and 1.0 respectively, then the exponent of normalized vertical stress is varied to obtain the best fit correlation. A prior knowledge of stress history is

required in Eq. 4.12. A method suggested by Eslaamizaad and Robertson (1996b) (Chapter 5) can be used to estimate overconsolidation ratio of sands from SCPT data. Equation 4.12 can be compared with the empirical formula proposed by Janbu (1963). It implies that for overconsolidated sands the stress exponent is equal to 0.185 and modulus number can be obtained from the following relationship:

$$[4.13] \quad k_M = 932.95 \frac{\left(\frac{q_c}{p_a}\right)^{0.1466}}{\left(\frac{V_s}{V_a}\right)^{0.2932} (OCR)^{0.3225}}$$

Figure 4.6 summarizes the relationship between tangent constrained modulus number ( $k_M$ ), normalized cone penetration, normalized shear wave velocity and overconsolidation ratio for uncemented sands. A series of contours constructed for modulus number  $k_M$  versus  $(q_c/p_a)(V_s/V_a)^2$  for uncemented sands with different stress history is shown. Figure 4.6 illustrates that in normally consolidated sands the correlation follows a parabolic trend. However, in overconsolidated sands the correlations display a gradual increase of modulus number with increasing  $(q_c/p_a)(V_s/V_a)^2$ . Figure 4.6 also shows that among the consolidated sands, higher overconsolidation ratio produces lower constrained modulus when all other variables are identical. This indicates the different level of influences of stress history on  $M_t$  and  $q_c$ . Nevertheless overconsolidated sands have much higher constrained modulus than normally consolidated sands. Figure 4.7 compares the predicted normalized constrained modulus (using Eq. 4.9 and 4.12) with the normalized constrained modulus measured in the calibration chamber test.

A prior knowledge of initial relative density is not required by the proposed relationships and OCR can be evaluated directly from seismic CPT results (Eslaamizaad and Robertson, 1996b) (Chapter 5). As mentioned earlier, the correlations have been derived based on the test results on uncemented unaged silica sands. Hence, their applications are limited to sands which meet those qualifiers. Nevertheless, the proposed framework seems to be applicable for highly compressible sands with high mica or carbonate content. Unfortunately, very limited calibration chamber tests have been performed on highly compressible sands.

#### 4.2.2 Bulk modulus

Tangent bulk modulus ( $B_t$ ) can be expressed by the following relationship:

$$[4.14] \quad B_t = k_B p_a \left( \frac{\sigma'_{vo}}{p_a} \right)^n$$

Tangent bulk modulus ( $B_t$ ) can be estimated from tangent constrained modulus ( $M_t$ ) using a factor of  $(1 + 2 K_o)/3$ , where  $K_o = \sigma'_{ho}/\sigma'_{vo}$  is the coefficient of earth pressure at rest and  $\sigma'_{ho}$  is horizontal effective stress (e.g. Byrne et al., 1987). Similar correlation exists between bulk modulus number ( $k_B$ ) and constrained modulus number ( $k_M$ ) as follows:

$$[4.15] \quad k_B = \frac{1 + 2K_o}{3} k_M$$

Based on a large number of calibration chamber tests, Eslaamizaad and Robertson (1996b) (Chapter 5) proposed a correlation between  $K_o$  and overconsolidation ratio in the form of

$$[4.16] \quad \text{OCR} = 5.8539 (K_o)^{2.1598}$$

This relationship can be rearranged to obtain  $K_o$  from OCR. Then, Eq. 4.15 is rewritten in the following form of:

$$[4.17] \quad k_B = (0.333 + 0.294 \text{OCR}^{0.463}) k_M$$

Equation 4.17 can be combined with Eq. 4.11 and Eq. 4.13 to develop relationships between bulk modulus number and  $(q_c/p_a)(V_c/V_s)^2$ . Figure 4.8 illustrates the resulting correlations for sands with different stress history. Figure 4.8 shows that bulk modulus number is approximately identical for overconsolidated sands with different OCR. Nevertheless, a considerable difference exists between bulk modulus of normally consolidated and overconsolidated sands.

### 4.2.3 Example Application

The Kidd and Massey sites are located near Vancouver, B.C. Both sites contain natural alluvial sediments as part of the Fraser River delta. At both sites, SCPT data are within a 20 to 30 m thick complex of distributary channel sands that underlies most of the delta plain (Monahan et al., 1995). Fraser River sand is a young, uncemented predominantly quartz sand with some mica and feldspar, has a  $D_{50} = 0.30$  mm and contains on average about 5% fines. Measured in-situ void ratio has been reported as 0.88 to 0.97 at Kidd site and 0.92 to 1.02 at Massey site. These represent a range of relative density of 25% to 50% for Kidd and 10% to 35% at Massey. Seismic CPT has been performed at various depths and locations at these sites (68 tests at Massey and 46 tests at Kidd). Both sites have been identified as normally consolidated sands having a coefficient of earth pressure at rest about 0.4 (Eslaamizaad and Robertson, 1996b). More details about the above soils, have been given in Chapter 2, Section 2.3 and in Appendix A.

Equations 4.9, 4.11 and 4.15 can be applied to the data from the combined measurement of shear wave velocity and cone penetration resistance to estimate constrained modulus, constrained modulus number and bulk modulus number.

For Massey sand, the constrained moduli are evaluated based on Eq. 4.9 and Fig. 4.6, to be between 31 to 46 MPa. The bulk moduli, based on Eq. 4.14 and Fig. 4.8, are evaluated as 19 to 28 MPa. Corresponding constrained modulus numbers extends from 520 to 730 and bulk modulus numbers are estimated to be in the range of 310 to 440. It should be noted that the constrained modulus varies with vertical effective stress whereas, the variation in modulus numbers is mainly due to variable relative density. The above results are in reasonable agreement with the constrained moduli based on consolidation test data of triaxial tests on frozen samples of the Massey site, from a target zone at a depth of 9 to 13 m, where  $M_1$  ranges from 25 to 43 MPa. The above results are also in good agreement with the average values reported by Byrne et al. (1987). Byrne et al. (1987) summarized the average values of soil parameters, as given in Table 4.2. Byrne et al. noted that there was considerable scatter in their data. Nevertheless, they suggested average values as a guidance. The relative density at Massey site, is between 10 to 35 per cent. On this basis, bulk modulus can be estimated as 9 to 24 MPa from the method by Byrne et al. (1987).

Similarly, for Kidd sand, constrained moduli are evaluated based on Eq. 4.9 to be between 37 to 52 MPa. The bulk moduli, hence, are evaluated as 22 to 31 MPa. Corresponding constrained modulus numbers are between 630 to 680 and bulk modulus numbers are estimated to be in the range of 380 to 410. The above results are in reasonable agreement with the constrained moduli based on consolidation test data of triaxial tests on frozen samples of the Kidd site, from a target zone at a depth of 12 to 16 m, where  $M_c$  ranges from 19 to 40 MPa. The above results are also in good agreement with the average values reported by Byrne et al. (1987) from laboratory tests. At Kidd site, the relative density is in the range of 25 to 50 percent. Hence, bulk modulus can be estimated as 15 to 32 MPa from the method by Byrne et al. (1987).

Table 4.3 summarizes the predicted constrained modulus and bulk modulus in comparison with consolidation test results on frozen samples and average bulk modulus suggested by Byrne et al. (1987). Based on Eq. 4.9 and Fig. 4.6, the constrained moduli predicted for Massey sand are in good agreement with test results on frozen samples. However, for Kidd sand higher values are predicted as compared with consolidation test results on frozen samples. In addition the predicted values based on the laboratory tests, as suggested by Byrne and his co-workers are in good agreement with those proposed in this study, based on field test results. The method proposed by Byrne et al. requires a knowledge of relative density which is not generally known. Hence, the suggested method based on SCPT results has the advantage that it requires no earlier information of initial relative density and OCR can be reasonably predicted by SCPT (Eslaamizaad and Robertson, 1996b).

### **4.3 Evaluation of sand compressibility from CPT results**

#### **4.3.1 Constrained modulus**

The method suggested by Baldi et al. (1986) has been widely used in practice, as illustrated by Fig. 4.2. However, this approach requires a prior knowledge of initial relative density as well as stress history of sand deposit. Baldi and his co-workers concluded that for the same initial relative density and mean effective stress, the ratio of  $M_c/q_c$  increases as OCR increases. However, a comprehensive review of calibration chamber test results, reported by Baldi et al. (1986), and Fioravante et al. (1991), indicates an opposite trend. That is to say an increase in OCR, where all other variables are identical, results in a decrease in the

ratio of  $M_t/q_c$ . This reflects the different degree to which the stress history, influences  $M_t$  and  $q_c$ , indicating that the increase in OCR produce larger cone penetration resistance than in-situ constrained modulus.

A regression analysis was performed as part of this study on the calibration chamber test results on uncemented normally consolidated Ticino sand and Toyoura sand (Baldi et al. 1986, and Fioravante et al. 1991), to develop a correlation between constrained modulus  $M_t$ , vertical effective stress  $\sigma'_{vo}$ , and cone penetration resistance  $q_c$ . A relationship is established for the evaluation of the tangent constrained modulus from CPT data in the form of:

$$[4.18] \quad \frac{M_t}{P_a} = 81.55 \left( \frac{q_c}{P_a} \right)^{0.4183} \left( \frac{\sigma'_{vo}}{P_a} \right)^{0.20}$$

Figure 4.9 presents a summary of the calibration chamber test results in the form of Eq. 4.18. The correlation factor for the above regression analysis is  $R = 0.8977$ . Equation 4.18 can be compared with the empirical relationship by Janbu (1963). This indicates that for normally consolidated sands, the stress exponent is 0.20 and the modulus number can be obtained from the following relationship:

$$[4.19] \quad k_M = 81.55 \left( \frac{q_c}{P_a} \right)^{0.4183}$$

Using a similar data base, that includes published calibration chamber test results on uncemented overconsolidated Ticino sand and Toyoura sand (Baldi et al. 1986, and Fioravante et al. 1991), the following relationship is developed for the evaluation of the tangent constrained modulus in overconsolidated sands from CPT data:

$$[4.20] \quad \frac{M_t}{P_a} = 1152.2 \frac{\left( \frac{q_c}{P_a} \right)^{0.1302} \left( \frac{\sigma'_{vo}}{P_a} \right)^{0.128}}{(OCR)^{0.3385}}$$

Figure 4.10 presents a summary of the calibration chamber test results in the form of Eq. 4.20. The correlation factor for the above regression analysis is  $R = 0.895$ . Equation 4.20 can be compared with the formula by Janbu (1963). It implies that the stress

exponent is equal to 0.128 and the modulus number for overconsolidated sands can be obtained from the following relationship:

$$[4.21] \quad k_M = 1152.2 \frac{\left(\frac{q_c}{P_a}\right)^{0.1302}}{(OCR)^{0.3385}}$$

Figure 4.11 summarizes the relationship between constrained modulus number  $k_M$ , normalized cone penetration  $q_c$ , and overconsolidation ratio OCR, for uncemented quartz sands. A series of contours are constructed for modulus number versus  $q_c/P_a$ . It suggests that in normally consolidated sands the correlation follows a parabolic trend. However, in overconsolidated sands a slight increase in modulus number is noted with increasing  $q_c/P_a$ . Figure 4.11 displays that among overconsolidated sands, higher overconsolidation ratio results in lower constrained modulus when all other variables are identical. This indicates the different level of influences of stress history on  $M_t$  and  $q_c$ . Nevertheless overconsolidated sands produce much higher constrained modulus than normally consolidated sands. Figure 4.12 compares the predicted normalized constrained modulus (using Eq. 4.18 and 4.20) with the normalized constrained modulus measured in the calibration chamber test.

### 4.3.2 Bulk modulus

A similar method as explained in Section 4.2.2 can be used to obtain a correlation between bulk modulus and cone penetration resistance. Equation 4.21 can be combined with Eq. 4.17 to develop relationships between bulk modulus number and  $q_c/P_a$ . Figure 4.13 illustrates the correlations for sands with different stress history.

### 4.3.3 Example Application

For Massey sand, from Fraser River delta in B.C., based on the method suggested in Section 4.3.1, using only CPT results, the constrained moduli are estimated to be between 41 to 60 MPa. The bulk moduli, hence, are evaluated as 25 to 36 MPa. Corresponding constrained modulus numbers extends from 410 to 520 and bulk modulus numbers are



evaluated to be in the range of 250 to 320. The above results are in reasonable agreement with the constrained moduli based on consolidation test data of triaxial tests on frozen samples of the Massey site, where  $M_c$  ranges from 25 to 43 MPa. The above results seems to be larger than the average values suggested by Byrne et al. (1987) from a comprehensive review of laboratory tests. The relative density at Massey site, is between 10 to 35 per cent. Hence, bulk modulus can be estimated as 9 to 24 MPa from the method by Byrne et al. (1987).

Similarly, for Kidd sand, from Fraser River delta in B.C., based on the method suggested, constrained moduli are evaluated to be between 45 to 75 MPa. The bulk moduli, hence, are evaluated as 27 to 45 MPa. Corresponding constrained modulus numbers are between 440 to 670 and bulk modulus numbers are estimated to be in the range of 260 to 400. The above results are in reasonable agreement with the constrained moduli based on consolidation test data of triaxial tests on frozen samples of the Kidd site, where  $M_c$  ranges from 19 to 40 MPa. The above results are also larger than the average values suggested by Byrne et al. (1987) from laboratory tests, as given in Table 4.2. At Kidd site, the relative density is in the range of 25 to 50 percent. On this basis, bulk modulus can be estimated as 15 to 33 MPa from the method by Byrne et al. (1987).

Table 4.4 summarizes the predicted constrained modulus and bulk modulus in comparison with consolidation test results on frozen samples and average bulk modulus suggested by Byrne et al. (1987). Based on Eq. 4.9 and Fig. 4.11, the constrained moduli predicted for Massey sand are in good agreement with test results on frozen samples. However, for Kidd sand higher values are predicted as compared with consolidation test results on frozen samples. In addition, the predicted values based on the laboratory tests, as suggested by Byrne and his co-workers are about 30 to 40 percent smaller than those proposed in this study, based on field test results. First, it should be noted that the values suggested by Byrne et al. (1987) are average values. As mentioned by Byrne et al., related data were scattered, hence, they include noticeable amount of uncertainty by averaging the test results. This is illustrated in Fig. 4.14. Secondly, sand compressibility based on reconstituted specimens is often smaller than the in-situ sand compressibility. Thirdly, the relationship seems to be valid for sands with different stress history, although it has been widely recognized that the sand compressibility is highly influenced based on whether sand is normally consolidated or is overconsolidated. In addition, many investigators noted different stress exponent for normally consolidated sands and overconsolidated sands, whereas the method by Byrne et al. recommends a constant stress exponent for sands

irrespective to the stress history. Finally, the method by Byrne et al. (1987) is based on the amount of relative density, which in sands can not be determined accurately. This can also increase the level of uncertainty in the determination of bulk modulus based on the method by Byrne et al. (1987).

Using CPT data from Drammen (Holmen) and Sleipner sands, Lunne (1996) compared the above proposed method with other available methods (Lunne and Christoffersen, 1983; Robertson and Campanella, 1983; Baldi et al., 1986). Holmen is a site in the Drammen river delta. Drammen sand was deposited 2000 to 4000 years ago. Drammen sand includes 55% quartz and 35% feldspar. It is known that it is not geologically overconsolidated and its coefficient of earth pressure at rest is about 0.4 (Lunne, 1991). Sleipner site is located in about 80 m water depth in North Sea. The upper 22 m of soil is a very dense fine sand estimated to have been deposited approximately 100,000 years ago. Sleipner sand (North Sea sand) is an uncemented very dense overconsolidated predominantly quartz sand with some feldspar. Sleipner sand is a subrounded sand of 92% quartz and 8% feldspar with a specific gravity of 2.62. The void ratio of Sleipner sand ranges from 0.54 to 1.00 (Lunne et al., 1997).

A summary of the comparison by Lunne (1996) is shown in Table 4.5. Lunne mentioned that the relationship proposed by Baldi et al. (1986), requires correction due to the uncertainty in the evaluation of relative density.

#### **4.4 Summary and conclusions**

Compression in granular soils involves both rearrangement and crushing of particles. The significant effect of sand mineralogy and confining pressures on compression behavior of sands has been broadly recognized. Other influencing factors include initial relative density, stress history, cementation, particles size, angularity and gradation.

Evaluation of compressibility in cohesionless soils based on laboratory tests can be difficult and unreliable due to the often unavoidable sample disturbance. In such circumstances in-situ tests are generally preferred. However, a comprehensive procedure for determining compressibility from in-situ tests, applicable to sands with different mineralogy ranging from clean silica sand to calcareous carbonate sand, has not yet been established. The cone penetration test (CPT) has become increasingly more popular due to

the continuous nature of the data, reliable and repeatable results and cost effectiveness. Many empirical correlations have been developed between cone penetration resistance and compressibility in sands. Many investigators suggested a linear correlation between constrained modulus of sands and cone penetration resistance (Mitchell and Gardner 1975, Lunne and Kleven 1981, Baldi et al. 1986). Others, noted an hyperbolic relationship relating constrained modulus to cone penetration resistance (Senneset et al. 1982, Robertson and Campanella 1983, Lunne and Christoffersen 1983, Fioravanta et al. 1991). Application of the available methods is limited to low to moderately compressible silica sands. Moreover, they often require a prior knowledge of relative density and stress history. In general, cone penetration test can not be used to determine the preconsolidation pressure in prestressed sands. Since the compressibility of sand is highly influenced by whether it is normally consolidated or overconsolidated, this can be a serious limitation if the stress history of the deposit is unknown.

A framework has been proposed to quantify sand compressibility from the combined measurement of shear wave velocity and cone penetration. An assessment of calibration chamber test results has provided an empirical basis to relate tangent constrained modulus with cone penetration resistance and shear wave velocity in sands. Hence, correlations have been developed to predict in-situ constrained modulus in uncemented and unaged silica sands with variable stress history using the seismic CPT. On this basis, relationships have also been presented from which bulk modulus can be evaluated using SCPT results. A prior knowledge of initial relative density is not required by this method and OCR can be evaluated directly from seismic CPT (Eslaamizaad and Robertson, 1996b). The proposed method has been applied to Seismic CPT results of the Kidd and Massey sites. The predicted constrained moduli and bulk moduli are in good agreement with consolidation test results on frozen samples and those reported by Byrne et al. (1987) from laboratory tests.

The method proposed by Baldi et al. (1986) has been examined with a large data base of calibration test results. The results for overconsolidated sands confirm a different trend from that suggested by Baldi et al. (1986), indicating that the ratio of  $M_t/q_c$  decreases as OCR increases, despite a positive exponent for OCR in the relationship.

In this study, attempts have also been made to establish empirical correlations to evaluate  $M_t$  from CPT data. The method has been based on regression analyses on calibration chamber test results on uncemented Ticino sand and Toyoura sand with different stress history. In the framework proposed by Janbu (1963), corresponding constrained modulus

numbers, stress exponents have been determined and related to CPT test results. A series of contours have been constructed to evaluate modulus numbers for sands with different history. Accordingly, correlations have been suggested to estimate bulk modulus from CPT test results in sands. The predicted constrained moduli and bulk moduli are in good agreement with consolidation test results on frozen samples and those reported by Byrne et al. (1987) from laboratory tests. The proposed method has the advantages that it requires no earlier information of initial relative density as compared with the method suggested by Baldi et al. (1986), and its application is not limited to normally consolidated sands as compared with the method suggested by Robertson and Campanella (1983). However, a prior knowledge of OCR, is needed. In addition, the application of the above method, based on CPT results, is limited to low to medium compressible sand. Hence, sand mineralogy should be known beforehand. Experimental evidence indicates that the penetration of the cone alters almost completely the previous stress and strain history of the sand (Baldi et al., 1986). Hence, in such circumstances, Seismic CPT which can provide insight into sands of different mineralogy and stress history, is preferred.

Reference	N.C. sand		O. C. sand	
	No. of sands	$\alpha_M$	No. of sands	$\alpha_M$
Veismanis (1974)	3	3 - 11	3	5 - 30
Parkin et al. (1980)	1	3 - 11	1	5 - 30
Chapman and Donald (1981)	1	3 - 4 3 absolute lower limit	1	8 - 15 12 = average
Baldi et al. (1979)	1	>3	1	3 - 6

Table 4.1 Summary of Calibration Chamber test results for constrained modulus factor  $\alpha_M$  (after Lunne and Kleven, 1981)

Dr	m	k <sub>B</sub>
25	0.25	200
50	0.25	350
75	0.25	500
100	0.25	700

where,

$$B_t = k_B P_a (\sigma'_3 / P_a)^m$$

k<sub>B</sub> = the bulk modulus number

m = the stress exponent

P<sub>a</sub> = atmospheric pressure

σ'<sub>3</sub> = the minor principal effective stress

Table 4.2 Average sand compressibility parameters from laboratory tests  
(after Byrne et al., 1987)

	Massey		Kidd		Reference
Dr (%)	10	35	25	50	
$k_M$	520	730	630	680	Fig. 4.6
$M_t$ (MPa)	31	46	37	52	Eq. 4.10
$k_B$	310	440	380	410	Fig. 4.8
$B_t$ (MPa)	19	28	22	31	Eq. 4.14
$M_t$ (MPa)	25	43	19	40	Frozen samples
$B_t$ (MPa)	9	24	15	32	Byrne et al., 1987

Table 4.3 Evaluation of proposed method of estimation of sand compressibility using SCPT

	Massey		Kidd		Reference
$D_r$ (%)	10	35	25	50	
$k_M$	410	520	440	670	Fig. 4.11
$M_t$ (MPa)	41	60	45	75	Eq. 4.10
$k_B$	250	320	260	440	Fig. 4.13
$B_t$ (MPa)	25	36	27	45	Eq. 4.14
$M_t$ (MPa)	25	43	18	40	Frozen samples
$B_t$ (MPa)	9	24	15	33	Byrne et al., 1987

Table 4.4 Evaluation of the proposed method of estimation of sand compressibility using CPT



Sand	Depth m	$\sigma'_{vo}$ kPa	OCR	$K_o$	$\sigma'_{mo}$ kPa	$q_L$ MPa	Dr %	$k_M$	Constrained Modulus, $M_1$ , MPa			
									Lunne & Christ. (1983)	Robertson & Camp. (1983)	Baldi et al. (1986)	Eslaamizaad & Robertson (1997)
Holmen	6	79	1	0.4	47.2	2.30	18	300	9.2	25	25.3	28.2
	10	117	1	0.4	70.4	3.10	16	360	12.4	37	34.1	36.6
	16	175	1	0.4	105	5.10	26	450	20.4	54	51.1	49.6
Sleipner	6	60	4-16	0.8- 1.6	52-84	60	>100	1180- 1560	250	80	360 - 480	109 - 144
	10	100	2.3-9	0.6- 1.2	73-113	60	>100	1220- 2000	250	110	270 - 420	120 - 197
	16	160	2-6	0.5- 1.0	96-160	58	>100	1440- 2100	250	130	230 - 320	150 - 219

Table 4.5 Validation of the proposed method of estimation of constrained modulus in sands (after Lunne, 1996)

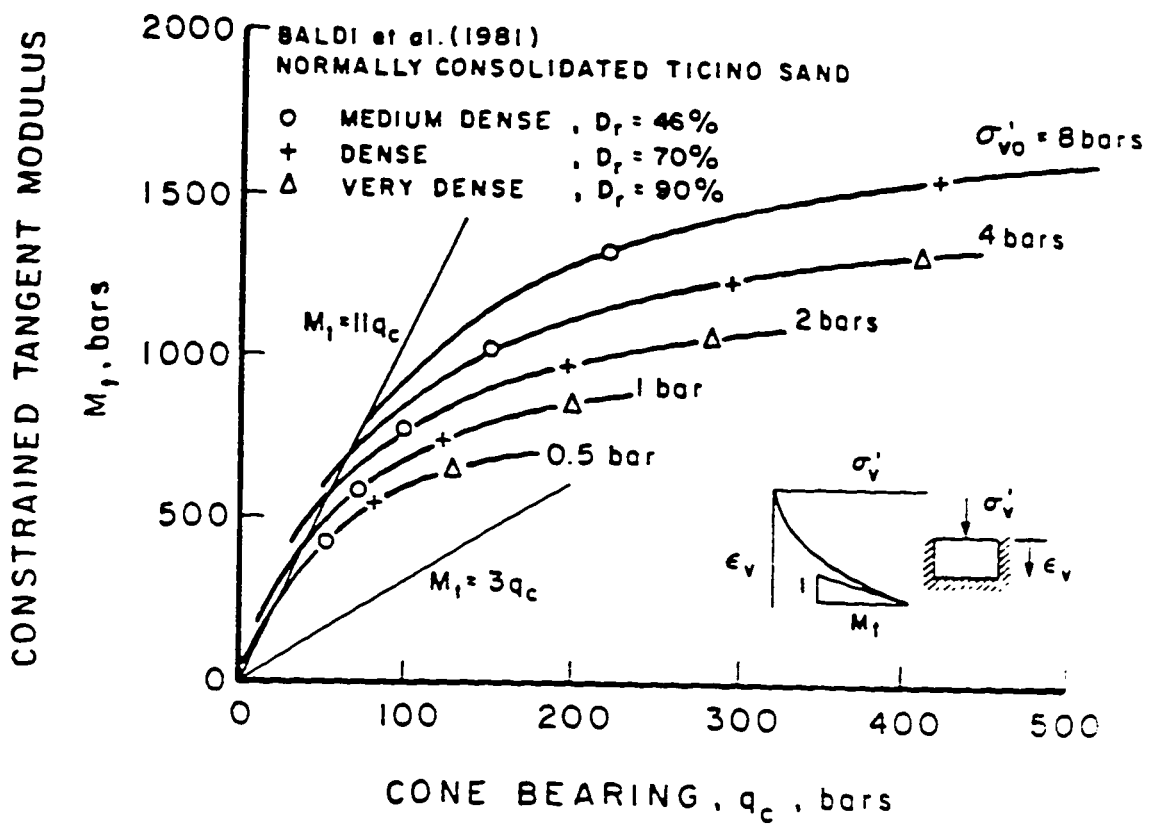


Fig. 4.1 Relationship between cone penetration resistance and constrained modulus for normally consolidated, uncemented quartz sands. (after Robertson and Campanella, 1983)

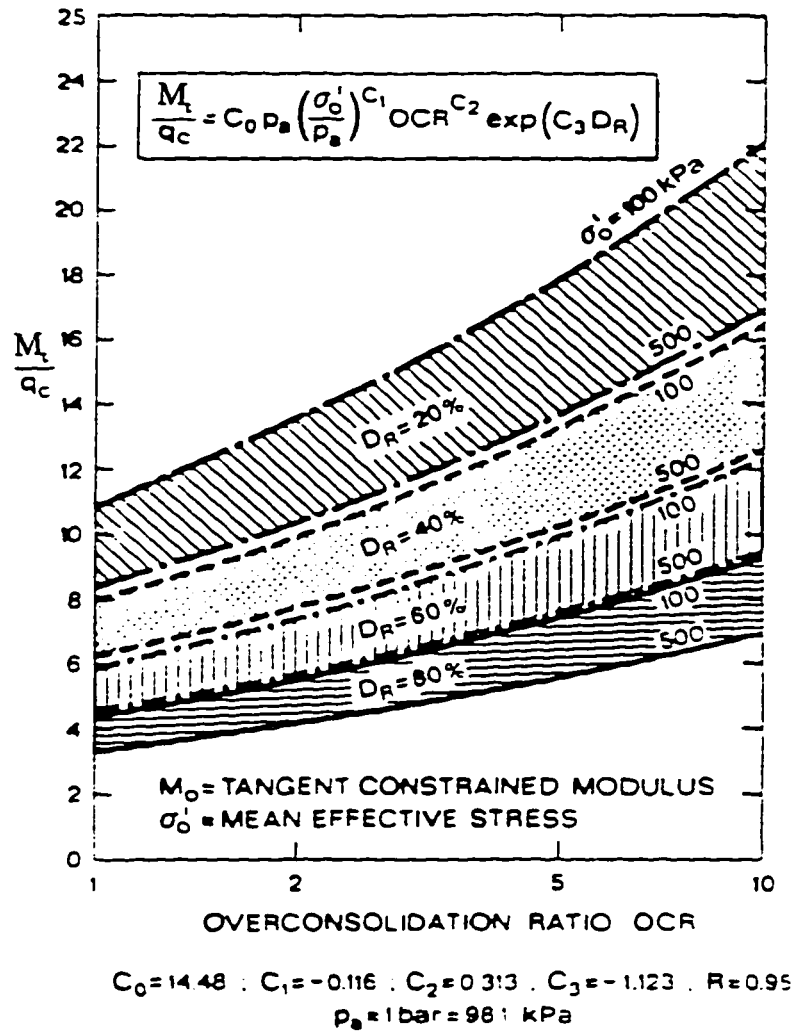


Fig. 4.2 Relationship between cone penetration resistance and constrained modulus for N.C. and O.C., uncemented unaged quartz sands. (after Baldi et al., 1986)

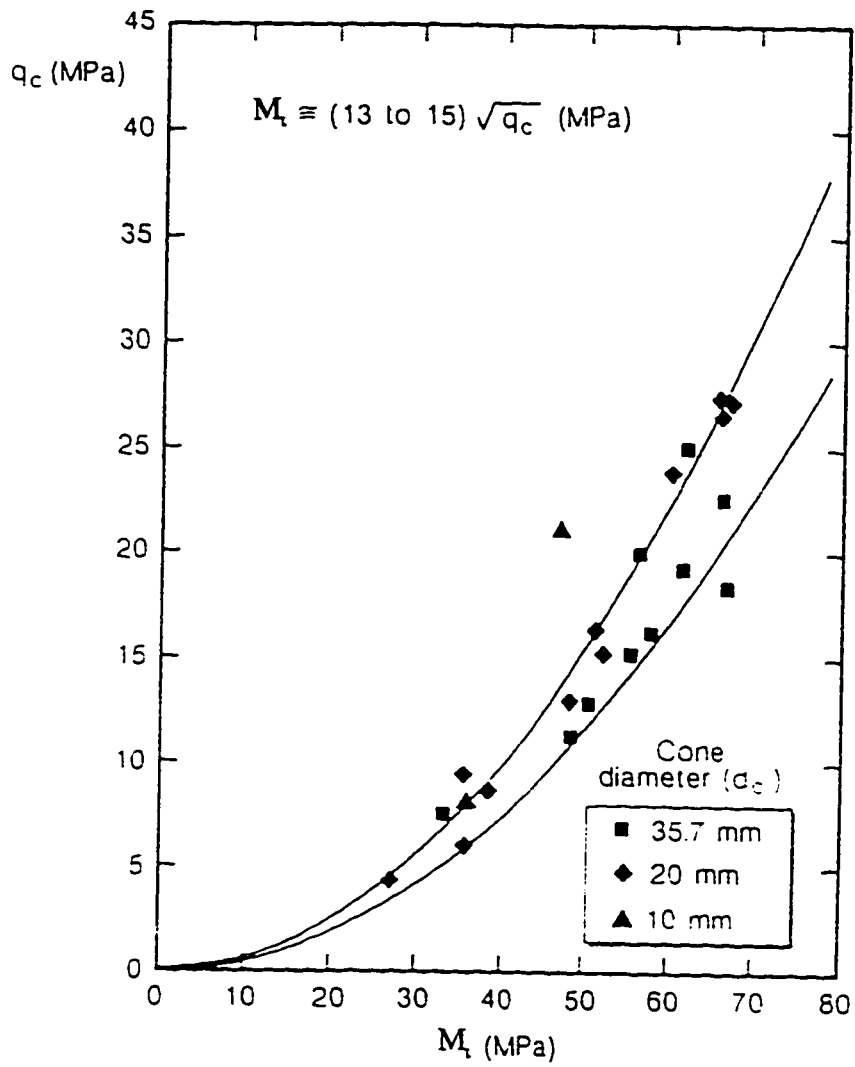


Fig. 4.3 Constrained modulus vs cone resistance based on calibration chamber tests in Toyoura sand. (after Fioravante et al., 1991)

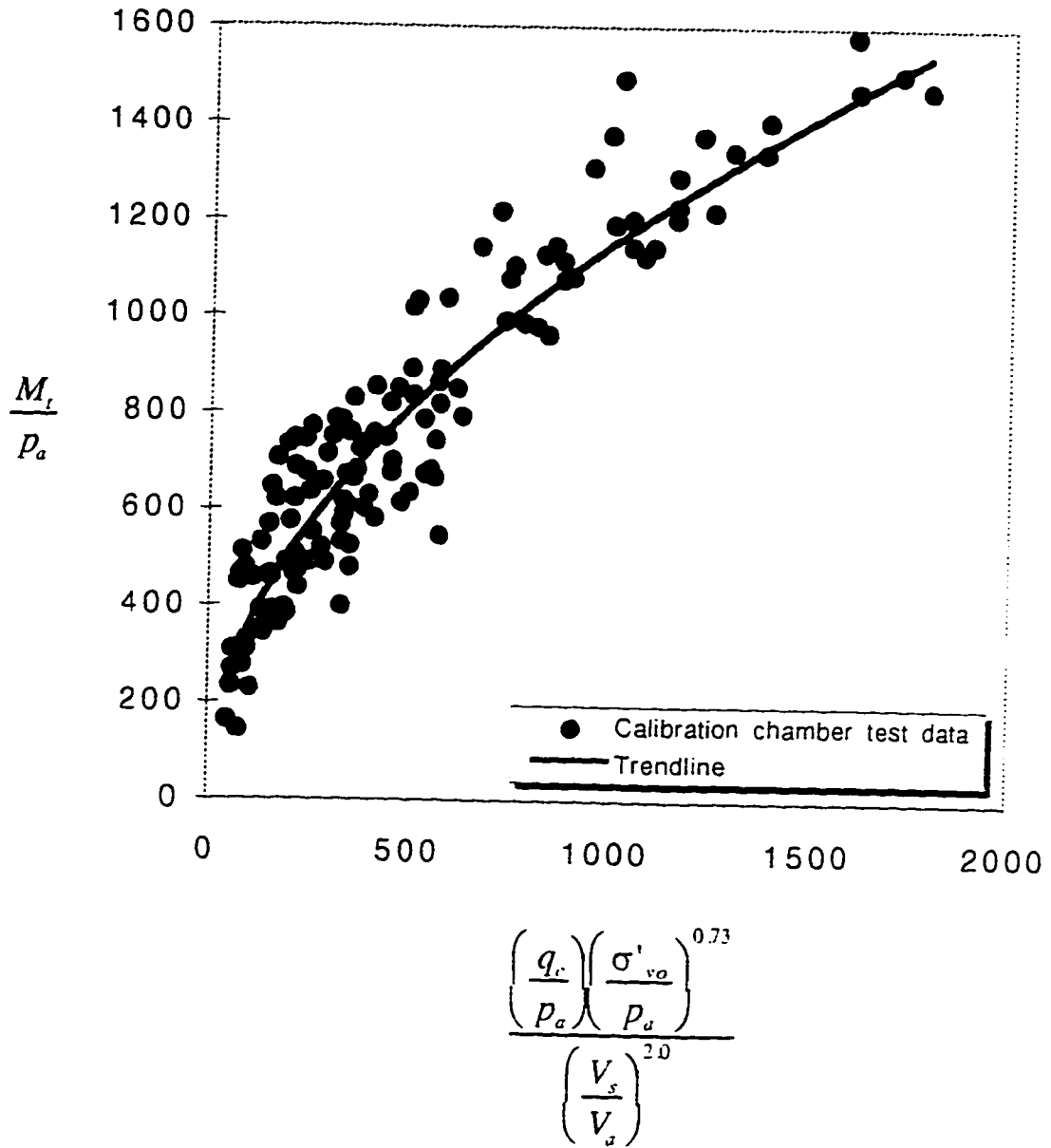
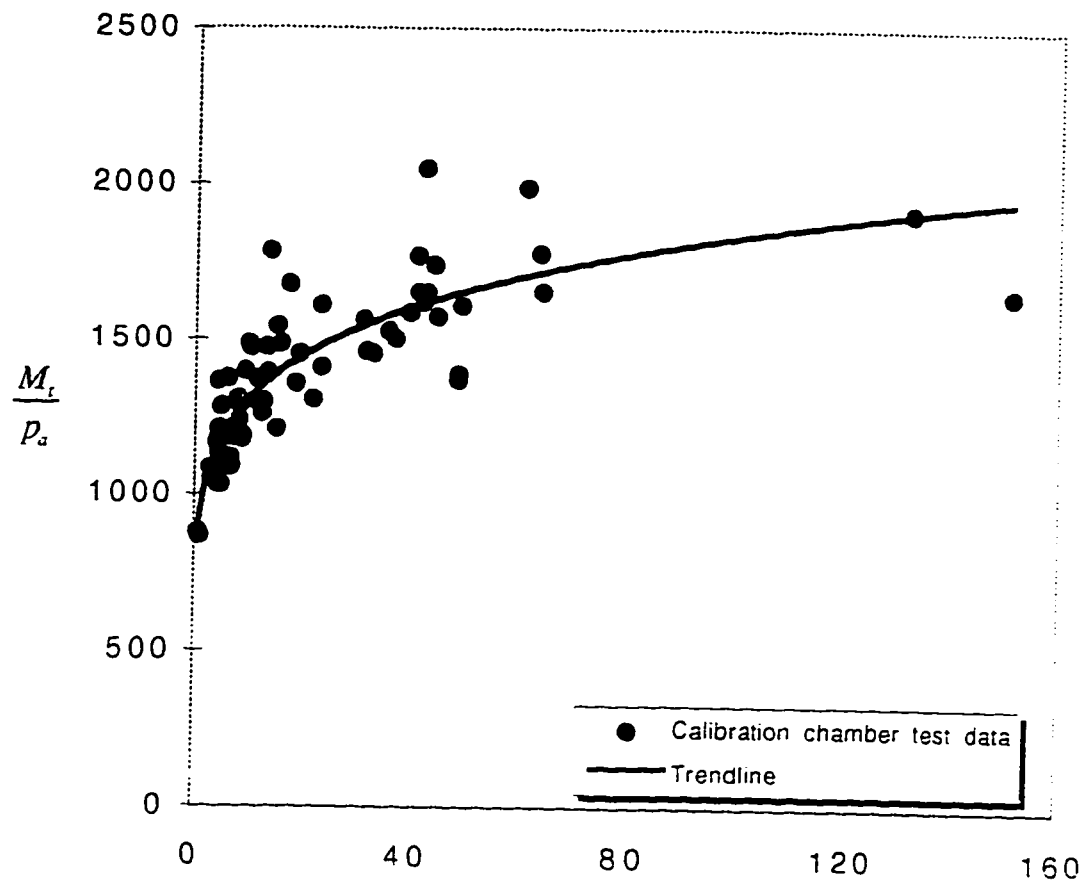


Fig. 4.4 Correlation between  $M_t$ ,  $q_c$  and  $V_s$  for normally consolidated uncemented sands.



$$\frac{\left(\frac{q_c}{p_a}\right) \left(\frac{\sigma'_{vo}}{p_a}\right)^{2.26}}{\left(\frac{V_s}{V_a}\right)^{2.0} (OCR)^{2.20}}$$

Fig. 4.5 Correlation between  $M_t$ ,  $q_c$ ,  $V_s$  and OCR for overconsolidated uncemented sands.

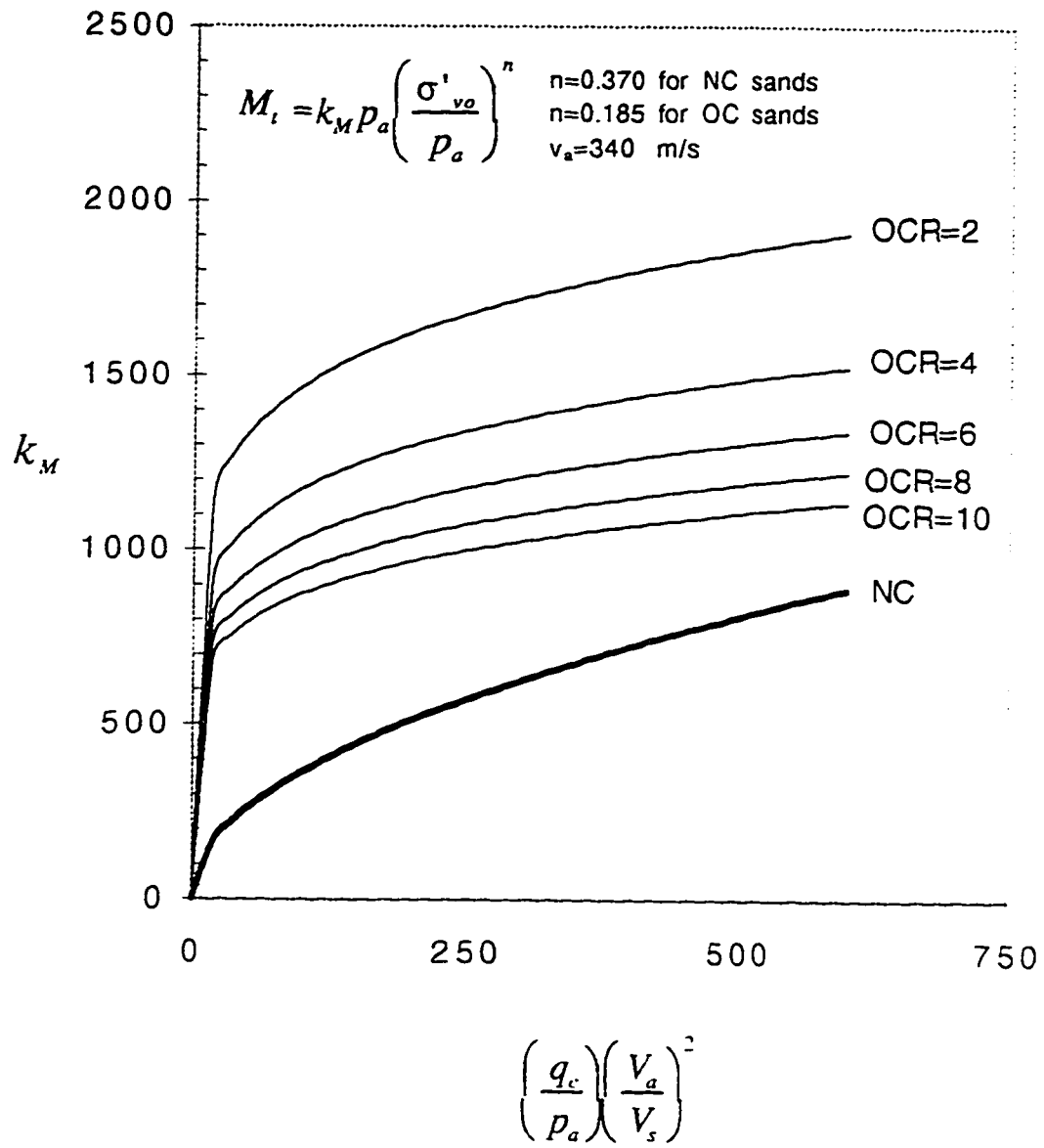


Fig. 4.6 Relationship between  $k_M$ ,  $q_c$  and  $V_s$  for uncemented sands.

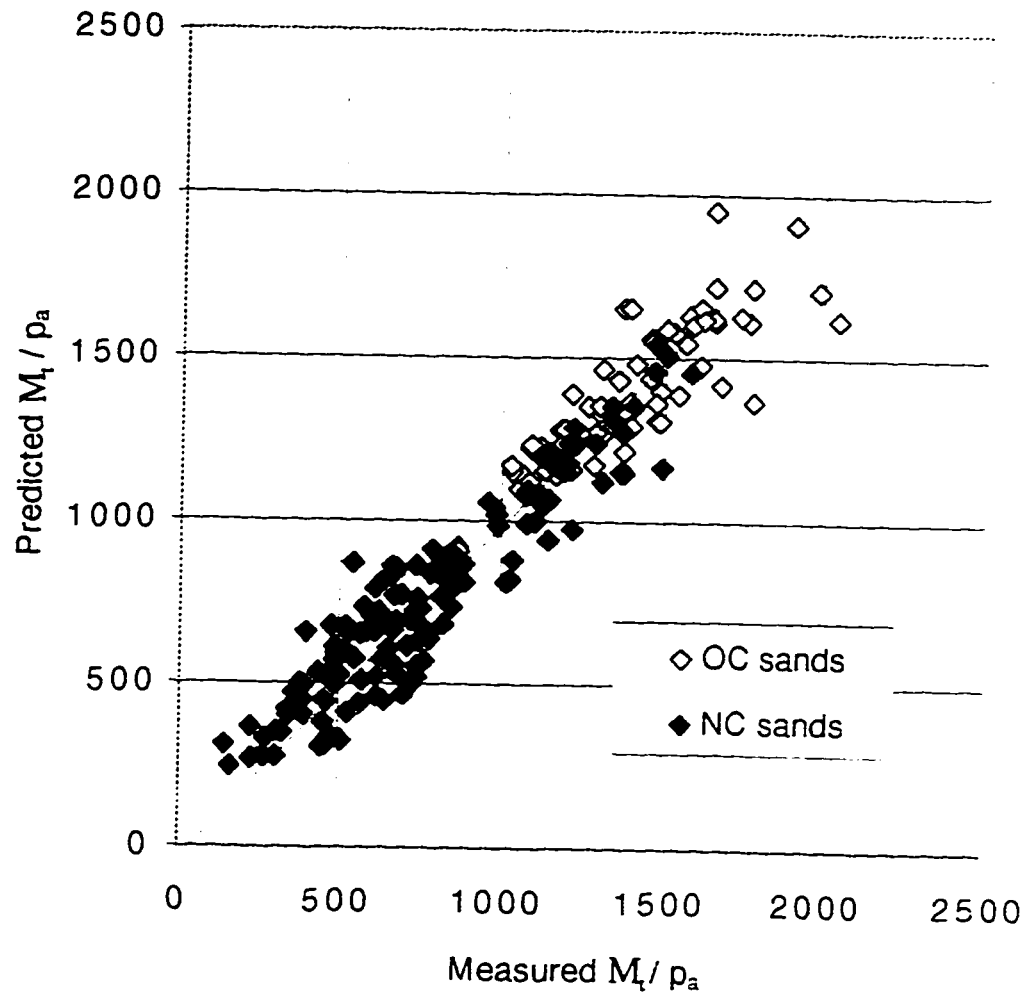


Fig. 4.7 Predicted versus measured normalized constrained modulus (using Eq. 4.9 and 4.12)



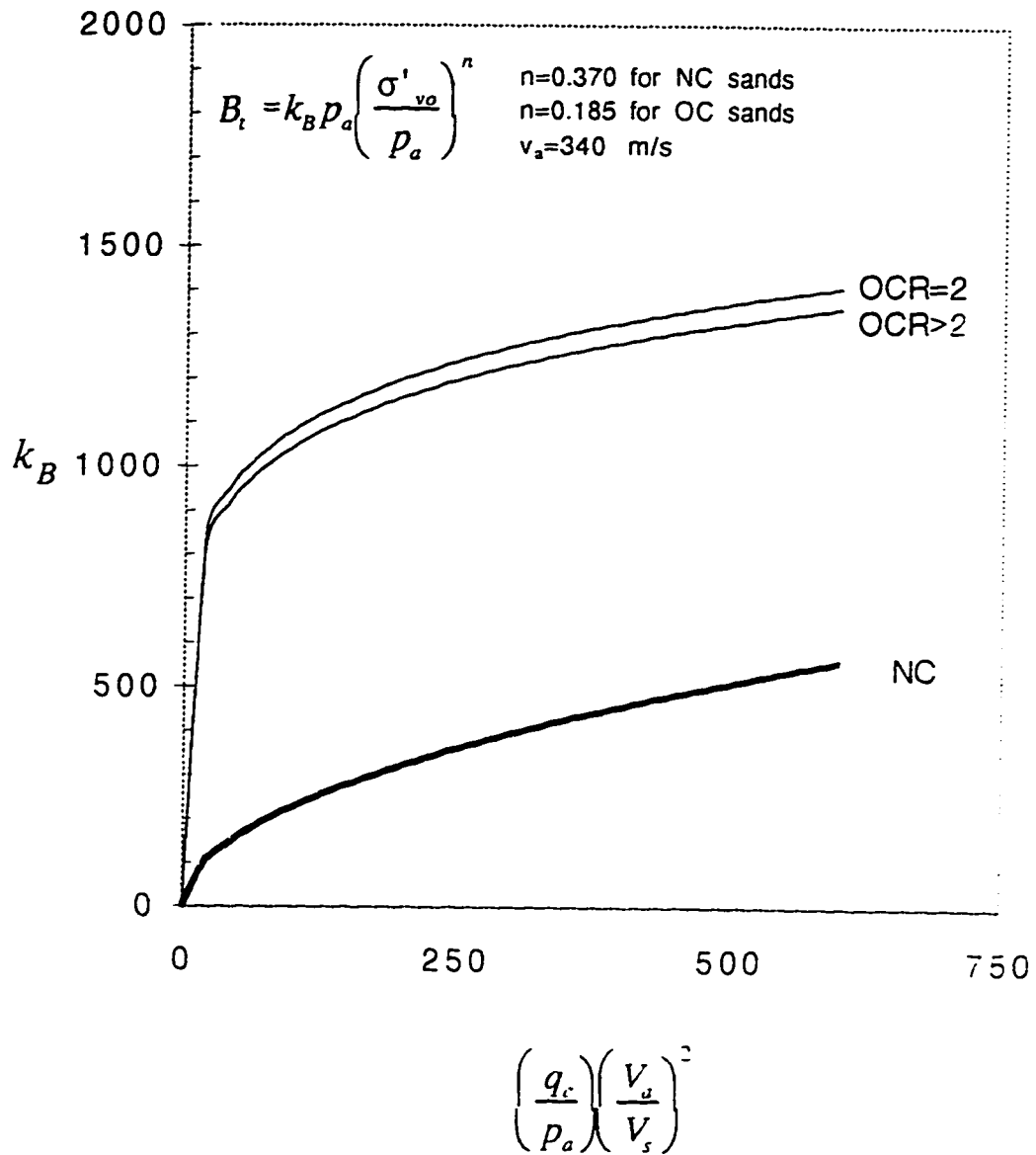


Fig. 4.8 Relationship between  $k_B$ ,  $q_c$  and  $V_s$  for uncemented sands.

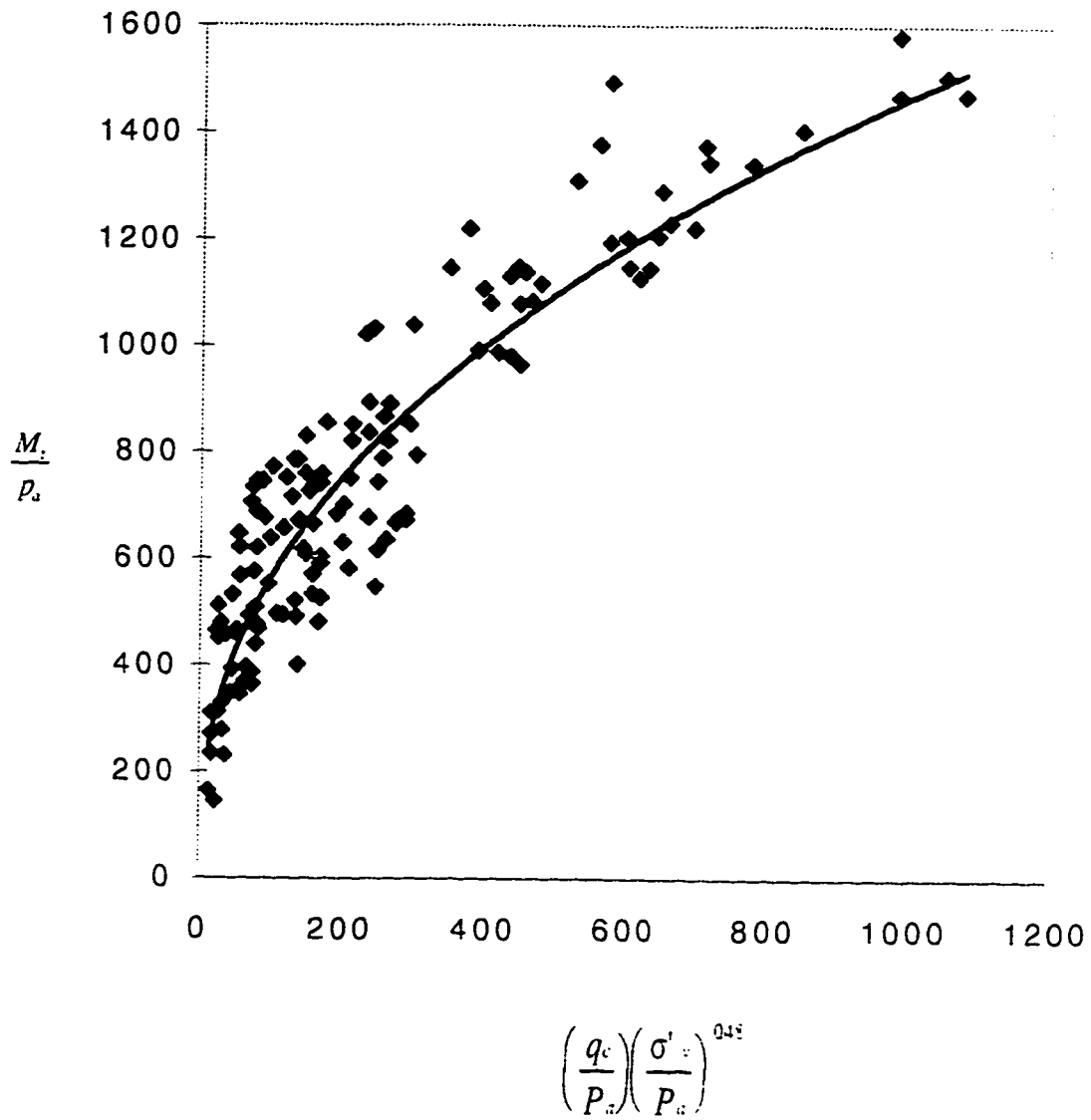


Fig. 4.9 Correlation between  $M_t$  and  $q_c$  for normally consolidated uncemented sands.

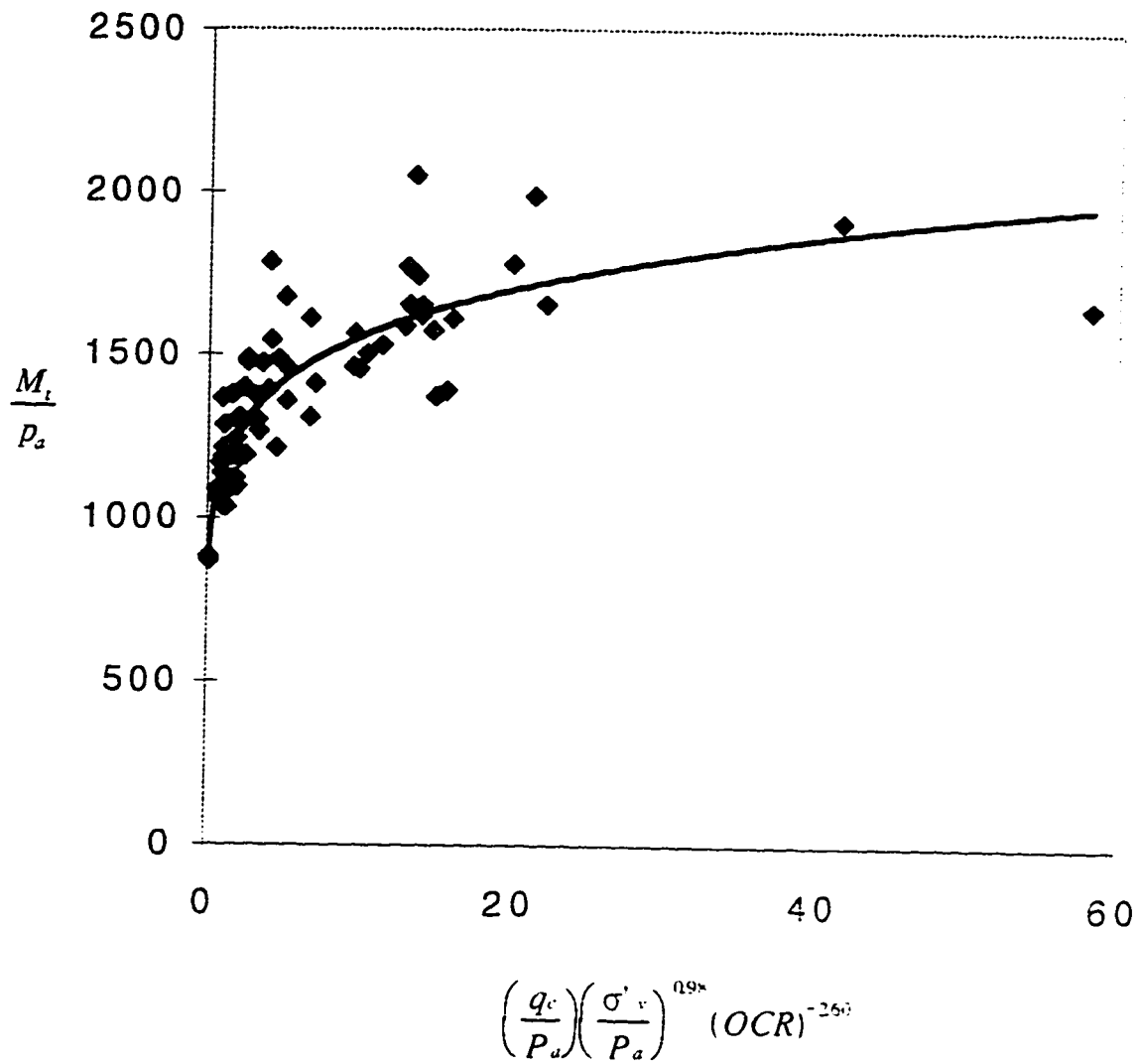


Fig. 4.10 Correlation between  $M_t$ ,  $q_c$  and OCR for overconsolidated uncemented sands.

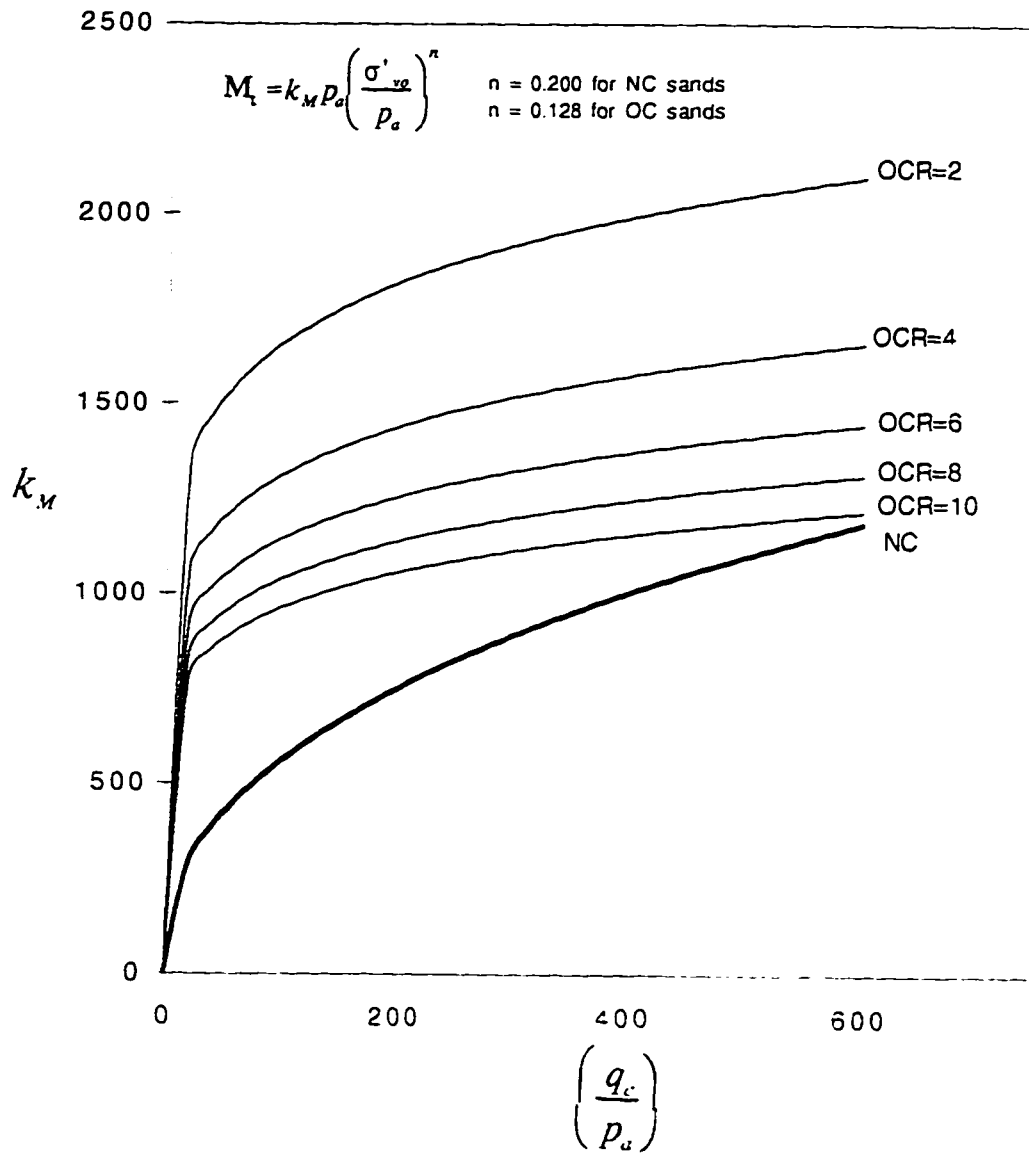


Fig. 4.11 Relationship between  $k_M$  and  $q_c$  for uncemented sands.

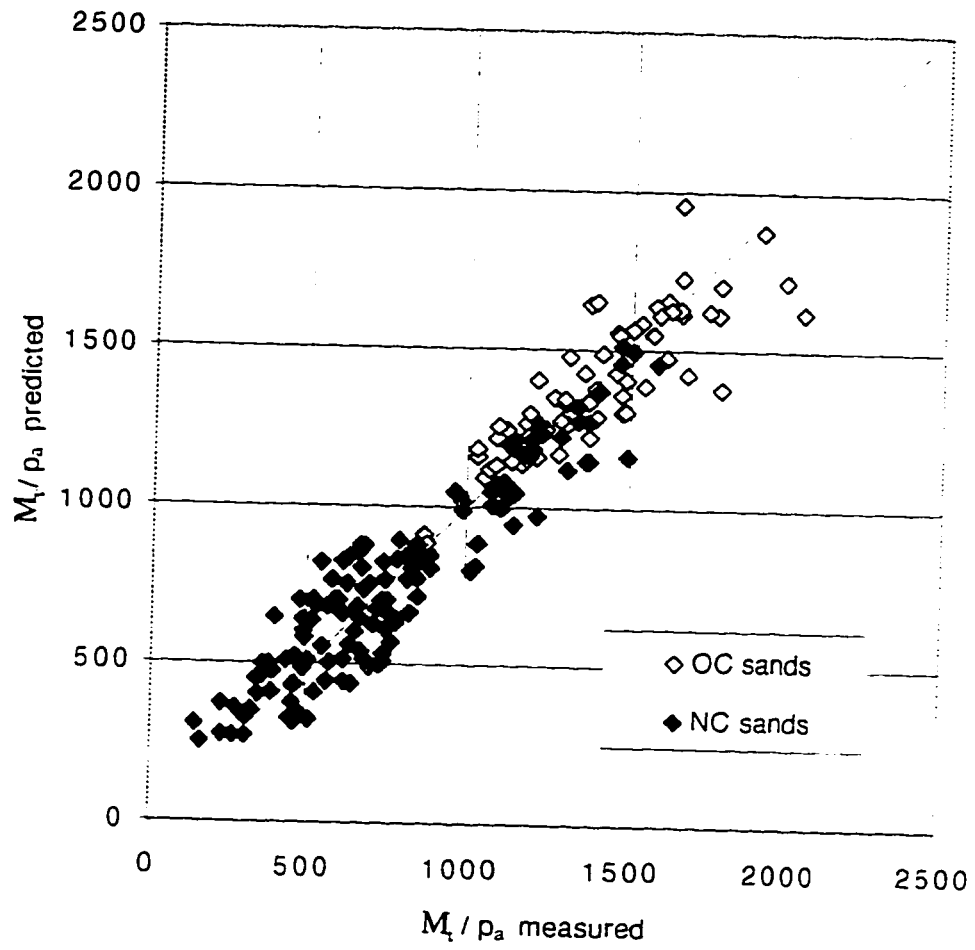


Fig. 4.12 Predicted versus measured normalized constrained modulus.  
(using Eq. 4.18 and 4.20)

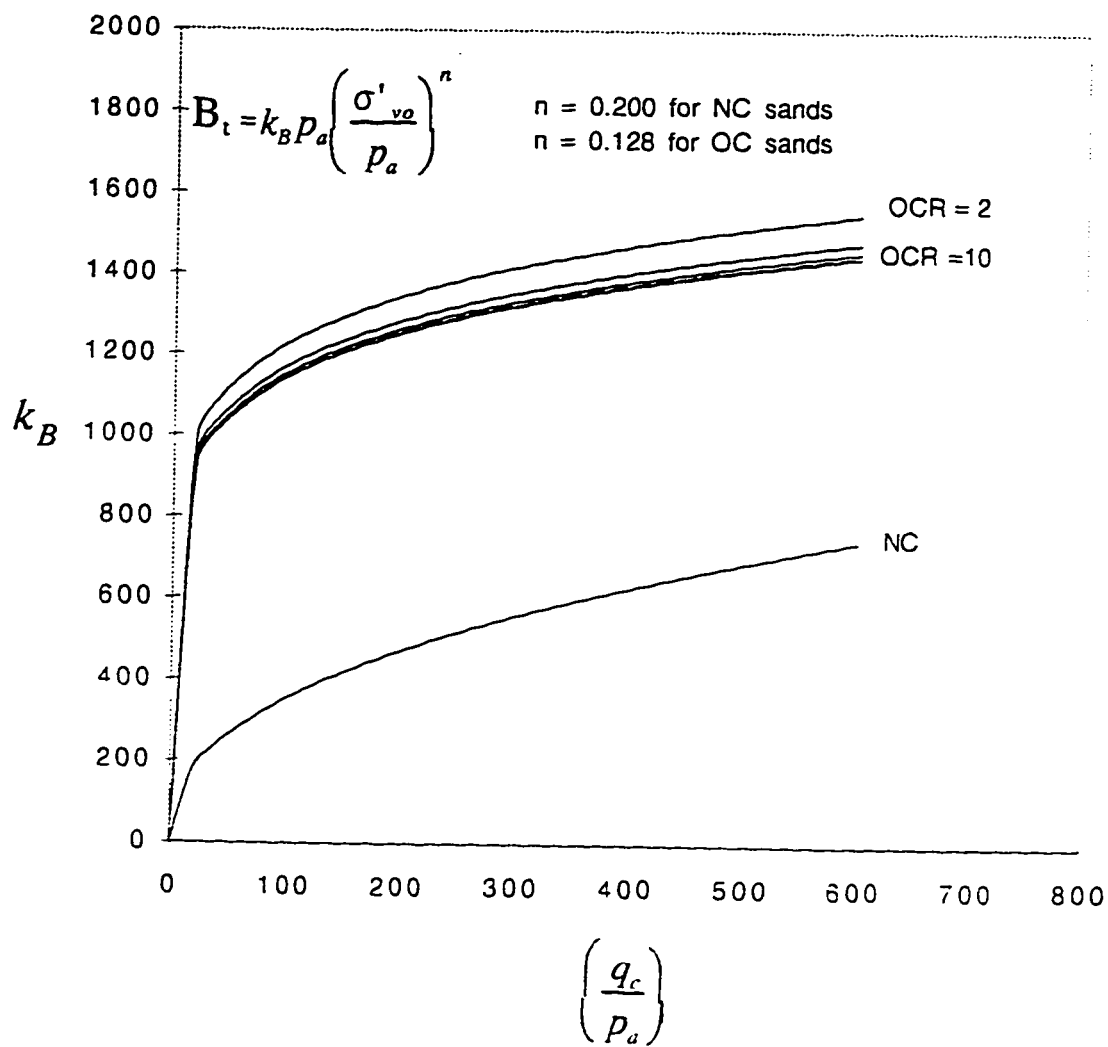


Fig. 4.13 Relationship between  $k_B$  and  $q_c$  for uncemented sands.

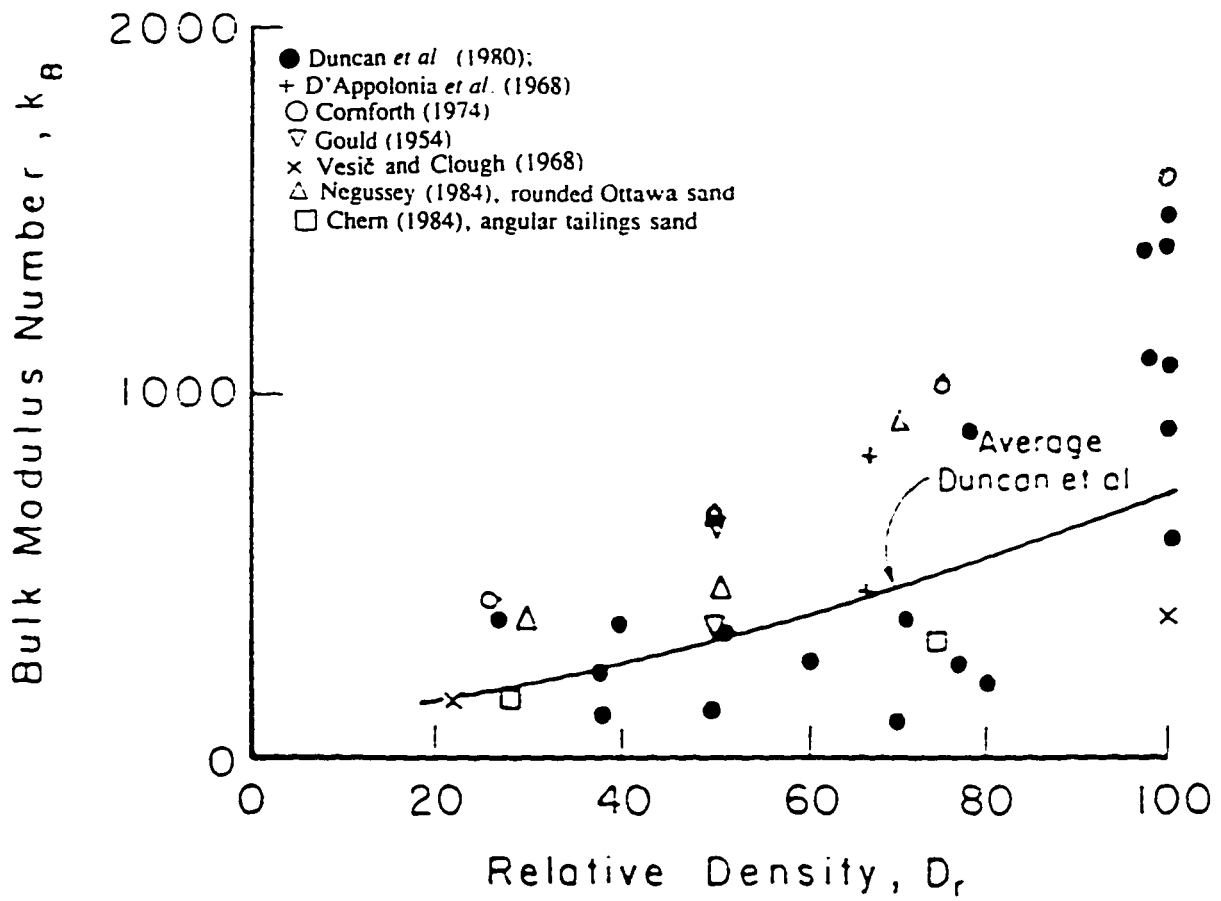


Fig. 4.14  $k_B$  values from laboratory and field tests.  
(after Byrne *et al.*, 1987)

## References

- Baldi G., Bellotti R., Ghionna V., Jamiolkowski M. and Pasqualini E. 1981. Cone resistance of a dry medium sand. Proceedings of Tenth International Conference on Soil Mechanics and Foundation Engineering, Stockholm, Vol. 2, pp. 427-432.
- Baldi G., Bellotti R., Ghionna V., Jamiolkowski M. and Pasqualini E. 1982. Design parameters for sands from CPT. Proceedings of second European symposium on penetration testing, ESOPT II, Amsterdam, May 1982, Vol. 2, pp. 425-438.
- Baldi G., Bellotti R., Ghionna V., Jamiolkowski M. and Pasqualini E. 1986. Interpretation of CPT's and CPTU's 2nd Part: Drained Penetration of Sands. Proceedings of Fourth International Geotechnical Seminar on Field Instrumentation and In-situ Measurements, Singapore.
- Baldi, G., Bellotti, R., Ghionna, V., Jamiolkowski M. and Lo Presti D.C.F. 1989. Modulus of sands from CPT's and DMT's. Proceedings, XII International Conference of Soil Mechanics and Foundation Engineering, Vol. 1, pp. 165-170., Rio De Janeiro.
- Byrne, P. M., Cheung, H., and Yan, L. 1987. Soil parameters for determination of sand masses. Canadian Geotechnical Journal, pp. 366-376.
- Duncan, J. M., Byrne, P. M., Wong, K. S., and Mabry, P. 1980. Strength, stress-strain and bulk modulus parameters for finite element analysis of stresses and movements in soil masses. University of California, Berkeley, CA, Report no. UCB/GT/80-01.
- Eslaamizaad, S. and Robertson, P.K. 1996a. A Framework for In-Situ Determination of Sand Compressibility, Proceedings of the 49th Canadian Geotechnical Conference, St. John's, Newfoundland, Canada, pp. 419-428.
- Eslaamizaad, S. and Robertson, P.K. 1996b. Estimation of in-situ lateral stress and stress history in sands. Proceedings of the 49th Canadian Geotechnical Conference, St. John's, Newfoundland, Canada, pp. 439-448.
- Eslaamizaad, S. and Robertson, P.K. 1997. Constrained modulus of sands from cone penetration testing (CPT), Submitted to the 50th Canadian Geotechnical Conference, St. John's, Ottawa, Canada.
- Fioravante V., Jamiolkowski M., Tanizawa F., and Tatsuoka F. 1991. Results of CPT's in Toyoura quartz sand., Proceedings of the First International Symposium on Calibration Chamber Testing ISOCCT1, Postdam, New York, Edited by An-Bin Haug, pp. 135-146.



- Iwasaki, K. and Tatsuoka, F. 1977. Dynamic soil properties with emphasis on comparison of laboratory tests and field measurements. Proc. 6th World Conference on Earthquake Engineering.
- Jamiolkowski, M., Ghionna V.N., Lancellotta R. and Pasqualini E. 1988. New correlations of penetration tests for design practice. Proceedings of the first international symposium on penetration testing/ ISOPT-1, Orlando, pp. 263-296
- Jamiolkowski, M., and Robertson, P.K. 1988. Future trends for penetration testing. Proceedings of conference, Penetration testing in the U.K., Birmingham, pp. 21-42.
- Janbu, N. 1963. Soil compressibility as determined by oedometer and triaxial tests, Proc. 3rd Eur. Conf. Soil Mech., Wiesbaden, Vol. 1, pp. 19-25
- Lo Presti, D. 1987. Behavior of Ticino sand during resonant column test. Ph.D. Thesis, Technological University of Turin.
- Lunne, T. 1991. Practical use of CPT correlations in sand based on calibration chamber tests. Proceeding of the International Symposium on Calibration chamber testing, Potsdam, New York, pp. 225-236,
- Lunne, T. 1996. Personal communications with P.K. Robertson and J.J.M. Powell.
- Lunne, T. and Christoffersen, H.P. 1983. Interpretation of cone penetration data for offshore sands. Proceedings, 15th Annual Offshore Technology Conf., Houston, pp. 181-192.
- Lunne, T. and Kleven, A. 1981. Role of CPT in North Sea Foundation Engineering. Proceedings, Symposium on Cone Penetration Testing and Experience, Geotechnical Engineering Division, ASCE, Oct. 1981, pp. 49-75.
- Lunne, T, Robertson, P.K. and Powell, J.J.M. 1997. CPT in Geotechnical Practice, Blackie Academic & Professional, Chapman & Hall.
- Mitchell, J.K and Gardner, W.S. 1975. In-situ measurement of volume change characteristics. State of the art report, Proceedings of the conference on in-situ measurement of soil properties, Specialty conference of the geotechnical division, North Carolina State University, Raleigh, Vol. II.
- Monahan, P. A., Luternauer, J. L., and Barrie, J. V. 1995. The geology of the CANLEX Phase II sites in Delta and Richmond, British Columbia. Proceedings of the 48th Canadian Geotechnical Conference, Vancouver, B.C., pp. 59-68.
- Rix G.J. and Stokoe K.H. II. 1991, Correlation of Initial tangent Modulus and Cone Penetration Resistance. Proceedings of the First International Symposium on Calibration Chamber Testing/ISOCCT1, Potsdam, New York, Edited by An-Bin Huang, pp. 351-362.

- Robertson, P. K. and Campanella, R. G. 1983, Interpretation of cone penetration tests.  
Part I: sand., Canadian Geotechnical Journal 20, pp. 718-733.
- Senneset, K., Janbu, N. and Svano, G. 1982. Strength and deformation parameters from cone penetration tests. Proceedings, 2nd European Symp. on Penetration Testing, Amsterdam, pp. 863-870.
- Thomas, D. 1968. Deepsounding test results and the settlement of spread footings on normally consolidated sands, Geotechnique, Vol. 18, pp. 472-488.
- Vesic, A.S. and Clough G.W. 1968. Behavior of granular materials under high stresses, Journal of Soil Mechanics and Foundations Division, ASCE, Vol. 94, No. SM3, pp. 661-688.
- Vesic, A.S. 1970. Tests on instrumented piles, Journal of Soil Mechanics and Foundations Division, ASCE, Vol. 96, No. SM2, pp. 561-584.

## CHAPTER 5

### EVALUATION OF IN-SITU LATERAL STRESS AND OCR IN UNCEMENTED SANDS<sup>1</sup>

#### 5.1 Introduction

A knowledge of the initial stress state is of great importance for the geotechnical characterization of natural and man-made soil deposits. However, a reliable procedure for determining horizontal in-situ stress has not yet been established for cohesionless soils. In addition, due to inherent difficulties in measuring or choosing an appropriate in-situ horizontal stress and assessing the stress history of natural sand deposits, the application of most of the existing empirical correlations for the CPT can be somewhat limited. Unfortunately, it is not possible to identify stress history of cohesionless soils directly from CPT data during drained penetration.

Traditionally many natural sands have been considered to be normally consolidated. However, considerable evidence exists to suggest that most natural sands with an age greater than about 1000 years behave similar to overconsolidated sands for most loading conditions. This is probably due to one or more of the following factors: aging, cementation, stress and strain history. The same factors have been recognized for some time to produce similar apparent preconsolidation in many clay soils (Robertson, 1990). The stress history and age of the deposit are among the important factors which control the soil modulus, and hence, the deformation characteristics of the soil. Extensive studies of penetration testing in calibration chamber have shown that the stiffness of sands is very sensitive to stress history. However stress history effects can be due to changes in horizontal effective stresses as well as strain hardening due to accumulated plastic strains. The increases in horizontal effective stresses are conventionally linked with mechanical overconsolidation, whereas strain hardening generally appears as a consequence of either,

---

<sup>1</sup> A version of part of this chapter has been published. *Eslaamizaad, S. and Robertson P.K. 1996. Estimation of in-situ lateral stress and stress history in sands, Proc. of the 49th Canadian Geotechnical Conference, St. John's, Newfoundland, 439-448.*

aging, desiccation, and/or low strain cyclic history. Calibration chamber studies have shown that penetration resistance is strongly influenced by the current level of horizontal effective stress and is almost totally insensitive to the effects of plastic strain hardening due to loading and unloading processes (Baldi et al, 1986).

Experimental evidence indicates that the penetration of the cone alters almost completely the previous stress and strain history of the sand (Baldi et al. 1986). Nevertheless, cone penetration resistance ( $q_c$ ) is strongly influenced by the current level of horizontal effective stress ( $\sigma'_{ho}$ ) (e.g. Baldi et al. 1986, and Parkin 1988). On this basis, Parkin (1988) suggested an empirical expression in the form of

$$[5.1] \quad \sigma'_{ho} = A q_c^2$$

for relatively dense sands regardless of the influence of stress history. Housby and Hitchman (1988) also noted a similar power function expression relating  $\sigma'_{ho}$  and  $q_c$ , but for a wide range of relative densities.

Kulhawy et al. (1989) obtained a relationship between  $K_o$ ,  $\phi'$ , and the normalized cone tip resistance ( $q_c/\gamma B$ ) based on the Durgunoglu and Mitchell theory (1979). Figure 5.1 illustrates this correlation for various depths of cone penetration. The width of the standard cone,  $B$ , is 35.7 mm, and depth,  $D$ , is included in the dimensionless ratio,  $D/B$ . This method requires a prior knowledge of effective stress friction angle of the sand.

Based on the assessment of CPT calibration chamber data compiled from 26 different test series on uncemented clean quartz sands, Mayne (1991,1995) developed an iterative approach which uses cone penetration resistance ( $q_c$ ) data. It requires an evaluation of OCR and estimation of soil compressibility beforehand. The method relates the effective horizontal stress  $\sigma'_{ho}$ , to the measured cone tip resistance  $q_c$  as a function of relative density  $D_r$ :

$$[5.2] \quad \sigma'_{ho} = (q_c)^{1.6} 10^{(1.144 - 0.0186 D_r)}$$

By including the effects of overconsolidation ratio OCR and effective vertical stress  $\sigma'_{vo}$ , an iterative approach can be used to obtain the in-situ  $\sigma'_{ho}$  from the following cumbersome expression:

$$[5.3] \quad \frac{\sigma'_{ho}}{P_a} = \frac{(q_c/P_a)^{1.6}}{145 \exp \left( \left[ \frac{(q_c/P_a)}{12.2(OCR)^{0.2}(\sigma'_{vo}/P_a)^{0.5}} \right]^{0.5} \right)}$$

A relationship between  $K_o$  and OCR, as developed by Mayne and Kulhawy (1982) is recommended to be used in the iteration.

A method by Masood and Mitchell (1993), which uses measured sleeve friction ( $f_s$ ), also requires an *a priori* knowledge of stress history. The method relates the unit sleeve friction measured during the penetration of a cone penetrometer and the effective stress friction angle of the displaced soil ( $\phi'$ ) and the effective overburden pressure  $\sigma'_v$ , assuming the angle of friction between soil and the sleeve is one third of the effective stress friction angle  $\phi'$ . On this basis, they recommended the following expression:

$$[5.4] \quad f_s = \sigma'_v \cdot \tan^2 \left( 45 + \frac{\phi'}{2} \right) \cdot \tan \left( \frac{\phi'}{3} \right)$$

Equation 5.4 can be solved to obtain the effective stress friction angle  $\phi'$  from the measured unit sleeve friction  $f_s$ . Then, the coefficient of earth pressure at rest  $K_o$  can be estimated using Jaki's (1944) formulae and the relationship between  $K_o$  and overconsolidation ratio OCR suggested by Mayne and Kulhawy (1982) where OCR should be known. Figure 5.2 illustrates the correlation by Masood and Mitchell from which  $K_o$  can be estimated using the normalized parameter  $f_s/\sigma'_v$  and OCR. The reliability of the method depends on the accuracy of the sleeve friction measurements and a knowledge of OCR. However, it is widely agreed that the sleeve friction is the least reliable and repeatable parameter in cone penetration testing.

Geotechnical engineers often use penetration resistance from the CPT to estimate the small strain shear modulus,  $G_o$ . Several correlations have been developed, mainly based on calibration chamber test and resonant column test results, to relate  $G_o$  with CPT tip resistance  $q_c$  for sands where the grain minerals are predominantly quartz (Robertson and Campanella 1983, Baldi et al. 1986, Jamiolkowski and Robertson 1988, Baldi et al. 1989, Fioravante et al. 1991, Rix and Stokoe 1991). However, with the advent of the seismic CPT (SCPT) in which both the cone resistance and small strain shear modulus are measured during the same sounding in the same soil, the application of such correlations is not justified in practice. During the SCPT, the shear wave velocity ( $V_s$ ) can be measured. Based on elastic theory, the small strain shear modulus ( $G_o$ ) can be determined from the seismic shear wave velocity ( $V_s$ ) using:

$$[5.5] \quad G_o = \rho(V_s)^2$$

where,  $\rho$  is soil mass density.

In this chapter, it is shown that a correlation between  $G_o$  and  $q_c$  is found to be highly dependent on the in-situ horizontal stress. Hence, the potential exists to evaluate in-situ horizontal stress for uncemented cohesionless soils using the SCPT measuring in-situ cone penetration resistance ( $q_c$ ) and small strain shear modulus ( $G_o$ ). A method is developed to evaluate in-situ lateral stresses in cohesionless deposits using the results from the SCPT. A large published database derived from 3 different series of CPT calibration chamber and resonant column tests on sands with different stress history and compressibility was reviewed to investigate a relationship between  $G_o$ ,  $q_c$  and  $\sigma'_{ho}$ .

High in-situ horizontal stresses are conventionally linked with mechanical overconsolidation. Hence, for uncemented sands which have experienced a simple load/unload history caused by mechanical overconsolidation a relationship should exist between the coefficient of earth pressure at rest,  $K_o = \sigma'_{ho}/\sigma'_{vo}$  and OCR. On this basis, a tentative procedure is also presented for estimating stress history of cohesionless deposits from the predicted coefficient of earth pressure at rest.

## 5.2 Evaluation of in-situ lateral stress in sands

Extensive studies have been conducted by several researchers (Robertson and Campanella 1983, Baldi et al. 1986, Jamiolkowski and Robertson 1988, Baldi et al. 1989, Fioravante et al. 1991, Rix and Stokoe 1991) to relate small shear modulus,  $G_o$ , with cone penetration resistance,  $q_c$ , performed in unaged, uncemented predominately quartz sands.

Jamiolkowski and Robertson (1988) presented a correlation in a diagram of  $G_o/q_c$  versus  $q_c/\sqrt{\sigma'_{vo}}$  for normally consolidated sand (OCR=1.0) and highly overconsolidated sand (OCR=10.0), where  $\sigma'_{vo}$  is the vertical effective stress. Baldi et al. (1989) noted that although the correlation was derived based on data for recently deposited, unaged sand, the results show good agreement with data of natural cohesionless soil deposits with an age of 3,000 years to 20,000 years at a maximum depth of 30 m. On this basis, Baldi et al. (1989) proposed a tentative correlation between  $G_o$  and  $q_c$  in a diagram of  $G_o/q_c$  versus  $q_c/\sqrt{\sigma'_{vo}}$  for uncemented predominantly silica sands in which, the influence of horizontal effective stress and hence, stress history on the relationship is shown by lines for overconsolidation ratios of 1 and 10 (see Fig. 2.5 in Chapter 2). Rix and Stokoe (1991) explained that these lines account for the residual horizontal stresses due to overconsolidation. These correlations can be expressed in the form of:

$$[5.6] \quad \frac{G_o}{q_c} = A \cdot \left( \frac{q_c}{\sqrt{\sigma'_{vo}}} \right)^B \cdot (OCR)^C$$

A, B and C have been back-calculated, in this study, as (1454, -0.758 and 0.053), respectively, from the diagram by Jamiolkowski and Robertson (1988) and, (970, -0.706 and 0.103) from the diagram by Baldi et al. (1989).

Rix and Stokoe (1991) examined the correlation suggested by Baldi et al. (1989) with data from a series of calibration chamber tests performed in washed mortar sand as well as in-situ seismic measurements and cone penetration tests in sands at the Herber Road site in the Imperial Valley of California. As a result, they proposed a correlation similar to Eq. 5.6 where A and B are equal to 1634 and -0.75 respectively. Rix and Stokoe (1991) did not include the influence of stress history in their correlation. However, they noted that parameter A varies between 817 and 2451. They further concluded that there may be factors such as fines content, particle angularity, and particle mineralogy that influence  $G_o$ .

and/or  $q_c$  that are not included in these correlations. In other words, they stated that these correlations may suffer from the influence of soil compressibility, although their applications have been primarily limited to low compressible silica sands.

Eslaamizaad and Robertson (1996a), also given in Chapter 2, investigated the influence of soil compressibility in its broadest sense, including grain crushibility on the above correlations. They concluded that sands with different compressibility plot essentially within the same band. The results suggest that the relationship between  $G_o$  and  $q_c$  is not highly influenced by soil compressibility. Hence, the potential exists to estimate stress history in uncemented sands with different compressibility from the correlation between small strain shear modulus and cone penetration resistance. This can be accomplished using the seismic CPT in which both the cone resistance and small strain shear modulus are measured during the same sounding in the same soil. However, it should be noted that such a correlation will be strongly influenced by the presence of cementation (Eslaamizaad and Robertson, 1996b), also given in Chapter 3.

Cone penetration resistance in uncemented, unaged sands is basically controlled by relative density ( $D_r$ ), vertical effective stress ( $\sigma'_{vo}$ ) and horizontal effective stress ( $\sigma'_{ho}$ ). An expression used for the relationship between cone penetration resistance, relative density and effective stresses for clean, uncemented and unaged sands is :

$$[5.7] \quad \frac{q_c}{p_a} = C_o \left( \frac{\sigma'_{vo}}{p_a} \right)^{C_1} \left( \frac{\sigma'_{ho}}{p_a} \right)^{C_2} \text{Exp}(C_3 D_r)$$

where  $C_2$  is reported to be about three times  $C_1$  for both Ticino sand and Toyoura sand. This illustrates the significance of horizontal stress on the cone penetration resistance.

Based mainly on the results of resonant column tests on reconstituted sand, the small strain shear modulus can be related to the mean effective stress  $p'$  and either void ratio or relative density. However, there is evidence to show that small strain shear modulus does not depend equally on all three principal stresses as often implied by the use of the mean effective stress. From the measurement of shear wave velocity in cubical samples of freshly deposited, uncemented sand, Roesler (1979) showed that the variation of shear modulus with stress can be given in the form of:



$$[5.8] \quad \frac{G_o}{p_a} = C \left( \frac{\sigma'_a}{p_a} \right)^m \left( \frac{\sigma'_b}{p_a} \right)^n$$

where  $C$  is a function of soil grain characteristics, soil fabric and void ratio,  $\sigma'_a$  and  $\sigma'_b$  are the effective stresses in the directions of seismic wave propagation and soil particle motion, respectively, and that the third principal stress has no effect. This concept has been supported by Knox et al. (1982), Yu and Richart (1984), and Lee and Stokoe (1986). In practice, when down hole seismic CPT (SCPT-DH) is performed, the direction of wave propagation is essentially vertical while the direction of particle motion is horizontal. This indicates that for SCPT-DH  $\sigma'_a = \sigma'_{vo}$  and  $\sigma'_b = \sigma'_{ho}$ . In the case of cross hole seismic CPT (SCPT-XH), shear waves are usually propagated horizontally with particle motion commonly vertical. Hence, for most SCPT-XH  $\sigma'_a = \sigma'_{ho}$  and  $\sigma'_b = \sigma'_{vo}$  should be considered. For resonant column tests, Yu and Richart (1984) showed that  $m$  and  $n$  are in general both close to 0.25. This shows a similar significance of both in-situ vertical effective stress and horizontal effective stress on the measured small strain shear modulus.

Equations 5.7 and 5.8 show that both  $q_c$  and  $G_o$  are dependent on the vertical and horizontal effective stresses and soil relative density. This suggests that, after eliminating the term of relative density, a correlation can be obtained in the form of:

$$[5.9] \quad \frac{G_o}{p_a} = B_o \left( \frac{q_c}{p_a} \right)^{B1} \left( \frac{\sigma'_{vo}}{p_a} \right)^{B2} \left( \frac{\sigma'_{ho}}{p_a} \right)^{B3}$$

This correlation is analogous to Eq. 5.6. Equation 5.6 can be rewritten as follows to illustrate its similarity with Eq. 5.9:

$$[5.10] \quad \frac{G_o}{p_a} = C_o \left( \frac{q_c}{p_a} \right)^{C1} \left( \frac{p_a}{\sigma'_{vo}} \right)^{C2} (OCR)^{C3}$$

in which  $C_1$  is close to 0.25.

Equation 5.9 implies that a potential exists to estimate in-situ horizontal stress from the measurement of small strain shear modulus  $G_o$ , and cone penetration resistance  $q_c$  for uncemented, unaged sands.

Based on a large number (222 tests) of published calibration chamber test results (Baldi et al. 1986, Fioravante et al. 1991 and Almeida et al. 1991) on uncemented normally consolidated and overconsolidated Ticino sand, Toyoura sand and Quiou sand, a relationship is developed for the evaluation of in-situ horizontal stress from SCPT data in the form of:

$$[5.11] \quad \frac{\sigma'_{ho}}{p_a} = \left( \frac{\left( \frac{G_o}{p_a} \right) \left( \frac{\sigma'_{vo}}{p_a} \right)^{0.13}}{334.90 \left( \frac{q_c}{p_a} \right)^{0.25}} \right)^{2.1635}$$

Toyourea sand is a quartzic sand of low compressibility which contains less than 5% fines. Ticino sand is a quartzic sand with about 5% feldspar and is a sand of moderate to low compressibility. Quiou sand contains on average about 70% of shell fragments and about 15% of calcium carbonate aggregates and hence, Quiou sand is a sand of high compressibility.

Figure 5.3 presents a summary of the calibration chamber test results in the form of Eq. 5.11. The correlation factor for the above regression analysis is  $R = 0.8959$ . It should be noted that to be consistent with previous research, the exponent of normalized small strain shear modulus and normalized cone resistance have been fixed in the regression analysis as 1.00 and 0.25, respectively. Figure 5.4 compares the predicted normalized horizontal stress (using Eq. 5.11) with the normalized horizontal stress measured in the calibration chamber tests. Equation 5.11 can be rearranged in terms of coefficient of earth pressure at rest ( $K_o$ ), small strain shear modulus ( $G_o$ ), and cone penetration resistance ( $q_c$ ) in the following form from which  $K_o$  can be evaluated:

$$[5.12] \quad \frac{G_o}{p_a} = 334.90 \left( \frac{q_c}{p_a} \right)^{0.25} \cdot \left( \frac{\sigma'_{vo}}{p_a} \right)^{0.332} \cdot K_o^{0.462}$$

A large portion of the published calibration chamber tests (147 tests, 66%), were carried out in normally consolidated sands. This may have an influence on the above correlations to provide a slightly better result in normally consolidated sands than in overconsolidated sands. Hence, practitioners should be cautious in using the above correlation for

uncemented overconsolidated sands where the correlation might underestimate the real  $K_o$ . The advantage of this method (Eq. 5.12) is that the approach is based on data from a whole range of different sands. Hence, the combined use of  $G_o$  and  $q_c$  appears to compensate variations in grain characteristics (i.e. sand compressibility).

### 5.3 Estimation of OCR in sands

High in-situ horizontal stresses are conventionally linked to mechanical overconsolidation of a soil. Hence, for uncemented sands which have experienced a simple load/unload history caused by mechanical overconsolidation a relationship should exist between  $K_o$  and OCR. Mayne and Kulhawy (1982) have shown that for many soils  $K_o$  may be expressed as a function of OCR, as follows:

$$[5.13] \quad K_o = K_{oNC} \text{OCR}^{1-K_{oNC}}$$

where  $K_{oNC}$  is the coefficient of earth pressure at rest for the normally consolidated soil. This is often obtained from the relationship by Jaki (1944) as:

$$[5.14] \quad K_{oNC} = (1 - \sin\phi_{cv})$$

in which  $\phi_{cv}$  is the constant volume friction angle. Mayne (1991) suggested a tentative relationship for practical use to estimate OCR from  $K_o$  as  $\text{OCR} = 5.04 (K_o)^{1.54}$ . This appears to be based on  $\phi_{cv} = 41^\circ$ .

Equation 5.12 is analogous to Eq. 5.10. Hence, comparison between these equations indicates that a relationship should exist between overconsolidation ratio and coefficient of earth pressure at rest  $K_o$ . Figure 5.5 shows a regression analysis based on the calibration test results and gives a correlation in the form of:

$$[5.15] \quad \text{OCR} = 5.8539 (K_o)^{2.1598}$$

The correlation factor for the regression is  $R = 0.9662$  which supports the observations by Mayne and Kulhawy (1982). Also shown in Fig. 5.5 is the proposed relationship by Mayne (1991). The relationship in Eq. 5.15 can be used to estimate OCR of uncemented, mechanically overconsolidated cohesionless soil deposits. For comparison with Eq. 5.13, Eq. 5.15 can be rearranged in the form of:

$$[5.16] \quad K_o = 0.441 \text{OCR}^{0.463}$$

This also indicates that a constant volume friction angle of between 26 and 32 degrees would appear to be more reasonable for the calibration chamber test sands.

#### 5.4 Applications

Figure 5.6 presents a summary of the proposed correlation given in Eq. 5.12. As seen in Figure 5.6, a set of contours has been generated from which  $K_o$  can be estimated from a set of  $G_o$  and  $q_c$  values in uncemented, unaged sands from the results of seismic CPT. Also shown on Fig. 5.6 is the application of these contours to estimate the in-situ  $K_o$  for the Kidd, Massey and Alaska sands.

The Kidd and Massey sites are located near Vancouver, B.C. Both sites contain natural alluvial sediments as part of the Fraser River delta. At both sites, SCPT data are within a 20 to 30 m thick complex of distributary channel sands that underlies most of the delta plain (Monahan et al., 1995). Fraser River sand is a young, uncemented predominantly quartz sand with some mica and feldspar, has a  $D_{50} = 0.30$  mm and contains on average about 5% fines. Massey and Kidd are sands of moderate to low compressibility. Alaska sand is a tailings deposit which has been deposited into the sea and has a 30% fines content. The fines have a high crushed shell content and, hence, Alaska sand has high compressibility.

Figure 5.6 illustrates a uniform trend for each site. This means that the proposed correlation appears not to be highly sensitive to possible errors in the measurement of shear wave velocity and cone penetration resistance. On average,  $K_o$  is estimated to be about 0.4 for Kidd sand, 0.35 for Massey sand, and 0.35 for Alaska sand. These results are in good agreement with those obtained from high quality self-boring pressuremeter testing in Kidd and Massey where  $K_o$  are reported to be between 0.4 and 0.5. Using Eq. 5.15, all three

sites are identified as normally consolidated deposits with  $OCR = 1.0$ . Unfortunately, there is limited SCPT data available from in-situ overconsolidated sands to fully evaluate the proposed methodology.

## 5.5 Discussion

Figure 5.4 compares the predicted normalized effective horizontal stress, based on Eq. 5.11, with the normalized horizontal stress measured in the calibration chamber. As illustrated, they agree quite well for the full range of normalized effective horizontal stress. However, the value of  $K_o$  which has been computed using Eq. 5.12, from an indirect evaluation, using a simple rearrangement of Eq. 5.11, demonstrates a noticeable disagreement with the measured  $K_o$ . Figure 5.7 illustrates the comparison between  $K_o$ , computed from Eq. 5.12 and the corresponding  $K_o$  measured in the calibration chamber test. Figure 5.7 illustrates the sensitivity of  $K_o$  to small variations in both  $\sigma'_{vo}$  and  $\sigma'_{ho}$ .

It should be noted that in the proposed Eq. 5.12, the exponent of  $G_o$  is about 2.16 when  $K_o$  is determined. In addition, small strain shear modulus,  $G_o$  is determined from the field measurement of shear wave velocity,  $V_s$ . As given in Eq. 5.5,  $G_o$  is related to  $V_s$  through an exponent of 2. Hence, the determination of  $K_o$  is based on the shear wave velocity measurement with an exponent of 4.32, and vertical effective stress with a power of 2.16. For instance, a 10 percent error in the measurement of the shear wave velocity would result in either a 51 percent overestimation or 36 percent underestimation of  $K_o$ . Similarly, a 10 percent error in the estimation of vertical effective stress can result in either a 21 percent overprediction or 19 percent underprediction. The  $K_o$  value predicted based on Eq. 5.12 is highly sensitive to the accuracy of the measurement of shear wave velocity in the field and prediction of vertical effective stress in depth.

Based on the above discussion, it could be an advantage to develop a correlation to estimate  $K_o$  directly. This can prevent any reduction in accuracy due to indirect evaluation. First, the correlation should include exponents less than unity to reduce the sensitivity of the prediction with respect to the field measurement and predictions. Secondly, it is better to correlate  $K_o$  directly with shear wave velocity rather than with small strain shear modulus. Finally, it seems that a linear correlation can be less sensitive to the field parameters and

predictions. These guidelines can be used to develop a new correlation for the prediction of  $K_o$  in sands. This approach will be presented and evaluated in the following section.

### 5.6 A modified method for a direct estimation of $K_o$

Based on the recent findings, explained in Section 5.5, an attempt has been made to correlate  $K_o$  with the measured shear wave velocity, cone penetration resistance and vertical effective stress for quartz sands. A regression analysis based on data from a large number (147 tests) of published calibration chamber test results (Baldi et al. 1986, Fioravante et al. 1991 and Almeida et al. 1991) on uncemented normally consolidated and overconsolidated Ticino sand and Toyoura sand gives the following correlation:

$$[5.17] \quad K_o = 10.197A_K - 4.2903$$

where,

$$[5.18] \quad A_K = \frac{\left(\frac{V_s}{V_a}\right)}{\left(\frac{q_c}{P_a}\right)^{0.07} \left(\frac{\sigma'_{v0}}{P_a}\right)^{0.19}}$$

where,  $V_s/V_a$  is normalized shear wave velocity, in which  $V_a$  is the velocity of sound in air, assumed to be 340 m/s (1110 ft/s),  $q_c/P_a$  is normalized cone penetration resistance and  $\sigma'_{v0}/P_a$  is normalized vertical effective stress.

Figure 5.8 presents a summary of the calibration chamber test results in the form of Eq. 5.17. The correlation factor for the above regression analysis is  $R = 0.8343$ . In general,  $\sigma'_{v0}/P_a$  varies between 0.5 to 2.0,  $V_s/V_a$  ranges from 0.35 to 0.9, and  $q_c/P_a$  extends from 50 to 500. Hence,  $A_K$  varies between 0.3 to 0.5. The above linear correlation seems to be more convenient when compared with Eq. 5.12, since a linear correlation with exponents less than unity can be less sensitive to the field parameters. In addition,  $K_o$  is directly related to the field parameters, which would prevent any inaccuracy induced by indirect evaluation of  $K_o$  from effective horizontal stress. Also  $K_o$  is directly correlated

with field measured value of shear wave velocity,  $V_s$ , rather than small strain shear modulus,  $G_o$ . Figure 5.9 compares the predicted  $K_o$ , using Eq. 5.17, with the corresponding  $K_o$  measured in the calibration chamber tests. Figure 5.9 illustrates that the accuracy of prediction for  $K_o$  is about  $\pm 0.1$ . Although some points are scattered, the general trend for the predictions for the full range of OCR, that is normally consolidated sands to highly overconsolidated sands, are reasonably good.

The exponents determined in Eq. 5.17 for  $V_s/V_{s1}$ , and  $\sigma'_{v0}/P_1$  are in good agreement with corresponding exponents in Eq. 5.12. However, the exponent for  $q_c/p_1$  is determined to be 0.07 compared with 0.125. The domain of the proposed correlation by Eq. 5.17 is  $0.55 > A_K > 0.45$  for  $K_o$  between 0.40 and 1.40. When  $A_K$  is less than 0.47, the proposed relationship gives negative value for  $K_o$ . However, the correlation should pass the origin to include the full range of parameter  $A_K$ , as seen in Eq. 5.12. For instance  $K_o$  value at the wall of an excavation can be zero while both normalized shear wave velocity and cone penetration resistance are close to zero.

Based on a review of the Seismic Cone Penetration Test results performed at the Kidd and Massey sites, the following correlations are recommended for the full range of  $A_K$ :

$$[5.19] \quad K_o = 10.197 A_K - 4.2903 \quad \text{for } A_K \geq 0.47$$

$$[5.20] \quad K_o = 0.90 A_K \quad \text{for } A_K < 0.47$$

The above bilinear relationship replicates a power function with two straight lines, which is the actual trend of the correlation, as earlier discussed in Section 5.5. These correlations are shown in Fig. 5.10.

As described earlier, the above proposed correlations are only applicable for uncemented low compressible quartz sands. However, the same framework can be applied to sands with highly compressible mineralogy. A regression analysis was carried out using calibration chamber test results (17 tests) on normally consolidated and overconsolidated carbonate Quiou sand (Almeida et al. 1991).  $K_o$  is correlated with parameter  $A_K$ , as given in Eq. 5.18. On this basis, a relationship is developed for the evaluation of in-situ  $K_o$  in highly crushable sands in the form of:

$$[5.21] \quad K_o = 7.9501 A_K - 3.6817$$

Figure 5.11 presents a summary of the calibration chamber test results in the form of Eq. 5.21. The correlation factor for the above regression analysis is  $R = 0.9918$ . Also shown in Fig. 5.11 are the test data for Ticino sand and Toyoura sand. As seen, low compressible sand data plot on a different line. For a given parameter  $A_K$ , a higher  $K_o$  can be estimated for low compressible quartz sands. The slope of Eq. 5.17, for low compressible quartz sands, is 0.42, while the slope of the correlation for highly compressible sands, as given by Eq. 5.21, is 0.46. Hence, they are found to be parallel to each other. This illustrates that the linear correlations proposed for sands with various compressibility have almost similar slope in the diagram of  $K_o$  versus parameter  $A_K$ . The higher the compressibility of sand, the further its correlation would be plotted from the origin in that diagram. The drawback with the proposed framework in this section is the need to have a prior knowledge of sand compressibility. Eslaamizaad and Robertson (1996a) developed a method to identify compressible sands using Seismic CPT. This approach can be used to determine whether a sand is low, medium or highly compressible. As explained earlier for low compressible sands, the corresponding correlation plotted in a diagram of  $K_o$  versus parameter  $A_K$ , should pass the origin. On this basis, the following relationships are proposed for highly compressible sands:

$$[5.22] \quad K_o = 7.9501 A_K - 3.6817 \quad \text{for } A_K \geq 0.51$$

$$[5.23] \quad K_o = 0.74 A_K \quad \text{for } A_K < 0.51$$

Figure 5.10 summarizes the correlations proposed for both low compressible and highly compressible sands. This chart can be used to estimate coefficient of earth pressure at rest  $K_o$ , for sands with various compressibility and different level of OCR.

The above proposed method are applied to the field data of low compressible Kidd and Massey sands and highly compressible Alaska sand. Based on Eqs. 5.19, 5.20, 5.22 and 5.23, on average,  $K_o$  is estimated to be about 0.41 for Kidd sand, 0.39 for Massey sand, and 0.27 for Alaska sand. These results are in good agreement with those obtained from high quality self-boring pressuremeter testing in Kidd and Massey where  $K_o$  are reported to



be between 0.4 and 0.5. Unfortunately there is limited field data available from overconsolidated sands to evaluate the proposed methodology.

## 5.7 Summary and conclusions

A knowledge of the initial stress state is of great importance for the geotechnical characterization of natural and man-made soil deposits. However, a reliable procedure for determining horizontal in-situ stress has not yet been established for cohesionless soils.

The stress history and age of the deposit are among the important factors which control the soil modulus, hence the deformation characteristics of the soil. Extensive study of penetration testing mostly in calibration chamber have shown that the stiffness of sands is very sensitive to stress history.

Experimental evidence indicates that the penetration of the cone alters almost completely the previous stress and strain history of the sand (Baldi et al. 1986). Nevertheless, cone penetration resistance ( $q_c$ ) is strongly influenced by the current level of horizontal effective stress ( $\sigma'_{ho}$ ) (Baldi et al. 1986, Parkin 1988, Houlsby and Hitchman 1988, and Mayne 1991). This correlation has often been illustrated in the form of  $q_c = A (\sigma'_{ho})^B$ , in which exponent B is determined to be between 0.5 and 0.63.

The method by Kulhawy et al. (1989), based on the Durgunoglu and Mitchell theory (1979), requires a prior knowledge of effective stress friction angle of sand to determine  $K_o$  from CPT data. An iterative approach by Mayne (1991,1995), based on the assessment of CPT calibration chamber data which uses cone penetration resistance ( $q_c$ ) data on quartz sands, requires an evaluation of OCR and estimation of sand relative density beforehand. A method by Masood and Mitchell (1993) uses sleeve friction ( $f_s$ ) but also requires an *a priori* knowledge of stress history. The reliability of the method depends on the accuracy of the sleeve friction measurements and knowledge of OCR, whereas it is widely known that sleeve friction is the least reliable and repeatable parameter in cone penetration testing.

The seismic CPT has the potential to provide a wide range of in-situ geotechnical properties from a single sounding. Cone penetration resistance and small strain shear modulus in uncemented sands depend significantly on the in-situ effective stress state. An assessment

of calibration chamber test results has provided an empirical basis to relate horizontal stress with cone resistance and small strain shear modulus. The proposed method is based on published data from a large number of CPT calibration chamber tests and resonant column tests performed on sands with various grain characteristics and stress histories. Hence, a correlation has been developed to predict in-situ horizontal stress in uncemented and unaged cohesionless soils using the seismic CPT. On this basis, a relationship is proposed to evaluate in-situ horizontal effective stress,  $\sigma'_{ho}$ , as well as the coefficient of earth pressure at rest,  $K_o$ . The influence of soil compressibility on the proposed relationship appears to be quite small. A preliminary and tentative procedure has also been presented for estimating stress history (OCR) of uncemented cohesionless deposits from the predicted coefficient of earth pressure at rest ( $K_o$ ). Limited field evidences have been used to illustrate the proposed correlations. The results have been found to be in good agreement with those obtained from high quality self-boring pressuremeter testing, mainly in normally consolidated sands, although more data are required to fully evaluate the method. A comparison between the  $K_o$  predicted by the proposed method and the corresponding  $K_o$  measured in the calibration chamber test illustrates that although the  $K_o$  value is estimated quite well for normally consolidated sands, it can be underpredicted in overconsolidated sands. Several parameters which can reduce the accuracy of the prediction of  $K_o$  have been identified, discussed and evaluated. They can be listed as follows: i) in calibration chamber a large portion of tests is often performed on normally consolidated sands, ii) indirect evaluation of  $K_o$ , iii) high exponents of field parameters in the proposed correlation, iv) inclusion of small strain shear modulus rather than shear wave velocity which is one of the first-hand product of field measurements. In this framework an alternative direct correlation has been developed for sands between  $K_o$ ,  $q_c$  and  $V_s$ . However, this correlation is found to be highly influenced by sand compressibility. Hence, different relationships are recommended for sands with low compressibility, and high compressibility. Very limited field data have been used to evaluate the new developed correlations. Although the results have been found to be in reasonable agreement with the limited field measurements, more data are required to perform a comprehensive evaluation of the method.

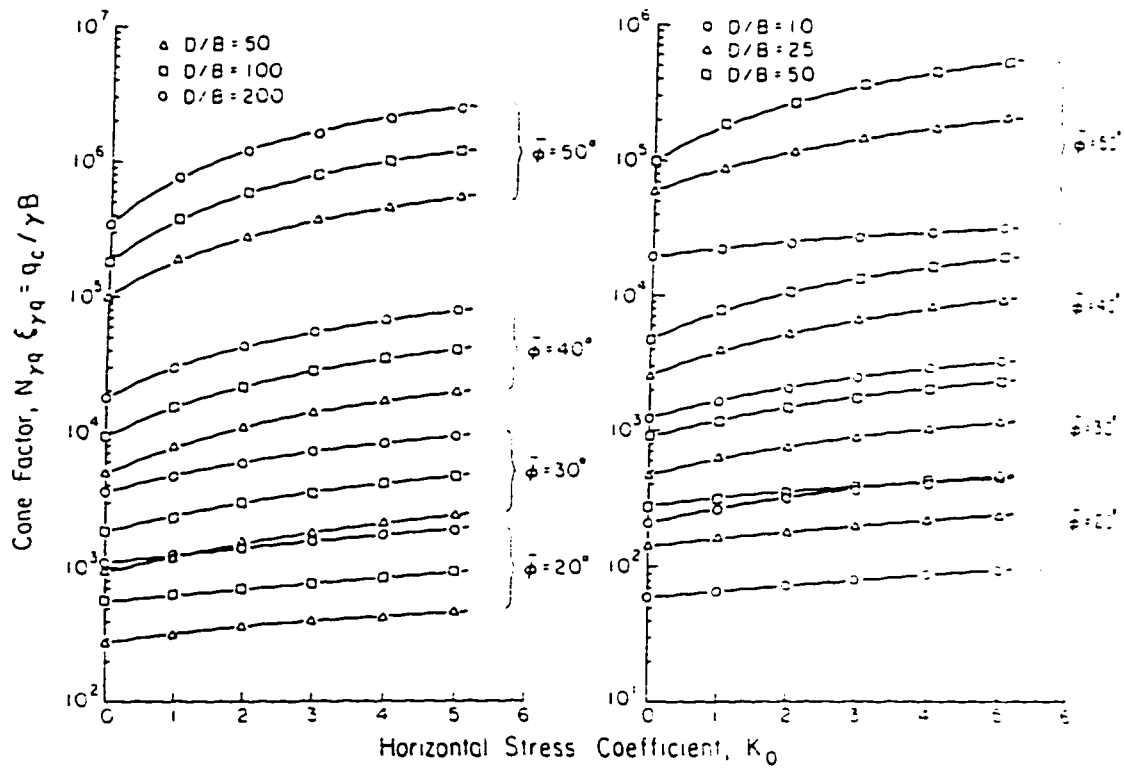


Fig. 5.1 Estimation of  $K_0$  from Durgunoglu and Mitchell, (after Kulhawy et al., 1989)

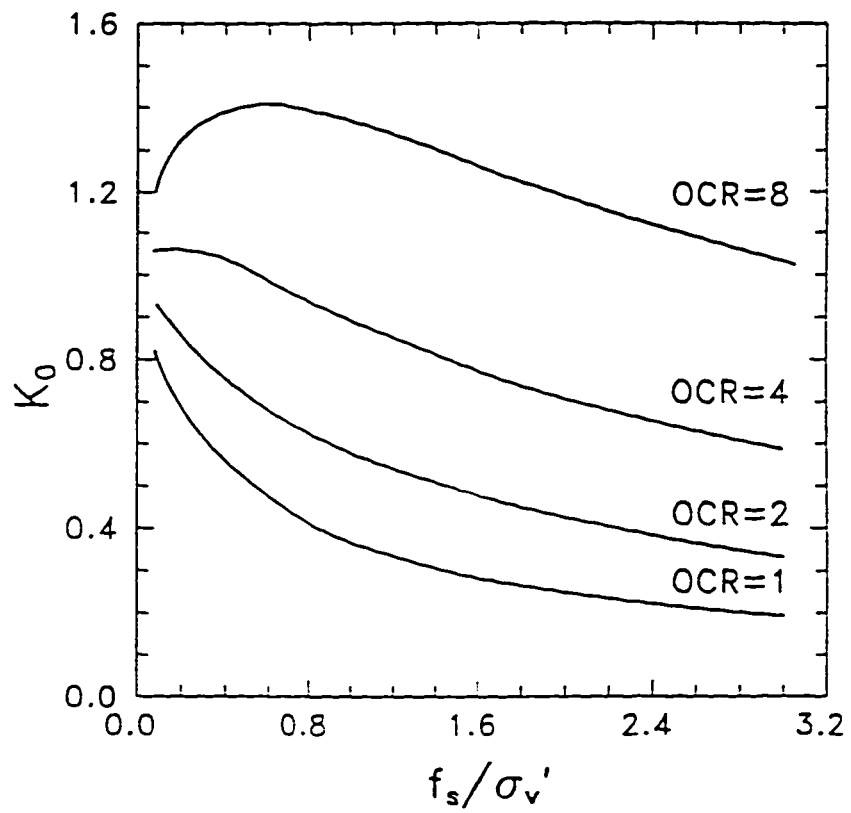


Fig. 5.2  $K_0$  as a function of sleeve friction and overconsolidation ratio (after Masood and Mitchell., 1993)

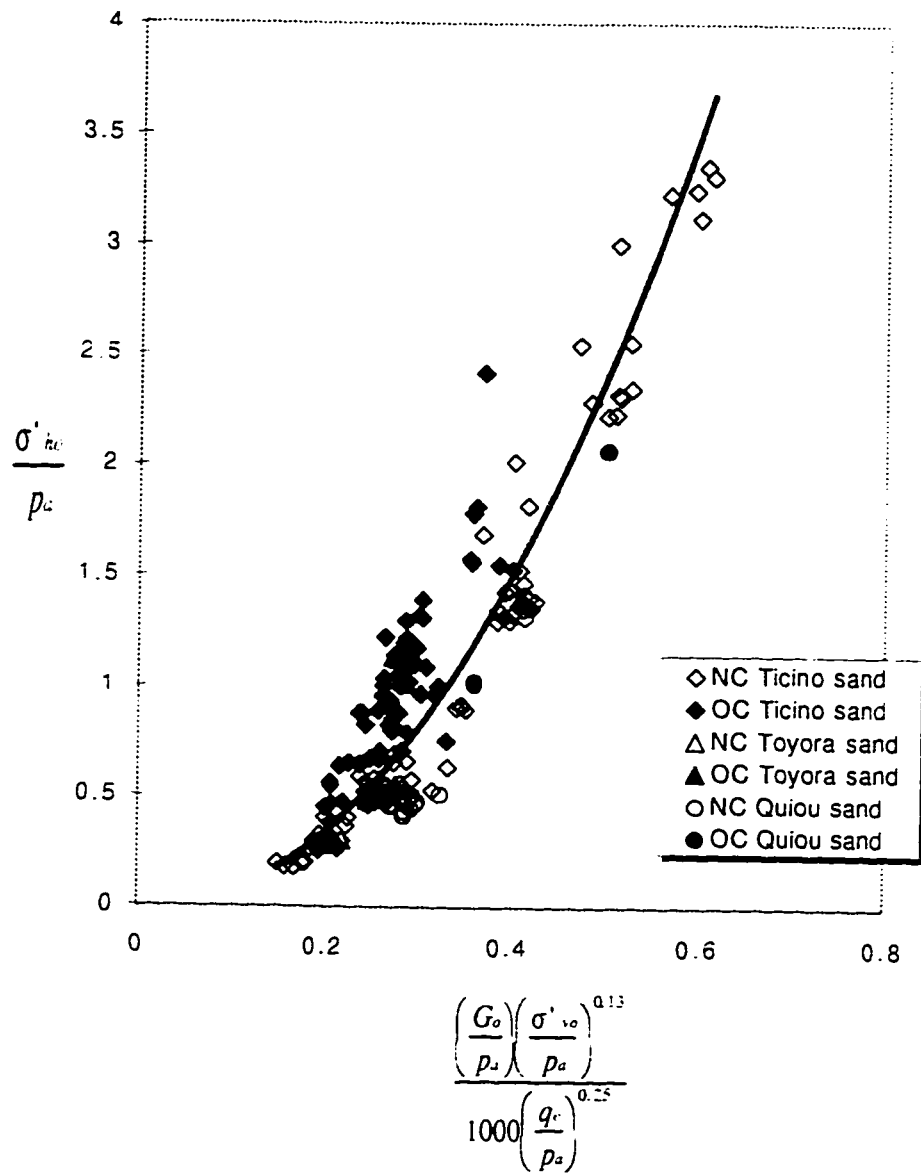


Fig. 5.3 Correlation between  $\sigma'_{hv}$ ,  $q_c$ ,  $G_0$  and  $\sigma'_{vo}$

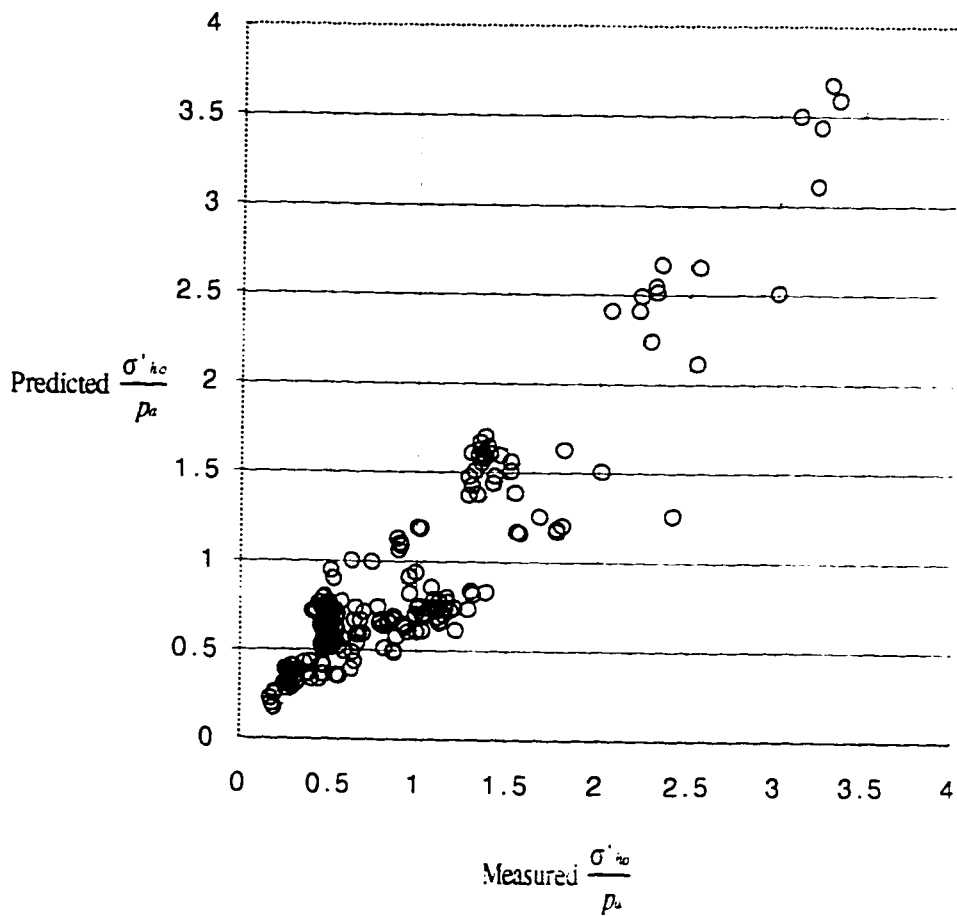


Fig. 5.4 Measured versus predicted normalized horizontal effective stress for calibration chamber tests

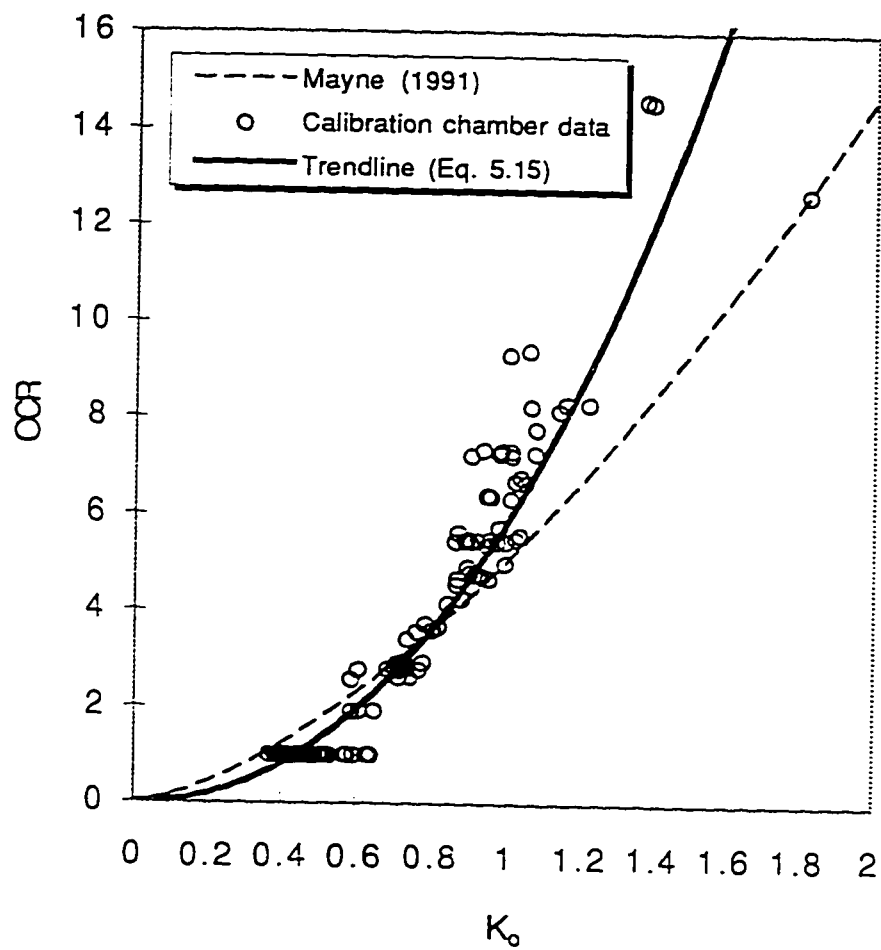


Fig. 5.5 Correlation between OCR and  $K_0$ .

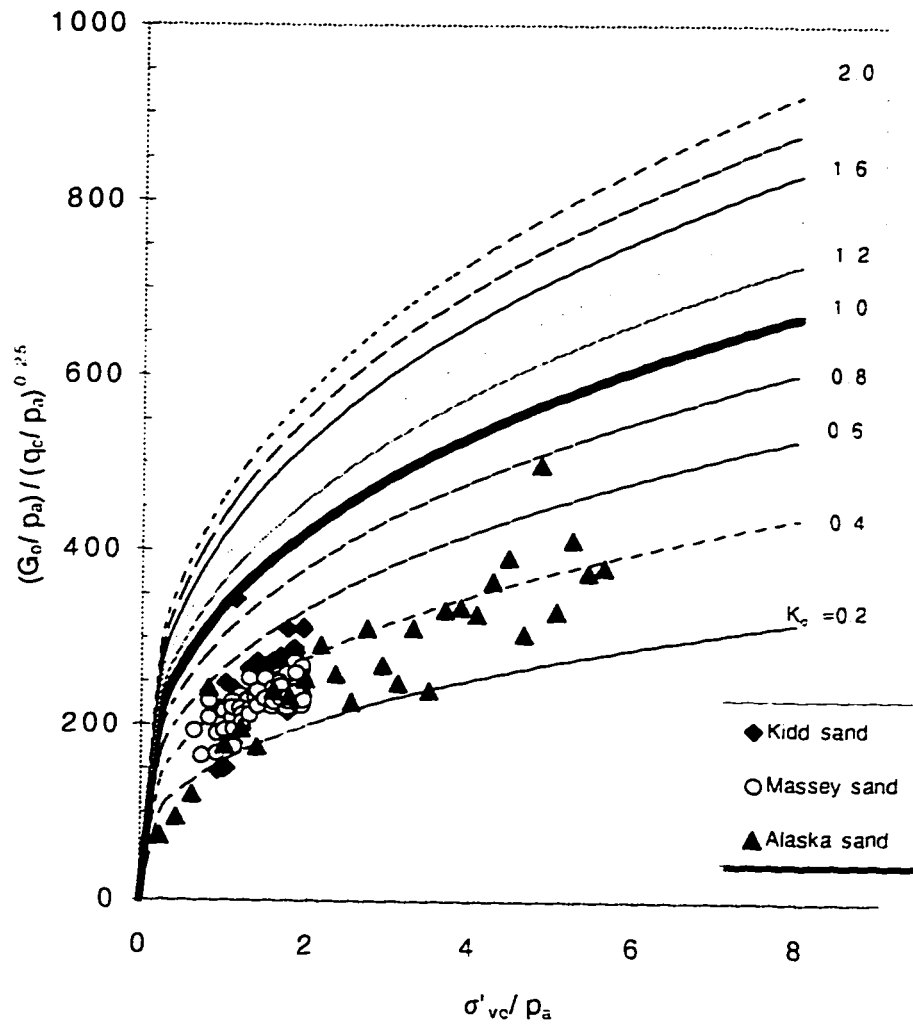


Fig. 5.6 Evaluation of  $K_0$  from SCPT for unaged, uncemented sands



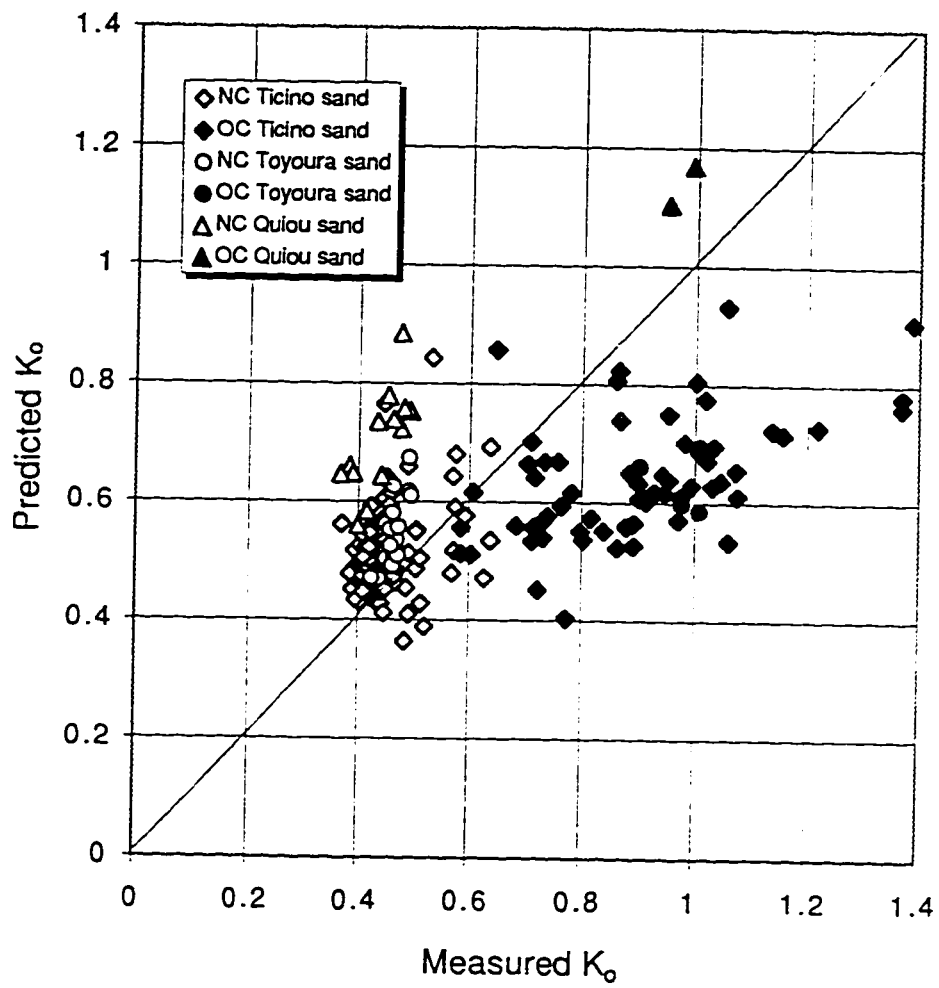


Fig. 5.7 Predicted  $K_0$  based on Eq. 5.12, versus measured  $K_0$  for calibration chamber tests

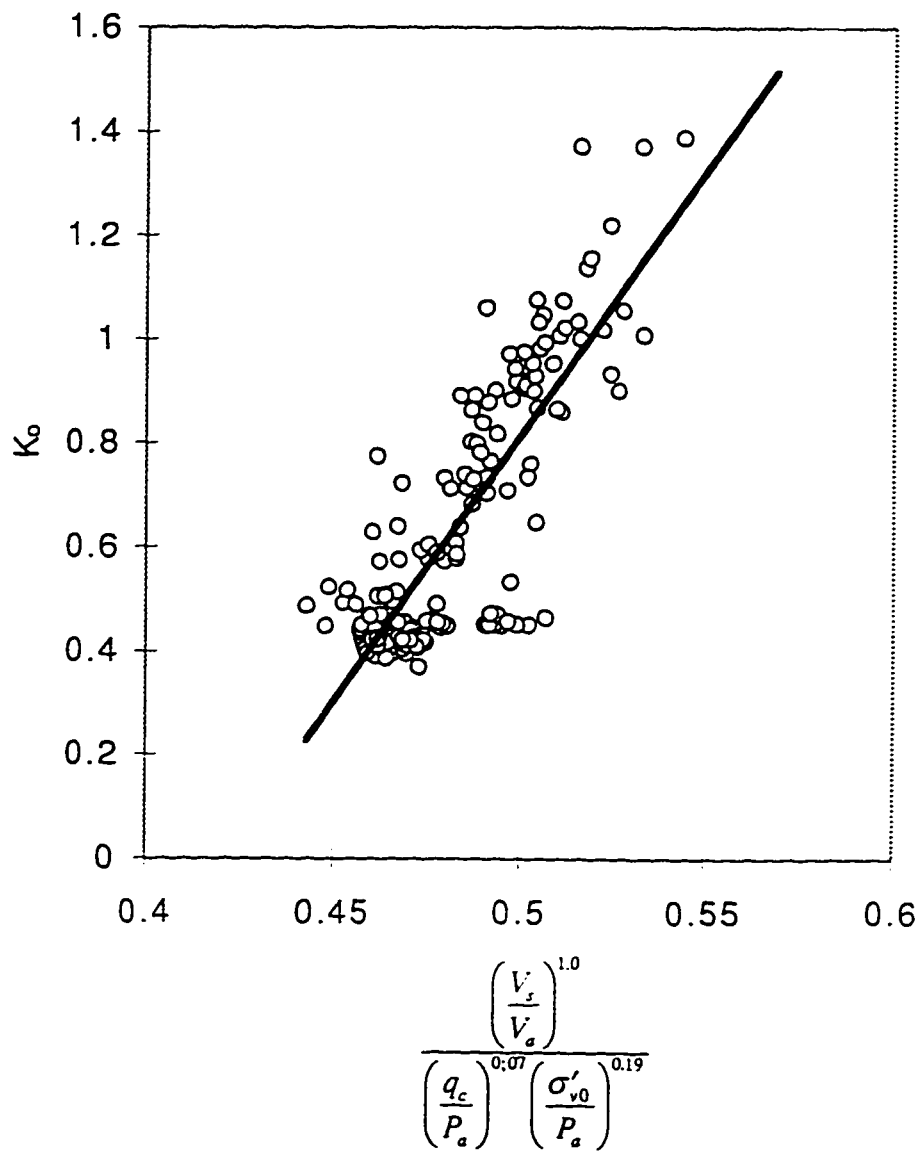


Fig. 5.8 Correlation between  $q_c$ ,  $V_s$  and  $\sigma'_{v0}$  for uncemented quartz sands

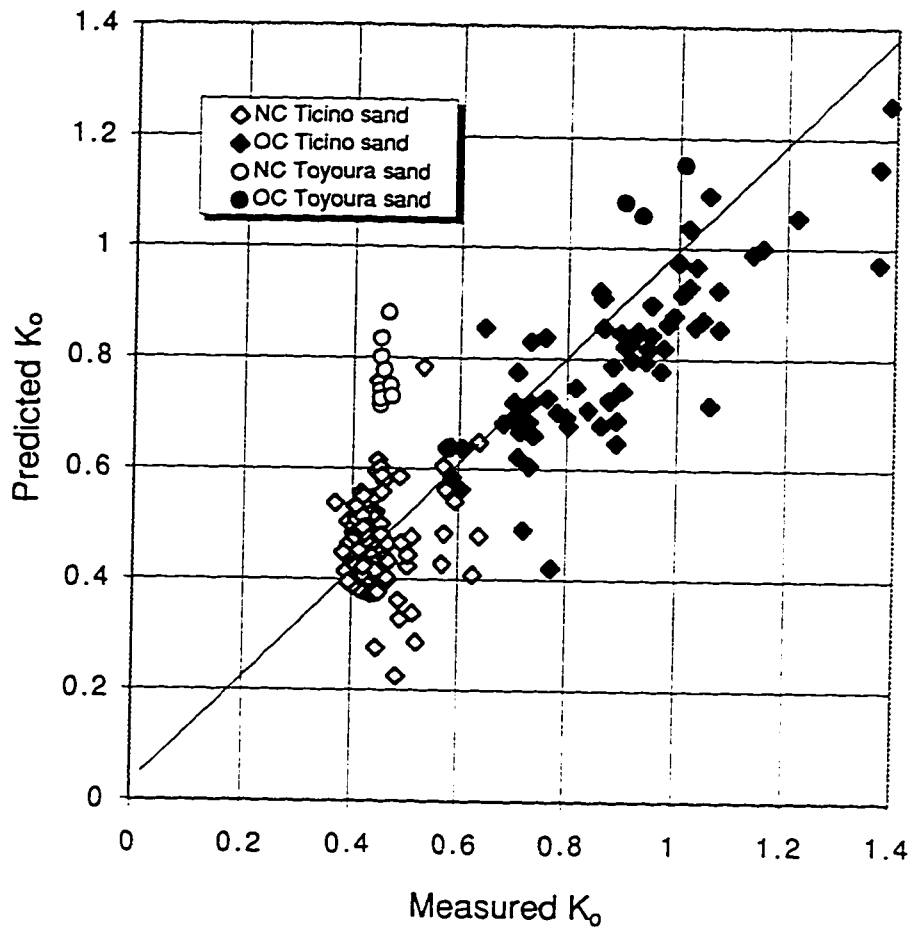


Fig. 5.9 Predicted  $K_0$  based on Eq. 5.17, versus measured  $K_0$

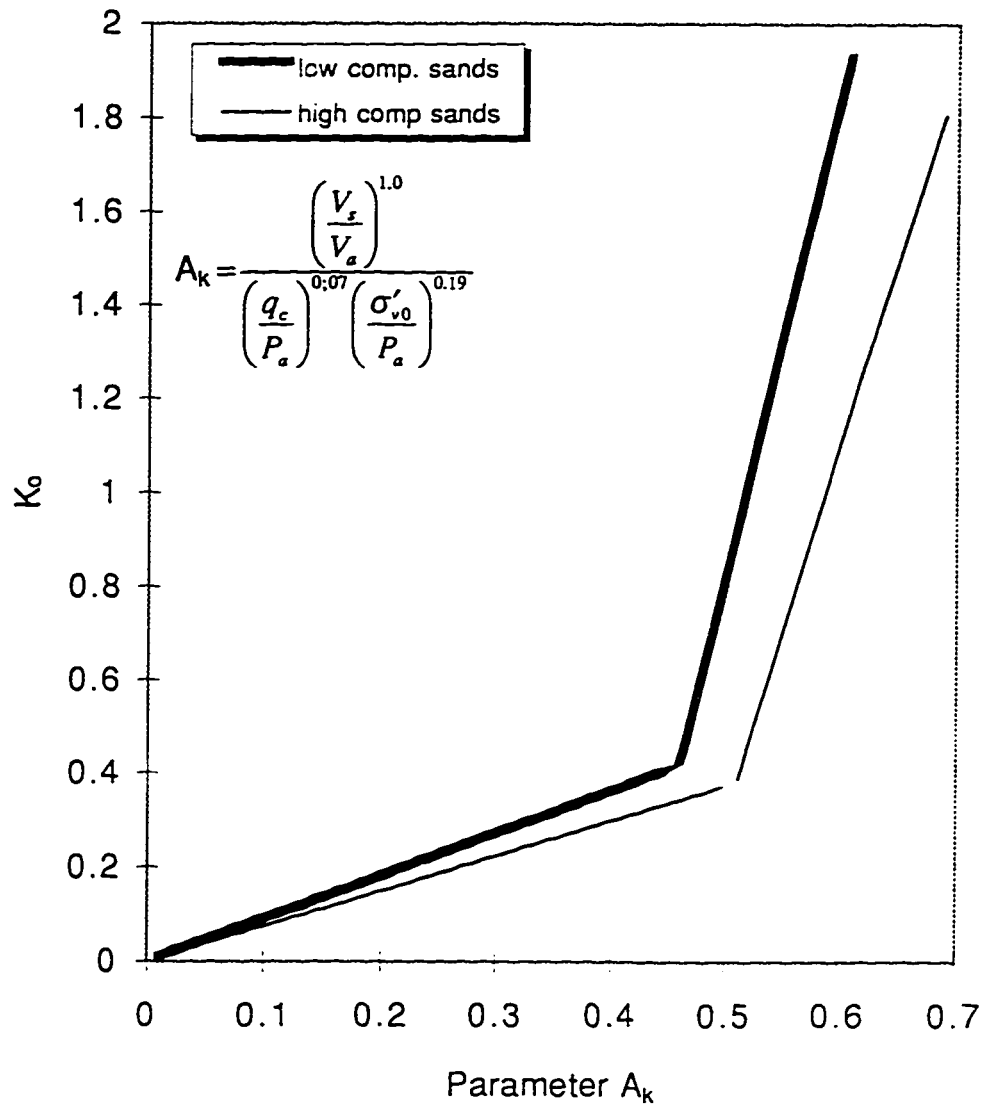


Fig. 5.10 Evaluation of  $K_0$  from SCPT for unaged, uncemented sands

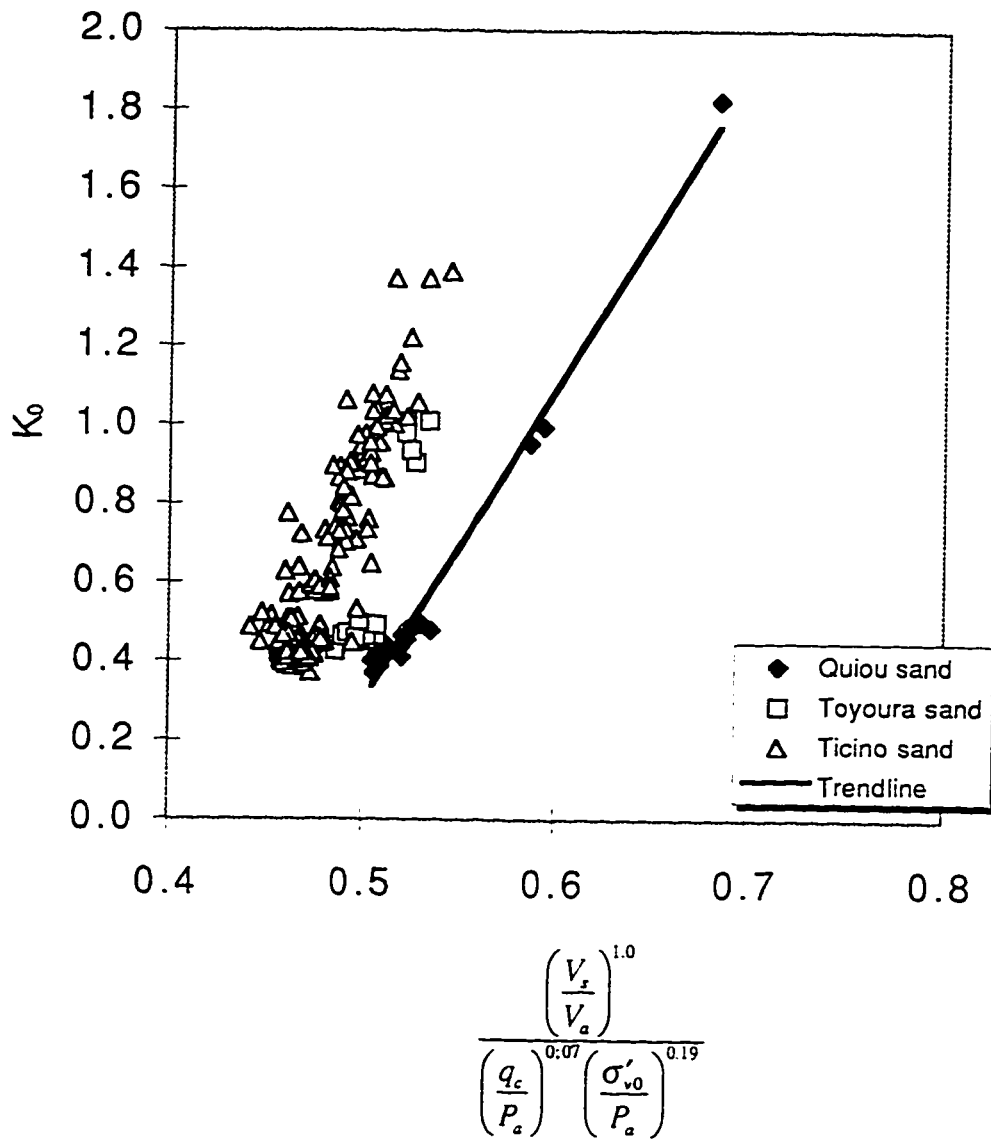


Fig. 5.11 Correlation between  $q_c$ ,  $V_s$  and  $\sigma'_{v0}$  for carbonate Quiou sands

## References

- Almeida M.S., Jamiolkowski M., and Peterson R.W. 1991. Preliminary results of CPT in tests in calcareous Quiou sand, Proceedings of the First International Symposium on Calibration Chamber Testing ISOCCT1, Postdam, New York, Edited by An-Bin Haung, pp. 41-53.
- Baldi G., Bellotti R., Ghionna N., Jamiolkowski M. and Pasqualini E. 1986. Interpretation of CPT's and CPTU's 2nd Part: Drained Penetration of Sands. Proceedings of Fourth International Geotechnical Seminar on Field Instrumentation and In-situ Measurements, Singapore.
- Baldi, G., Bellotti, R., Ghionna, V., Jamiolkowski M. and Lo Presti D.C.F. 1989. Modulus of sands from CPT's and DMT's. Proceedings, XII International Conference of Soil Mechanics and Foundation Engineering, Vol. 1, pp. 165-170.. Rio De Janeiro.
- Durgunoglu, H.T., and Mitchell J.K. 1975. Static penetration resistance of soils, Proc. of ASCE Conf. In-situ Meas. Soil, Raleigh, pp. 151-189.
- Eslaamizaad, S. and Robertson, P.K. 1996a. A framework for in-situ determination of sand compressibility. 49th Canadian Geotechnical Conference, St. John's, NF, Canada.
- Eslaamizaad, S. and Robertson, P.K. 1996b. Seismic cone penetration test to identify cemented sands. 49th Canadian Geotechnical Conference, St. John's, NF, Canada.
- Fioravante V., Jamiolkowski M., Tanizawa F., and Tatsuoka F. 1991. Results of CPT's in Toyoura quartz sand., Proceedings of the First International Symposium on Calibration Chamber Testing ISOCCT1, Potsdam, New York , Edited by An-Bin Huang, pp. 135-146.
- Houlsby, G. T. and Hitchman, R. 1988, Calibration chamber tests of a cone penetrometer in sand. Geotechnique 38, No.1, pp. 39-44.
- Jaky, J. 1944. The coefficient of earth pressure at rest. J. Soc. of Hungarian Arch. and Engrs., Budapest, Hungary, pp. 355-358 (in Hungarian)
- Jamiolkowski, M., and Robertson, P.K. 1988. Future trends for penetration testing., Proceedings of conference, Penetration testing in the U.K., Birmingham, pp. 21-42.
- Knox, D. P., Stokoe, K. H., II., and Kopperman, S. E. 1982. Effect of state of stress on velocity of low- amplitude shear wave propagating along principal stress directions in dry sand. Report GR 82-23, University of Texas at Austin.

- Kulhawy F. H., Jackson C. S., and Mayne P. W. 1989. First -order estimation of  $K_0$  in sands and clays. *Foundation Engineering: Current principles and practices (GSP 22)*, Vol. 1, ASCE, New York, pp. 121-134.
- Lee, S. H. and Stokoe, K. H., II. 1986. Investigation of low-amplitude shear wave velocity in anisotropic material. Report GR 86-6, University of Texas at Austin.
- Masood, T. and Mitchell, J. K. 1993. Estimation of in-situ lateral stresses in soils by cone penetration test. *Journal of Geotechnical Engineering*, Vol. 119, No. 10, ASCE, pp. 1624-1639.
- Mayne, P.W. 1991. Tentative method for estimating  $\sigma'_{ho}$  from  $q_c$  data in sands. *Proceedings of the First International Symposium on Calibration Chamber Testing ISOCCT1, Potsdam, New York*, Edited by An-Bin Huang, pp. 249-256.
- Mayne P.W. 1995. CPT determination of overconsolidation ratio and lateral stresses in clean quartz sands., *Proceedings of CPT' 95, Volume 2, Section 2.14*, pp. 215-220.
- Mayne, P.W., and Kulhawy, F.H. 1982.  $K_0$ -OCR relationships in soil., *Journal of Geotechnical Engineering*, Vol. 108, No. 6, ASCE, pp. 851-872.
- Monahan, P. A., Lutemauer, J. L., and Barrie, J. V. 1995. The geology of the CANLEX Phase II sites in Delta and Richmond, British Columbia. *Proceedings of the 48th Canadian Geotechnical Conference, Vancouver, B.C.*, pp. 59-68.
- Parkin A. K. 1988, The calibration of cone penetrometers. *Proceedings of the First International Symposium on penetration Testing/ISOPT1, Orlando*, Edited by J. De Ruyter, pp. 221-243.
- Rix G.J. and Stokoe K.H. II. 1991, Correlation of Initial tangent Modulus and Cone Penetration Resistance. *Proceedings of the First International Symposium on Calibration Chamber Testing/ISOCCT1, Potsdam, New York*, Edited by An-Bin Huang, pp. 351-362.
- Robertson, P. K. and Campanella, R. G. 1983, Interpretation of cone penetration tests. Part I: sand., *Canadian Geotechnical Journal* 20, pp. 718-733.
- Robertson, P. K. 1990, Estimation of foundation settlements in sand from CPT, ASCE, *Journal of Geotechnical Engineering*, pp. 764-775.
- Roesler, S. K. 1979. Anisotropic shear modulus due to stress anisotropy. *Journal of Geotechnical Engineering*, Vol. 105, GT5, ASCE, pp. 871-880.
- Yu, P. and Richart, F. E. 1984. Stress ratio effects on shear modulus for sand. *Journal of Geotechnical Engineering*, Vol. 110, No. 3, ASCE, pp. 331-345.

## CHAPTER 6

### A METHOD FOR EVALUATING BEARING CAPACITY OF FOUNDATIONS IN SANDS FROM CONE PENETRATION TEST (CPT)<sup>1</sup>

#### 6.1 Introduction

The bearing capacity of foundations depends both on the nature of the soil and the dimensions and layout of the foundations. Undisturbed sampling in soils with little or no cohesion can be difficult and expensive. In addition, some natural cohesionless soils may be lightly cemented and standard sampling techniques often break the bonds, resulting in disturbance. In such circumstances, in-situ tests are preferred. The cone penetration test (CPT) has become increasingly more popular due to the continuous nature of the data, reliable and repeatable results and cost effectiveness. Empirical and theoretical relations exist relating cone penetration resistance ( $q_c$ ) to a full range of geotechnical soil parameters. Extensive research has been performed to correlate cone resistance to the end bearing capacity of deep footings (de Ruiter and Beringen 1979, Bustamante and Gianselli 1982). However, few attempts have been made to estimate bearing capacity ( $q_{ult}$ ) of shallow footings directly from CPT data. The most widely used procedure for computing  $q_{ult}$  using CPT data is based on the general bearing capacity theory in which either internal friction angle ( $\phi$ ) or bearing capacity factors ( $N_\gamma$  and  $N_q$ ) are estimated from empirical correlations or published charts. However, the ultimate bearing capacity of footings on sand can be overpredicted using correlations that relate cone resistance to friction angle because such relationships are most frequently based on test results from calibration chamber tests performed on uncemented unaged sands while some natural sands are lightly cemented. In addition, general bearing capacity theory does not consider the effect of soil compressibility.

Based on bearing capacity theory, and the relationship between SPT blow number  $N$  and

---

<sup>1</sup> A version of part of this chapter has been published. Eslaamizaad, S. and Robertson P.K. 1996. Cone Penetration Test to evaluate bearing capacity of foundations in sands, Proc. of the 49th Canadian Geotechnical Conference, St. John's, Newfoundland, 429-438.



angle of internal friction of cohesionless soils, Meyerhof (1956) developed a correlation between penetration resistance  $N$  and bearing capacity of shallow footings. Meyerhof further assumed  $q_c = 4N$  ( $\text{kg}/\text{cm}^2$ ) to relate cone penetration resistance directly with ultimate bearing capacity ( $q_{ult}$ ) of shallow footings, in the form of :

$$[6.1] \quad q_{ult} = \frac{q_c}{C} B \left( 1 + \frac{D}{B} \right)$$

where  $q_c$  is the average cone resistance within a depth  $B$  below the base of the footing,  $C$  is an empirical constant equal to 12.2 in meters, and  $B$  and  $D$  are the width and depth of the footing in meters, respectively. Based on a factor of safety of 3, Fig. 6.1 illustrates the ratio between allowable bearing capacity and cone tip resistance as a function of depth and width of the footing in the form of Eq. 6.1.

In an attempt to obtain a direct relationship between cone resistance and bearing capacity, Goel (1982) conducted a series of plate load tests on sands at different relative densities under both dry and submerged conditions. Using the relationship between settlement and size of the plate and those of the footing, he related the allowable bearing capacity for 2.5 cm settlement for different sizes of footings to the average cone resistance within the pressure bulb under the footings. Goel noted that the allowable bearing capacity reduces by about 10% when footing width increases from 1.5 m to 4.5 m. He further concluded that submergence of sand reduces the value of cone tip resistance  $q_c$  by about 10% while the allowable bearing capacity reduces by about 20 to 25% of its value under dry condition. Figure 6.2 summarizes his proposed correlations between average cone resistance under the footing and the allowable bearing capacity of footing with different size. Goel did not address the impact of the depth of the footing on the bearing capacity of footings on cohesionless sands.

Recently, Briaud and Jeanjean (1994) studied the results of loading tests of five full scale footings on sands and proposed an approximate relationship for all footing sizes as

$$[6.2] \quad q_{ult} = 0.25 q_c$$

in which  $q_{ult}$  is defined as the pressure at a relative displacement of  $s/B = 0.1$ , where  $s$  is the settlement and  $B$  is footing width.

Tand et al. (1995) reviewed load test results of nine full scale footings on medium dense sand. They also performed a numerical analysis to study the effect of embedment and footing size on ultimate bearing capacity and to extrapolate the test results to footings of different sizes and embedment. They assumed that there is a direct ratio between  $q_{ult}$  and  $q_c$ . Nevertheless, they further explained that this assumption is not entirely correct because the mode of failure is different between a cone penetrometer and a shallow footing. Accordingly, they proposed a correlation between  $q_{ult}$  and  $q_c$  in the form of:

$$[6.3] \quad q_{ult} = R_k \cdot q_c + \sigma'_{vo}$$

where  $q_{ult}$  is assumed to occur at a relative settlement of  $s/B = 0.05$ ,  $\sigma'_{vo}$  is the initial vertical effective stress at the base of footing, and  $R_k$  is a factor which varies between 0.14 to 0.19 depending on depth, and width of the footing, as given in Fig. 6.3.

Determination of pile capacity from the CPT data is one of the original application of the cone penetration test. A major problem with the prediction of pile capacity in sands is the large variety of pile installation techniques and their influence on the ultimate bearing capacity. Thus, methods based on CPT test data should include the influence of installation technique for the determination of ultimate bearing capacity.

For pile foundations, Meyerhof (1956) noted that the ultimate end bearing capacity of piles in sands varied from about 0.66 to 1.50 times the cone resistance  $q_c$ . Regardless of the size and depth of the deep footing, he proposed that on average:

$$[6.4] \quad q_{ult} = q_c$$

This simple correlation has been supported by many researchers to relate cone resistance to the ultimate end bearing capacity of piles (e.g. Ghionna et al., 1993). However, for large diameter bored piles in granular soils, the end resistance mobilized at a relative settlement ranging between 5 and 10% is often considered in the design, since the ultimate end bearing capacity ( $q_{ult}$ ) occurs at a very large relative settlement of  $s/B \geq 100\%$  (Fioravante et al., 1995).

Nottingham (1975), Schmertmann (1978), and de Ruiter and Beringen (1979) proposed to take the end resistance of a pile equal to the average cone resistance in a zone of 8D above the pile end, and between 0.7D to 4D below the pile end (where, the actual value depends on the trend of  $q_c$  values, and D = pile diameter). They introduced an increasing correction factor for overconsolidation and gradation in cohesionless soils. However, the major problem is the difficulty in estimating the overconsolidation ratio in sands. They further imposed an upper limit of 15 MPa for the end resistance of piles in cohesionless soils. Figure 6.4 illustrates the methods by Schmertmann, de Ruiter and Beringen.

Based on a large number of full-scale loading tests, Bustamante and Ganeselli (1982) proposed a method for predicting the end bearing capacity of deep foundations from the cone resistance  $q_c$ . They assumed that there is a direct ratio between end bearing capacity of piles and  $q_c$  in the form of:

$$[6.5] \quad q_{ult} = k_c \cdot q_c$$

The correlation factor  $k_c$  was established from full scale loading tests. For bored piles in loose to dense sands where  $q_c$  is less than 12000 kPa,  $k_c = 0.4$ , and in very dense sands with  $q_c$  greater than 12000 kPa,  $k_c = 0.3$  are recommended. For driven piles in loose to dense sands where  $q_c$  is less than 12000 kPa,  $k_c = 0.5$ , and in very dense sands with  $q_c$  greater than 12000 kPa,  $k_c = 0.4$  are recommended. These values also appear to account for some level of limited deformation.

Eslami and Fellenius (1995) proposed a direct method, very similar to the Schmertmann and de Ruiter and Beringen methods, for determining the pile end resistance from cone resistance. In their approach, the geometric average of all  $q_c$ - values within the zone at the vicinity of pile end, similar to that proposed by the Schmertmann and de Ruiter and Beringen methods, are considered. They mentioned that the proposed method of averaging is independent of the judgment in filtering data and in choosing correlation factors as required by all the current methods. According to their method the end bearing capacity of a pile can be estimated as follows:

$$[6.6] \quad q_{ult} = (q_{c1} \cdot q_{c2} \cdot \dots \cdot q_{cn})^{1/n}$$

where n is the number of  $q_c$ -values in the considered zone and  $q_{ci}$  is ith  $q_c$ -value.

Bottiau (1995) reviewed the approach recommended by the French code (DTU13.2) for the assessment of the end bearing capacity of a single pile from CPT results. The method was originally based on the LCPC (Laboratoires des Ponts et Chaussees) experiments and recommendations by Bustamante and Gianceselli (1982). The French code evaluates the end bearing capacity as

$$[6.7] \quad q_{ult} = \alpha_b \cdot k_c \cdot q_c$$

where  $q_c$  is the cone resistance at the pile base level, and  $\alpha_b$  is the installation coefficient. For displacement (or driven) piles  $\alpha_b = 1.0$ .  $k_c$  is a reduction factor depending on the soil type and the pile type. In sand,  $k_c = 0.4$  where  $q_c < 2500$  kPa, and  $k_c = 0.3$  where  $q_c > 10000$  kPa. Bottiau (1995) discussed that the major problem of the method is the selection of the  $q_c$ -value to use for the computation of the bearing capacity, especially in the case of a discontinuous or intermediate layer.

The objective of this chapter is to present a direct method for predicting ultimate bearing capacity of footings in cohesionless soils using measured cone penetration resistance. The results of full-scale loading tests from 9 large spread footings are used to develop the proposed relationship. The effect of the shape, size and depth of footings on the correlation between cone penetration resistance and ultimate bearing capacity of footings is also investigated. Finally, the proposed method is evaluated and compared with other available methods. Application of the proposed correlation for determination of end bearing capacity of deep footings is discussed and evaluated.

## 6.2 Proposed method for evaluation of bearing capacity of footing in sands

The ultimate bearing capacity of footings in sands is a function of size and depth of the footing as well as both density and shear strength of the ground. Cone penetration resistance in sands is influenced by the in-situ effective stress and density of the soil. The role of size and shape of the footing in the ultimate bearing capacity of footings is well recognized and quantified in the general bearing capacity theory.

The significance of the influence of size of the footing on the bearing capacity of sands has also been widely recognized. According to Vesic (1973) the mode of failure in sands is a function of the shape of footing as well as the relative embedment depth expressed as B/D which are largely different for CPT and shallow footing. Therefore, to assume a single constant ratio between  $q_{ult}$  and  $q_c$  for all footings is not entirely correct because the mode of failure of a cone penetrometer and a shallow footing will be different. Hence, a linear proportionality of  $q_{ult} = k q_c$  excludes the influence of the size and shape of footing. Such simple correlations predict the same bearing capacity for footings with different sizes and shapes but at the same depth. As a result, any correlation factor between  $q_{ult}$  and  $q_c$  should also include the above factors.

Many researchers have analyzed cone penetration as a bearing capacity problem (e.g. Janbu and Senneset 1974). In this study, the general bearing capacity formula which includes the influence of the size and shape of footing, is adopted as the bases to develop a new correlation between  $q_{ult}$  and  $q_c$ .

For a footing in cohesionless soils the bearing capacity equation can be written as

$$[6.8] \quad q_{ult} = \gamma' D N_q + F \gamma B N_\gamma$$

where B and D are width (or diameter) and depth of the footing, respectively.  $N_q$  and  $N_\gamma$  are bearing capacity factors which depend on the friction angle of the cohesionless soil and mode of failure. F is a factor which accounts for the influence of the shape of footing which is equal to 0.3 for circular foundation and is equal to  $(0.5-0.1B/L)$  for a rectangular foundation with length L. Substituting  $\sigma'_{vo} = \gamma' D$ , the above relationship can be rearranged in the form of

$$[6.9] \quad q_{ult} = \sigma'_{vo} N_q \left(1 + F \frac{B N_\gamma}{D N_q}\right)$$

To correlate  $q_{ult}$  with  $q_c$ , here it is assumed that

$$[6.10] \quad \sigma'_{vo} N_q = \alpha_f \bar{q}_c$$

where  $\bar{q}_c$  is defined as an average value of cone resistance within the pressure bulb (zone of influence) of the footing. It is recommended to average the cone resistance over a depth of 1.0B below the bottom level for shallow footings in which  $D \leq B$ , and over a depth of 1.5B above and 1.5B below the bottom level of deep footings in which  $D > B$  (Bustamante and Gianselli, 1982). A relationship similar to Eq. 6.10 is approximated by Koumoto (1988), and by Peterson (1991) to determine penetration resistance of cohesionless materials. This seems to be a reasonable assumption since both  $\sigma'_v$ ,  $N_q$  and  $q_c$  are functions of the same basic variables of vertical effective stress and relative density or internal friction angle.  $N_q$  is also a function of mode of failure which in turn is influenced by size, shape and depth of the footing whereas,  $q_c$  is not influenced by such factors. Hence, the factor  $\alpha_f$  in Eq. 6.10 should be a function of shape, size and depth of the footing. The ultimate bearing capacity can then be expressed as follows:

$$[ 6.11 ] \quad q_{ult} = \alpha_f \bar{q}_c \left( 1 + F \kappa \frac{B}{D} \right)$$

where,

$$\kappa = \frac{N_\gamma}{N_q}$$

$\alpha_f$  = empirical correlation factor

F = shape factor

= 0.3 for circular footing

= (0.5-0.1B/L) for rectangular footings

According to Vesic (1973), as illustrated in Fig. 6.5, when the relative density of sand is smaller than about 75%, either local shear failure or punching shear failure is likely, and for dense sands with relative density greater than about 75%, general shear failure is probable. Examination of the ratio  $\kappa$  for various internal friction angles indicates that, for general shear failure in sand when  $35^\circ < \phi < 45^\circ$  the value of  $\kappa$  varies between 1.0 and 1.7, and for local shear failure in sand when  $25^\circ < \phi < 35^\circ$ ,  $\kappa$  has a value between 0.52 and 0.60, which is almost constant. In the above evaluation of the ratio  $\kappa$ , the bearing capacity

factors  $N_r$ , given by Terzaghi (1943), and  $N_q$  developed by Vesic (1963) are used. In this study,  $\kappa$  is taken as 0.55 for loose to medium dense sands and 1.00 for dense sands.

As described earlier, the empirical correlation factor  $\alpha_r$  is basically influenced by the shape, size and depth of footing. Here it is assumed that, the factor  $\alpha_r$  is a function of B/D ratio as a variable to quantify the effect of both footing size and embedment. A regression analysis is performed to correlate the factor  $\alpha_r$ , back-calculated from Eq. 6.11, with the variable B/D using the test results of full size foundations on sand.

Recently, the results of 9 load tests of full size shallow footings on sand have been reported in the literature. The footings were loaded to failure to measure  $q_{ult}$  and displacements (Briaud and Gibbens 1994, Tand et al. 1994). At the Texas Experiment Site, where the subsoils are middle Eocene sand formed in a coastal environment, five square footings were tested with a width from 1 to 3 m at a depth of about 0.80 m (Briaud and Gibbens, 1994). At the Texas Gulf Coast Site, in which the subsoils are fluvial deposits of late-Pleistocene age, 4 circular footings were tested with a diameter about 2.0 m at a depth of 2.3 m (Tand et al., 1994). All these experiments, at the two sites, were performed on lightly cemented, medium dense quartz sand.

For foundations located at a shallow depth, the ultimate load may occur at a foundation settlement of between 4 to 10% of B. This is true when general shear failure occurs, however, in the case of local punching shear failure, the ultimate load may occur at settlements of between 15 to 25% of the width of foundation (Das, 1990). Some researchers defined the ultimate bearing capacity ( $q_{ult}$ ) as the pressure for which settlement is equal to 10% of the width (e.g. Briaud and Jeanjean 1994). At the two test sites the relative density of the sands in the depth of influence of the footings was about 55% to 70%, indicating that a local shear failure is more probable (Fig. 6.5). Hence,  $q_{ult}$  is taken as the pressure at a relative displacement of  $s/B = 0.1$  (i.e. 10%).

Figure 6.6 presents the results of the 9 footing tests in terms of  $\alpha_r$  versus B/D, based on Eq. 6.11. The resulting correlation is given by:

$$[6.12] \quad \alpha_f = 0.1849 \left( \frac{B}{D} \right)^{-0.5093}$$

The correlation factor for the above regression analysis is 0.99. This correlation is valid for shallow footings in medium dense quartz sand with  $0.8 \leq D \leq 2.3$  m and  $1.0 \leq B \leq 3.0$  m (i.e.  $0.7 < B/D < 4.0$ ).

Recent data and evidence suggest that many natural sands may be very weakly cemented (Puppala et al. 1995). Apparently, the presence of low levels of cementation in the sands tested at the above sites might limit the application of the method developed in this study to lightly cemented sands. Fortunately, the effect of low levels of cementation on the factor  $\alpha_f$ , back-calculated using Eq. 6.11, is small since the ultimate friction angle of a cemented sand is similar to that of uncemented sand (Dupas and Pecker 1979; Clough et al. 1981) and based on the bearing capacity theory by Janbu and Senneset (1974) the increase in  $q_{ult}$  and  $q_c$  due to low levels of cementation can be assumed identical. Hence, the proposed method should be applicable to both lightly cemented and uncemented sands.

Combining Eq. 6.11 and Eq. 6.12, the final correlation between  $q_{ult}$  and  $\bar{q}_c$  can be obtained as follows:

$$[6.13] \quad q_{ult} = 0.1849 \bar{q}_c \left( \frac{B}{D} \right)^{-0.5093} \left( 1 + F \kappa \frac{B}{D} \right)$$

The application of Eq. 6.13 is limited to uncemented or lightly cemented predominantly silica sands since the available correlations and field test results were obtained in such sands. The ultimate bearing capacity of footings on heavily cemented sands may be overestimated using Eq. 6.13.

Equation 6.13 can be rearranged to derive the ratio between  $q_{ult}$  and  $\bar{q}_c$  in the form of:

$$[6.14] \quad K = \frac{q_{ult}}{\bar{q}_c} = 0.1849 \left( \frac{B}{D} \right)^{-0.5093} \left( 1 + F \kappa \frac{B}{D} \right)$$



where  $\kappa = 0.55$  for loose to medium dense sands  
 $\kappa = 1.00$  for dense sands

Figure 6.7 shows the resulting correlation of  $K$  with  $B/D$  ratio for various sand density and shape of footing. As shown in Fig. 6.7, in deep footings ( $B/D < 1.0$ ), an increase in width of footing results in a decrease in end bearing capacity. However, for shallow footings ( $B/D > 1.0$ ), the ultimate bearing capacity increases as the width of footing increases. This is shown by a trough at about  $B = D$ . This is controlled by  $\kappa$  ratio. Figure 6.7 shows that the factor  $K$  is almost constant beyond a  $B/D$  ratio of 2.0. This finding is in good agreement with the findings and recommendations of other investigators (Briaud and Jeanjean, 1994; Tand et al., 1995). However, its magnitude is found to be slightly different based on size and shape of the footing and mode of failure. Nevertheless, for most practical cases for shallow footings a constant ratio can be reasonably estimated between cone resistance and bearing capacity. A ratio of 0.16 can provide a reasonably conservative estimate for  $q_{ult}/\bar{q}_c$  for shallow footings on sands with any shape and for a wide range of soil density. Submergence of sand due to presence of ground water table within a depth of  $B$  beneath the footing, reduces the corresponding vertical effective stress, and hence the average cone penetration resistance. Therefore, the influence of ground water table is included in the predicted ultimate bearing capacity. If the water table is likely to rise due to seasonal changes, it is recommended to reduce the estimated bearing capacity under dry condition, by about 10% for the effect of submergence.

### 6.3 Estimation of the ultimate end bearing capacity of deep foundations

For deep foundations, the ultimate end bearing capacity does not constantly increase with depth but reaches an asymptotic value at a certain depth often called the critical depth (de Beer 1963), beyond which the capacity remains essentially constant. According to Meyerhof (1976), the value of critical depth depends on soil density and varies between  $5B$  and  $12B$  in loose and medium dense sands in which  $25^\circ < \phi < 35^\circ$  and ranges between  $12B$  and  $28B$  in dense sands in which  $35^\circ < \phi < 45^\circ$ . On this basis, and using Eq. 6.14, the maximum ratio between bearing capacity and cone resistance can be estimated as 0.66

in loose and medium dense sands and 1.02 in dense sands. This is in reasonable agreement with the findings of other researchers who noted that the difference between the ultimate end bearing capacity of a pile and measured cone penetration resistance is small. They further suggested that for practical purposes in deep footings  $q_{ult} = q_c$  (e.g. Ghionna et al. 1993). In most practical cases the magnitude of depth of penetration of piles into dense sand layer is greater than  $6B$  (i.e.  $B/D \leq 0.17$ ). Hence, for deep footings  $q_{ult} = q_c$  seems to be a reasonable average relationship. Based on the above discussion, Figure 6.8 displays an expanded view of  $K$  for  $B/D < 0.50$  based on Eq. 6.14 with the suggested limits of  $K = 0.66$  for  $D/B \geq 12$  for loose to medium dense sands and,  $K = 1.00$  for  $D/B \geq 28$  for dense sands. Fig. 6.8 is based on a relative settlement  $s/B = 0.10$ . For smaller values of relative settlement, the values of  $K$  would be smaller.

#### 6.4 Summary and conclusions

This chapter serves to present a review of the available methods for predicting ultimate bearing capacity of foundations in cohesionless soils by means of cone penetration testing (CPT). Extensive research has been performed to correlate cone resistance to the end bearing capacity of deep footings. However, few attempts have been made to estimate bearing capacity of shallow footings directly from CPT data. The most widely used procedure for computing  $q_{ult}$  using CPT data is indirect and based on the general bearing capacity theory in which either internal friction angle or bearing capacity factors are estimated from empirical correlations or published charts. However, the ultimate bearing capacity of shallow footings on sand is often overpredicted using correlations that relate cone resistance to friction angle because such relationships are most frequently based on test results from calibration chamber tests performed on uncemented unaged sands while some natural sands are lightly cemented. In addition, general bearing capacity theory does not consider the effect of soil compressibility.

For shallow foundations, the method by Meyerhof (1956) and recently the method by Tand and Funegard (1995) are distinguished since they predict the ultimate bearing capacity directly from the CPT data and include the effect of embedment and footing size on the estimated ultimate bearing capacity of shallow footings.

For deep foundations, many researchers propose a single constant ratio between end bearing of piles and cone penetration resistance regardless of the size and depth effect.

This seems to be a reasonable assumption since the penetration of the cone is analogous to the driving of a pile into the ground. These correlations have been developed based on the results of a number of pile load tests. The scale effect and the influence of installation procedure are embodied in the proportional factor between  $q_{ult}$  and average  $q_c$  around the pile end. The most widely used methods to estimate end bearing capacity of piles in sands directly from CPT results are the methods by Schmertmann (1978), de Ruiter and Beringen (1979), and Bustamante and Gianselli (1982).

In this chapter, a procedure has been proposed to evaluate the ultimate bearing capacity of shallow and deep footings in sands using in-situ cone penetration test results. The application of the procedure is limited to uncemented or lightly cemented, predominantly silica sands. The ultimate bearing capacity of footings on heavily cemented sands could be overestimated. The results of full scale load tests from 9 full scale spread footings have been used to develop the proposed relationship for bearing capacity. A regression analysis has been performed to investigate the effect of the shape, size and depth of footing on the predicted bearing capacity. It has been concluded that for practical purposes a conservative constant ratio of 0.16 can be reasonably assumed between average cone resistance and bearing capacity for shallow footings on sands with any shape and for a wide range of soil density. When the correlation is extended to predict end bearing capacity of deep foundations in sand, results are found to be in good agreement with field observations. Hence, a single correlation developed in this study can be used to estimate either ultimate bearing capacity of shallow footings or end bearing capacity of deep footings. In deep foundations, where  $D/B$  can be greater than 10, the ratio between end bearing capacity and cone penetration resistance varies between 0.66 in loose to medium dense sands and 1.00 in dense sands. The proposed correlations are based on a settlement to width ratio,  $s/B=0.10$  at the ultimate bearing capacity.

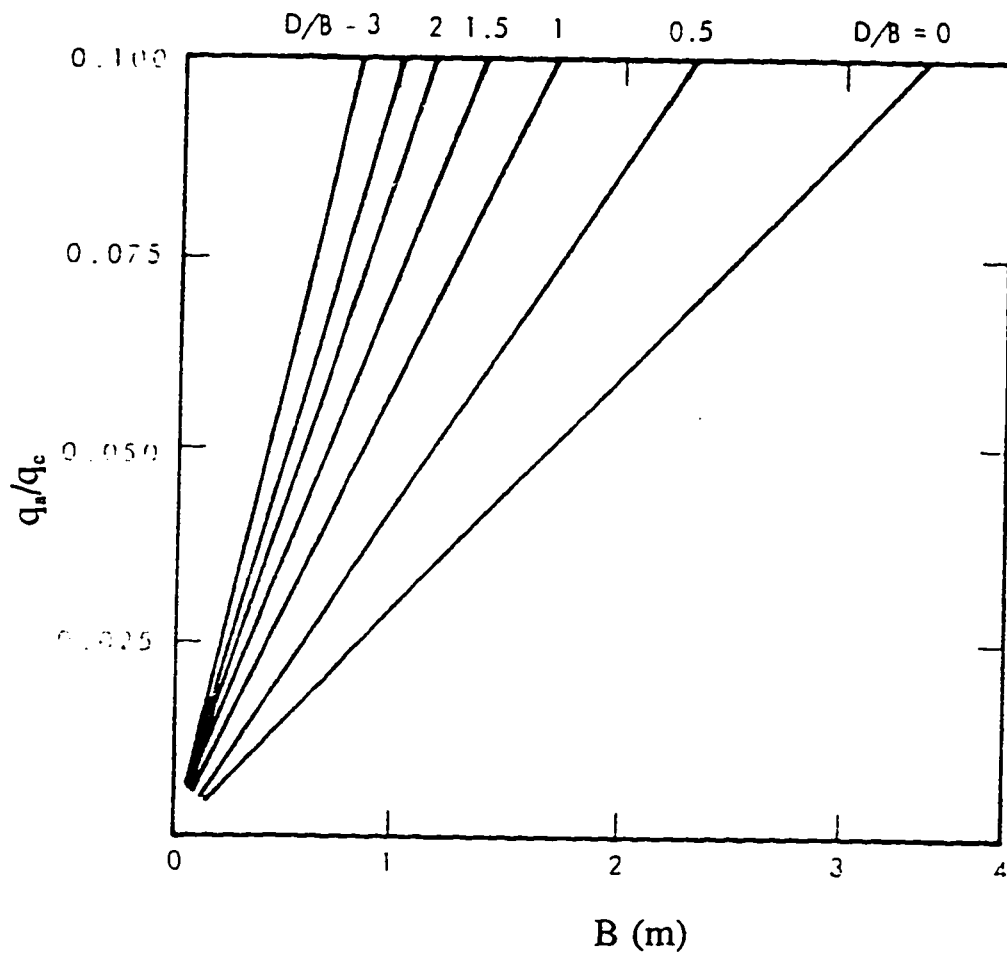


Fig. 6.1 Allowable bearing pressure estimated from Cone Penetrometer (after Meyerhof, 1956)

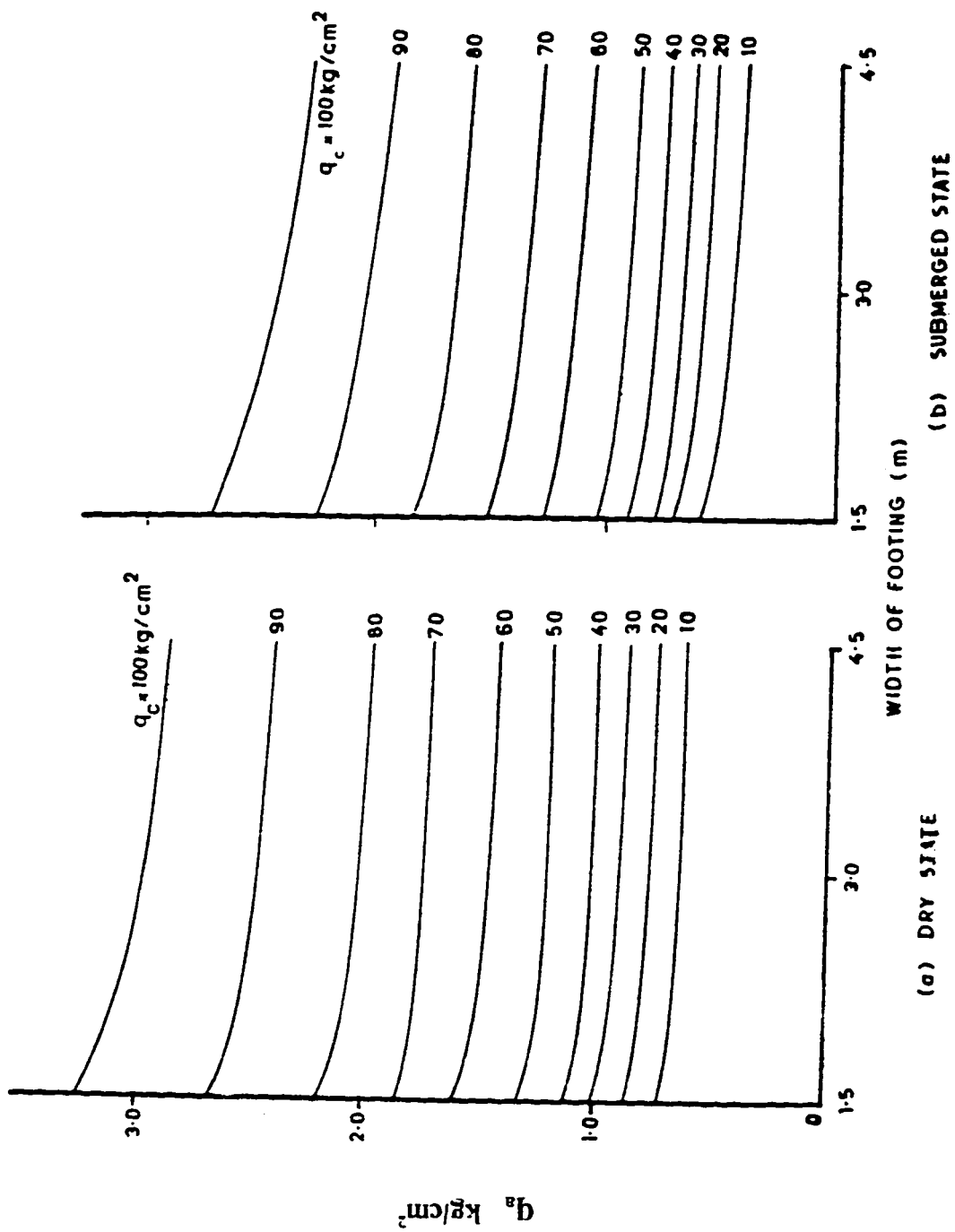


Fig. 6.2 Correlation between  $q_u$  and allowable bearing pressure  $q_a$ , for various sizes of footings (after Goel, 1982)

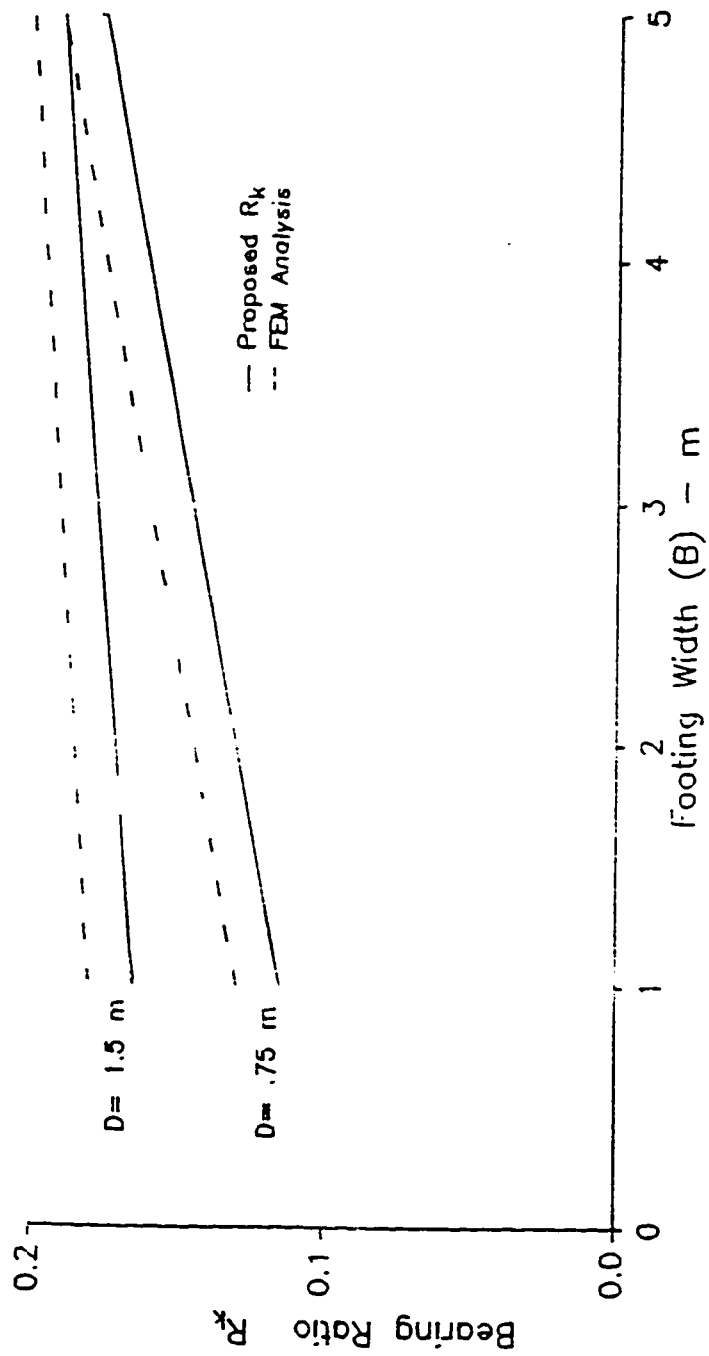
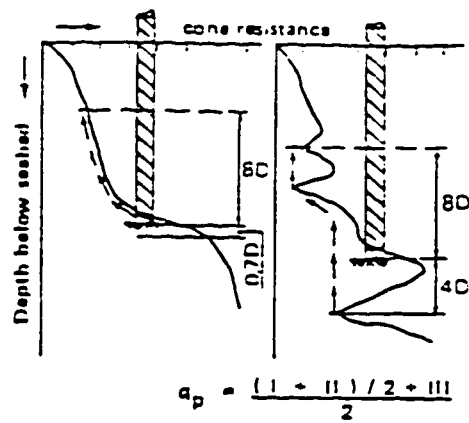


Fig. 6.3 Bearing ratio versus width of the footing (after Tand et al., 1995)



Key

- D : Diameter of the pile
- I : Average cone resistance below the tip of the pile over a depth which may vary between 0.7D and 4D
- II : Minimum cone resistance recorded below the pile tip over the same depth of 0.7D to 4D
- III : Average of the envelope of minimum cone resistances recorded above the pile tip over a height which may vary between 6D and 8D. In determining this envelope, values above the minimum value selected under II are to be disregarded
- $q_p$  : Ultimate unit point resistance of the pile

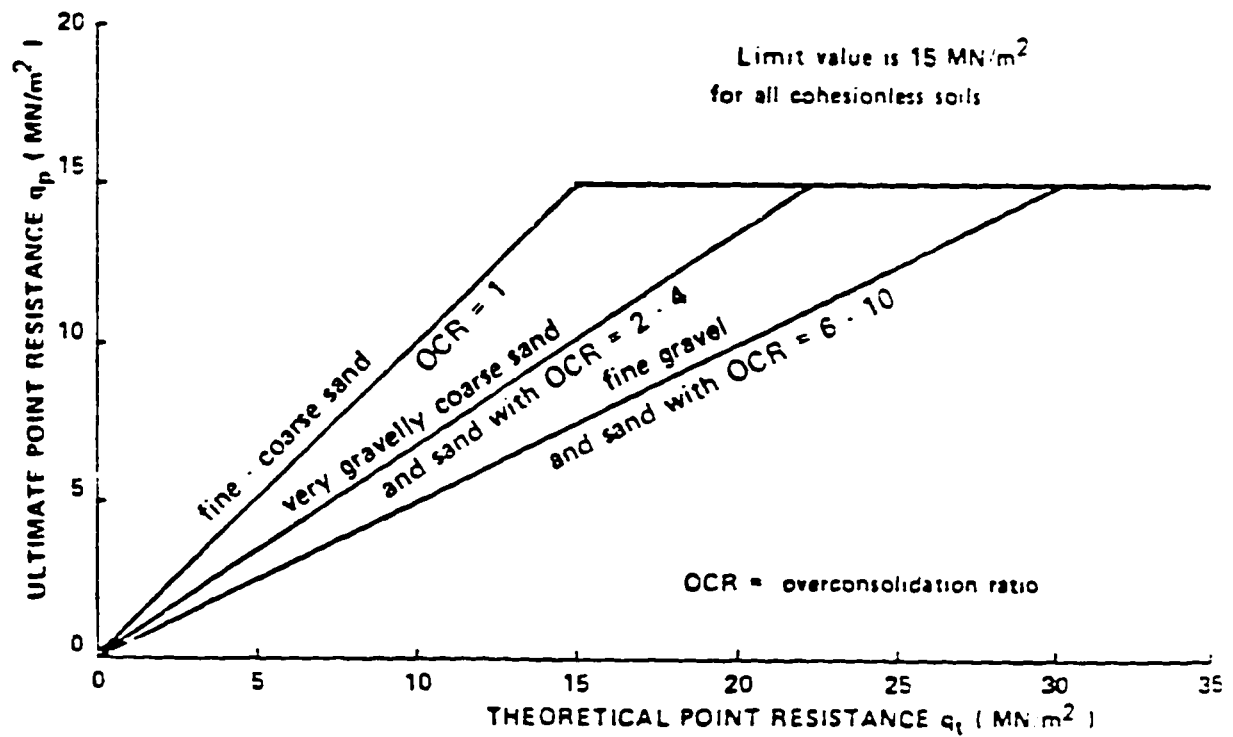


Fig. 6.4 Application of CPT to pile design (after Schmertmann, 1978)

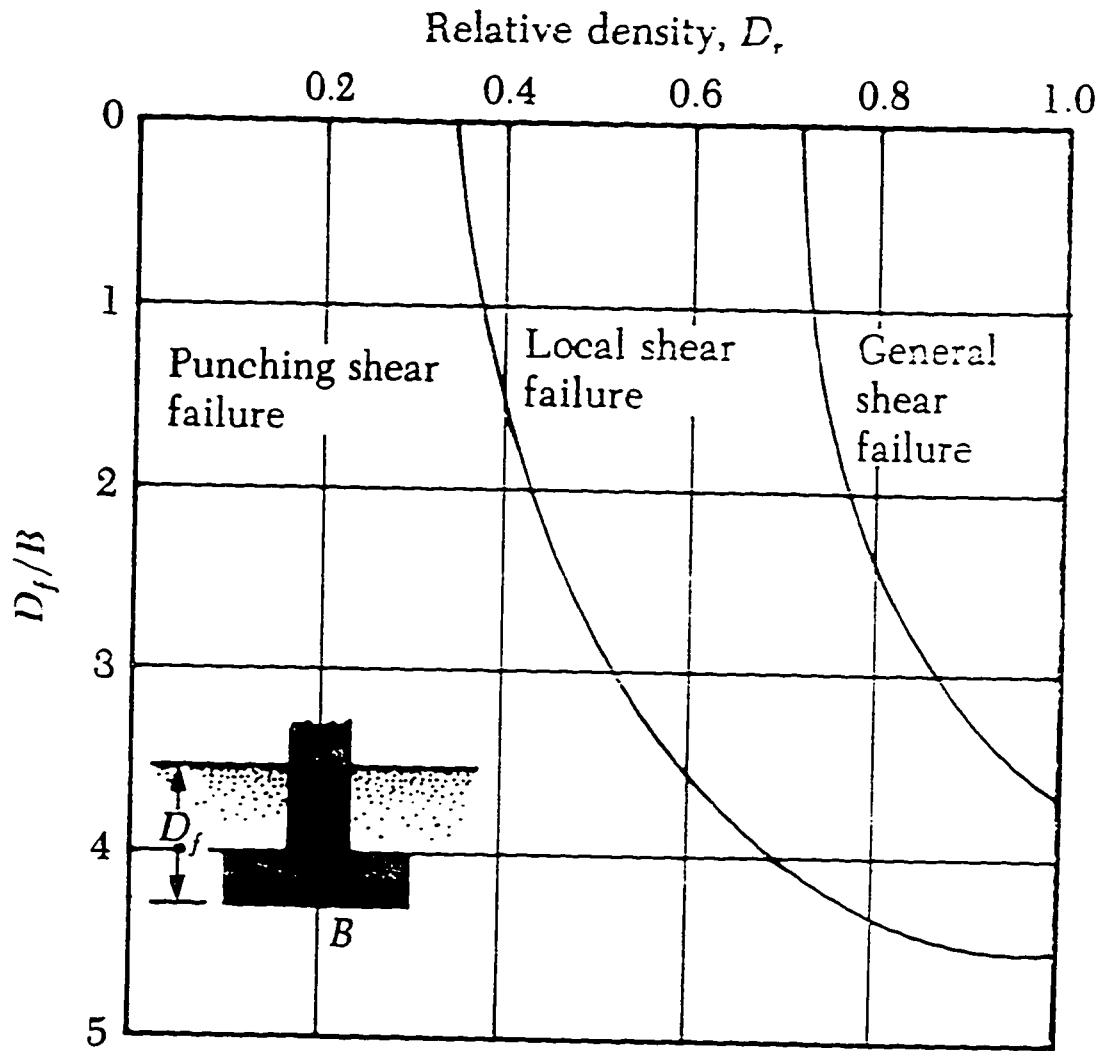


Fig. 6.5 Modes of foundation failure in sand (after Vesic, 1973)



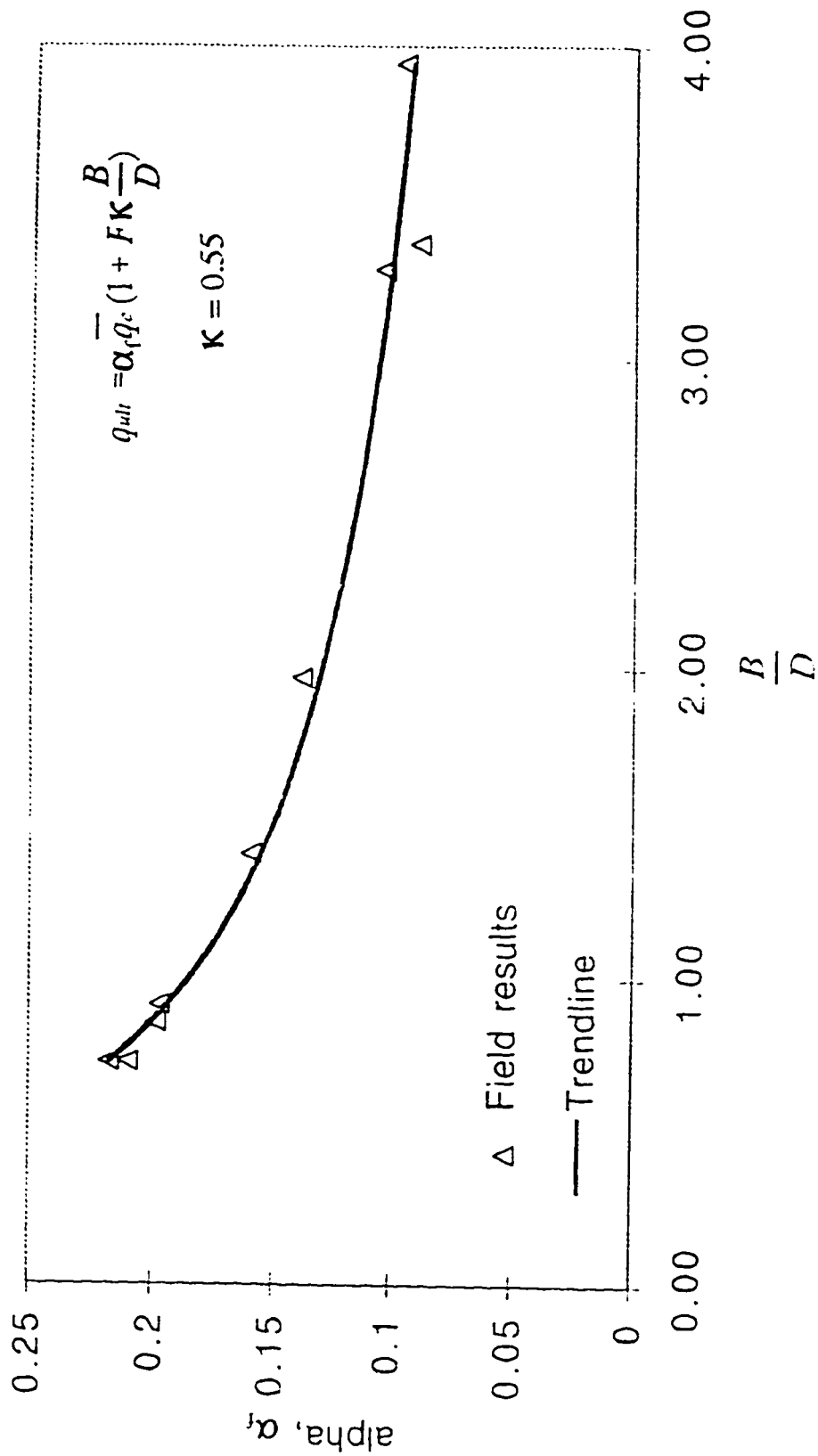


Fig. 6.6 Regression analysis to evaluate the empirical correlation factor,  $\alpha_r$

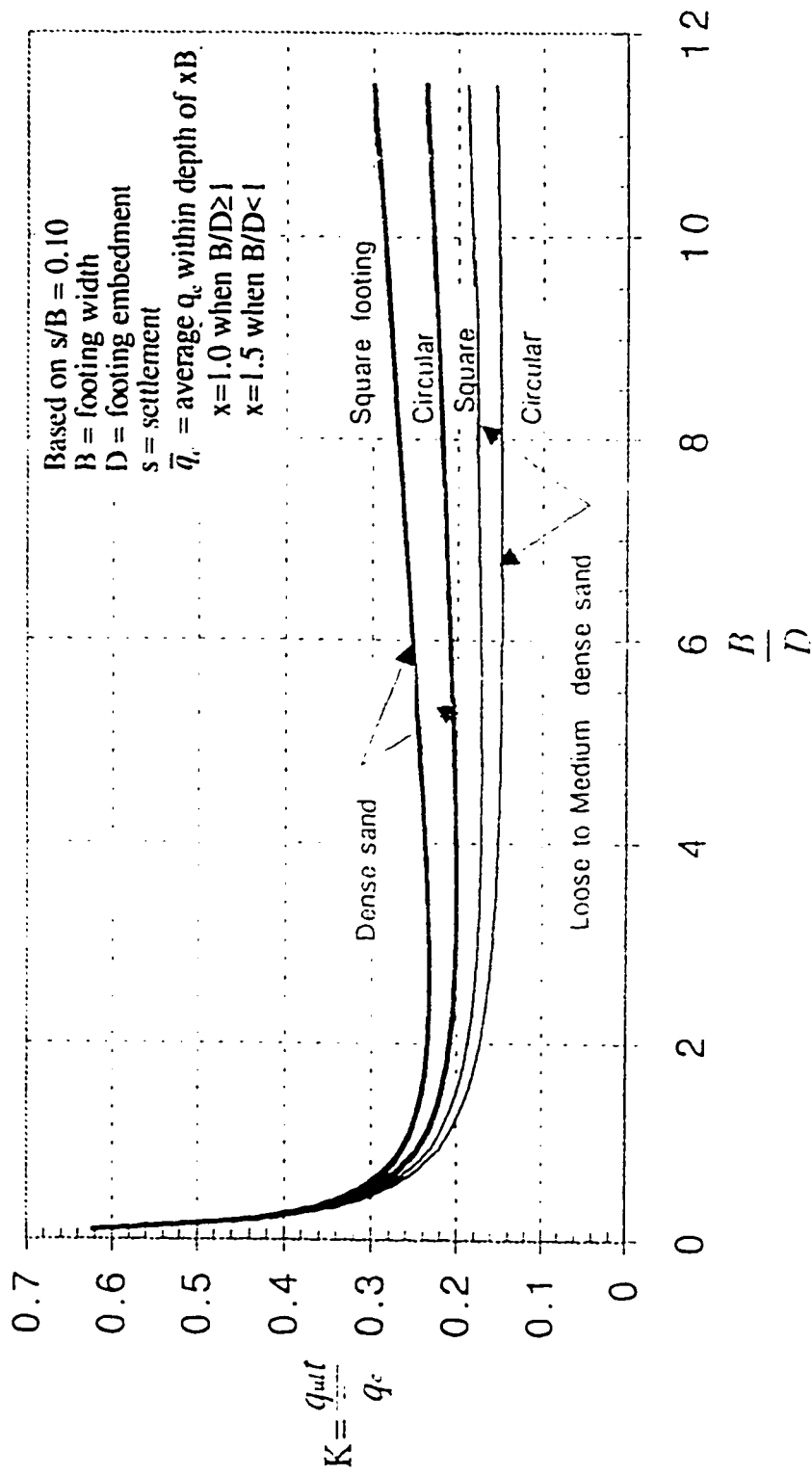


Fig. 6.7 Correlation between bearing capacity of footings on cohesionless soils and average cone resistance,  $\bar{q}_c$ .

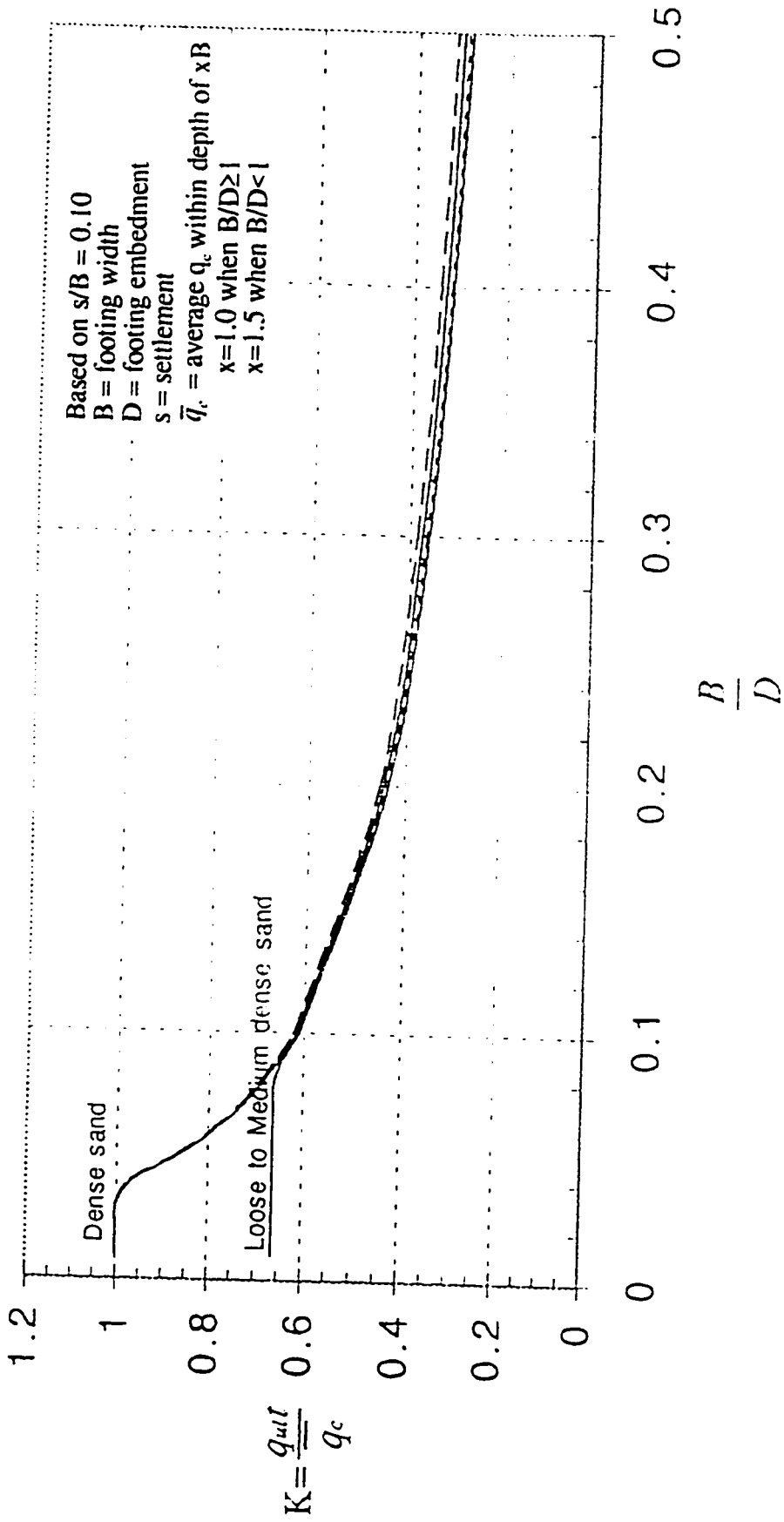


Fig. 6.8 Correlation between bearing capacity and average cone resistance,  $\bar{q}_c$ , in deep footings,  $\bar{q}_c$ .

## References

- Bottiau, M., 1995. Comparative assessment of the bearing capacity out of CPT-results, Proceedings of CPT'95, pp. 399-406.
- Briaud, J. L. and Gibbens, R. 1994. Test and prediction results for five large spread footing on sand. Predicted and Measured Behavior of five spread footing on sand, ASCE Geotechnical Special Publication No. 41, pp. 92-128.
- Briaud, J. L. and Jeanjean, P. 1994. Load settlement curve method for spread footings on sand. Vertical and Horizontal Deformations of Foundations and Embankments, ASCE Geotechnical Special Publication No. 40, Vol. 2, pp. 1774-1804.
- Bustamante, M. and Gianceselli, L. 1982. Pile bearing capacity prediction by means of static penetrometer CPT. Proceedings of the second European symposium on penetration testing, ESOPT II, Amsterdam, pp. 493-500.
- Clough, G. W., Sitar, N., Bachus, R. C., and Rad, N. S. 1981. Cemented sands under static loading, Journal of Geotechnical Engineering, Vol. 107, No. GT6, ASCE, pp. 799-816.
- Das, B. M. 1990. Principles of Foundation Engineering, Second Edition, PWS-KENT Publishing Company, Boston, 731p.
- De Beer, E. E., 1963. The scale effect in the transposition of the results of deep-sounding tests on the ultimate bearing capacity of piles and caisson foundations, Geotechnique, 13, pp. 39-75.
- De Ruiter, J. and Beringen, F. L. 1979. Pile foundations for large North Sea structures, Marine Geotechnology, Vol. 3, No. 3, pp. 267-314.
- DTU13.2, Document Technique Unifie no 13.2 1978, 1985. Centre Scientifique et Technique du Batiment.
- Dupas, J. M. and Pecker, A., 1979. Static and dynamic properties of sand-cement, Journal of Geotechnical Engineering, Vol. 105, No. GT3, ASCE, pp. 419-436.
- Eslami A. and Fellenius B. H., 1995 Toe bearing capacity of piles from cone penetration test (CPT) data, Proceedings of International Symposium on cone penetration testing, CPT'95, Linkoping, Sweden, Vol. 2, 3.12, pp. 453-460.
- Fioravante, V., Ghionna, V., Jamiolkowski and M., Pedroni S. 1995. Load carrying capacity of large diameter bored piles in sand and gravel. Tenth Asian Conference on Soil Mechanics and Foundation Engineering

- Ghionna, V. N., Jamiolkowski, M., Pedroni S. and Lancellotta R. 1993. Base capacity of bored piles in sands from in-situ tests. Proceedings of 2nd international geotechnical seminar on deep foundation on bored and auger piles, Ghent, Edit. W. F. Van Impe, pp. 67-75.
- Goel M. C. 1982. Correlation of static cone resistance with bearing capacity. Proceedings of the second European symposium on penetration testing, ESOPT II, Amsterdam, pp. 575-579.
- Janbu, N., and Senneset, K. 1974. Effective stress interpretation of in-situ static penetration tests. Proc. European Symp. on Penetration Testing, ESOPT I, A.A. Balkema, Rotterdam, The Netherlands, Vol. 1.2., pp. 479-488.
- Koumoto, T. 1988. Ultimate bearing capacity of cones in sand. Penetration Testing 1988, ISOPT-1, De Ruyter (ed.), pp. 809-813.
- Meyerhof, G.G. 1956. Penetration tests and bearing capacity of cohesionless soils. Journal of Soil Mechanics and Foundations Division, ASCE, Vol. 82 No. SM 1, pp. 1-19.
- Meyerhof, G.G. 1976. Bearing capacity and settlement of pile foundations. Journal of Geotechnical Engineering, Vol. 102, No. GT3, ASCE, pp. 197-228.
- Nottingham, L.C. 1975. Use of quasi-static friction cone penetrometer data to predict load capacity of displacement piles. Ph.D. thesis, Dept. of Civil Engineering, University of Florida, 553p.
- Peterson, R. W. 1991. Penetration resistance of fine cohesionless materials., Proceedings of the First International Symposium on Calibration Chamber Testing/ISOCCT1, Potsdam, New York, Edited by An-Bin Huang, pp. 315-328.
- Puppala, A. J., Acar, Y. B. and Tumay, M. T. 1995. Cone penetration in very weakly cemented sand, Journal of Geotechnical Engineering, Vol. 121, ASCE, pp. 589-601.
- Schmertmann, J. H. 1978. Guidelines for cone test, performance and design. Federal Highway Administration, report FHWA-TS-78209, Washington, 145p.
- Tand K. E., Funegard E.G. and Warden P. E. 1994. Footing Load Test on Sand. Vertical and Horizontal Deformations of Foundations and Embankments, ASCE Geotechnical Special Publication No. 40, Vol. 1, pp. 164-178.
- Tand K. E., Funegard E.G. and Warden P. E. 1995. Predicted/ Measured Bearing Capacity of Shallow Footings on Sand. Proceeding of CPT'95, Linkoping, Volume 2, Sec. 3.33, pp. 589-594.
- Terzaghi, K. 1943. Theoretical soil mechanics, Wiley, New York.

- Vesic, A., 1963. Bearing capacity of deep foundations in sands. Highway research Record No. 39, National Academy of Sciences, pp. 112-153.
- Vesic, A., 1973. Analysis of ultimate loads of shallow foundations. Journal of Soil Mechanics and Foundations Division, ASCE, Vol. 99, No. SM 1, pp. 45-73.

## CHAPTER 7

### EVALUATION OF SETTLEMENT OF FOOTINGS ON SAND FROM SEISMIC IN-SITU TESTS<sup>1</sup>

#### 7.1 Introduction

The inevitable disturbance that occurs during sampling and subsequent handling of samples severely alters the compressibility and stiffness of granular materials. Consideration is therefore directed to alternative methods of in-situ testing to determine moduli for estimating settlement of footings. For lightly-loaded structures supported on sands the consequences of overestimating soil compressibility are minor, typically resulting in conservative sizing of footings. For heavily loaded high-rise structures, however, unrealistically high settlement estimates can lead to the use of costly deep foundations that may not be warranted.

Numerous articles have appeared in the literature related to the prediction of settlement of footings on sand by means of in-situ tests. Most of these methods have been based on the conventional elastic formula, where the ground is assumed to be an elastic homogeneous medium, in the form of:

$$[7.1] \quad s = I_s \frac{q \cdot B}{E}$$

in which  $q$  is net foundation pressure supported by the soil in excess of the pressure caused by the surrounding soil at the foundation level,  $B$  is the width of foundation,  $E$  is the strain compatible soil stiffness,  $I_s$  is an influence factor depending on the shape and rigidity of the foundation and the Poisson's ratio of the ground.  $I_s$  is theoretically 0.785 for circular footings and 0.815 for square footings. Typically,  $I_s$  can be taken as 0.8 for practical purposes. Sand deposits are often non-homogeneous in nature in which the

---

<sup>1</sup> A version of part of this chapter has been submitted to the 50th Canadian Geotechnical Conference in Ottawa, Eslamizaad, S. and Robertson P.K. 1997. Evaluation of settlement of footings on sand from seismic in-situ tests.

stiffness varies with depth. Hence, an equivalent soil modulus is frequently estimated based on in-situ testing measurements. Empirical correlations exist relating in-situ testing results to the ground stiffness from which the equivalent ground modulus can be obtained and used in Eq. 7.1. In general, a depth of influence is defined within which an average value of soil modulus, is computed. The depth of stress influence is somewhat uncertain and has been subjected to many research activities. It is a function of factors such as foundation width to length ratio ( $B/L$ ), and variation of ground stiffness with depth. Depth of influence is often assumed to be equal to two times the width of footing, i.e.  $2B$ .

Over the past three decades geotechnical researchers have studied and proposed a number of methods for obtaining more realistic estimates of the stiffness of sands. Lambe and Whitman (1969) proposed using the reload cycle of triaxial compression tests to estimate the modulus of deformation of sand. Experience has shown that moduli measured during the initial load cycles of triaxial tests overestimate the in-situ compressibility of sands. Lambe and Whitman (1969) reported that the second cycle of loading gives a better estimate of in-situ modulus. Eisenstien and Morrison (1973) evaluated the use of pressuremeter tests for settlement analyses. Swiger (1974) proposed using seismic velocity surveys in combination with cyclic laboratory tests to estimate strain-compatible Young's and shear moduli for use in settlement analyses. Schmertmann (1978) presented settlement prediction methods based on cone penetrometer tests.

The procedure originally proposed by Schmertmann (1970) and modified by Schmertmann et al. (1978) is now widely used for the systematic computation of the static settlement of isolated, rigid, concentrically loaded shallow foundations over nonhomogeneous sand. Its application is limited to sands with predominantly quartz minerals. Use of this method for unusual sands such as highly compressible carbonate sands and cemented sands, can be misleading and sometimes unsafe. The procedure consists of dividing the sand below the footing into  $n$  layers. The method employs elastic half-space theory in a simplified form and uses the static cone penetration resistance,  $q_c$ , as a practical means for determining in-situ stiffness of sands,  $E$ . The estimate of  $E$  from  $q_c$  is in the form of:

$$[7.2] \quad E = \alpha_E q_c$$

where  $q_c$  is cone penetration resistance and  $\alpha_E$  is recommended to be 2.5 for axisymmetrical conditions and 3.5 for plain strain conditions for normally consolidated



sands (Schmertmann et al., 1978). The penetration of the cone alters almost completely the previous stress and strain history of the sand (Baldi et al. 1986). Hence,  $\alpha_E$  should vary with stress history and compared to normally consolidated sands higher values of  $\alpha_E$  should be used for highly overconsolidated sands. As a result of above discussion, an oversimplified correlation such as Eq. 7.2 will involve considerable amount of uncertainty that could result in costly dimensioning for the footing over sand.

Seismic tests are among the few in-situ tests that produce little or no soil disturbance. Such techniques induce very small strain in the ground that preserve its natural features. Swiger (1974) applied in-situ seismic techniques in the evaluation of ground settlement using conventional linear elastic theory. In his approach, the measured small strain moduli are softened using reduction curves developed by Seed (1969) based on the strain level in the ground. However, the curves given by Seed do not distinguish between sand stress history and sand grain mineralogy. More realistic computation of settlement of footings on sands can be obtained when appropriate modulus degradation curves are utilized in determining operational modulus of the ground from the measured small strain modulus. Hence, prior knowledge of stress history and compressibility of sand are required to select an appropriate modulus degradation curve. However, such information can not be provided by means of seismic testings alone.

Seismic methods can measure the small strain response of a large volume of the ground, whereas the penetration of the cone measures the large strain response of the ground since average stress levels around the cone approximately equals failure in the soil. Hence, the seismic CPT (SCPT) which measures both small and large strain responses of the ground can provide more information about geotechnical properties. During the SCPT, the shear wave velocity ( $V_s$ ) can be measured. Based on elastic theory, the small strain shear modulus ( $G_o$ ) can be determined from the seismic shear wave velocity ( $V_s$ ) using:

$$[7.3] \quad G_o = \rho(V_s)^2$$

where,  $\rho$  is mass density of soil.

Recently, Eslaamizaad and Robertson (1996a, 1996b, 1996c) (Chapter 3, Chapter 4, Chapter 5) investigated the potential of using seismic CPT (SCPT) for the in-situ

determination of degree of cementation, compressibility, and stress history of sands. They proposed correlations to identify unusual sands and to estimate the stress history of sands from a combined measurement of shear wave velocity and cone resistance in sands.

In this chapter, two methods are presented to evaluate the settlement of footings on sand using seismic methods. The methods employ elastic half-space theory and use the measured shear wave velocity for determining the in-situ stiffness of sands. They can be used for the systematic computation of the settlement of isolated, rigid, concentrically loaded shallow foundations over nonhomogeneous sand. One method is based on an assumed homogenous ground beneath the footing. Hence, an equivalent operational modulus, for the nonhomogeneous layered ground within the depth of influence beneath the footing, is computed. Then, the equivalent modulus is incorporated into conventional elastic formulae. In the second approach, the ground is divided into layers, in which the operational modulus of each layer is computed for the evaluation of the settlement of the corresponding layer. A summation of settlement of layers within the depth of influence provides the total settlement. The latter proposed method has a similar framework as the method developed by Schmermann (1970). However, in this method the operational modulus is computed from the direct in-situ measurement of shear wave velocity rather than using an empirical correlation. A set of curves are constructed to soften the measured small strain modulus of the sand layers based on the degree of loading, stress history and grain mineralogy.

In the following sections, the methods are developed to evaluate the equivalent small strain soil modulus beneath the footing and to compute the operational soil modulus of the ground.

## **7.2 Depth of influence and evaluation of equivalent modulus**

### **7.2.1 Background**

Many investigators have proposed to use a simple arithmetic mean of soil modulus over an assumed depth of influence, below which it is assumed that stresses have negligible influence on the computed settlement, to obtain an equivalent modulus for the computation of settlement. Several researchers identified the significance of thickness and depth of

different layers within the stress influence zone and recommended a weighted average rather than a simple averaging of values (e.g. Schmertmann, 1970). Others have considered an average point within the pressure bulb whose property is taken as an equivalent value into the calculation (e.g. Lambe and Whitman, 1969). The depth of influence is somewhat uncertain and has been the subject of many research activities. A depth of influence equal to  $2B$  has been widely used.

Menard (1965), in his approach to predict settlements from pressuremeter testing results, introduced a procedure to determine equivalent value of distortional modulus in heterogeneous soil. In that approach, the ground underneath the footing is divided into sixteen layers of equal thickness of  $B/2$ . The pressuremeter modulus at the center of each layer is measured and called  $E_1$  to  $E_{16}$ . The equivalent modulus is then obtained from following equation:

$$[7.4] \quad \frac{1}{E_{eq}} = \frac{1}{4} \left[ \frac{1}{E_1} + \frac{1}{0.85E_2} + \frac{1}{E_{3/4/5}} + \frac{1}{2.5E_{6/7/8}} + \frac{1}{2.5E_{9/16}} \right]$$

where  $E_{p/q}$  is the harmonic mean of the moduli of layers  $p$  to  $q$

Schmertmann (1970) and Schmertmann et al. (1978) in their method to predict settlement on sands, assumed an influence depth of  $2B$  and  $4B$  beneath a square footing and strip footing, respectively. Based on elastic half-space theory they employed variable strain influence factors with depth,  $I_z$ . This incorporates the significance of both the thickness and depth of different layers within the depth of influence. The procedure consists of dividing the assumed depth of influence  $H$ , into  $n$  layers of thickness  $\Delta z_i$ . The settlement is then calculated from:

$$[7.5] \quad s = q \sum_{i=1}^n \left( \frac{I_z}{E_n} \right) \Delta z_i$$

where  $E_n$  = stress-strain modulus estimated from cone penetration resistance for layer  $i$ .

Based on the statistical analysis of a number of settlement observations Schultze and Sherif (1973) presented a method for predicting the settlement of foundations on sand. They developed a relationship to evaluate modulus from the number of blows  $N$  of the

standard penetration test (SPT). It was assumed that the thickness of the compressible layer below the foundation is less than  $2B$ . The arithmetic mean of the blows in within the depth of  $2B$  is used in the computation. Where several layers are found within the depth of influence, they recommended to evaluate the mean value of blows  $N_m$  from following equation:

$$[7.6] \quad N_m = \frac{f_n}{\sum_1^n \frac{f_n - f_{n-1}}{N_n}}$$

where  $n$  is number of the layer concerned, and  $f_n$  is the influence factor for the settlements according to the tables for the elastic isotropic half space for a Poisson ratio  $\nu = 0$ .

Parry (1978) developed a procedure to estimate foundation settlement in sand based on SPT  $N$ -values. To choose a representative value  $N_m$  from the measured values of  $N$ , he assumed an influence depth of  $2B$  below the foundation. In order to place greater influence on values immediately below the foundation, he suggested taking an average value of  $N$ , denoted  $N_1$ , from foundation level to a depth of  $\frac{2}{3}B$  below foundation level,  $N_2$  from  $\frac{2}{3}B$  to  $\frac{4}{3}B$  and  $N_3$  from  $\frac{4}{3}B$  to  $2B$ .  $N_m$  is then given by:

$$[7.7] \quad N_m = \frac{1}{6}(3N_1 + 2N_2 + N_3)$$

He explained that the emphasis placed on different  $N$  values within a depth  $2B$  by the above method corresponds very well to the vertical strain distribution idealized from experimental observation by Schmertmann (1970).

Based on analysis of over 200 records of foundations, Burland and Burbidge (1985) developed a method to predict settlement of foundations on sands and gravels. In their method, the arithmetic mean of the SPT  $N$ -value over the depth of influence of foundation  $Z_1$ , is used. They assumed that the depth of influence is the depth within which 75% of the surface settlement takes place. In their method of settlement computation, they assumed a unique relationship between  $Z_1$  and  $B$  for cases where  $N$  increases or is constant with depth as illustrated in Fig. 7.1. Where  $N$  shows a consistent decrease with depth, they

recommend to take the depth of influence as  $2B$  or to the bottom of the soft layer. However, Burland and Burbidge emphasized that the depth of influence corresponding to a given value of  $B$  will not be unique and will depend on the variation of stiffness with depth. By means of a finite element analysis, they plotted the normalized distribution of settlement ( $s/s_0$ ) with  $(z/2a)$  beneath the center of a rigid rough circular footing of radius  $a$ , where  $2a = B$ , on a non-homogeneous ground having an increasing Young's modulus with depth for various values of  $(E_s/ak)$ , as shown in Fig 7.2. They concluded that the higher is the rate of increase of Young's modulus, the shallower will be the depth of influence.

Based on a study of the Boussinesq pressure profiles, Schmertmann's strain profiles, and vertical strain profiles based on the equations by Timoshenko and Goodier (1951), Bowles (1987) concluded that for all practical purposes the soil mass below a depth of  $4B$ - $5B$ , has little influence on the foundation settlement. In addition, from an examination of the stress and strain profiles, he indicated that taking the depth of influence as  $5B$  seems reasonable and slightly conservative over using  $4B$ . He further noted that in homogeneous sand deposits the stress-strain modulus  $E_s$  generally increases with depth and would be much larger at  $5B$  than at the foundation base. Based on this consideration, he suggested that for computing the elastic settlement of a foundation on sand deposit using the conventional elastic settlement, one should use an average value of the stress-strain modulus  $E_s$  over the depth of  $H = 4B$  to  $5B$  and not the value in the zone of  $B$  to  $2B$  beneath the foundation.

Bowles recommended a weighted average rather than a simple arithmetic average of values. The weighted average is computed as:

$$[7.8] \quad E_s = \frac{\sum H_i E_{si}}{H}$$

He also pointed out that additional weighting should be used as necessary with corresponding adjustment in both  $H_i$  and  $H$ . However, Bowles did not evaluate these weighting factors for various depth beneath the footing.

Leonards and Frost (1987) developed a procedure using a combination of dilatometer and cone-penetration test results to include the effects of overconsolidation on the settlement of shallow foundations on granular soils. They assumed the thickness of the granular stratum to be equal or less than  $2B$  in a generalized form of Schmertmann's expression.

### 7.2.2 Proposed method for the evaluation of equivalent modulus

Among the available methods for evaluation of equivalent stiffness, those which include the significance of both the thickness and depth of different layers within the depth of influence are distinguished, for example the method by Schmertmann (1970) and Schmertmann et al. (1978). The procedure proposed here has a similar framework.

The computation of settlement requires an integration of strains in the form of:

$$[7.9] \quad s = \int_0^H \epsilon_z dz = q \int_0^H \left( \frac{I_z}{E_z} \right) dz = q \sum_0^H \left( \frac{I_z}{E_z} \right) \Delta z$$

where H is the depth of influence,  $\epsilon_z$  and  $E_z$  are vertical strain and Young's modulus at depth z, respectively. The last form of Eq. 7.9 can be used for nonhomogeneous soils. When soil is homogeneous in depth with uniform modulus of E, Eq. 7.9 can be written in the following form:

$$[7.10] \quad s = \frac{q}{E} \sum_0^H I_z \Delta z$$

A comparison between Eqs. 7.9 and 7.10 results in the following relationship for the computation of equivalent modulus for nonhomogeneous ground:

$$[7.11] \quad E_{eq} = \frac{\sum_{i=1}^n I_i \Delta z_i}{\sum_{i=1}^n \frac{I_i \Delta z_i}{E_i}}$$

where, the influence depth below the footing is divided into n layers not thicker than 0.5B. This equation can be further simplified by taking layers of equal thickness. Here a minimum depth of 2B is used for square footings.  $I_i$  is the average strain influence factor based on the operational Poisson's ratio, for layer i whose thickness and Young's modulus are  $\Delta z_i$  and  $E_i$ , respectively.

The values of strain influence factors  $I_i$  can be obtained from tables given by Ahlvin and Ulery (1962) for use in an equation presented by them for vertical strain beneath a uniform circular load on an elastic homogeneous isotropic halfspace in the form of:

$$[7.12] \quad \varepsilon = \frac{q}{E_i} I_i$$

in which

$$[7.13] \quad I_i = (1 + \nu)[(1-2\nu)A + B]$$

where  $\nu$  is Poisson's ratio and A and B are functions whose values vary with depth and radial distance from the load axis. Figure 7.3 illustrates the distribution of the strain influence factors with depth on the axis of loading for Poisson's ratio from 0.1 to 0.5. It displays a noticeable variation only within the depth of  $0.5B$  beneath the footing and the rest is little affected by variation of Poisson's ratio. Although the variation of Poisson's ratio is limited, the strain level dependency of Poisson's ratio has been noted by several researchers. Shibuya et al. (1992) reported that the small strain Poisson's ratio in sands ranges from 0.1 to 0.2. However, the large strain or operational value of Poisson's ratio in sand is commonly in the range from 0.2 to 0.4. Figure 7.4 illustrates the recommended simplified distribution of the strain influence factors with depth on the axis of loading for both small strain ( $\nu = 0.15$ ), and large strain ( $\nu = 0.30$ ) range of loading.

Assuming a constant Poisson's ratio Eq. 7.11 can be written in terms of shear modulus in the form of:

$$[7.14] \quad G_{eq} = \frac{\sum_{i=1}^n I_i \Delta z_i}{\sum_{i=1}^n \frac{I_i \Delta z_i}{G_i}}$$

in which  $G_i$  and  $G_{eq}$  represent shear modulus at the midpoint of layer  $i$  and equivalent shear modulus beneath the footing, respectively.

Based on Eq. 7.14 and taking layers of equal thickness of  $0.5B$  the following simple relationship can be derived for small strain shear modulus:

$$[7.15] \quad G_{\text{oeq}} = 10 / (4/G_{o1} + 3/G_{o2} + 2/G_{o3} + 1/G_{o4})$$

in which  $G_{o1}$ ,  $G_{o2}$ ,  $G_{o3}$  and  $G_{o4}$  are the small strain shear moduli at the middle of layer 1, 2, 3 and 4, respectively, beneath the footing.

### 7.3 Operational stiffness of ground

Seismic methods, such as Spectral Analysis of Surface Waves (SASW), Downhole, Uphole or Crosshole techniques and Seismic cone penetration test (SCPT) can provide reliable small strain shear modulus profiles of sandy soils. However, the elastic moduli derived from the seismic methods reflect the stiffness of soils at very low strain levels. Two changes can occur to the soil moduli due to stresses induced by loading from a shallow foundation. While the increase in shear strains can decrease the ground stiffness, increased confinement due to loading of a footing will increase the soil stiffness.

Soils exhibit non-linear stress-strain behavior, becoming softer at higher strain levels. The rate of reduction in modulus depends on grain mineralogy, stress history and density of the sand. For low compressible sands with various stress history and relative density, Teachavorasinskun et al. (1991) performed high quality tests and plotted corresponding shear modulus reduction curves. In this study, these diagrams are used to establish relationships between  $G/G_o$  and  $\tau/\tau_{\text{max}}$  based on curve fitting techniques.  $\tau/\tau_{\text{max}}$  can be used as a measure of the degree of loading, and should be computed. Then, knowing the stress history and sand mineralogy, the appropriate  $G/G_o - \tau/\tau_{\text{max}}$  relationships can be used to evaluate the proper reduction in soil stiffness and the corresponding operational modulus can be calculated.

The stiffness of soils is affected by the effective confining stress. Based on laboratory tests on sands, moduli were found to increase approximately in proportion to the square root of the average effective confining stress. Hence, sandy soils become stiffer due to increases in confinement induced by loading. On this basis, the small strain moduli should be



adjusted for increased confining stress under a footing. In this section a factor is computed to evaluate the increase in soil moduli at a given depth as a function of the degree of loading.

### 7.3.1 Modulus degradation relationships

The results of ground deformation analyses can be realistic and meaningful if the stress-strain characteristics of the ground can be reasonably estimated. This is difficult because the stress-strain characteristics of soils are extremely complex and the behavior of soil is nonlinear, inelastic and stress level dependent. The small strain as well as large strain behavior of soils is important when evaluating deformation of ground. In a single laboratory or in-situ test, however, the examination of stiffness from an extremely small strain to the peak is technically difficult. Hence, for a variety of geotechnical engineering materials, the general picture of their stress-strain nonlinearity has not been truly quantified.

The hyperbolic stress-strain relationships were developed to provide a simple framework encompassing the most important characteristics of soil stress-strain behavior, using data from conventional laboratory tests. In the pioneering work of Konder (1963) a hyperbolic stress-strain relation was proposed to model monotonic prefailure behavior of the ground in the form of:

$$[7.16] \quad \tau = \frac{\gamma}{\frac{1}{G_0} + \frac{\gamma}{\tau_{\max}}}$$

in which,  $\tau_{\max}$  is the shear strength and  $G_0$  is the initial shear modulus.

The hyperbolic stress-strain relationship was developed for use in nonlinear incremental analysis of soil deformation. In each increment of such analysis the stress-strain behavior of the soil is treated as being linear and the relationship between stress and strain is assumed to be governed by the generalized Hooke's Law of elasticity. The use of the hyperbolic equation for modeling the stress-strain relation of soils and rocks is popular and has been widely in use for the following reasons: It has a simple form using only two parameters each having a clear physical meaning, the determination of the parameters for a given stress-strain curve is straight forward, and it is considered as a versatile model which

can simulate stress-strain relations of most types of soils and rocks by selecting the appropriate parameters. However, the original hyperbolic equation is only a crude approximation for the entire range of strain and the stress strain curves of real soils are not truly hyperbolic. In this light, Hardin and Drnevich (1972a, 1972b) proposed to use a distorted normalized strain in a modified hyperbolic model in which two additional empirical constants were employed. Other models have been proposed to attain a better degree of fitting to the behavior of real soil. They can be classified into the following types: the original form of hyperbolic equation modified using constant coefficients of correction for either the peak strength and/or the initial stiffness, the original hyperbolic equation modified using strain dependent coefficients of correction, or a modified form of the hyperbolic equation.

Tatsuoka and Shibuya (1991) investigated the stress-strain relationships of various geotechnical materials, ranging from a soft clay to soft rocks. They performed high quality resonant column, triaxial and plane strain compression tests over a large strain range from about 0.0001% to that at peak. Tatsuoka and Shibuya examined the original hyperbolic function for the stress-strain relations of soils and rocks and concluded that the hyperbolic fitting was not capable of representing the overall stress-strain relation of any of the materials. According to their work, generally the hyperbolic function underestimates the stiffness of rocks and overestimates that of clays and sands. In addition, both normally consolidated and overconsolidated soils show a much greater rate of reduction in modulus than suggested by the basic hyperbolic model.

The basic hyperbolic equation, as given by Eq. 7.16, can be written in terms of normalized shear stress in the following linear form independent of confining stress level

$$[7.17] \quad \frac{G}{G_o} = 1 - \frac{\tau}{\tau_{\max}}$$

Fahey and Carter (1991) proposed the following formulae to adjust the simple hyperbolic form:

$$[7.18] \quad \frac{G}{G_o} = 1 - f \left( \frac{\tau}{\tau_{\max}} \right)^s$$

in which parameter  $g$  dictates the curvature of the curve. In this study, attempts were made to derive  $f$  and  $g$  parameters based on the high quality laboratory results by Tatsuoka et al. (1991) and Teachavorasinskun et al. (1991). However, in many cases Eq. 7.18 failed to model nonlinear stress-strain relationship over the entire range of strain level. As a result, a slight modification to the Fahey and Carter formulae is suggested here, as follows:

$$[7.19] \quad \left( \frac{G}{G_o} \right) = \left[ 1 - f \left( \frac{\tau}{\tau_{max}} \right)^g \right]^k$$

A new parameter  $k$  is introduced to increase the flexibility of the curve for a better fit.

Teachavorasinskun et al. (1991) reported the results of drained simple shear testing to evaluate the stiffness of low compressible Toyoura sand for strains from  $10^{-6}$  to those at peak strength. They obtained the relationship between the secant shear modulus and the corresponding shear stress for loose ( $Dr = 35\%$ ) and dense ( $Dr = 75\%$ ) Toyoura sand with stress history of  $OCR = 1.0$  and  $OCR = 4.0$ . These relationships are shown in Fig. 7.5 where  $G$  is the operational shear modulus corresponding to the stress level of  $\tau/\tau_{max}$  and  $G_o$  is the maximum or small strain shear modulus which can be obtained from measured in-situ shear wave velocity in the ground. As given in Table 7.1, Teachavorasinskun et al. (1990) presented detailed data for each test.

It should be noted that degradation curves are almost identical for loose and dense sands. However, the influence of stress history is noticeable. Also shown in Fig. 7.5, is the commonly used hyperbolic stress-strain curve which highly overestimates operational shear modulus in normally consolidated sands.

In this study, based on the experiments performed by Teachavorasinskun et al. (1991) the parameters  $f$ ,  $g$  and  $k$ , given in Eq. 7.19 are determined for sands with different stress history. Figure 7.6 and Fig. 7.7 demonstrate experimental points and corresponding fitted curves. Hence, the following relationships were obtained for low compressible sands to evaluate large strain modulus from the measured small strain shear modulus based on the normalized shear stress:

$$[7.20] \quad \left(\frac{G}{G_o}\right) = \left[1 - 0.75\left(\frac{\tau}{\tau_{\max}}\right)^{0.50}\right]^{2.70} \quad \text{for normally consolidated sands}$$

$$[7.21] \quad \left(\frac{G}{G_o}\right) = \left[1 - 0.72\left(\frac{\tau}{\tau_{\max}}\right)^{0.88}\right]^{3.00} \quad \text{for over consolidated sands (OCR = 4)}$$

Similar correlations can be developed for highly compressible sands, in which the rate of reduction of shear modulus with degree of loading can be high compared with low compressible sands.

### 7.3.2 Increase in soil stiffness due to loading of footing

The stiffness of soils is affected by confining stress. At low strain levels (about  $10^{-4}$  percent), based on laboratory tests on sands, moduli were found to increase approximately in proportion to the square root of the average effective confining stress. Increased confinement due to loading can result in substantial increase in the moduli of sands. Hence, the small strain moduli should be adjusted for the increased confining stress under foundation loading assuming that modulus increases in proportion to the square root of the average confining stress increase. Based mainly on the results of resonant column tests, the variation of  $G_o$  with mean effective stress  $p'$  is of the form:

$$[7.22] \quad \frac{G_o}{p_a} = C \left(\frac{p'}{p_a}\right)^n$$

where,  $C$  is a function of void ratio and angularity of sand. The power term  $n$  is about 0.5. The impact of increase in confining pressure due to a footing can be evaluated by a factor as:

$$[7.23] \quad \alpha(z) = \left(\frac{p'_o + 0.50\Delta p'}{p'_o}\right)^{0.5}$$

where,

$$[7.24] \quad \Delta p' = (\Delta\sigma_x + \Delta\sigma_y + \Delta\sigma_z)/3$$

$$[7.25] \quad p'_o = (1 + 2K_o) \sigma'_{vo}/3$$

in which factor 0.50 is applied to include average amount of increased confining pressure due to loading. Equation 7.23 can be combined with Eqs. 7.24 and 7.25 as:

$$[7.26] \quad \alpha(z) = \left( 1 + \frac{0.50(\Delta\sigma_x + \Delta\sigma_y + \Delta\sigma_z)}{(1 + 2K_o)\sigma'_{vo}} \right)^{0.5}$$

where,  $\sigma'_{vo} = \gamma z$ , in which  $\gamma'$  is the effective soil weight density and  $z$  is the depth of interest. Eq. 7.26 can be simplified into following form:

$$[7.27] \quad \alpha(z) = \left( 1 + \frac{0.50\Delta\sigma_z}{\sigma'_{vo}} \right)^{0.5}$$

Assuming 1:2 gradient for  $\Delta\sigma_z$  in depth, Eq. 7.27 can be rearranged as follow:

$$[7.28] \quad \alpha(z) = \left( 1 + \frac{0.50 \frac{q}{B\gamma'}}{\frac{z}{B} \left( 1 + \frac{z}{B} \right)^2} \right)^{0.5}$$

Eq. 7.28 can be used to evaluate the increase in soil stiffness at a depth of  $z/B$ , due to a load level of  $q/B\gamma'$ . Numerical integration is applied over the depth of influence of  $2B$  to obtain an average factor for the increase in moduli of sands as a function of degree of loading  $q/B\gamma'$ . The factor can be expressed in the final form of:

$$[7.29] \quad \bar{\alpha} = 1.0 + 0.08 \left( \frac{q}{B\gamma'} \right)^{0.74}$$

According to Terzaghi (1943) for a footing on the surface of cohesionless soils

$$[7.30] \quad q_{ult} = 0.4 \gamma' B N_\gamma$$

in which  $N_\gamma$  is the bearing capacity factor as given by Terzaghi (1943). For a dense sand the internal friction angle can be estimated as high as 40 degree, hence,  $q_{ult} \cong 32 B \gamma'$ . On this basis, the maximum average increasing factor from Eq. 7.29 can be around 2.0, showing an increase of about 100 percent in small strain moduli due to the increase in confinement from a footing.

The ratio  $q/B\gamma'$  can be written in terms of  $q/q_{ult}$  which is a normalized form of degree of loading and has a physical meaning as:

$$[7.31] \quad \frac{q}{B\gamma'} = \lambda \left( \frac{q}{q_{ult}} \right)$$

in which,

$$[7.32] \quad \lambda = 0.4 N_\gamma$$

Here, general shear failure is assumed to calculate  $N_\gamma$ . Practitioners are recommended to assume similar mode of failure for the sake of consistency. Based on the data summarized in Table 7.1,  $\lambda$  and  $q_{ult}$  can be computed for typical low compressible sands, as given in Table 7.2. Hence, Eq. 7.29 and Eq. 7.31 can be combined and written in the following form:

$$[7.33] \quad \bar{\alpha} = 1.0 + 0.08 \left( \lambda \frac{q}{q_{ult}} \right)^{0.74}$$

Figure 7.8 illustrates average increase in sand moduli versus degree of loading for sands with various densities and stress histories.

#### 7.4 First proposed method to estimate settlement based on an equivalent homogeneous medium beneath the footing

This proposed method employs elastic half-space theory and uses the measured shear wave velocity for determining in-situ stiffness of sands. In this method, non-homogenous ground within the depth of influence is replaced with an equivalent homogeneous ground. On this basis an equivalent small strain modulus within the depth of influence is computed using Eq. 7.14. Then, the corresponding large strain or operational modulus within the depth of influence beneath the footing, based on the methods explained in Sections 7.3.1 and 7.3.2, is computed. Finally, the equivalent operational modulus is incorporated into the conventional elastic formulae. The method can be used for the computation of the settlement of isolated, rigid, concentrically loaded shallow foundations over nonhomogeneous sand.

##### 7.4.1 A summary of the first method

The proposed method can be summarized in the following steps:

- i. Based on the profile of small strain modulus beneath the footing resulting from seismic tests and using Eq. 7.14 or 7.15, an equivalent small strain shear modulus,  $G_{ocq}$  within a depth of influence of  $2B$  is computed.
- ii. Equation 7.33, or Fig. 7.8 gives the average increasing factor,  $\bar{\alpha}$ , based on degree of loading.
- iii. Since both  $\tau/\tau_{max}$  and  $q/q_{ult}$  display degree of loading, within the depth of influence beneath the footing it is assumed:

$$[7.34] \quad \tau/\tau_{max} = q/q_{ult}$$

Hence, knowing degree of loading,  $q/q_{ult}$ , Eq. 7.20 or 7.21 can be used to calculate

$$[7.35] \quad \beta = G/G_o$$

Figure 7.9 illustrates average decreasing factor,  $\beta$ , of sand moduli beneath the footing versus degree of loading,  $q/q_{ult}$  for sands with various stress history.

iv. Average operational large strain shear modulus can be estimated by

$$[7.36] \quad G_{eq} = \alpha \cdot \beta \cdot G_{oocq}$$

v. Assuming a Poisson's ratio of 0.3, the average operational Young's modulus can be calculated by

$$[7.37] \quad E_{eq} = 2(1 + \nu) G_{eq} \cong 2.6 G_{eq}$$

vi. Finally, conventional elastic formula, as given by Eq. 7.1, can be used to evaluate settlement of footing on sand. Using  $I_r = 0.8$  and  $\nu = 0.3$ , Eq. 7.1 can be written as:

$$[7.38] \quad s = 0.28 qB/G_{eq}$$

or

$$[7.39] \quad s = 0.28 qB/\psi \cdot G_{oocq}$$

in which  $\psi = \alpha \cdot \beta$ . Figure 7.10 illustrates factor  $\psi$  versus  $q/q_{ult}$  for sands with various density and stress history. In general,  $\psi_{oc} = 2 \psi_{nc}$  which is in agreement with previous methods (Schmertmann et al., 1978).

#### 7.4.2 Worked example

Briaud and Gibbens (1994) reported the results load tests of full size shallow footings on sand. At the Texas Experimental Site, 5 square footings were tested with width from 1 to 3 m at a depth of about 0.80 m. The site is located at the Texas A&M University Riverside Campus. The subsoils are middle Eocene sand in age, and they were deposited in a coastal environment. The soil at the Texas Experimentation Site, is predominantly sand from 0 to 11 m. Below the sand layers is a clay layer which extends until a depth of at



least 33 m. The sand is a lightly cemented medium dense overconsolidated soil. The sand is overconsolidated by desiccation of the fines and removal of 1 meter of overburden. Table 7.3 summarizes the in-situ and laboratory test results at the site (Tand et al., 1995). The in-situ relative density was estimated from SPT blow counts and CPT values as being approximately 55%.

The footings were loaded to failure (where  $s/B > 0.05$ ) to measure  $q_{ult}$  and displacements. The unit weight of sand is approximately  $16 \text{ kN/m}^3$ . Briaud and Gibbens (1994) reported average small strain shear moduli, as summarized in Table 7.4. Table 7.5 summarizes the predicted settlement based on the proposed method for various loadings on a square footing with 3 meter width. The results are in good agreement with observed settlements from full scale testing in low and medium degree of loading, as illustrated in Fig. 7.11. Also shown in Fig. 7.11 is the prediction based on the method by Schmertmann et al. (1978) where it is assumed  $E = 5q_c$  for overconsolidated sand. As illustrated, it displays larger settlement at low amounts of loading and underpredicts the settlement at higher values of loading. Hence, the method by Schmertmann et al. can not capture the nonlinearity of force-settlement curve properly.

### **7.5 Second proposed method to estimate settlement for a non-homogeneous medium beneath the footing**

In the second approach, the ground is divided into layers, in which the operational modulus of each layer is computed for the evaluation of settlement of the corresponding layer. A summation of settlement of layers within the depth of influence provides the total settlement. The method employs elastic half-space theory and uses the measured shear wave velocity for determining the in-situ stiffness of sands. The proposed method has a similar framework as the method developed by Schmertmann (1970) and Schmertmann et al. (1978). However, in this method the operational modulus is computed from the direct in-situ measurement of shear wave velocity rather than using empirical correlations that can include considerable uncertainty. A set of curves are constructed to soften measured small strain modulus of sand layers based on degree of loading, stress history and grain mineralogy.

### 7.5.1 Computation of settlement

Equation 7.9 can be used to evaluate settlement of footings on nonhomogeneous layered medium of sand. Assuming a depth of influence of  $2B$ , Eq. 7.9 can be written as follows:

$$[7.40] \quad s = q \sum_0^{2B} \left( \frac{I_z}{E_z} \right) \Delta z$$

in which  $E_z$  is the average operational Young's modulus of a layer with thickness  $\Delta z$  whose midpoint is at depth  $z$ .  $E_z$  can be written in terms of small strain shear modulus of ground prior to loading of footing as:

$$[7.41] \quad E_z = 2(1 + \nu) G_z$$

where,  $G_z$  is operational (large strain) shear modulus of the ground.  $G_z$  can be written as

$$[7.42] \quad G_z = \alpha(z) \cdot \beta(z) \cdot G_{\alpha z}$$

in which,  $\alpha(z)$  is the increase in shear modulus due to increase in confinement pressure in depth,  $\beta(z)$  is reduction in shear modulus due to increase in shear stresses in depth, and  $G_{\alpha z}$  is the corresponding shear modulus in depth. Hence, Eq. 7.40 can be written as:

$$[7.43] \quad s = q \sum_0^{2B} \left( \frac{I_z}{2(1 + \nu)\alpha(z)\beta(z)G_{\alpha z}} \right) \Delta z$$

Equation 7.43 can be written in the following simple form:

$$[7.44] \quad s = q \sum_0^{2B} \left( \frac{I'_z}{G_{\alpha z}} \right) \Delta z$$

in which:

$$[7.45] \quad I'_z = \frac{I_z}{2(1+\nu)\alpha(z)\beta(z)}$$

Poisson's ratio can be assumed as 0.3 for large strain range of loading. The following sections describes the methods for determination of  $\alpha(z)$ ,  $\beta(z)$ , and the strain influence factor  $I_z$ .

### 7.5.2 Evaluation of increase in modulus with depth, $\alpha(z)$ due to increase in confinement stress

Equation 7.26 can be used to determine the increase of modulus with depth due to increased confinement. Since confining pressure is a function of loading, the following relationship holds:

$$[7.46] \quad (\Delta\sigma_x + \Delta\sigma_y + \Delta\sigma_z) = \eta q$$

in which  $\eta$  is a function of depth.

Equation 7.26 can be rewritten in the following form:

$$[7.47] \quad \alpha(z) = \left[ 1 + \frac{0.5\eta q}{(1+2K_o)\gamma z} \right]^{0.5}$$

where,  $\sigma'_{vo} = \gamma z$

Equation 7.47 can be further rearranged as:

$$[7.48] \quad \alpha(z) = \left[ 1 + \frac{0.5\eta \left( \frac{q}{B\gamma} \right)}{(1+2K_o) \left( \frac{z}{B} \right)} \right]^{0.5}$$

in which  $B$  is the width of a rectangular footing, and ratio of  $q/B\gamma$  is a measure of degree of loading. Eq. 7.48 and Eq. 7.31 can be combined and written in the following form:

$$[7.49] \quad \alpha(z) = \left[ 1 + \frac{0.5\eta\lambda \left( \frac{q}{q_{ult}} \right)}{(1 + 2K_o) \left( \frac{z}{B} \right)} \right]^{0.5}$$

$\alpha(z)$  measures the increasing ratio in small strain shear modulus of a layer at depth  $z$ , due to loading of a footing. Equation 7.49 can be used to determine  $\alpha(z)$  in depth based on degree of loading,  $q/q_{ult}$ , and normalized depth,  $z/B$  for sands with different relative density and stress history using Table 7.1 and Table 7.2.

### 7.5.3 Evaluation of reduction of modulus in depth, $\beta(z)$ due to increase in shear stress

Equations 7.20 and 7.21, can be used to determine

$$[7.50] \quad \beta(z) = G_z/G_{oz}$$

To establish a correlation between  $\tau/\tau_{max}$  in depth and  $q/q_{ult}$  following relationship is adopted:

$$[7.51] \quad (\tau/\tau_{max})_z = \mu(z)(q/q_{ult})$$

in which  $\mu(z)$  is a factor which depends on depth of corresponding layer.

The distribution of induced shear stress,  $\tau$ , due to loading is based on the theory of elasticity for a certain Poisson's ratio. For Poisson's ratio of 0.3, Fig. 7.12 illustrates distribution of shear stress for a concentric loading as a function of normalized depth,  $z/B$ , and loading,  $q$  (Poulos and Davis, 1974). Based on the distribution given in Fig. 7.12, conservatively it is assumed here that at  $q = q_{ult}$  ( $q/q_{ult} = 1.0$ ), the peak shear stress at about

$z/B = 0.4$ , is equal to  $\tau_{\max} = 0.33q$ . Hence, to determine  $\tau/\tau_{\max}$  with depth, shear stresses are normalized to  $\tau_{\max} = 0.33q$ . This gives  $\mu(z)$  in depth. Figure 7.13 illustrates the variation of  $\mu(z)$  with depth. Knowing  $q/q_{ult}$  and  $\mu(z)$ , normalized shear stress with depth,  $(\tau/\tau_{\max})_z$  can be estimated from Eq. 7.50.

Finally, Equations 7.20 and 7.21, are used to determine  $\beta(z)$  which measures the reduction in small strain shear modulus of a layer at depth  $z$  due to loading of a footing.

#### 7.5.4 Strain influence factor $I_z$

Using the recommended distribution of strain influence as illustrated by Fig. 7.4 for large strain and using Eq. 7.45 and Eq. 7.49 and Eq. 7.50, a series of diagrams are prepared to compute  $I'_z$  based on the degree of loading, sand relative density and sand stress history. Figures 7.14 and 7.15, or Table 7.6 can be used to determine  $I'_z$ .

#### 7.5.5 A summary of the second method

The settlement is calculated from the following relationship:

$$[7.52] \quad s = K_1 K_2 q \sum_0^{2B} \left( \frac{I'_z}{G_{oz}} \right) \Delta z$$

where,

$G_{oz}$  = small strain modulus measured by means of seismic methods for layer  $i$

$K_1$  = a correction factor for the depth of the foundation, as suggested by

Schmertmann (1970) and Schmertmann et al. (1978) =  $1.0 - 0.50(q/\sigma_{vo})$ ,

where  $\sigma_{vo}$  is the overburden pressure at the foundation level.

According to Burland and Burbidge (1985), the net pressure rather than gross amount of pressure on the footing as  $(q - 0.67\sigma_{vo})$  can be considered to incorporate the influence of overburden pressure. This gives a factor of  $[1.0 - 0.67(q/\sigma_{vo})]$ , showing a higher

influence of embedment, as compared with  $[1.0 - 0.50(q/\sigma_{vo})]$  by Schmertmann et al. (1978). Hence, factor  $[1.0 - 0.67(q/\sigma_{vo})]$  can result in a lower amount of settlement. Nevertheless, for the sake of conservatism and the larger experience behind the method by Schmertmann (1970), it is recommended to consider the impact of embedment of footing into settlement calculation from the relationship proposed by Schmertmann (1970) and Schmertmann et al. (1978).

$K_2$  = a correction factor for creep as suggested by Schmertmann (1970)  
 $= 1.0 + 0.2 \log_{10} 10t$ , in which  $t$  is time in years after the application of foundation loading for which the settlement value is required.

$I'_z$  = influence factor as shown in Figure 7.14 and 7.15., or Table 7.6, based on the degree of loading, sand relative density and sand stress history .

The following information should be gathered before a settlement estimate can be calculated by the method suggested here:

1. A profile of small strain shear modulus over the depth of influence ( $2B$ ) below the footing, or to a boundary layer that can be assumed incompressible.
2. The width of footing ( $B$ ), its depth of embedment ( $D$ ), and the average foundation contact pressure ( $q$ ).
3. Grain mineralogy, relative density and stress history of sand. Seismic CPT can be used to characterize sands (Eslaamizaad and Robertson, 1996a, 1996b and 1996c).
4. The approximate unit weights of surcharge soils, and the position of the water-table.  
 These data are required for the estimate of  $\sigma_{vo}$ , which is needed for the computation of correction factor,  $K_1$ .
5. Over the depth of influence,  $2B$ , divide the  $G_o$  profile into a convenient number of layers, each with a constant value of small strain shear modulus.
6. When CPT data are available, the method developed in Chapter 6, as illustrated by Fig. 6.7 can be applied to predict ultimate bearing capacity  $q_{ult}$ . Otherwise, Table 7.2 can be used to estimate ultimate bearing capacity  $q_{ult}$ , which is needed to determine degree of loading  $q/q_{ult}$ .
7. Using Fig. 7.14 or 7.15 or Table 7.6, evaluate strain influence factor  $I'_z$  for each layer, based on degree of loading  $q/q_{ult}$ , stress history and relative density of sand.

8. Calculate  $[I'_z / G_o(z)].\Delta z$  for each layer. This represents the settlement contribution of each layer.
9. Finally, using Eq. 7.52, effects of embedment and creep can be incorporated and settlement of the footing is computed.

### 7.5.6 Worked example

The second proposed method is evaluated with the results of load tests of full size square footing with 3 meter width on a medium dense sand. Briaud and Gibbens (1994) reported the tests at the Texas experimental site. The footings were loaded to failure to measure settlements. The detailed geotechnical information of site has been given in Section 7.4.3.

Using the above method of prediction of settlement, depth of influence of  $2B = 6$  m, beneath the footing is divided into 8 layers of identical thickness equal to  $B/4 = 0.75$  m. Small strain shear moduli at the midpoint of each layer is computed. At this point  $I'_z$  is evaluated based on degree of loading, for a medium dense overconsolidated sand using Fig. 7.15 or Table 7.6. Using  $s_i = [I'_z / G_o(z)].\Delta z$ , the settlement of each layer is computed. Since the footing is at a depth of 0.8 m, factor  $K_1$  is greater than 0.99, hence it is neglected in this example. A summation of the settlement of layers provides the total settlement.

Table 7.7 summarizes the predicted settlement based on the proposed method for various loadings. This method, for this example predicts slightly larger settlement at various levels of  $q/q_{ult}$ . This can be due to the conservative assumption in the evaluation of reduction in  $\beta(z)$ , as discussed in Section 7.5.3. Nevertheless, the results are in reasonable agreement with the observed settlements from full scale testing for the full range of loading, as illustrated in Fig. 7.16. Also shown in Fig. 7.16 is the prediction based on the method by Schmertmann et al. (1978), in which it is assumed  $E = 5q_c$  for overconsolidated sand.

## 7.6 Summary and conclusions

The inevitable disturbance that occurs during sampling and subsequent handling of samples severely alters the compressibility and stiffness of granular materials. Consideration is

therefore directed to alternative methods of in-situ testing to determine moduli for estimating settlement. Numerous articles have appeared in the literature related to the prediction of settlement of footings on sand by means of in-situ tests. Most of these methods have been based on the conventional elastic formula, where the ground is assumed to be an elastic homogeneous medium. Sand deposits are often non-homogeneous in nature in which the stiffness varies with depth. Hence, an equivalent soil modulus is frequently estimated based on in-situ testing measurements. Empirical correlations exist relating in-situ testing results to the ground stiffness from which the equivalent ground modulus can be obtained. In general, a depth of influence is defined within which an average value of soil modulus, is computed. The depth of stress influence is somewhat uncertain and has been subjected to many research activities. It is a function of factors such as foundation width to length ratio ( $B/L$ ), and variation of ground stiffness with depth. Depth of influence is often assumed to be equal to two times the width of footing,  $2B$ .

Seismic tests are among the few in-situ tests that produce little or no soil disturbance. Such techniques induce very small strain in the ground that preserve its natural features. Swiger (1974) applied in-situ seismic techniques in the evaluation of ground settlement using conventional linear elastic theory. In his approach, the measured small strain moduli are softened using reduction curves developed by Seed (1969) based on the strain level in the ground. However, the curves given by Seed do not distinguish between sand stress history and sand grain mineralogy. More realistic computation of settlement of footings on sands can be obtained when appropriate modulus degradation curves are utilized in determining operational modulus of the ground from the measured small strain modulus. Hence, prior knowledge of stress history and compressibility of sand are required to select an appropriate modulus degradation curve. However, such information can not be provided by means of seismic testings.

Recently, Eslaamizaad and Robertson (1996a, 1996b, 1996c) investigated the potential of using seismic CPT (SCPT) in in-situ determination of degree of cementation, compressibility, and stress history of sands. These methods have also been presented in this thesis (Chapters 2, 3, 4 and 5). Correlations are proposed to identify and to evaluate unusual sands and to determine stress history of sands from a combined measurement of shear wave velocity and cone resistance in sands.



In this chapter, a method has been developed to evaluate equivalent soil modulus beneath the footing. Increased confinement due to loading results in substantial increases in the moduli of sands. A relationship has been proposed to evaluate this increase within the depth of influence. Based on high quality laboratory test results by Teachavorasinskun et al. (1991), reduction curves have been formulated to soften the average small strain shear modulus based on degree of loading (strain level).

In this chapter, two methods have been presented to evaluate settlement of footings on sand using seismic methods. The methods employ elastic half-space theory and use the measured shear wave velocity for determining in-situ stiffness of sands. They can be used for the systematic computation of the settlement of isolated, rigid, concentrically loaded shallow foundations over nonhomogeneous sand. One is based on a homogenous ground beneath the footing. Hence, an equivalent operational modulus, for nonhomogeneous layered ground within depth of influence beneath the footing, is computed. Then, the equivalent modulus is incorporated into conventional elastic formulae. In the second approach, the ground is divided into layers, in which operational modulus of each layer is computed for the evaluation of settlement of the corresponding layer. A summation of settlement of layers within depth of influence provides the total settlement. The second proposed method has a similar framework as the method developed by Schmertmann. However, in this method the operational modulus is computed from the direct in-situ measurement of shear wave velocity rather than using an empirical correlation. A set of curves are constructed to soften measured small strain modulus of sand layers based on degree of loading, stress history and grain mineralogy. The operational shear modulus is then introduced into the conventional elastic settlement formula to compute settlement of footings on sand. The effects of soil compressibility, relative density and stress history on the large strain shear modulus have also been discussed. The methods have been validated using the results of a limited number of full scale loading tests of large spread footings. Both methods have been illustrated and evaluated with test results of a full size shallow footing. The predicted settlements for both methods are in good agreement with the observed settlements. The first method that uses an equivalent operational modulus is simpler to apply since it uses less steps (see Table 7.5 and Table 7.7). For the example studied, second method appears to predict higher settlements.

Sand	Density	$\phi'$ (degree)	$K_o$	OCR
NC	Loose	32.4	0.42	1.0
NC	Dense	36.5	0.36	1.0
OC	Loose	34.4	0.92	4.0
OC	Dense	38.8	0.85	4.0

Table 7.1 Detailed data for tested low compressible Toyoura sand (after Teachavorasinskun et al., 1991)

Sand	Density	$\phi'$ (degree)	$\lambda$	$q_{ult}$
NC	Loose	32.4	10.8	10.8By
NC	Dense	36.5	22.0	22.0 By
OC	Loose	34.4	15.2	15.2By
OC	Dense	38.8	29.5	29.5 By

Table 7.2  $q_{ult}$  and  $\lambda$  values for typical low compressible sands with density and stress history

Depth	Description	$\phi'$	w	$\gamma_d$	N	$q_c$	$P_L$	$E_{PMT}$
m		degree	%	kN/m <sup>3</sup>		kPa	kPa	MPa
0-3.5	Silty sand	36	12	14.6	15	7200	700	8
3.5-7	Clean sand	36	25	14.9	20	9600	1000	11
7-11	Sand & clay	36	25	14.9	15	7200	4200	14
11	Clayey shale		30		50	9000		

- $\phi'$  : Drained friction angle  
w : water content  
 $\gamma_d$  : Dry weight density  
N : SPT blow count  
 $q_c$  : Cone Penetration resistance  
 $P_L$  : Limit pressure measured by Pressuremeter  
 $E_{PMT}$  : Young's modulus determined by Pressuremeter

Table 7.3 Summary of subsoil condition at the Texas Experimentation Site (after Tand et al., 1995)

Depth, m	Average shear wave velocity, m/s	Average shear Modulus, MPa
2	221	88.5
4	256	121
6	246	111
8	185	61.5
10	234	98.5

Table 7.4 Cross hole test results at Texas Experimentation Site  
(after Briaud and Gibbens, 1994)

Load, MN	4.0	6.0	8.0	Reference
$q$ , MPa	0.45	0.67	0.89	Applied load
$q_{ult}$ , MPa	1.2	1.2	1.2	Fig. 6.7
$q/q_{ult}$	0.38	0.56	0.74	
$\psi$	0.42	0.24	0.13	Fig. 7.10
$G_{ooq}$ , MPa	57	57	57	Eq. 7.15
Predicted $s$ , mm	16	41	101	Eq. 7.39
Observed $s$ , mm	15 - 20	37 - 64	70 - 110	

Table 7.5 Evaluation of settlement for a 3.0 m square footing on sand based on the first proposed method

z/B	q/quit=0.3						q/quit=0.5						q/quit=0.75						q/quit=1					
	NC			OC			NC			OC			NC			OC			NC			OC		
	LOOSE	DENSE		LOOSE	DENSE		LOOSE	DENSE		LOOSE	DENSE		LOOSE	DENSE		LOOSE	DENSE		LOOSE	DENSE		LOOSE	DENSE	
0	0.50	0.50	0.33	0.33	0.64	0.64	0.39	0.39	0.83	0.83	0.48	0.48	1.06	1.06	0.60	0.60								
0.125	0.96	0.87	0.58	0.51	1.36	1.36	0.77	0.77	2.31	2.31	1.34	1.34	3.97	3.97	2.58	2.58								
0.25	1.78	1.44	1.04	0.86	2.74	2.74	1.60	1.60	4.92	4.92	3.27	3.27	9.81	9.81	9.00	8.46								
0.375	2.43	2.10	1.39	1.23	4.11	3.39	2.41	2.04	8.27	6.57	5.81	4.76	19.07	14.76	21.11	16.86								
0.5	2.35	2.13	1.37	1.26	3.67	3.19	2.09	1.86	6.37	5.34	3.92	3.38	11.63	9.49	8.73	7.33								
0.625	2.00	1.88	1.18	1.12	3.01	2.73	1.71	1.58	4.89	4.30	2.87	2.58	8.10	6.95	5.33	4.68								
0.75	1.66	1.58	1.00	0.96	2.37	2.21	1.36	1.28	3.60	3.27	2.06	1.90	5.46	4.85	3.30	2.99								
0.875	1.38	1.34	0.85	0.83	1.91	1.82	1.10	1.06	2.76	2.58	1.56	1.48	3.96	3.62	2.30	2.13								
1	1.12	1.10	0.71	0.69	1.50	1.44	0.88	0.85	2.06	1.95	1.17	1.12	2.79	2.60	1.58	1.49								
1.125	0.93	0.91	0.60	0.59	1.20	1.17	0.72	0.70	1.60	1.54	0.92	0.89	2.10	1.99	1.19	1.14								
1.25	0.74	0.73	0.49	0.48	0.94	0.92	0.57	0.56	1.21	1.17	0.71	0.69	1.53	1.47	0.87	0.84								
1.375	0.58	0.57	0.39	0.39	0.71	0.70	0.45	0.44	0.88	0.86	0.53	0.52	1.08	1.04	0.62	0.61								
1.5	0.44	0.44	0.31	0.30	0.54	0.53	0.34	0.34	0.66	0.65	0.40	0.39	0.79	0.77	0.46	0.45								
1.625	0.32	0.32	0.22	0.22	0.38	0.38	0.25	0.25	0.46	0.45	0.28	0.28	0.54	0.53	0.32	0.32								
1.75	0.20	0.20	0.15	0.15	0.24	0.24	0.16	0.16	0.28	0.28	0.18	0.18	0.33	0.33	0.20	0.20								
1.875	0.10	0.10	0.07	0.07	0.11	0.11	0.08	0.08	0.13	0.13	0.08	0.08	0.15	0.15	0.09	0.09								
2	0.00	0.00	0.00	0.00	0.00	0.00	0.00	0.00	0.00	0.00	0.00	0.00	0.00	0.00	0.00	0.00								

Table 7.6 Distribution of factor  $I'_v$  in depth for NC and OC sands

Layer i	$G_{oz}$ (MPa)	$\Delta z$ (m)	$z/B$	$q/q_{ult} = 0.38$		$q/q_{ult} = 0.56$		$q/q_{ult} = 0.74$	
				$\Gamma'_z$	$s_r = q \Gamma'_z \Delta z / G_{oz}$ (m)	$\Gamma'_z$	$s_r = q \Gamma'_z \Delta z / G_{oz}$ (m)	$\Gamma'_z$	$s_r = q \Gamma'_z \Delta z / G_{oz}$ (m)
1	17	0.75	0.125	0.65	0.013	0.92	0.027	1.05	0.041
2	50	0.75	0.375	1.66	0.011	2.94	0.029	3.75	0.050
3	88	0.75	0.625	1.35	0.005	1.91	0.011	2.20	0.0167
4	117	0.75	0.875	0.92	0.0026	1.21	0.005	1.33	0.0076
5	139	0.75	1.125	0.64	0.0016	0.75	0.0027	0.80	0.0038
6	151	0.75	1.375	0.40	0.0009	0.42	0.0014	0.45	0.0020
7	154	0.75	1.625	0.20	0.0004	0.22	0.0007	0.25	0.0011
8	146	0.75	1.875	0.10	0.0002	0.10	0.0003	0.10	0.0005
Predicted settlement					0.034		0.077		0.123
Observed settlement					0.015- 0.020		0.037- 0.064		0.070- 0.110

Table 7.7 Evaluation of settlement for a 3.0 m square footing on sand based on the second proposed method



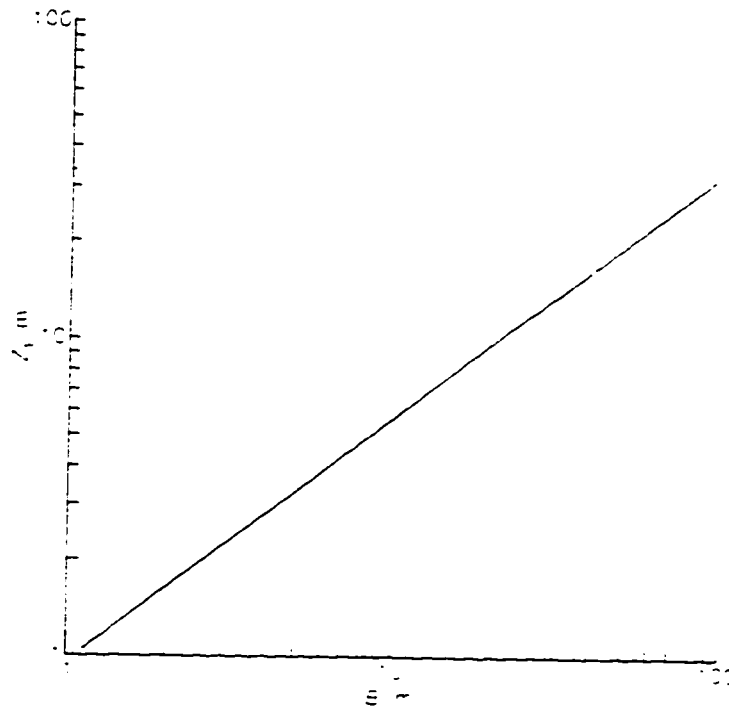


Fig. 7.1 Relationship between B and depth of influence  $Z_1$   
(after Burland and Burbidge, 1985)

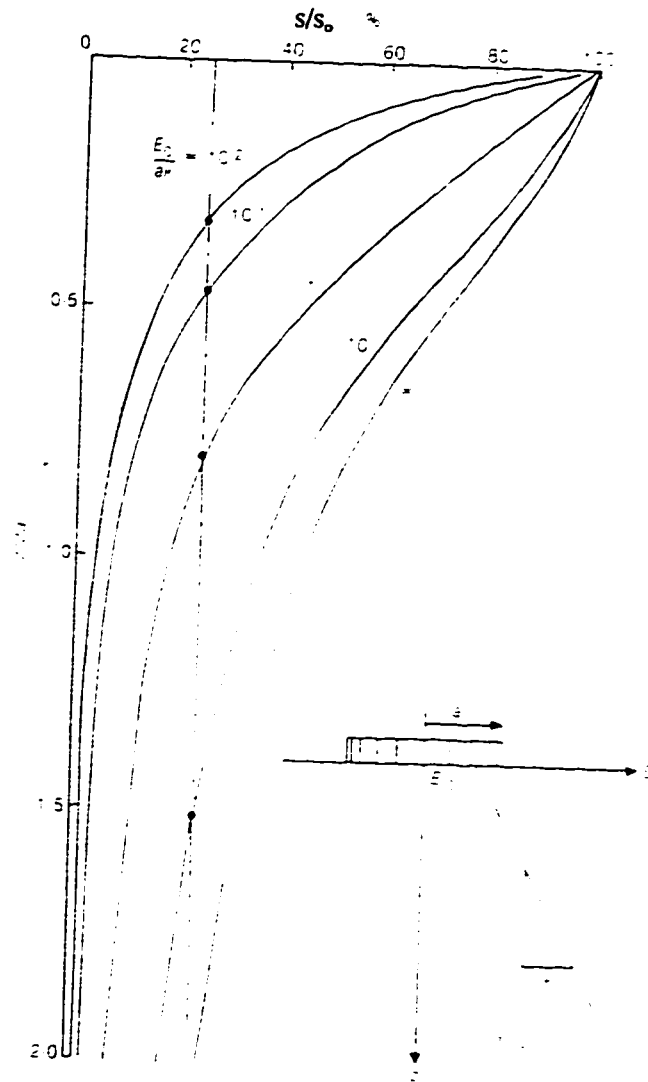


Fig. 7.2 Distribution of settlement with depth for a circular rough rigid foundation on isotropic non-homogeneous elastic soil (after Burland and Burbidge, 1985)

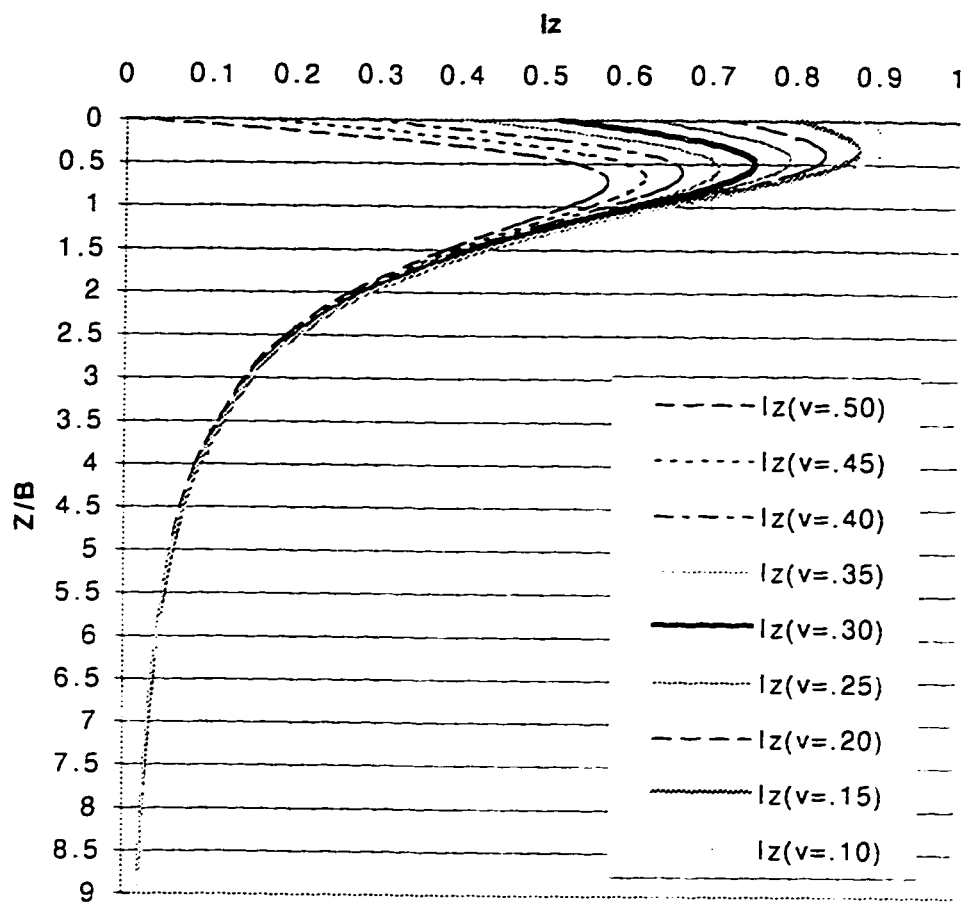


Fig. 7.3 Distribution of the strain influence factors in depth for various Poisson's ratios

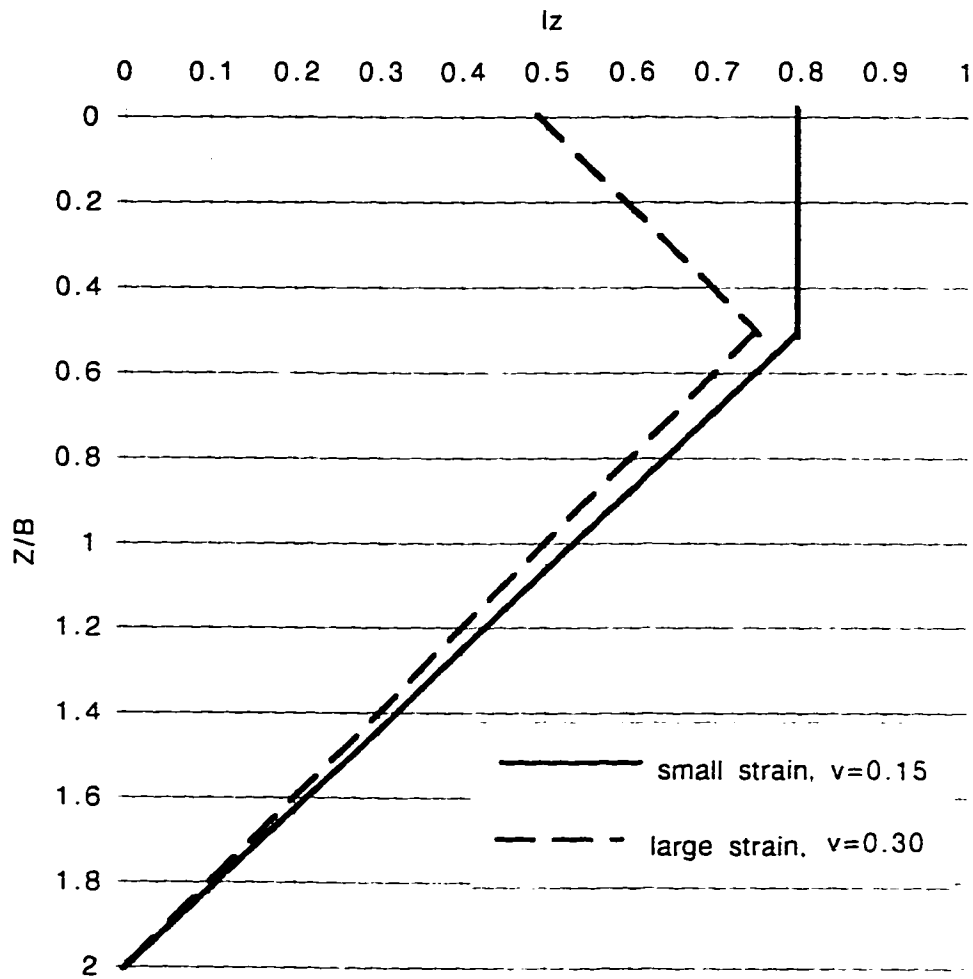


Fig. 7.4 Recommended distributions of strain influence factors in depth

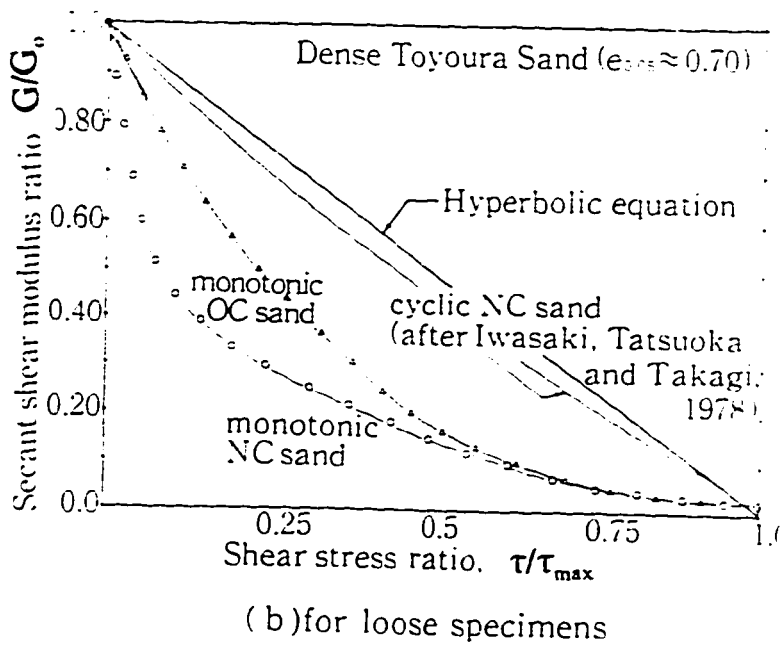
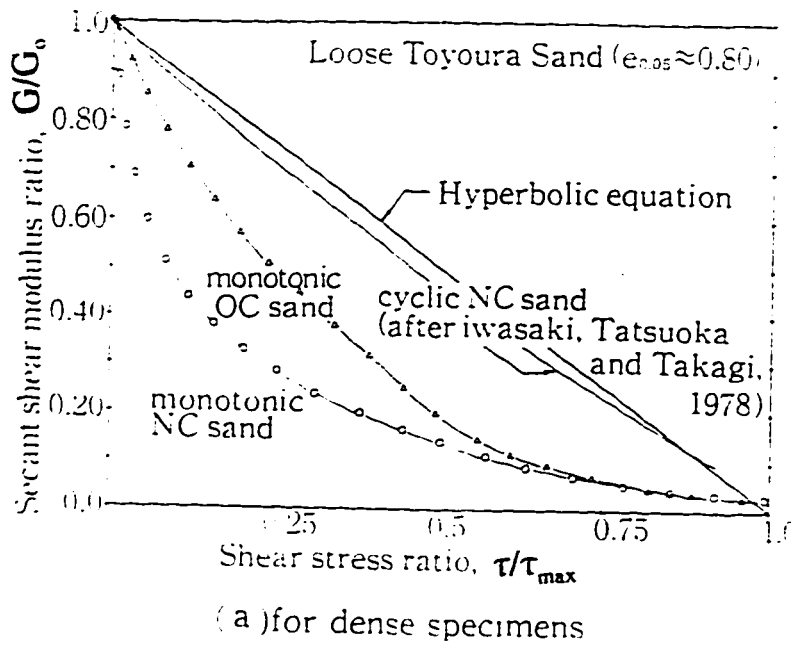


Fig. 7.5 Secant shear moduli for NC sand specimens and OC sand specimens (after Teachavorasinskun et al., 1991)

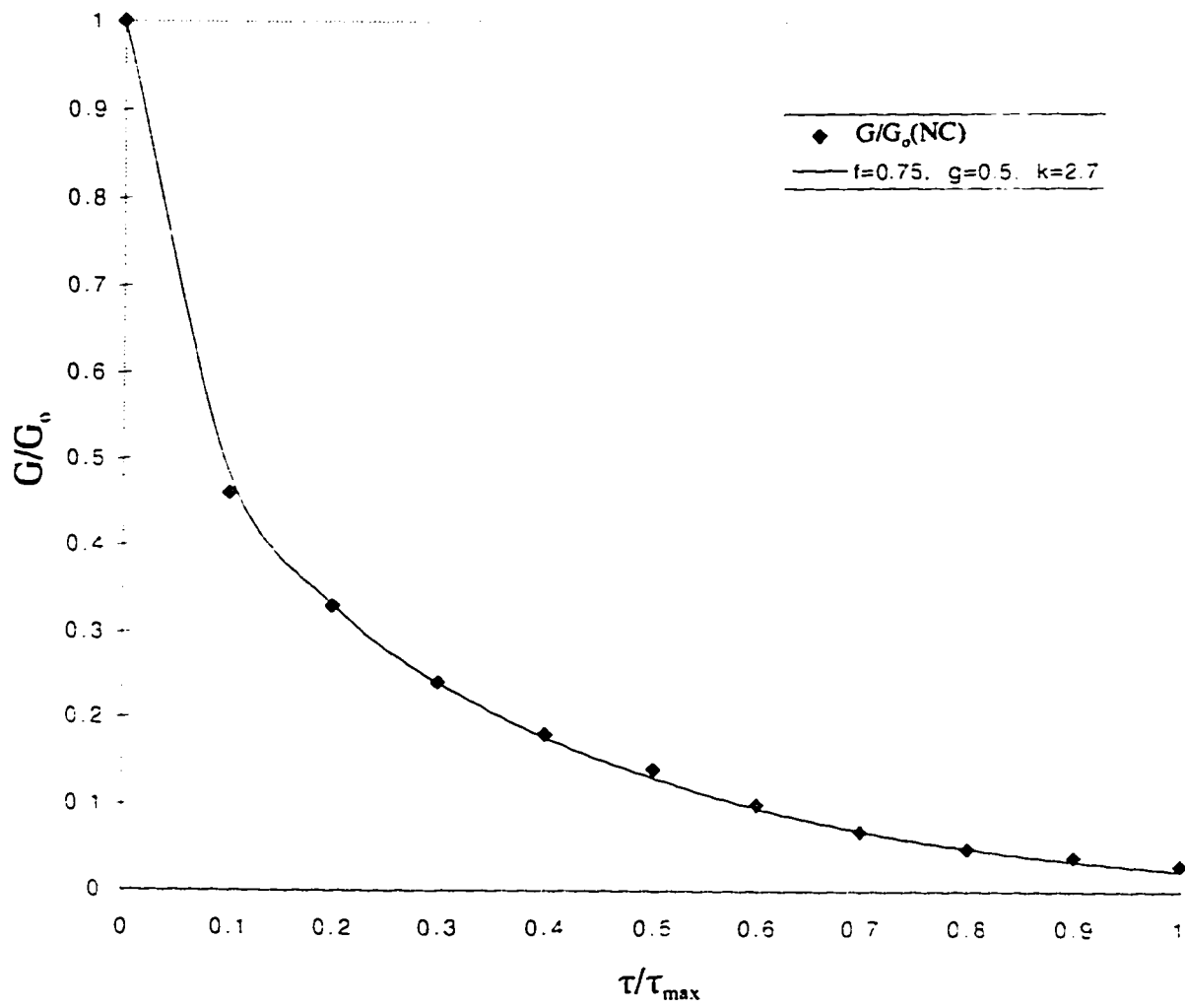


Fig. 7.6 Curve fitting for NC sands

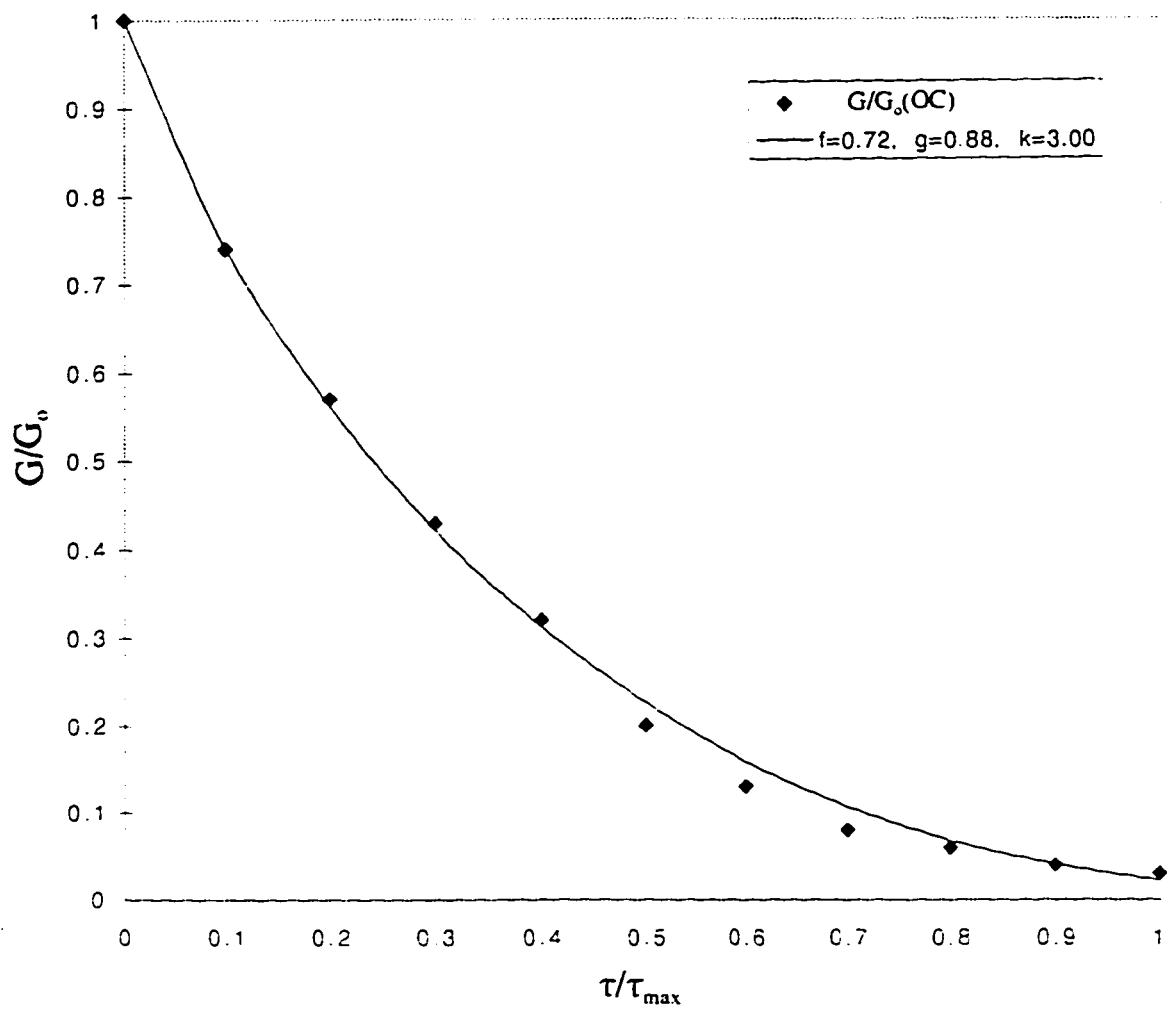


Fig. 7.7 Curve fitting for OC sands

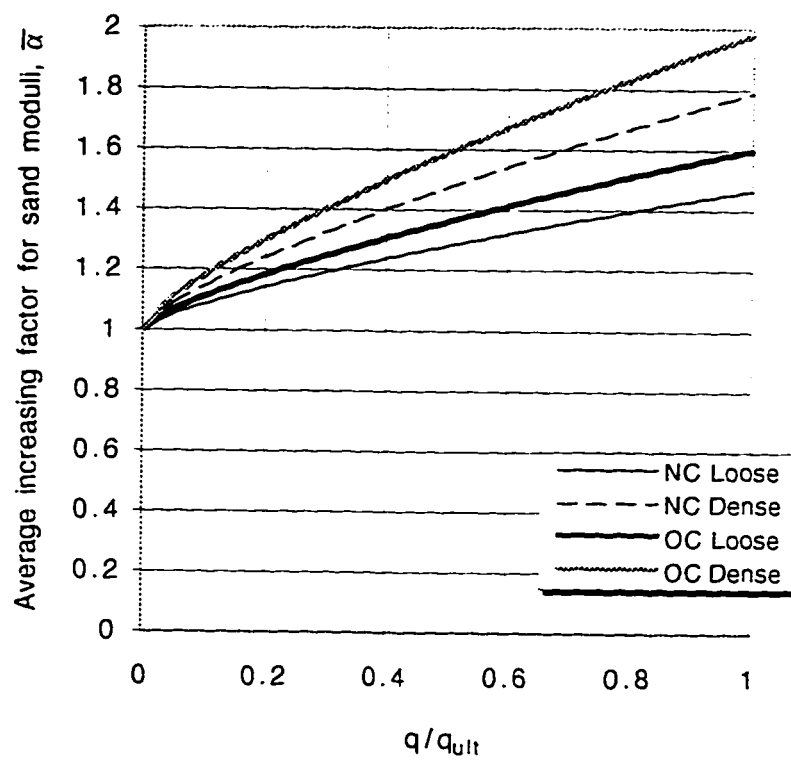


Fig. 7.8 Average increasing factor,  $\bar{\alpha}$ , of sand moduli due to increase in confinement



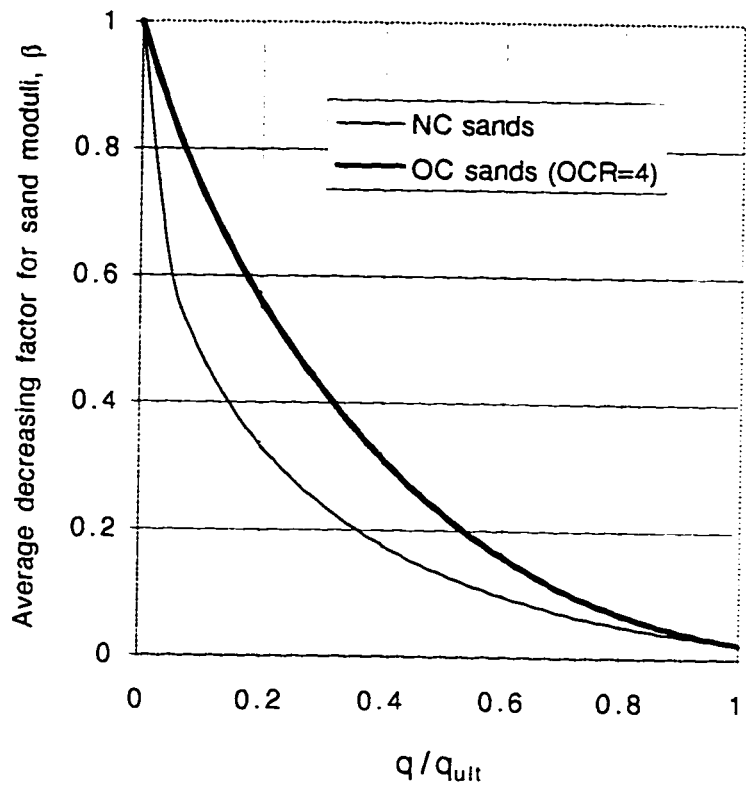


Fig. 7.9 Average decreasing factor,  $\beta$ , of sand moduli due to increase in shear strain

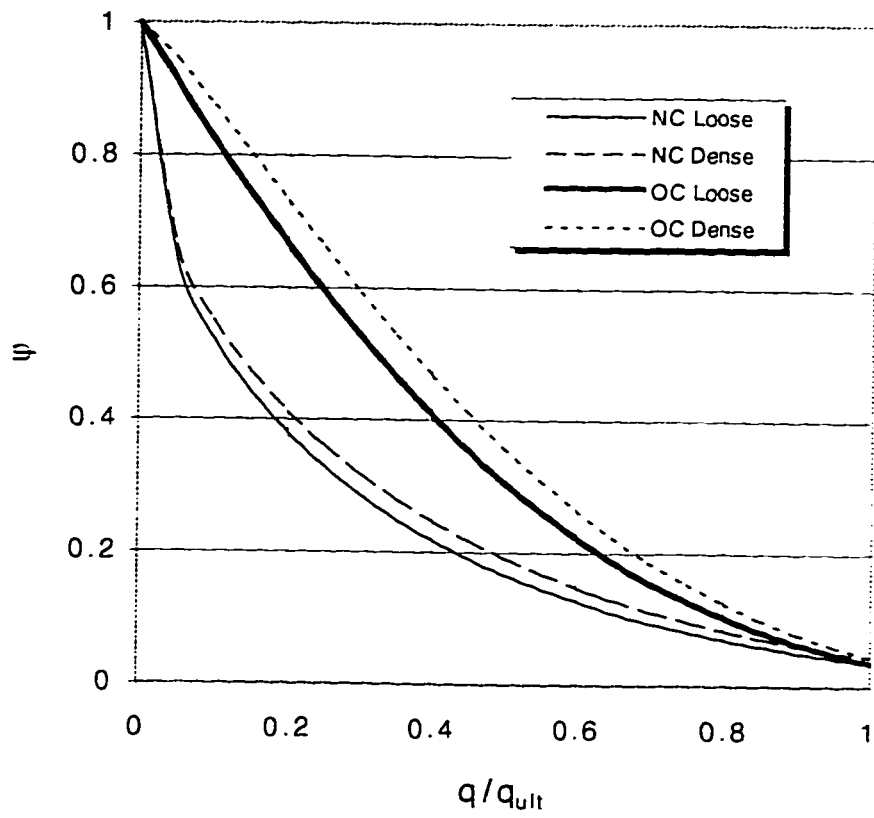


Fig. 7.10 Factor,  $\psi$ , versus  $q/q_{ult}$ , for sands with various density and stress history

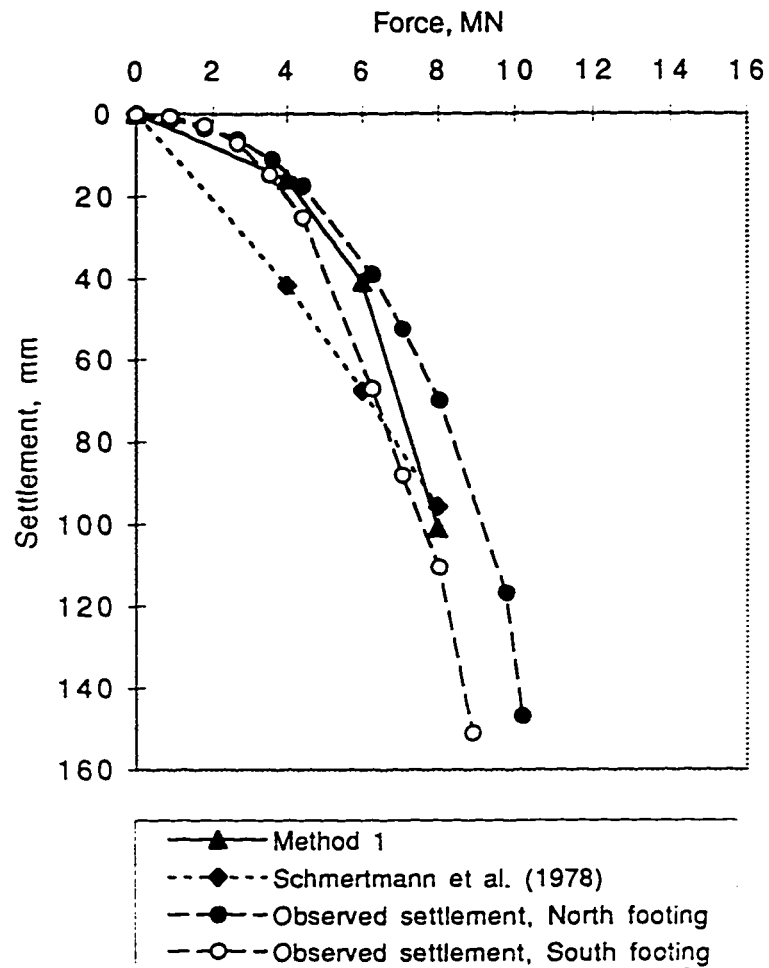


Fig. 7.11 Comparison of the first method of prediction of settlement with load settlement curve of 3m square footings at Texas Experimentation site

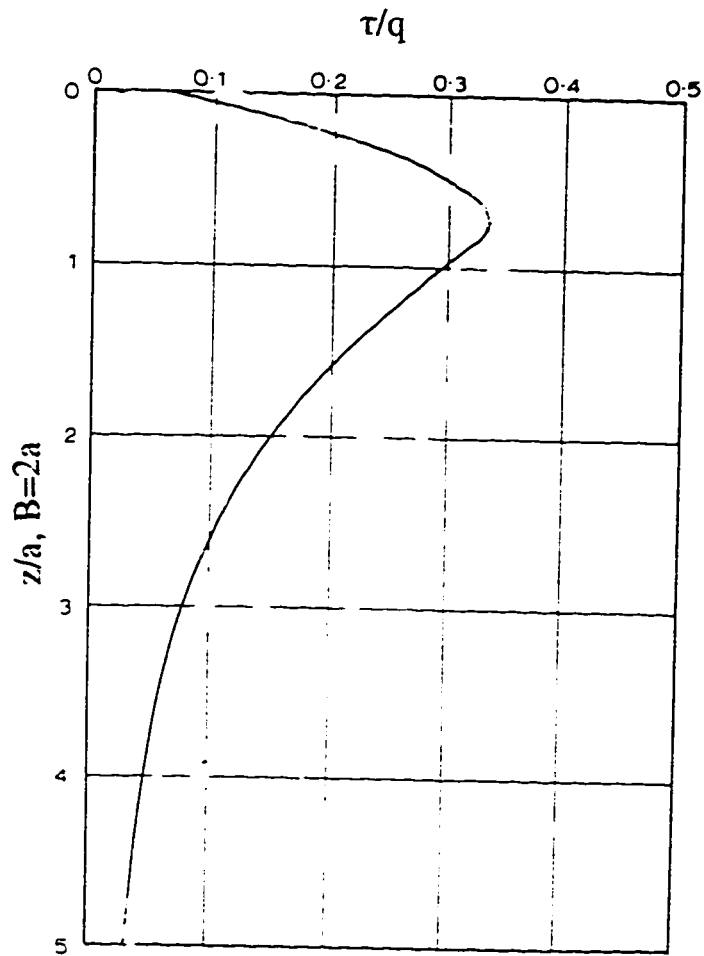


Fig. 7.12 Distribution of shear stress in depth for Poisson's ratio of 0.30 (after Poulos and Davis, 1974)

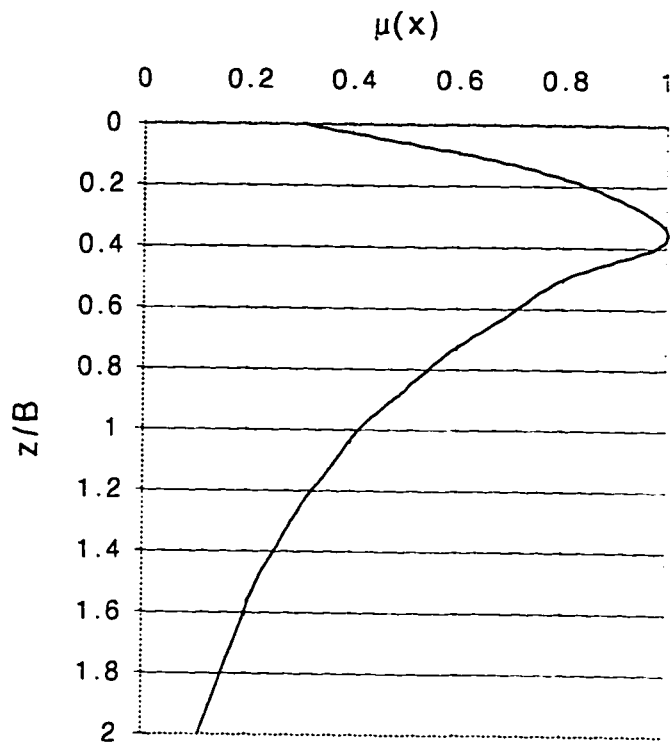


Fig. 7.13 Variation of  $\mu(z)$  with depth

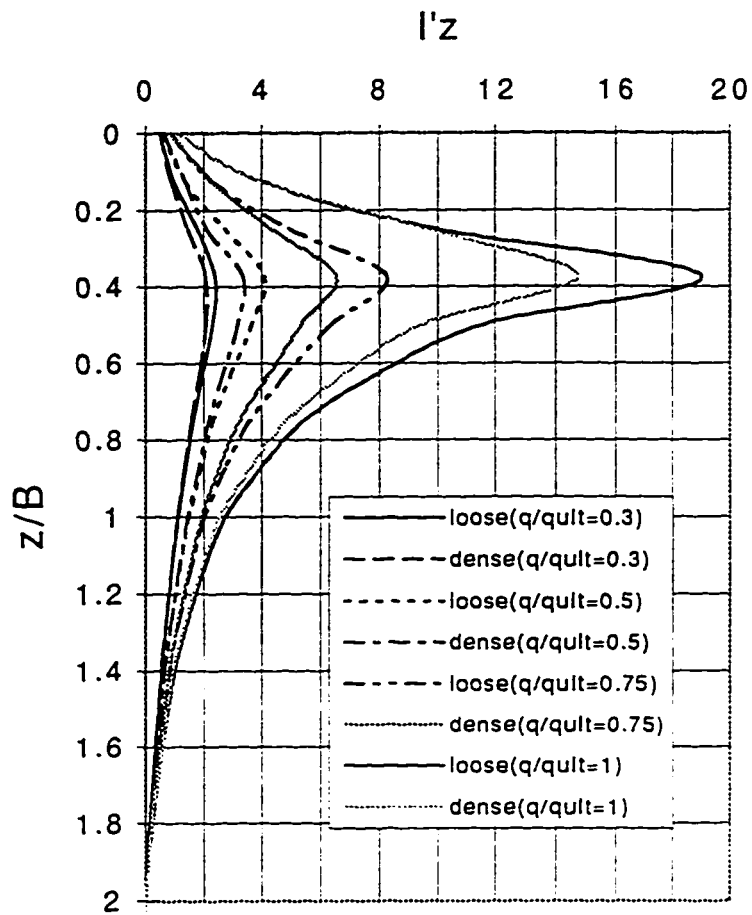


Fig. 7.14 Distribution of factor  $I'_z$  in depth for NC sands

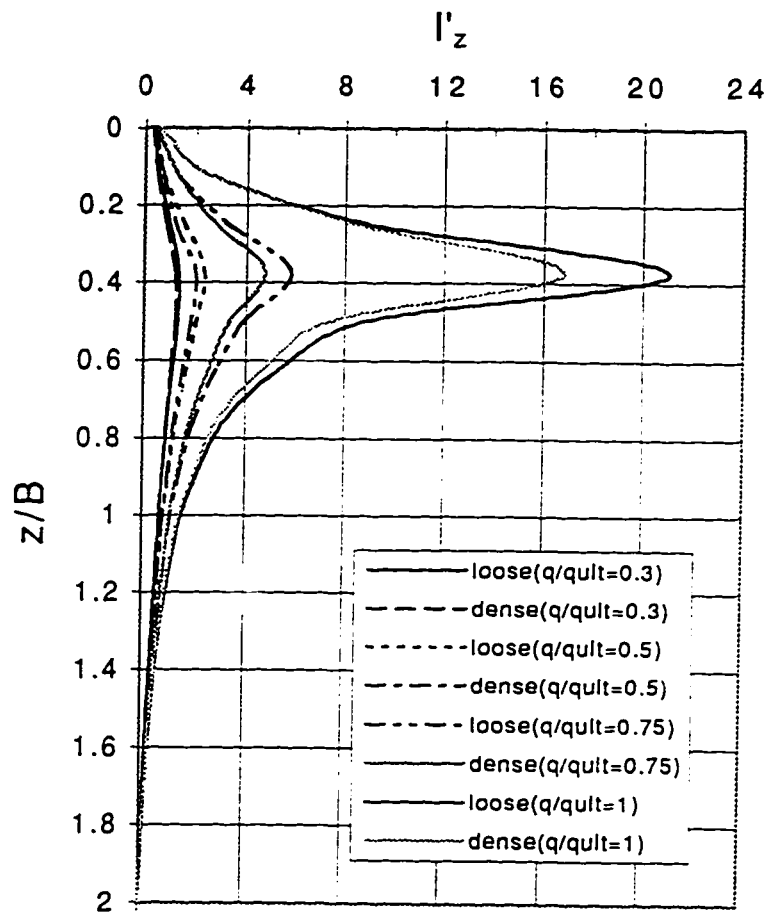


Fig. 7.15 Distribution of factor  $I'_z$  in depth for OC sands

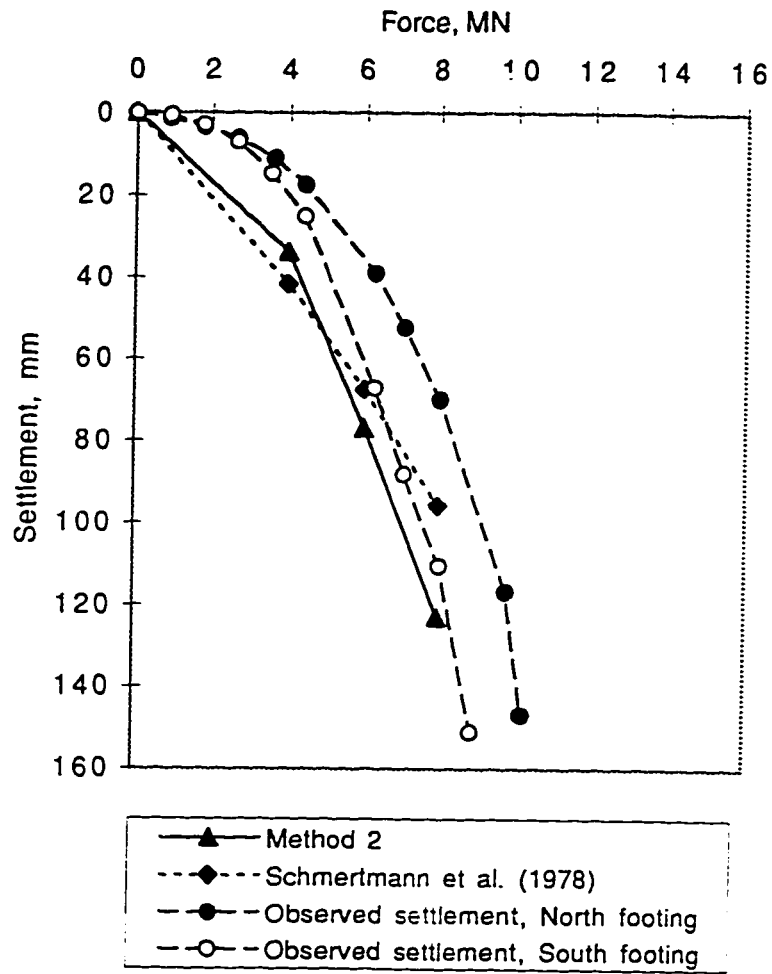


Fig. 7.16 Comparison of the second method of prediction of settlement with load settlement curve of 3m square footings at Texas Experimentation site



## References

- Ahlvin, R. G., and Ulery, H. H. 1962. Tabulated values for determining the complete pattern of stresses, strains, and deflections beneath a uniform load on a homogeneous half space, Highway Research Board Bulletin No. 342, pp. 1-13
- Baldi G., Bellotti R., Ghionna N., Jamiolkowski M. and Pasqualini E. 1986. Interpretation of CPT's and CPTU's 2nd Part: Drained Penetration of Sands. Proceedings of Fourth International Geotechnical Seminar on Field Instrumentation and In-situ Measurements, Singapore.
- Bowles, J. E. 1987 . Elastic Foundation Settlement on Sand Deposits. Journal of Geotechnical Engineering, Vol. 113, No. 8, ASCE, pp. 846-860.
- Briaud, J. L., and Gibbens, R. M. 1994. Predicted and measured behavior of five spread footings on sand. ASCE Geotechnical special publication No. 41.
- Burland J. B. and Burbidge M. C. 1985. Settlement of foundations on sand and gravel. Proceeding of the Institution of Civil Engineers, Part 1, 78, 1325-1381.
- Eisenstien, Z., and Morrison, N.A. 1973. Predictions of foundation deformations in Edmonton using an in-situ pressure probe. Can. Geotech. Jnl., Vol. 10, pp. 193-210.
- Eslaamizaad, S. and Robertson, P.K. 1996b. Seismic cone penetration test to identify cemented sands. 49th Canadian Geotechnical Conference, St. John's, NF, Canada.
- Eslaamizaad, S. and Robertson, P.K. 1996a. A framework for in-situ determination of sand compressibility. 49th Canadian Geotechnical Conference, St. John's, NF, Canada.
- Eslaamizaad, S. and Robertson, P.K. 1996c. Estimation of in-situ lateral stress and stress history in sands. Proceedings of 49th Canadian Geotechnical Conference, St. John's, NF, Canada.
- Fahey M. and Carter J. P. 1991. Finite element simulation of the pressuremeter test in sand using a Mohr Columb model with nonlinear elasticity, The University of Western Australia, Department of Civil and Environmental Engineering, Research Report No. G1026.
- Hardin, B.O. and Drnevich, V.P. 1972a. Shear modulus and damping in soils: measurement and parameter effects. Journal of the Soil Mechanics and Foundations Division, ASCE, Vol. 98, SM6, 603-624.
- Hardin, B.O. and Drnevich, V.P. 1972b. Shear modulus and damping in soils: design equations and curves. Journal of the Soil Mechanics and Foundations Division, ASCE, Vol. 98, SM7, 667-692.

- Konder, R. L. 1963. Hyperbolic stress strain response: cohesive soils. *Journal of the Soil Mechanics and Foundations Division, ASCE*, vol. 89, No. SM1, 115-143.
- Lambe T. W. and Whitman R. V. 1969 *Soil Mechanics*. John Wiley & Sons, Inc.
- Leonards, G.A., and Frost, J.D. 1987. Settlement of shallow foundations on granular soils, *Journal of Geotechnical Engineering*, Vol. 114, pp. 791-809.
- Menard L. 1965. Rules for the calculation of bearing capacity and foundation settlement based on pressuremeter tests, 6th ICSMFE, Vol. 2, pp. 295-299.
- Parry R. H. G. 1978. Estimating foundation settlements in sand from plate bearing tests. *Geotechnique* 28, No. 1, 107-118
- Poulos H. G. and Davis E. H. 1974. *Elastic solutions for soil and rock mechanics*. John Wiley & Sons, Inc. 411p.
- Schmertmann John H., 1970. Static Cone to compute static settlement over sand, *Journal of Soil Mechanics and Foundations Division, ASCE*, Vol. 96, No. SM3, pp. 1011-1043.
- Schmertmann H., Hartman J. Paul and B. Philip R. 1978. Improved strain influence factors diagrams, *Journal of Geotechnical Engineering Division, ASCE*, Vol. 104, No. GT8, pp. 1131-1135.
- Schultze E. and Sherif G. 1973. Prediction of settlements from evaluated settlement observations for sand. *Proc. of Eighth International Conference on Soil Mechanics and Foundations Engineering Vol. II*
- Seed H. B. 1969. Influence of local soil conditions on earthquake damage. *Proc., 7th International Conference on Soil Mech. and Found. Eng., Mexico city* .
- Swiger W. F. 1974. Evaluation of soil moduli. *Proc., Conference on Analysis and Design in Geotech. Engrg., ASCE, Austin, Texas, Vol. 2*.
- Shibuya, S., Tatsuoka, F., Teachavorasinskun S., Kong X. J., Abe F., Kim Y., and Park C. 1992. Elastic deformation properties of geomaterials, *Soils and Foundations, Japanese Society of Soil Mechanics and Foundation Engineering*, Vol. 32, pp. 26-46.
- Tand K. E., Funegard E.G. and Warden P. E. 1995. Predicted/ Measured Bearing Capacity of Shallow Footings on Sand. *Proceeding of CPT'95, Linkopig, Volume 2, Sec. 3.33, pp. 589-594*.
- Tatsuoka F., Shibuya S., Abe F., Kim Y. and Park C. 1991. Non-linearity in Stress-Strain Relations of a Wide Range of Geotechnical Engineering Materials-Part I Experimental results, *The University of Tokyo, Institute of industrial Science, Vol. 43 No. 2*.

- Teachavorasinskun S., Shibuya S. and Tatsuaka F. 1991. Stiffness of sands in monotonic and cyclic simple shear. Proceeding of Geotechnical Engineering Congress, Boulder, Colorado, ASCE, pp. 863-878.
- Teachavorasinskun S., Shibuya S. and Tatsuaka F. 1990. Stress history dependency of stiffness of a sand observed in simple shear. Institute of industrial science, University of Tokyo, Vol. 42, No. 3.
- Terzaghi K. 1943. Theoretical soil mechanics, Wiley, New York.
- Timoshenko, S., and Goodier, J. N. 1951. Theory of Elasticity , 2nd edition McGraw-Hill, 506p.

## CHAPTER 8

### CONCLUSIONS AND RECOMMENDATIONS

#### 8.1 Conclusions

The objective of this research has been to identify new ways to evaluate cohesionless soils, based on seismic techniques, such as the Seismic CPT. The research has focused on the identification of unusual sands, such as, highly compressible and/or cemented sands, and the quantification of their compressibility, stiffness, level of cementation, and in-situ stress and stress history. Relationships and methods have also been developed to evaluate the bearing capacity, and settlement of shallow footings on sand.

A re-evaluation of calibration chamber test results has provided an empirical basis to identify unusual highly compressible sands and/or cemented sands and to evaluate the level of cementation in cemented sands. Relationships have been developed in this research to estimate horizontal stress and constrained modulus of sands from combined measurement of cone resistance and small strain shear modulus using SCPT. The proposed relationships are based mainly on published data from a large number of CPT calibration chamber tests and resonant column tests performed on sands with various grain characteristics and stress histories.

A relationship has been proposed to evaluate the ultimate bearing capacity of shallow and deep footings in sands using in-situ cone penetration test results. The results of full scale load tests from 9 full scale spread footings have been used to assist in the development of the proposed relationship for bearing capacity.

Two methods have been presented to evaluate settlement of footings on sand using seismic methods. They can be used for the systematic computation of the settlement of isolated, rigid, concentrically loaded shallow foundations over nonhomogeneous sand. In these methods the sand modulus is computed from the direct in-situ measurement of shear wave velocity rather than using empirical correlations.

### 8.1.1 Identification of unusual sands

Unusual sands have been defined as sands in which the primary constituent are not quartz particles and/or sands which are cemented and/or aged. In Chapter 2, a procedure has been presented to identify 'unusual' sands using in situ seismic CPT results. The method is based on the correlation between small strain shear modulus and cone penetration resistance. It has been suggested to normalize cone penetration resistance with the square root of effective stress. It has also been noted that in a diagram of  $G_s/q_c$  versus normalized cone penetration resistance, sands with different compressibility plot essentially on the same band. This indicates that the correlation between  $G_s$  and  $q_c$  is not highly influenced by sand mineralogy. However, more compressible sands have low values of normalized cone resistance  $q_{c1}$  and high ratios of  $G_s/q_c$ . Compressible sands with high  $G_s/q_c$  (often greater than 10) and low  $q_{c1}$  (less than 50) can be distinguished as they plot in the lower half of the bounded zone. Cemented sands, however, fall outside the bounded zone. Hence, the proposed chart can be used to identify potentially cemented sands and to compare sands of different compressibility. Seismic CPT testing can be performed to obtain both the cone resistance and small strain shear modulus during the same sounding in the same soil. These data should then be plotted in the proposed chart to identify compressible and/or cemented sands.

### 8.1.2 Evaluation of level of cementation

Based on calibration chamber test results on artificially cemented sands, in Chapter 3, relationships have been developed from which the level of cementation in terms of the attraction parameter can be obtained and hence, the relative density of cemented sands estimated. These correlations are in good agreement with similar relationships developed for uncemented sands by other researchers. Application of the proposed procedure to natural sand deposits has been illustrated. Further field data from SCPT in cemented sands is required to evaluate the proposed relationships. It should be noted that, the available data base is limited since only one type of sand, a medium compressible Monterey No. 0/30 sand, has been used in the present study. Therefore, the developed interpretation correlation and method are considered valid only for cemented medium compressible sands.

### 8.1.3 Evaluation of compressibility

In Chapter 4, a framework has been proposed to quantify sand compressibility (Bulk/constrained modulus) from the combined measurement of shear wave velocity and cone penetration. Correlations have been developed to predict in situ constrained modulus in uncemented and unaged silica sands with variable stress history using the seismic CPT. Relationships have also been presented from which bulk modulus can be evaluated using SCPT results. A prior knowledge of initial relative density is not required by this method and OCR can be evaluated directly from seismic CPT (Eslaamizaad and Robertson, 1996). The proposed method has been applied to Seismic CPT results of the Kidd and Massey sites. The predicted bulk moduli are in good agreement with those reported by Byrne et al. (1987).

In Chapter 4, attempts have also been made to establish empirical correlations to evaluate  $M_c$  from CPT data only. The method has been based on regression analyses on calibration chamber test results on uncemented Ticino sand and Toyoura sand with different stress history. The proposed method has the advantage that it requires no additional measurements of shear wave velocity as well as earlier information of initial relative density as compared with the method suggested by Baldi et al. (1986). However, a prior knowledge of OCR, is needed. In the framework proposed by Janbu (1963), corresponding constrained modulus numbers, stress exponents have been determined and related to CPT test results. A series of contours have been constructed to evaluate modulus numbers for sands with different history. Accordingly, correlations have been suggested to estimate bulk modulus from CPT test results in sands.

### 8.1.4 Evaluation of in-situ lateral stress and stress history

In Chapter 5, a correlation has been developed to predict in situ horizontal stress in uncemented and unaged cohesionless soils using the seismic CPT. On this basis, a relationship is proposed to evaluate the coefficient of pressure at rest ( $K_0$ ). The influence of soil compressibility on the proposed relationship has been investigated. A preliminary and tentative procedure has also been presented for estimating stress history (OCR) of uncemented cohesionless deposits from the predicted coefficient of earth pressure at rest ( $K_0$ ). Limited field evidences have been used to illustrate the proposed correlations. The

results have been found to be in good agreement with those obtained from high quality self-boring pressuremeter testing, mainly in normally consolidated sands, although more data are required to fully evaluate the method. A comparison between the  $K_o$  predicted by the proposed method and the corresponding  $K_o$  measured in the calibration chamber test illustrates that although the  $K_o$  value is estimated quite well for normally consolidated sands, it can be underpredicted in overconsolidated sands. Several factors which can reduce the accuracy of the prediction of  $K_o$  have been identified, discussed and evaluated. They can be listed as follows: i) in calibration chamber a large portion of tests is often performed on normally consolidated sands, ii) indirect evaluation of  $K_o$ , iii) high exponents of field parameters in the proposed correlation, iv) inclusion of small strain shear modulus rather than shear wave velocity which is one of the first-hand product of field measurements. In this framework a direct correlation has been developed for sands between  $K_o$ ,  $q_c$  and  $V_s$ . However, this correlation is found to be highly influenced by sand compressibility. Hence, different relationships are recommended for sands with low compressibility, and high compressibility. Very limited field data have been used to evaluate the new developed correlations. Although the results have been found to be in reasonable, more data are required to perform a comprehensive evaluation of the method.

### 8.1.5 Evaluation of bearing capacity

In Chapter 6, a procedure has been proposed to evaluate the ultimate bearing capacity of shallow and deep footings in sands using in-situ cone penetration test results. The application of the procedure is limited to uncemented or lightly cemented, predominantly silica sands. The ultimate bearing capacity of footings on heavily cemented sands could be overestimated. The results of full scale load tests from 9 full scale spread footings have been used to develop the proposed relationship for bearing capacity. A regression analysis has been performed to investigate the effect of the shape, size and depth of footing on the predicted bearing capacity. It has been concluded that for practical purposes a conservative constant ratio of 0.16 can be reasonably assumed between average cone resistance and bearing capacity for shallow footings on sands with any shape and for a wide range of soil density. When the correlation is extended to predict end bearing capacity of deep foundations in sand, results are found to be in good agreement with field observations. Hence, a single correlation developed in this study can be used to estimate either ultimate bearing capacity of shallow footings or end bearing capacity of deep footings. In deep foundations, where  $D/B$  can be greater than 10, the ratio between end bearing capacity and

cone penetration resistance varies between 0.66 in loose to medium dense sands and 1.00 in dense sands. The proposed correlations are based on a settlement to width ratio,  $s/B=0.10$  at the ultimate bearing capacity. Smaller values of  $q_{ult}/q_c$  may apply for smaller values of  $s/B$ .

### 8.1.6 Evaluation of Settlement

In situ seismic techniques can be applied in the evaluation of ground settlement using conventional elastic formula, where the ground is assumed to be an elastic homogeneous medium. However, sand deposits are often non-homogeneous in nature in which the stiffness varies with depth. Hence, an equivalent soil modulus is evaluated within the depth of influence based on in situ testing measurements. Seismic methods can provide reliable modulus profiles of sandy soils. However, The moduli derived from the seismic methods reflect the stiffness of soils at very low strain levels. Two changes can occur to the moduli due to stresses induced by loading from a shallow foundation. While increased confinement due to loading of a footing can increase the soil stiffness, the increase in shear strains will decrease the ground stiffness. The stiffness of soils is affected by effective confining stress. Hence, soils become stiffer due to increases in confinement induced by loading. On this basis, the low strain moduli should be adjusted for increased confining stress under a footing. Soils exhibit non-linear stress-strain behavior, becoming softer at higher strain levels. The rate of reduction in modulus depends on grain mineralogy, stress history and density of the sand. More realistic computation of settlement of footings on sands can be obtained when appropriate modulus degradation curves are utilized in determining operational modulus of the ground from the measured small strain modulus. Hence, prior knowledge of stress history and compressibility of sand are required to select an appropriate modulus degradation curve.

In Chapter 7, two methods have been presented to evaluate settlement of footings on sand using seismic methods. They can be used for the systematic computation of the settlement of isolated, rigid, concentrically loaded shallow foundations over nonhomogeneous sand. One is based on a homogenous ground beneath the footing. Hence, an equivalent operational modulus, for nonhomogeneous layered ground within depth of influence beneath the footing, is computed. Then, the equivalent modulus is incorporated into conventional elastic formulae. In the second approach, ground is divided into layers, in which operational modulus of each layer is computed for the evaluation of settlement of the



corresponding layer. A summation of settlement of layers within depth of influence provides the total settlement. The second proposed method has a similar framework as the method developed by Schmertmann (1970) and et al. Schmertmann (1978). However, in this method the operational modulus is computed from the direct in-situ measurement of shear wave velocity rather than using an empirical correlation. A set of curves are constructed to soften measured small strain modulus of sand layers based on degree of loading, stress history and grain mineralogy. Both methods have been illustrated and evaluated with test results of a full size shallow footing. The predicted settlements in both methods are in good agreement with the observe settlements. The first method based on an equivalent operational modulus is, however, simpler to apply.

## 8.2 Recommendations

1. The available data base in the present study has been limited. Hence, the developed interpretation correlations and methods are considered valid only for sands with the same characteristics. It is necessary to enlarge the database and complement them with field studies before precise predictions could be made.
2. Very limited calibration chamber tests have been performed on highly compressible sands. Hence, in general, the proposed correlations are valid for low to medium compressible sands. Further data are required to develop reliable relationships applicable for sands with high mica or carbonate content made up of shell fragments.
3. Limited field evidence has been used to evaluate the proposed correlations. Although the results have been found to be in reasonable agreement with field measurements, more data are required to perform a comprehensive evaluation of the methods.
4. During SCPT, cone penetration resistance is usually measured at 2 to 5 centimeter in depth, whereas shear wave velocity is often measured every 1 meter. Further developments are required to provide shear wave velocity data at 2 to 5 centimeter interval. This will enhance the accuracy of interpretation remarkably.
5. It is well recognized that Poisson's ratio varies with loading. Evaluation of a more accurate Poisson's ratio, rather than an average constant value, can increase the

accuracy of settlement prediction based on the field measurement of shear wave velocity and conventional elastic formulae.

6. In the conversion of shear wave velocity to the corresponding small strain shear modulus, soil mass density should be known. The accuracy of small strain shear modulus profile is directly proportioned to accuracy of soil mass density. However, a reliable method to evaluate mass density with depth with a reasonable accuracy has not been established.
7. Further studies are required to distinguish aged sands from cemented sands and to evaluate age of a sand using seismic CPT.
8. In the proposed chart for identification of unusual sands, definition of compressibility involves both rearrangement and crushing of particles. Further research is required to identify sands with a high mica or carbonate content made up of shell fragment with low resistance to fracturing.

## References

- Byrne, P. M., Cheung, H., and Yan, L. 1987. Soil parameters for determination of sand masses. *Canadian Geotechnical Journal*, pp. 366-376.
- Eslaamizaad, S. and Robertson, P.K. 1996. Estimation of in situ lateral stress and stress history in sands. *Proceedings of the 49th Canadian Geotechnical Conference*, St. John's, Newfoundland, Canada, pp. 439-448.
- Janbu, N. 1963. Soil compressibility as determined by oedometer and triaxial tests, *Proc. 3rd Eur. Conf. Soil Mech., Wiesbaden, Vol. 1*, pp. 19-25.
- Schmertmann J. H., 1970. Static Cone to compute static settlement over sand, *Journal of Soil Mechanics and Foundations Division, ASCE, Vol. 96, No. SM3*, pp. 1011-1043.
- Schmertmann J. H., Hartman J. P. and Brown P. R. 1978. Improved strain influence factors diagrams, *Journal of Geotechnical Engineering Division, ASCE, Vol. 104, No. GT8*, pp. 1131-1135.

## **APPENDIX A**

Parameter	Phase II (Fraser River Sand)	
	Massey	Kidd
Approx. age of deposit	200 years *	4 000 years *
Target Zone Depth (m)	8 to 13	12 to 17
Average depth to GWT (m)	1.5	1.5
$\gamma$ (kN/m <sup>3</sup> ) above GWT	18.5	18.5
below GWT	19.5	19.5
Mineralogy (of silt size fraction of soil)	70% quartz 15 % feldspar 5% mica 5% kaolinite 5% chlorite & smectite	70% quartz 15 % feldspar 5% mica 5% kaolinite 5% chlorite & smectite
Grain Size $C_u$ ( $D_{60}/D_{10}$ )	2.14 (0.30/0.14)	2.5 (0.35/0.14)
Average FC (%) from SPT	3	6.8
$e_{max}^{\dagger}$	1.056	1.061
$e_{min}^{\ddagger}$	0.677	0.703
$G_s$	2.68	2.72 <sup>&amp;</sup>
$K_o^{**}$	$\approx 0.5$	$\approx 0.5$

\* Monahan et al. (1995)

\*\* Estimated from pressuremeter testing results

<sup>†</sup> Values of  $e_{max}$  and  $e_{min}$  determined by U. of A.

<sup>&</sup> Some void ratios calculated by UBC for the Kidd site were based on  $G_s=2.74$

Table A.1 Index parameters for Phase II CANLEX sites  
(after Wride and Robertson, 1997)

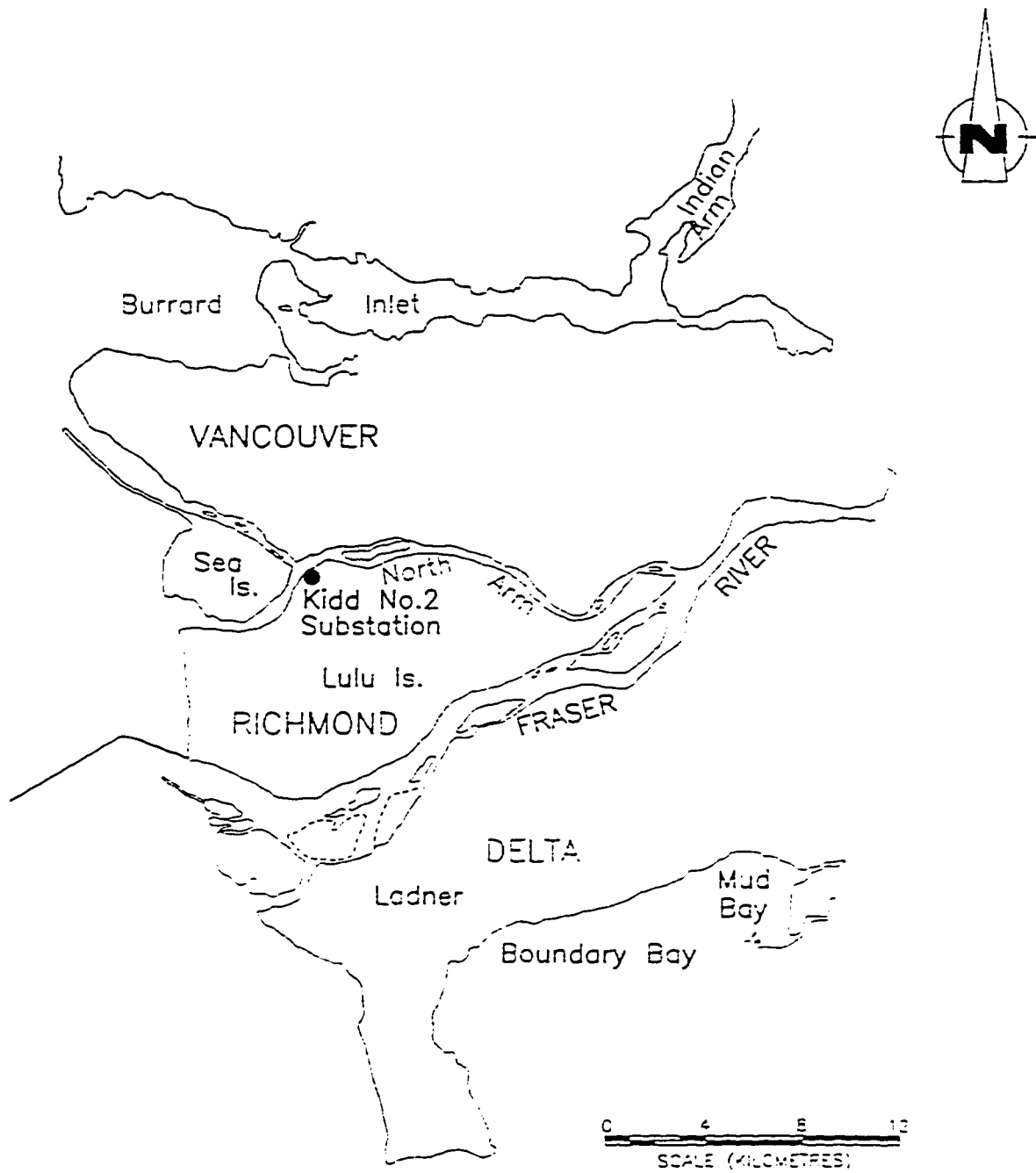


Fig. A.1 Kidd Site in the Fraser River Delta (after Lawrence et al., 1995)

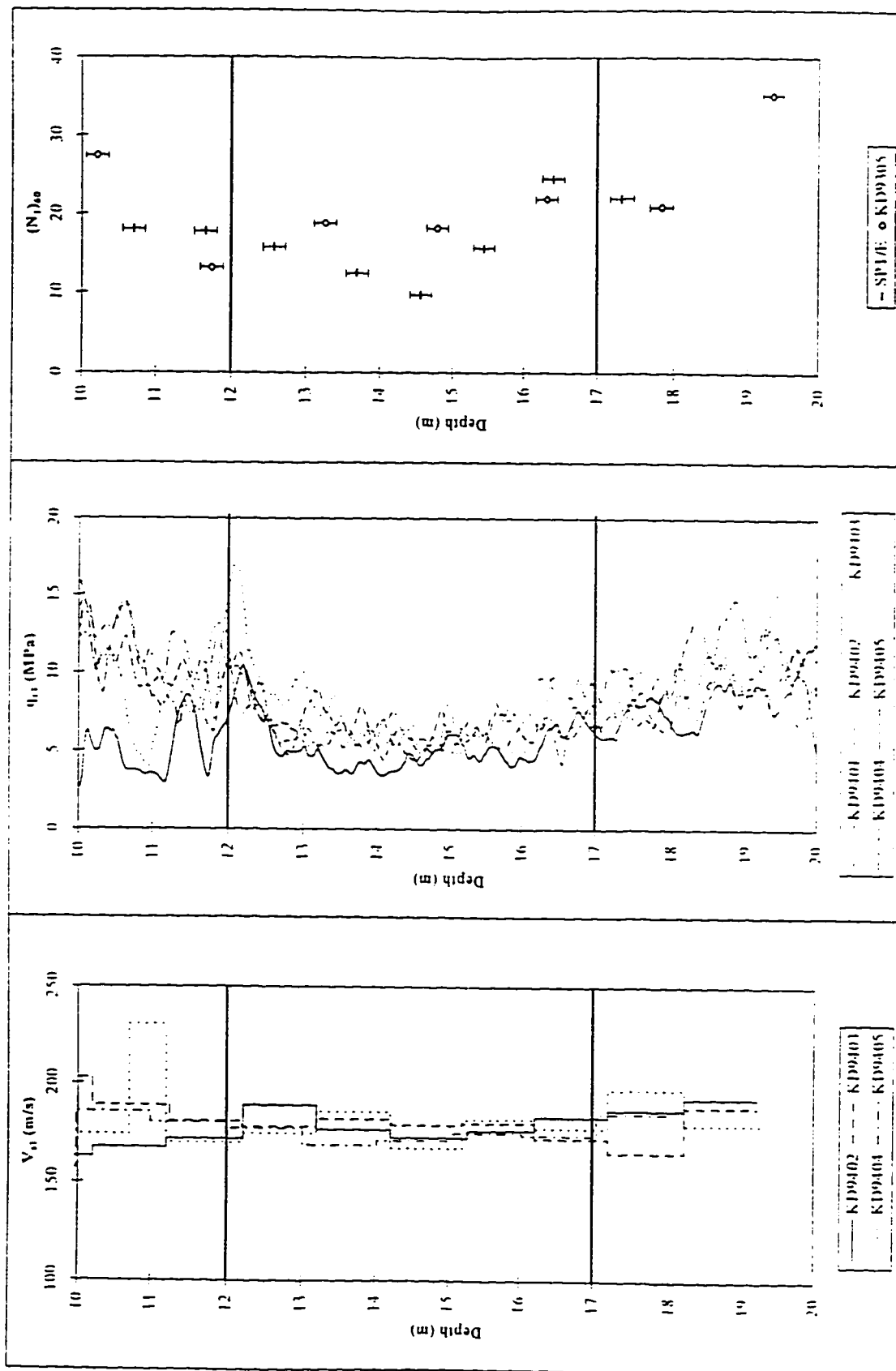


Fig. A.2 Corrected (a) SPT, (b) CPT and  $V_p$  profiles at the Kidd Site

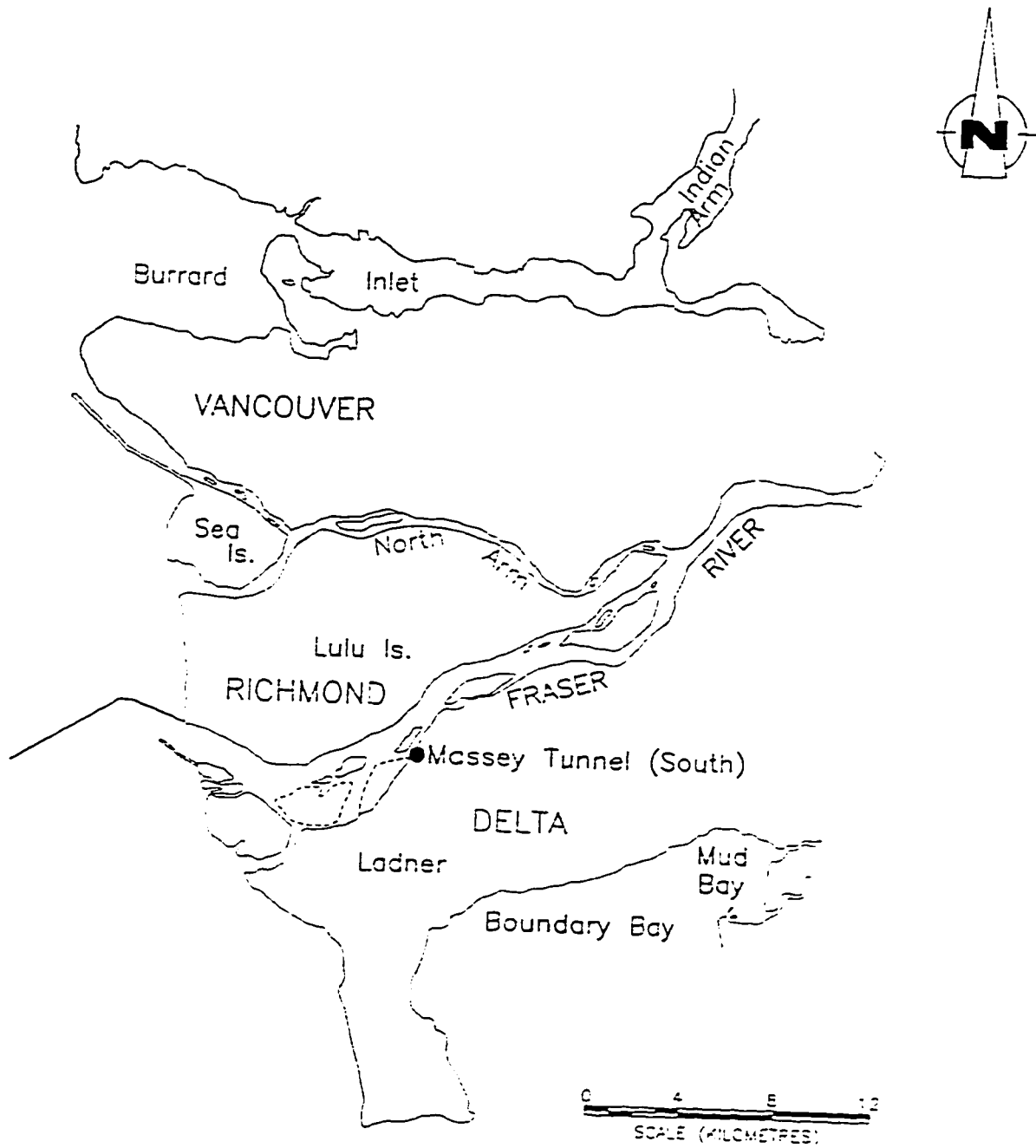


Fig. A.3 Massey Site in the Fraser River Delta  
(after Lawrence et al., 1995)



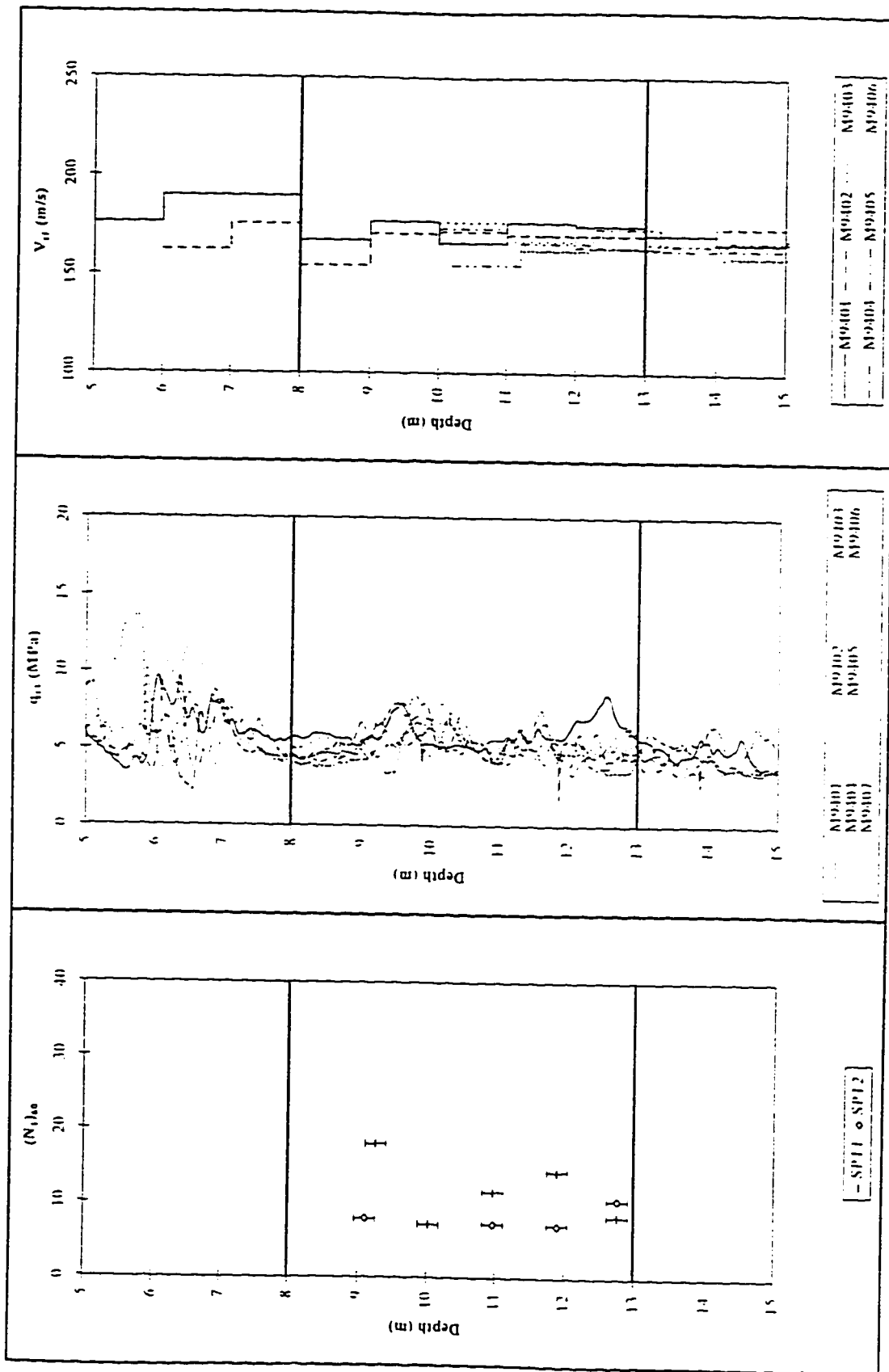


Fig. A.4 Corrected (a) SPT, (b) CPT and  $V_s$  profiles at the Massey Site

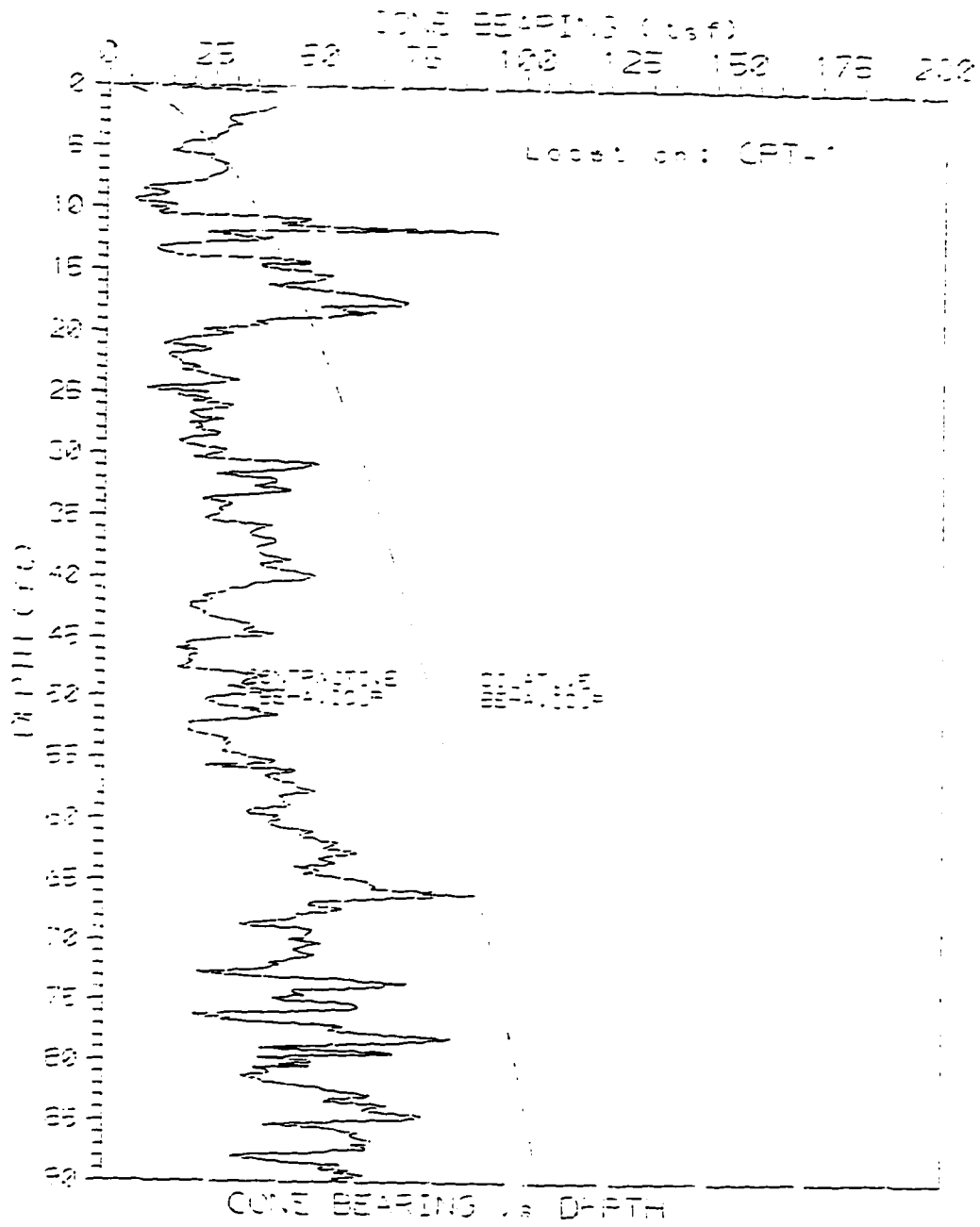


Fig. A.5 CPT profile at the Alaska Site

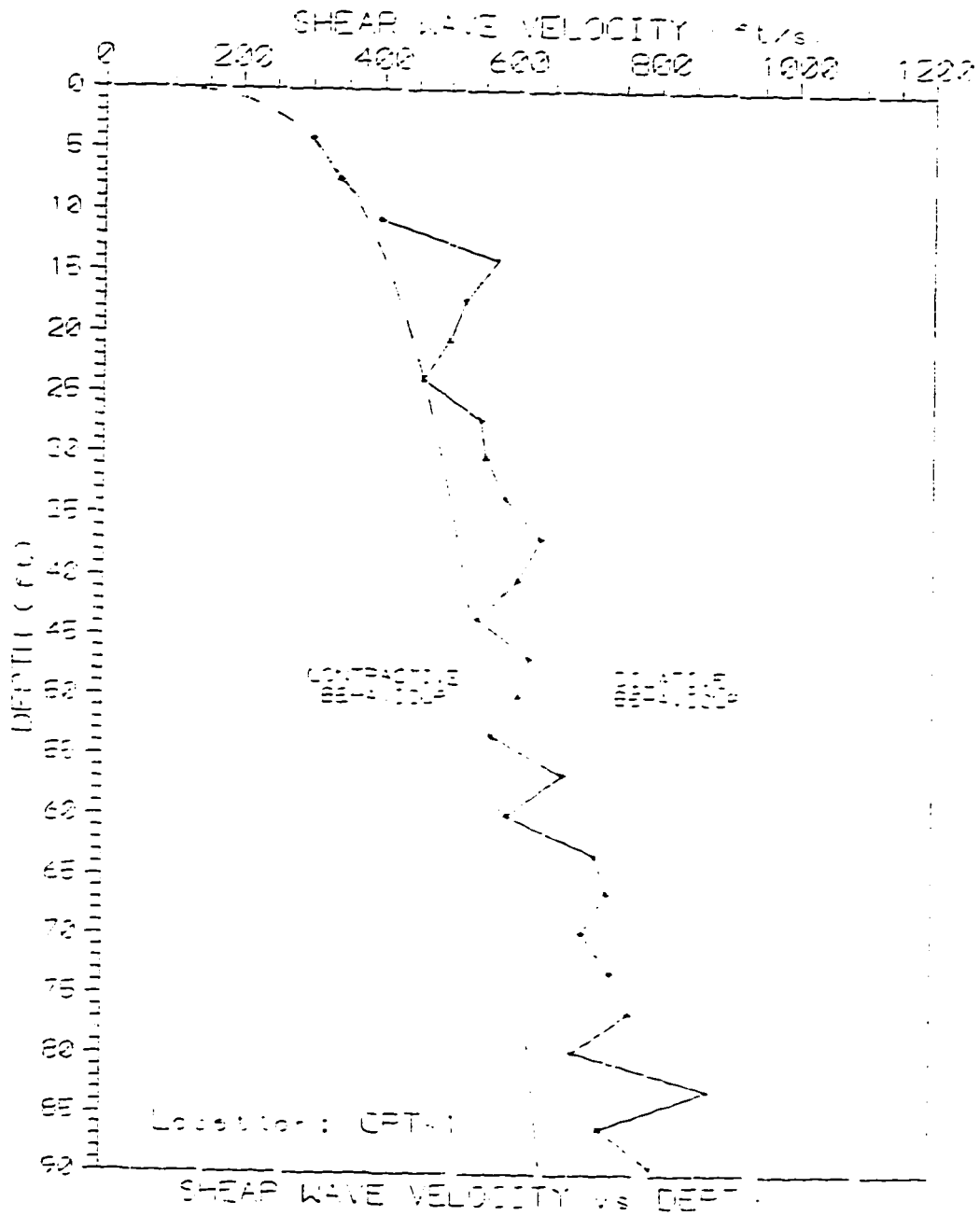


Fig. A.6  $V_s$  profile at the Alaska Site

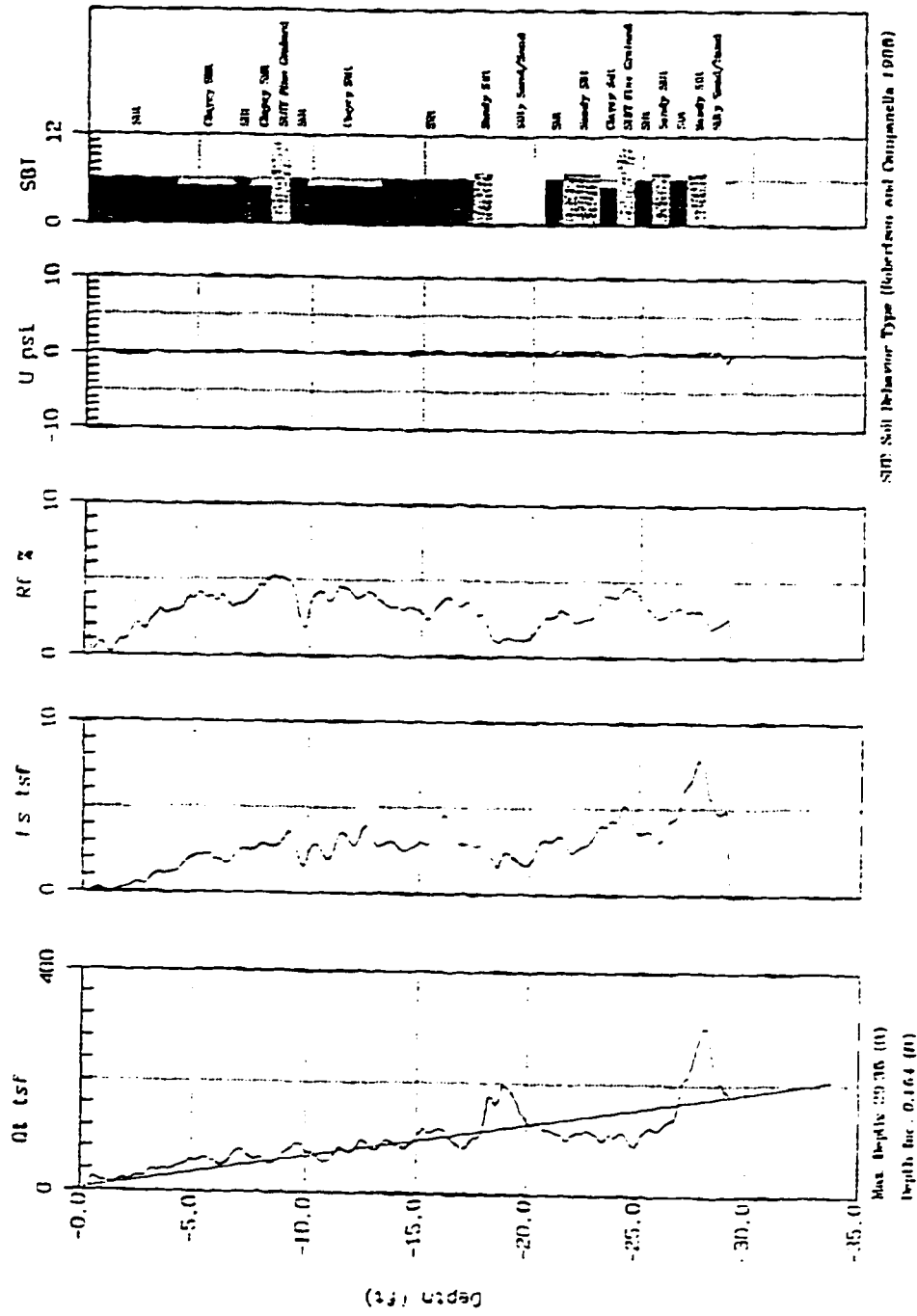


Fig. A.7 CPT profile of Utah tailings sand

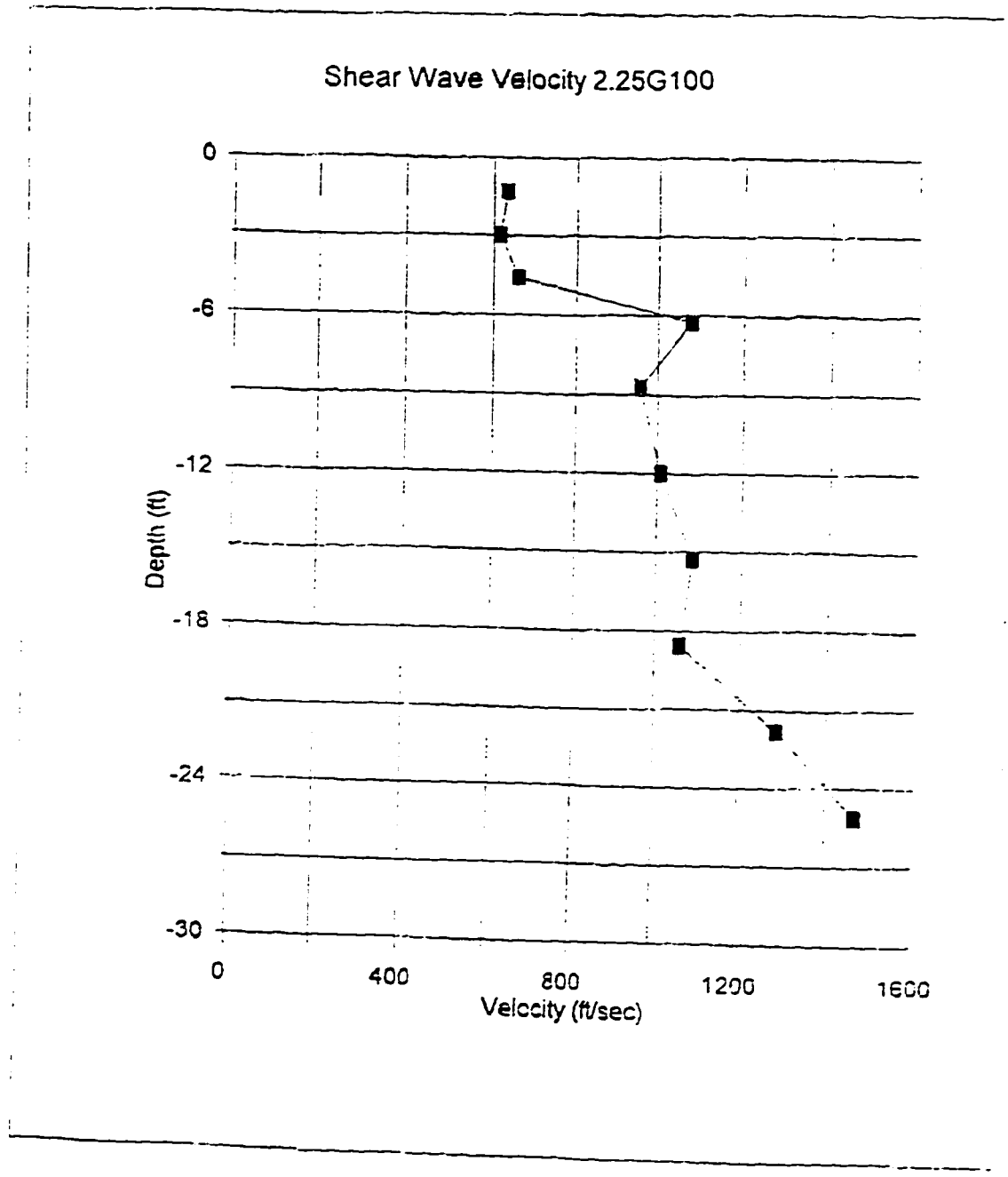


Fig. A.8  $V_s$  profile of Utah tailings sand

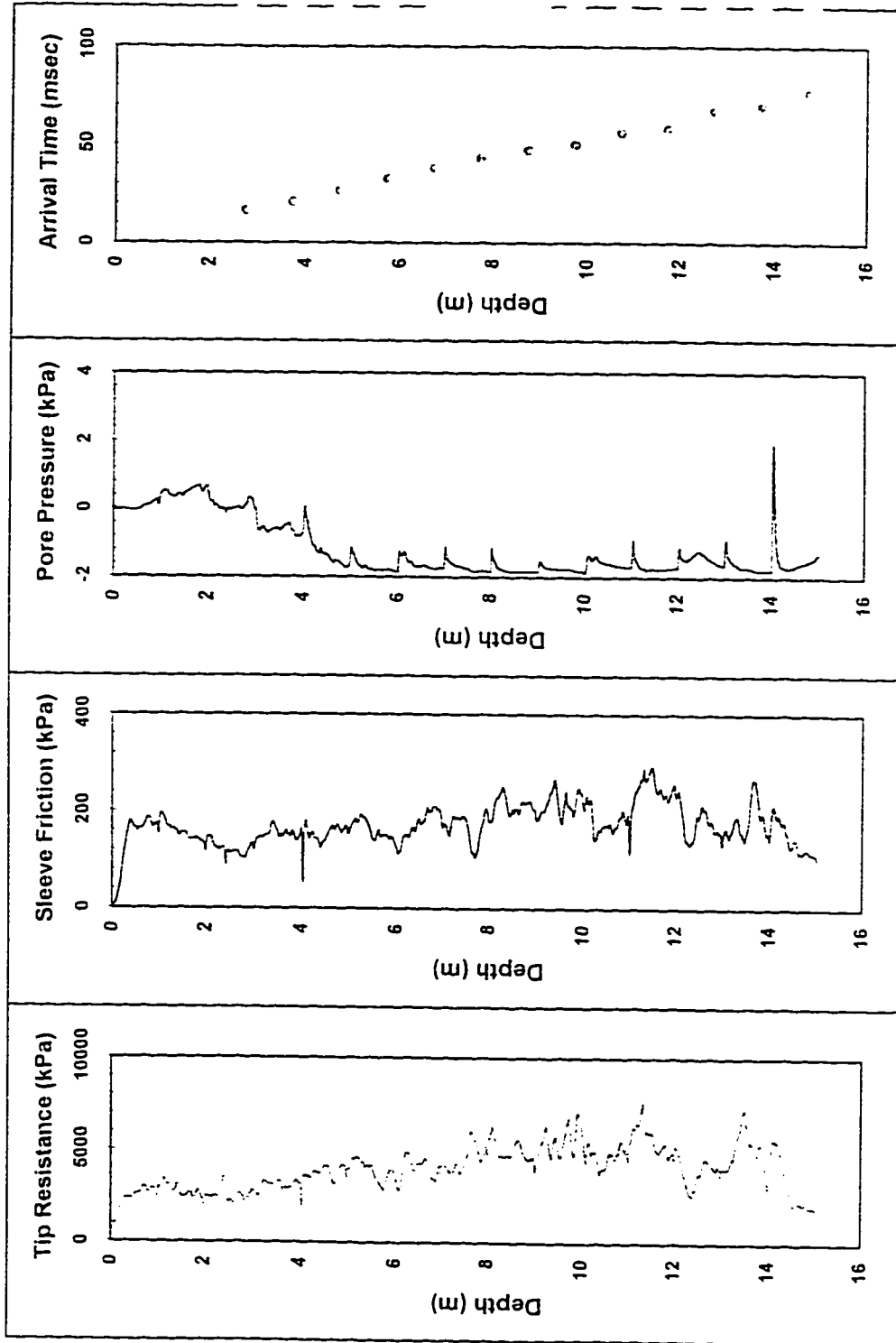


Fig. A.9 CPT profile of Alabama residual soil at Auburn University Test Site, Test C41

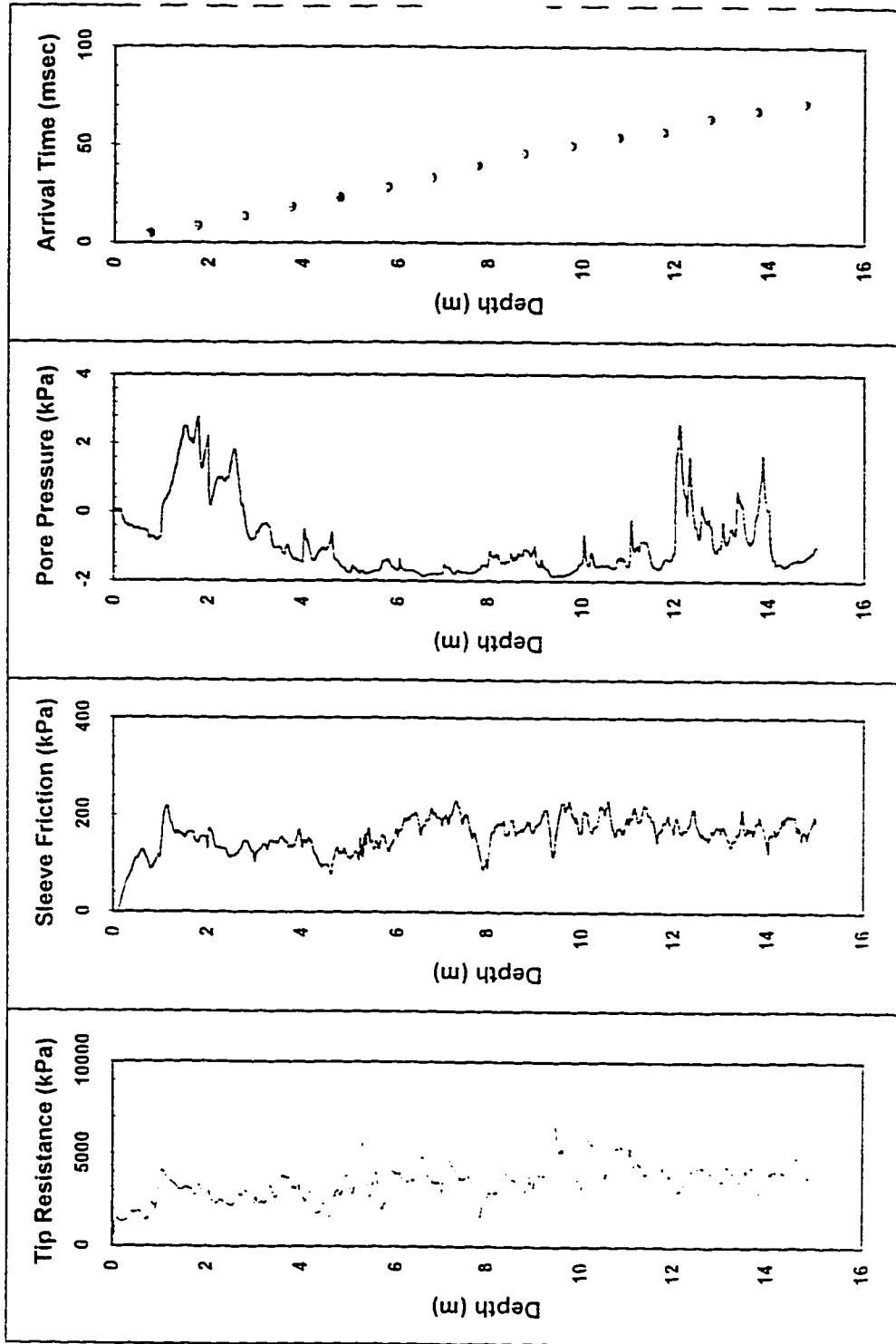


Fig. A.10 CPT profile of Alabama residual soil at Auburn University Test Site, Test C42

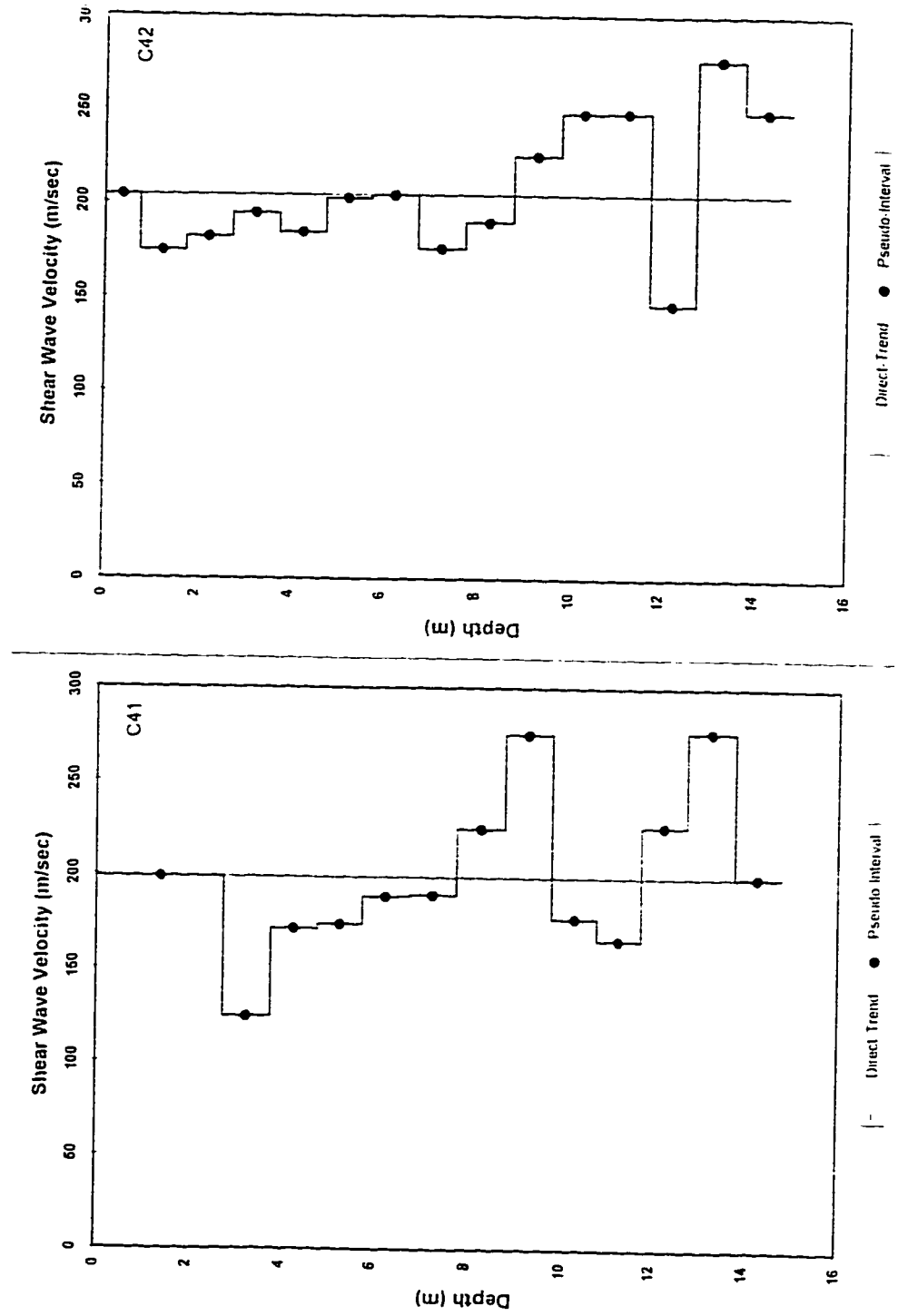


Fig. A.11  $V_s$  profile of Alabama residual soil at Auburn University Test Site, Test C41 and Test C42



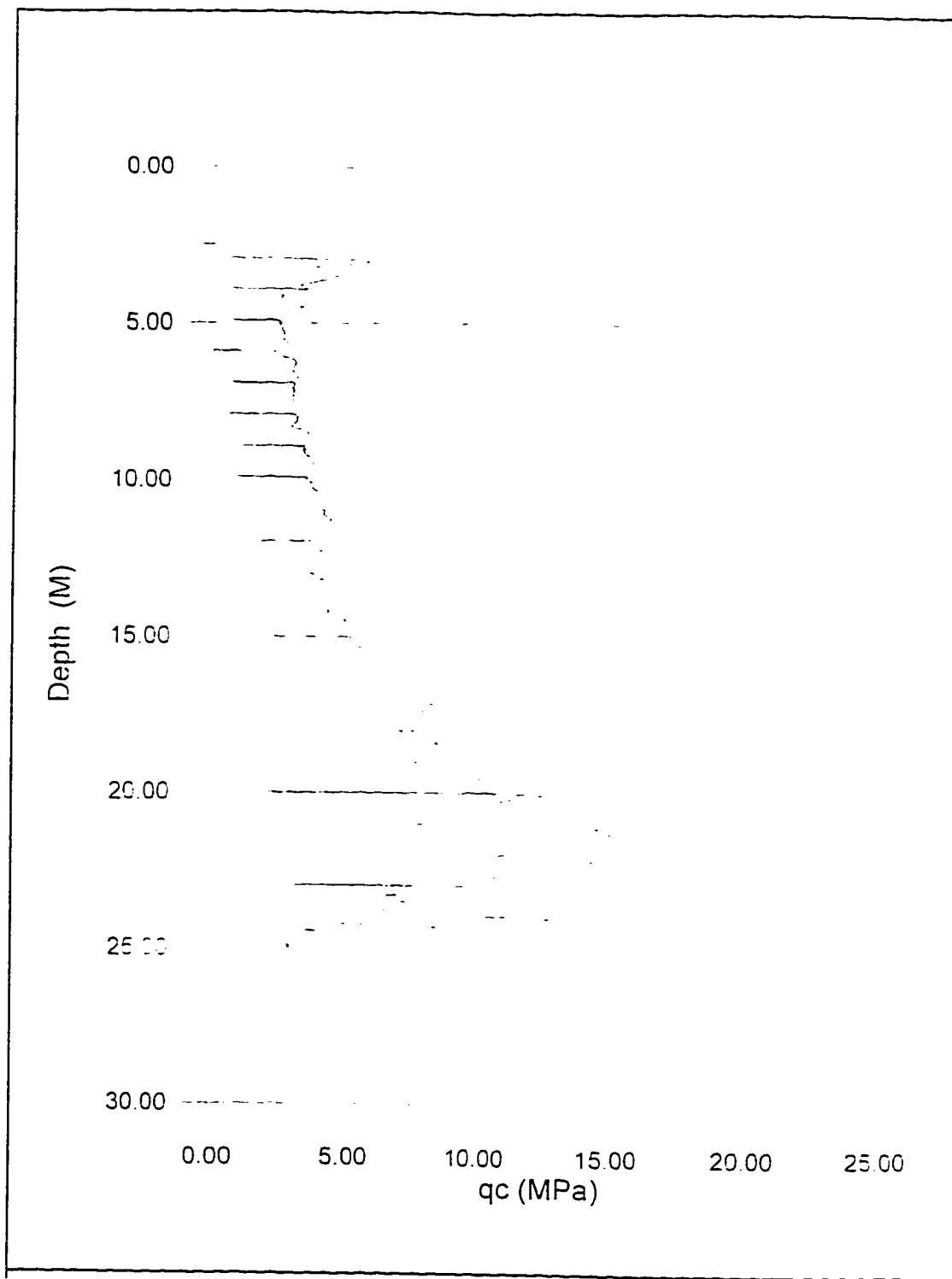


Fig. A.12 CPT profile at Holmen, Norway

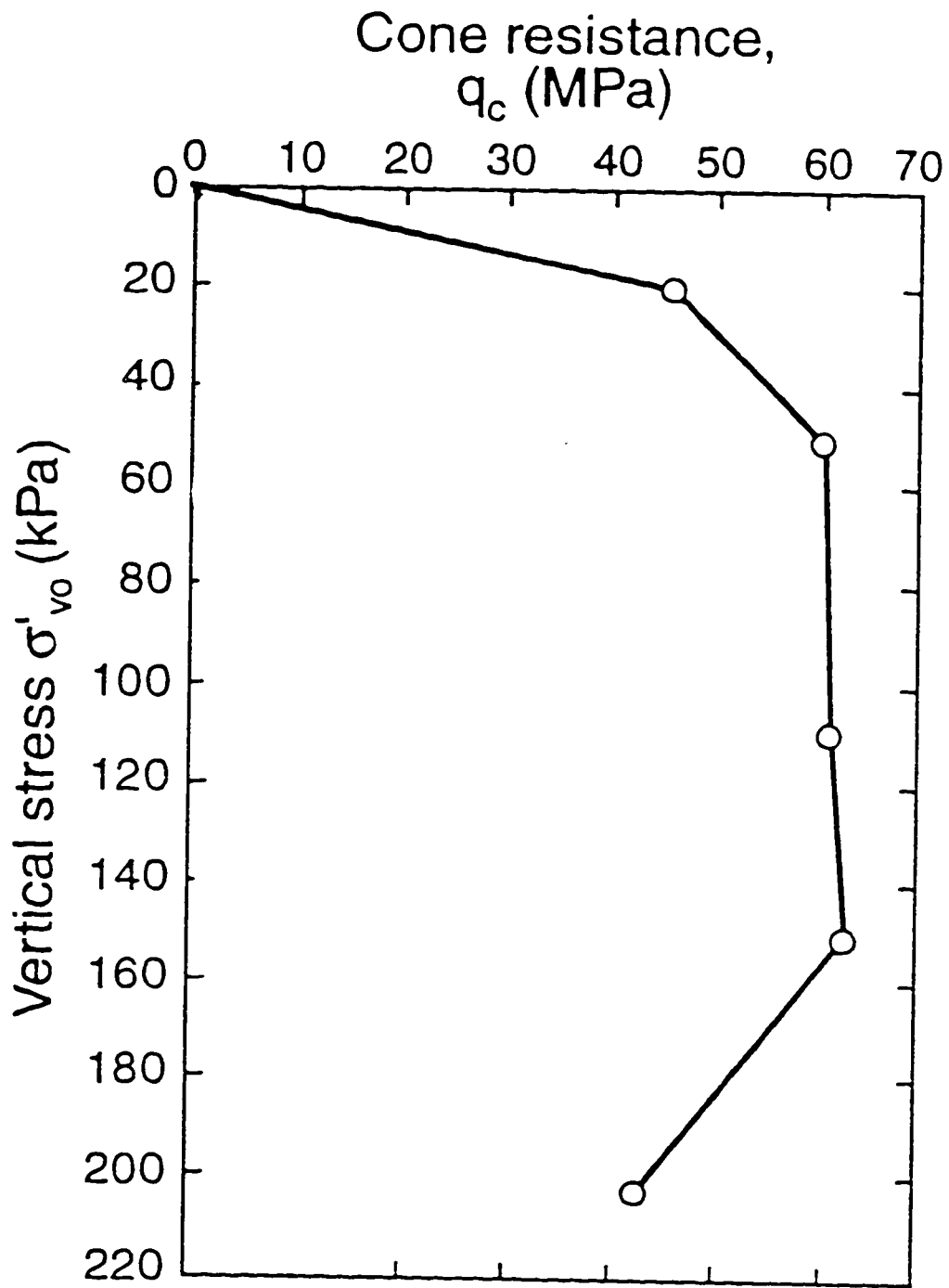


Fig. A.13 CPT profile at Sleipner, North Sea